# Novel PTA-derivatives as Ligands for Selective Catalytic Hydrogenation and Hydroformylation Reactions

*Antonella Guerriero*

**UNIVERSITA' DEGLI STUDI DI FIRENZE**

Dottorato di Ricerca in Scienze Chimiche – Ciclo XXIII
Settore CHIM/06 – Chimica organica
Settore CHIM/03 – Chimica generale e inorganica

# Novel PTA-derivatives as Ligands for Selective Catalytic Hydrogenation and Hydroformylation Reactions

**Doctoral Thesis**

Submitted by

**Guerriero Antonella**

Coordinator:

Prof. Andrea Goti

Tutors:

Dr. Gianna Reginato

Dr. Luca Gonsalvi

*Ai miei genitori e a mia sorella*

*per essermi stati sempre vicini*

# TABLE OF CONTENTS

# FREQUENTLY USED ABBREVIATIONS

| | |
|---|---|
| BZA | Benzylidene acetone |
| CD | Cyclodextrin |
| CNA | Cinnamaldehyde |
| Cod | 1,5-cyclooctadiene |
| Cp | Cyclopentadienyl |
| Cp* | Pentamethylcyclopendadienyl |
| DABCO | Diazobicylooctane |
| DFT | Density functional theory |
| DMC | Dichloromethane |
| DME | 1,2-dimethoxyethane |
| DMSO | Dimethyl sulfoxide |
| ESI-MS | Electrospray ionisation mass spectrometry |
| FT-IR | Infrared spectroscopy |
| GC | Gas-cromatography |
| $^{i}$PrOH | Isopropanol |
| LDA | lithium diisopropylamide |
| MS | Mass spectrometry |
| $^{n}$BuLi | *n*-buthyllithium |
| NMR | Nuclear magnetic resonance |
| OTf | $OSO_2CF_3$ |
| PTA | 1,3,5-triaza-7-phosphadamantane |
| RAME-β-CD | Randomly methylated β-cyclodextrin |
| RT | Room temperature |
| $^{t}$BuOK | *Tert*-potassium butoxide |
| TH | Transfer hydrogenatio |
| THF | Tetrahydrofuran |
| THP | *Tris*-(hydroxymethyl)phosphine |
| THPC | *Tetrakis*-(hydroxymethyl)phosphonium chloride |
| TOF | Turn over frequency |
| TON | Turnover number |
| Tos | *p*-toluensolfonate |
| XRD | Single-crystal X-ray diffraction |

## X-RAY CRYSTAL STRUCTURES: ATOM COLOUR CODE

| | |
|---|---|
| Carbon | Gray |
| Chlorine | Violet Red |
| Hydrogen | White |
| Iridium | Neon blue |
| Iodine | Violet |
| Nitrogen | Blue |
| Oxygen | Red |
| Phosphorous | Green |
| Selenium | Medium Forest Green |
| Ruthenium | Orange |
| Zinc | Indian Red |

# *Chapter 1*

# Introduction

## 1.1 Overview

This chapter provides an introduction to the fundamental principles of catalysis focusing in particular on aqueous-phase catalytic processes. After a brief review of some of the most common hydrophilic phosphine ligands used in catalysis, the physical, chemical and coordination properties of the phosphine PTA (1,3,5-triaza-7-phosphaadamantane) are treated in details. Some examples of the numerous transition metal complexes containing PTA or its derivatives, and the description of their use for several applications are also reported. A brief overview on the catalytic application of hydrophilic ligands to hydroformylation and hydrogenation reactions is also given. In the last part of the Chapter, the main objectives of the PhD project are described.

## 1.2 Aqueous-phase catalysis

The increasing cost of waste disposal and the need to preserve the environment and replace old technologies with more sustainable approaches, have prompted a renewed interest in the search for alternative media for chemical transformations and a re-evaluation of more "green" methodologies.[1] The area of catalysis is often referred to as a fundamental pillar of green chemistry.[2] Catalytic reactions, in fact, reduce energy requirements and minimize the quantities of reagents needed due to the enhancement of selectivity. Sustainable processes envisage also the reduction or, where possible, the elimination of environmentally hazardous substances and the replacement of traditional organic solvents with water. Organic solvents have a number of attractive features: they dissolve a wide range of organic compounds, they are volatile and easily removed but on the other hand, they are often toxic, flammable and non-renewable and originate a significant portion of chemical processes waste. Since solventless processes are unlikely to be realized in most cases, water represent an attractive alternative.

Water is completely benign in its pure form, it is ubiquitous, nonvolatile and environmentally friendly.[3] It is cheap and can also offer advantages in terms of chemical reactivity and selectivity.[4] Water is highly polar and provides effective solvation for ionic species, it can in some cases accelerate reactions of hydrophobic compounds[5] and gives the opportunity to finely tune the pH of the reaction system. Additionally, water itself can work as an acid, base, nucleophilic reagent and even as an $H_2$ source. In organic chemistry, the use of water as solvent implies the elimination of protection-deprotection processes of functional groups and water-soluble compounds such as carbohydrates can be used directly without any derivatization.[6]

The employment of water in catalysis has received renewed attention in the last years, in particular in homogeneous transition metals catalyzed processes.[7] These reactions have been growing in importance for both academic and industrial communities and the design of homogeneous catalysts represents a challenge for their implementation on a large scale.[8] In addition to the advantages of

homogeneous catalysis, that is high selectivity and activity, the possibility to use mild reaction conditions and well-defined molecular catalysts, an important advantage by using aqueous-phase catalysis is the unique ability of water to change the nature of the reaction. The formation of macrocycles, for examples, is accelerated in water by taking advantage of the low water-solubility of organic substrates.[6]

The first aspect to consider in the quest for a water-soluble homogeneous catalyst is to design a molecular structure able in principle to convey the electronic and steric properties of known active organometallic complexes into water. Therefore, a catalyst need to be stable in water in order to produce catalytic transformations with high activity and selectivity. In fact, an obvious limitation for aqueous-phase metal catalyzed processes is due to the limited stability of some metal-carbon bonds (M–C) in water. M–C bonds can be attacked by water either through electrophilic reaction (proton transfer) or *via* nucleophilic reaction operated by oxygen. For these reasons, conventional transition-metal catalyzed reactions are often carried out under an inert atmosphere and the exclusion of moisture is essential. However, several studies have recently shown that some of these reactions can be facilitated in water and can be carried out also in open air.[9] As for example, the functional groups of homoallylic alcohols were repositioned to give allylic alcohols with controlled regioselectivity, by using the water-soluble complex $[RuCl_2(PPh_3)_3]$ as catalyst (Scheme 1.1).[10] This C–H catalytic activation reaction was performed in water and in air. Finally, the low solubility of oxygen gas in water can facilitate the stability of moderately air-sensitive catalysts in this solvent.

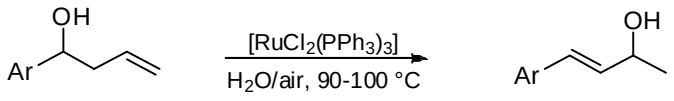


**Scheme 1.1.** Ru-catalyzed C-H activation reaction in water and air.[10]

Another aspect to consider in homogeneous aqueous-phase catalysis is the recovery of the catalyst by simply phase separation from the hydrophobic products. The most common metals used in catalysis (Ru, Ir, Rh, Pd, Pt) are expensive and

rare, so their recovery is important for industrial applications of homogeneous catalysts. In the conventional processes, thermal operations such as distillation, decomposition, transformations which normally lead to thermal stresses on the catalyst, are in fact required for separation of products and catalysts. These operations seldom give quantitative recovery, which causes failure of productivity and loss of the metal.

Catalyst-product separation can be easily obtained in heterogeneous catalysis but solid catalysts are often not selective for several important chemical transformations.[11] Thus, by using an aqueous-biphasic catalytic system incorporating a water-soluble catalyst, separation can be achieved more easily and with lower costs.[12] The water-soluble homogeneous catalyst (organometallic coordination complex) is in solution in the water phase and the substrates/products are located in a second phase (organic). Applying strong stirring they react at the interphase region or in the catalyst containing phase and, at the end of the reaction, catalyst and products distribute in the two phases and can be separated off simply by phase separation (Figure 1.1). Therefore, this system maintains the beneficial properties of homogeneous catalysis, and at the same time allows to avoid or reduce the use of organic solvents and to recover the catalyst for its possible reuse.

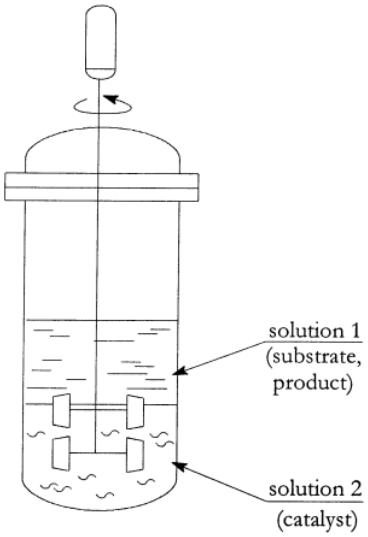


**Figure 1.1.** Representation of two-phase catalysis (aqueous/organic). Adapted from ref.12b.

## 1.3 Homogeneous catalysts design: water-soluble phosphines

In order to constrain a catalyst into the aqueous phase, several approaches can be utilized. Supported aqueous-phase catalysts (SAP) represent one of the possible methods. These are produced by the adsorption of the aqueous solution of the water soluble catalyst precursor onto a hydrophilic support such as silica, forming an immobilized catalyst.[13] Another possibility is to include organometallic catalysts in the pores of aluminosilicates or aluminophosphates and use them in water phase reactions involving water-soluble organic reagents.[14] An alternative strategy is to carry out the reactions in water by using surfactants or phase transfer agents such as modified cyclodextrins, which, depending on their composition, can accommodate into their cavity a wide range of hydrophobic guest molecules and convey them into water.[15] The most frequently used approach to exploit an organometallic compound as catalyst for an aqueous phase reaction is to obtain water-soluble complexes using ligands with hydrophilic polar groups.[16] Since phosphines, especially triarylphosphines are the most widely used class of ligands in catalytic processes thanks to their stability, a variety of water soluble tertiary phosphines have been prepared by many research groups. Generally, known phosphines are modified by the introduction of polar charged groups, *i.e*. $SO_3^-$, $CO_2^-$, $PO_3^{2-}$, $NR_3^+$, which causes the increase of water solubility due to solvation and/or separate ion couple formation.[17]

The most common class of hydrophilic phosphine ligands is that carrying anionic substituents (Figure 1.2). In particular, sulfonate, phosphonate and carboxylate are the most used anions because of their weakly basic features and their stability over a broad pH range, which allow to solubilize organometallic species in a variety of catalytic processes. Additionally, these weakly basic groups do not bind strongly to transition metals and do not interfere with the catalytic cycle.

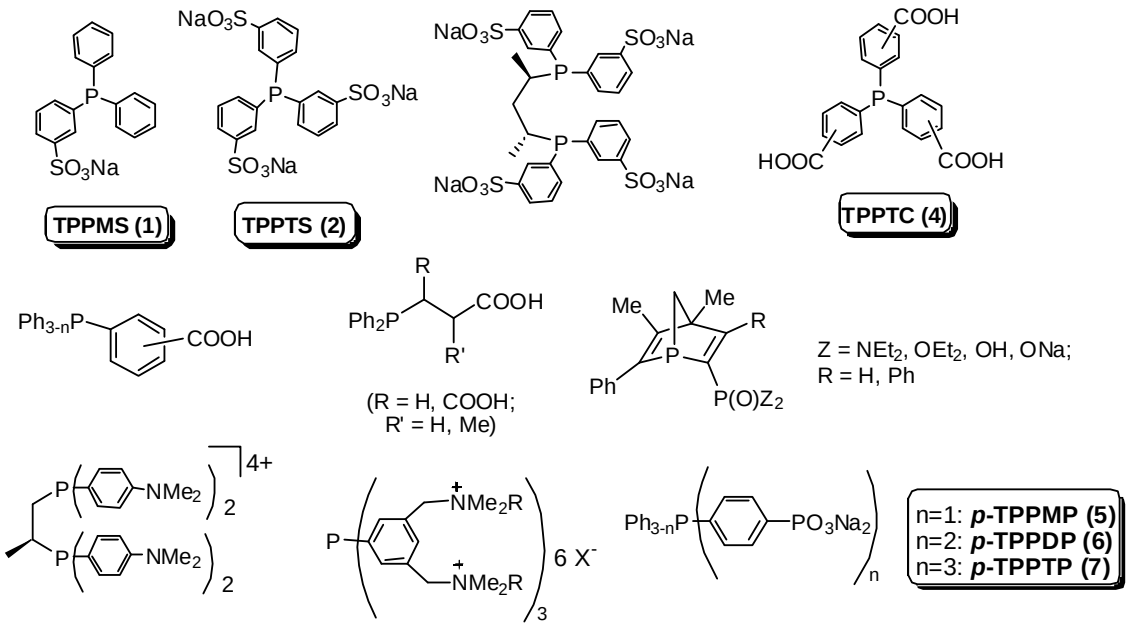


**Figure 1.2.** Some examples of water-soluble phosphines with anionic substituents.

The sulfonate group, for istance, is an attractive water-solubilizing moiety stable under numerous conditions and easy to introduce. Sulfonation of aryl rings is achieved through electrophilic substitution by using $SO_3/H_2SO_4$ or in some cases just $H_2SO_4$, followed by neutralization with metal hydroxides. When aryl rings are directly connected to the phosphorus atom, sulfonation occurs exclusively in *meta*-position due to the effect of the protonated P atom. Monosulfonated triphenylphosphine, *m*-TPPMS (**1**, Figure 1.2), is the first example of sulfonated phosphine ligand.[18] The study of the hydroformylation of 1-hexene catalyzed by a rhodium complex of TPPMS showed that this phosphine has a surfactant-like structure so it may be surface active, which means it will tend to accumulate at the boundary between the aqueous and the organic phase and its aqueous solutions have a tendency to form emulsions that separate slowly.[19] The trisulfonated derivative, *m*-TPPTS (**2**, Figure 1.2) was first prepared by the reaction of $PPh_3$ in 20% oleum at 40 °C for 24h, followed by neutralization with NaOH.[20] This reaction gave a mixture of *m*-TPPTS and its oxide *m*-TPPOTS, which can be removed due to its higher solubility in water/methanol compared to **2** or by separation using Sephadex columns.[21] Numerous sulfonation protocols have been developed to give *m*-TPPTS

in high yield, avoiding the oxidation of the phosphorus centre. The preparation of the partially sulfonated ligands *m*-TPPMS and *m*-TPPDS (**3**) is more difficult and often the reaction produces a mixture of the mono-, di- and tris-sulfonated products. In all cases, electrophilic sulfonation results exclusively in *meta*-sulfonated phenylphosphines and the presence of sulfonate in *meta*-position increases the cone angle of the phosphine, which may have a negative effect on its catalytic application. The inclusion of $SO_3$ group in *ortho* or *para*-positions can be achieved by involving a $S_NAr$ substitution reaction of phosphide nucleophile anions on *o*- or *p*-substituted aryl fluorides (Scheme 1.2) and, since sulfonation can be carried out on the aryl fluoride precursor before the reaction with phosphine, phosphorus oxidation is avoided. Contrary to TPPMS, *m*-TPPTS and *m*-TPPDS do not show surface active character.[22]

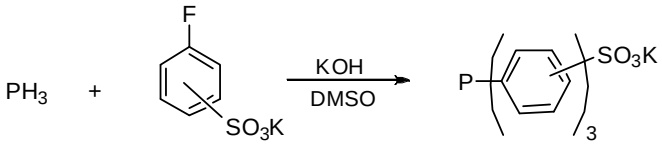


**Scheme 1.2.** Preparation of *p*-sulfonated phosphines. Adapted from ref. 16c.

Carboxylate and phosphonate substituents are also frequently used to prepare hydrophilic phosphines, although the examples of these ligands are few if compared to the sulfonated ones. This is due to the fact that they cannot be prepared by simple electrophilic substitutions of known ligands. The carboxylated analogs of TPPTS, *m*- or *p*-TPPTC (**4**, Figure 1.2) were prepared by lithiation of tris-(bromophenyl)phosphine followed by quenching with $CO_2$,[23] while *o*-, *m*- and *p*-TPPMC and TPPDC were obtained by nucleophilic addition of phosphides to fluorobenzoic acid derivatives.[24] Changing from the sulfonate substituent of *m*-TPPTS to the carboxylate of *m*-TPPTC does not alter the cone angle of the ligand (170°, obtained from crystallographic data[25]). Another approach used to prepare carboxylated phosphine is the condensation of hydroxymethylphosphines with amino acids.[26]

The mono (*p*-TPPMP, **5** Figure 1.2), di- (*p*-TPPDP, **6** Figure 1.2) and tris-phosphonated (*p*-TPPTP, **7** Figure 1.2) triphenylphosphine analogs were synthesized by reacting phosphorus nucleophiles ($Ph_2PK$, $PhPLi_2$ or red phosphorus) with fluorophenylphosphonate esters followed by hydrolysis of the esters.[27] Phosphonated $PPh_3$ can also be prepared by Pd-catalyzed P–C coupling of aryl halides to introduce both phosphine and phosphonate substituents.[28]

The insertion of cationic functionalities such as ammonium ions, is another method to prepare hydrophilic ligands. Quaternary ammonium ions are used to give ligands which will remain ionic regardless of pH. On the contrary, amines allow the solubility of the ligand to be controlled as a function of pH, consequently phosphine ligands substituted with amines can partition into both the organic and the aqueous phase as a function of pH and so can be used for both homogeneous and biphasic catalysis. Trialkylphosphines with ammonium groups are generally prepared by adding phosphine nucleophiles to haloalkylamines or ammonium salts.[29] Guanidinium ion has also been used and its higher hydrogen bonding ability compared to ammonium substituents provides higher water-solubility. Some mixed aryl alkylphosphines substituted with guanidinium were prepared in good yield by the reaction of 3-aminopropylphosphine with 1*H*-pyrazole-1-carboxamidine (**a**, Figure 1.3).[30] The guanidine-functionalized $PPh_3$ analogs (**8** *m*-TPPMG, **9** *m*-TPPDG, **10** *m*-TPPTG, Figure 1.3) were also obtained by reacting the corresponding *m*-aminophenylphosphines with dimethyl cyanamide.[31]

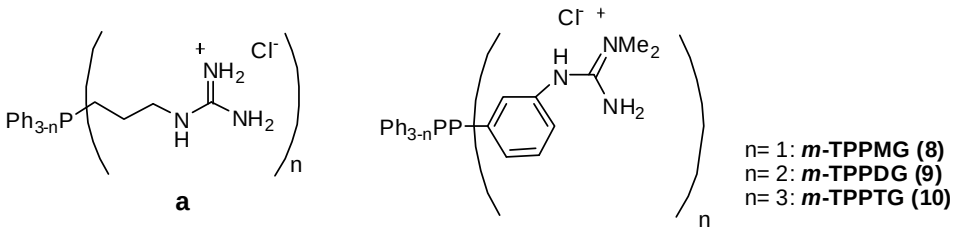


**Figure 1.3.** Some examples of phosphines with cationic substituents.

Although ionic functionalities are the most widely used water-solubilizing substituents, in the last years there has been a growing interest in the use of non-ionic hydrophilic functional groups. These substituents are attractive as they are often soluble both in organic solvents and in water and this property simplifies the synthesis of hydrophilic ligand. Carbohydrates, polyethers or polyamines are the most commonly used substituents. In particular, carbohydrates are useful for the synthesis of hydrophilic chiral phosphines because they are readily available in enantiomerically pure form and can be easily functionalized. An example is represented from BASPHOS (**11**, Figure 1.4) which was obtained from D-mannitol and then complexed to rhodium(I) (**12**, Figure 1.4), the corresponding complex was used for asymmetric hydrogenation of functionalized olefins and dehydroamino acids by up to 96% *ee* in water.[32]

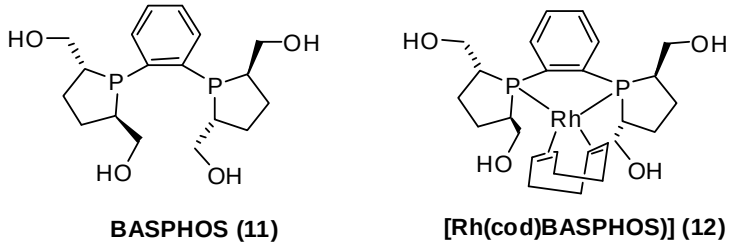


**Figure 1.4.** Water-soluble phosphine BASPHOS and its Rh(I) complex.

In all the cases described, the introduction of water-solubilizing groups can affect the steric and the electronic properties of the ligand, as well its electron-donating ability.

## 1.4 PTA, a versatile neutral water-soluble phosphine

As described before, phosphine are the most common ancillary ligands used in organometallic chemistry, owing to their ability to stabilize low metal oxidation states and their capacity to influence both steric and electronic properties of the catalytic species. In recent years, the cage-like water-soluble monodentate phosphine 1,3,5-triaza-7-phosphatricyclo[3.3.1.1]decane, known as PTA (**13**, Figure 1.5), has received a renewed interest.[33] Due to its ability to form transition metal

complexes stable in water, a large number of coordination complexes containing this ligand have appeared in the literature and their catalytic,[34] medicinal[35] and electrochemical properties[36] have been investigated.

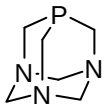

**PTA (13)**

**Figure 1.5.** The cage-like water-soluble phosphine PTA.

PTA was synthesized for the first time by Daigle *et al*. in 1974[37] and the synthetic procedure has been improved in the following years.[38] This alkyl phosphine is stable in air as solid in contrast to $PMe_3$ and $PEt_3$, which are both known to violently ignite in air. It is also thermally stable decomposing at temperatures higher than 260 °C. PTA shows high water solubility (*S*= 1.5 M, *ca*. 235 g/L) given only by the presence of tertiary amine and phosphine functionalities. Its water-solubility is higher than the sulfonated phosphine *m*-TPPMS (*S*= 0.2 M) and comparable to that of *m*-TPPTS (*S*= 1.9 M).[20a] The water solubility of PTA can be increased up to 2.2 M in 0.1 M HCl solution due to the formation of its N-protonated form. PTA is also soluble in MeOH and EtOH, but less soluble in heavier alcohols such as 2-propanol or *n*-butanol and THF at room temperature.[38a] Additionally, **13** is soluble in DMSO, acetone, chloroform, dichloromethane, but not in toluene, benzene or hexane at room temperature. Even if this phosphine is very water-soluble, its solubility in water can be further enhanced by alkylation of the nitrogen atoms (derivatization of *lower rim*) to give PTA cations or by tailored derivatization on $C_\alpha$ atoms of the methylene groups bound to the phosphorus (derivatization of *upper rim*). The synthesis and the properties of all these derivatives will be treated in details in Chapter 2. The basicity of PTA is similar to that of $PMe_3$ measured with a p$K_a$ of 5.70[39] and its overall reactivity is comparable to that of other alkyl phosphine. Favourably, it appears to have higher resistance to oxidation than other types of water-soluble phosphines, including TPPMS and TPPTS.

The crystal structure of PTA (Figure 1.6)[40] reveals that P–C and N–C bonds are typical and shows no indication of strain. The cone angle is relatively small (103°), equal to that of $PH_2Me$ and affords the possibility to prepare transition metals complexes containing more than one PTA molecule. The small compact steric property together with the chemical and thermal stability as well the high hydrophilicity, makes this ligand unique in comparison with less encoumbering phosphines such as $PMe_3$.

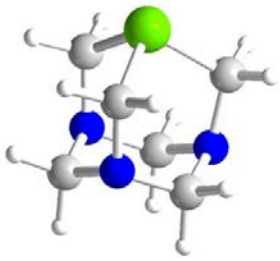

**Figure 1.6.** X-ray crystal structure of PTA (see atom colour code).

The $^1$H NMR of **13** in $D_2O$ shows a signal at 4.42 ppm (AB system, $^1J_{HAHB}$= 12.5 Hz) corresponding to the six protons of NC*H*$_2$N and a doublet at 3.89 ppm ($^1J_{HP}$= 9.0 Hz) corresponding to the three methylene groups bound to phosphorus. The derivatization of both *lower* and *upper rim* causes a decrease of molecular symmetry resulting in highly complex $^1$H NMR spectra. On the contrary, the $^{31}$P{$^1$H} NMR ($D_2O$) shows only the singlet at -98.7 ppm. This is an important tool to determine the coordination properties of PTA and to investigate *in situ* the mechanism of reactions catalyzed by PTA complexes. Infrared is poorly diagnostic for **13** with two adsorption bands at 452 and 405 cm$^{-1}$, but can be useful for the characterization of PTA complexes.

The coordination chemistry of PTA involves either the phosphorus atom which coordinates soft transition metals or nitrogen atoms which coordinate preferentially hard metals,[33] albeit an increasing number of examples of coordination via both P and N atoms is appearing in the literature. The PTA complexes coordinated by phosphorus are more numerous and present different

properties of solubility and several applications. Some examples of PTA complexes coordinated by phosphorus atom are shown in the Figure below (Figure 1.7).

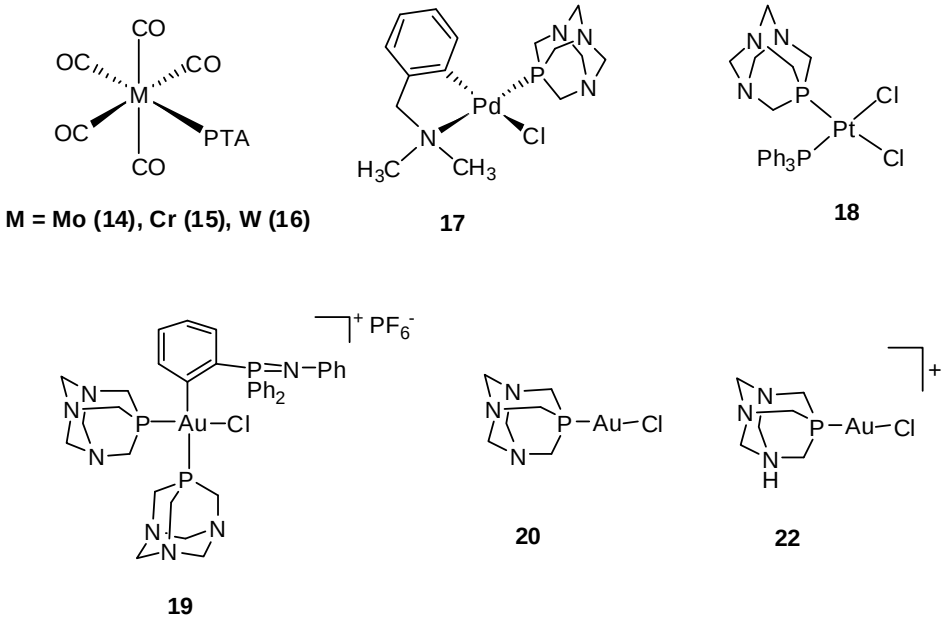


**Figure 1.7.** Some examples of PTA metal complexes.

Historically, the first PTA-metal complex $Mo(CO)_5(PTA)$ (**14**, Figure 1.7) was synthesized through ligand exchange by refluxing PTA with $Mo(CO)_6$ in dry diglyme or alternatively, by reacting PTA with the THF adduct of $Mo(CO)_5$. This procedure, applied also to $Cr(CO)_6$ and $W(CO)_6$, gave the corresponding $Cr(CO)_5(PTA)$ (**15**) and $W(CO)_5(PTA)$ (**16**) complexes.[41] Some late transition metal coordination complexes bearing PTA have also been synthesized. They have found interesting applications in the recent literature. For instance, the reaction of the dimeric complex $[Pd(dmba)(\mu\text{-}Cl]_2$ with 2 equivalents of PTA in $CH_2Cl_2$ yields the monomeric complex [Pd(dmba)Cl(PTA)] (**17**, Figure 1.7) as an air-stable solid, which decomposes above 220 °C under $N_2$.[42] This complex was tested as catalyst in the Sonogashira cross-coupling reaction of either aryl bromides or aryl chlorides with terminal alkynes leading good results when MeCN was used as solvent and $Cs_2CO_3$ as base, in the presence of 1.5 equivalents of tetrabutylammonium chloride.[42] Interesting applications have been found also with platinum compounds as for istance for *cis*-$[PtCl_2(PPh_3)(PTA)]$ (**18**, Figure 1.7), which was synthesized by the reaction of *cis*-

$[PtCl_2(PPh_3)_2]$ with 1 equivalent of PTA. This complex was tested in cell growth inhibition tests, showing that the Pt(PTA)($PPh_3$) group could confer to the complex the ability to dissolve in water-based biological fluids and to across the lipophilic membranes of the cell and then of the nucleus, reaching the nucleic acids, which represent the biological targets.[43]

The Au-PTA complex $[Au\{\kappa^2\text{-}C,N\text{-}C_6H_4(PPh_2{=}N(C_6H_5))\text{-}2\}(PTA)_2Cl]PF_6$ (**19**, Figure 1.7) has been prepared by the reaction of $[Au\{\kappa^2\text{-}C,N\text{-}C_6H_4(PPh_2{=}N(C_6H_5))\text{-}2\}Cl_2]$ with 1 equivalent of $NaPF_6$ and subsequent addition of 1 equivalent of PTA.[44] This complex, which is only soluble in DMSO or in DMSO/$H_2O$ mixtures, has been tested as potential anticancer agent in vitro experiments against HeLa human cervical carcinoma and Jurkat-T acute lymphoblastic leukemia cells. Preferential induction of apoptosis in HeLa cells after treatment with this compound was observed.

Finally, the dicoordinate mono-substituted PTA-gold complex [AuCl(PTA)] (**20** Figure 1.7), has been synthesized by reacting the dimethylsulfide complex $[AuCl(SMe_2)]$ with **13** in chloroform, and its bromide analog [AuBr(PTA)] (**21**) easily obtained by halogen exchange with either HBr in $H_2O$/acetone or KBr in $CH_2C_{l2}$/acetonitrile.[45] These compounds were the first luminescent complex featuring PTA and, together with the protonated derivative [AuCl(PTAH)]Cl (**22**, Figure 1.7) obtained by treating [AuCl(PTA)] with 0.1 M HCl solution, showed strong temperature-dependent emissions in the solid state. In particular, **20** and **22** have a single strong emission at low temperature which dramatically decreases in intensity and blue-shifts (400 $cm^{-1}$ for **20** and 700 $cm^{-1}$for **22**) when measured at room temperature.

Several rhenium complexes (Scheme 1.3) were obtained by stepwise replacement of one or more halides in $[ReBr_3(CO)_3](NEt_4)_2$ by PTA (Scheme 1.3).[46] Complex $[ReBr_3(CO)_3(PTA)_2]$ (**23**) has shown good solubility characteristics for potential applications in biphasic catalysis and the water-solubility of all these Re(I) complexes are also important in the context of developing their $^{188}Re$ analogs which have therapeutic and diagnostic applications in nuclear medicine.

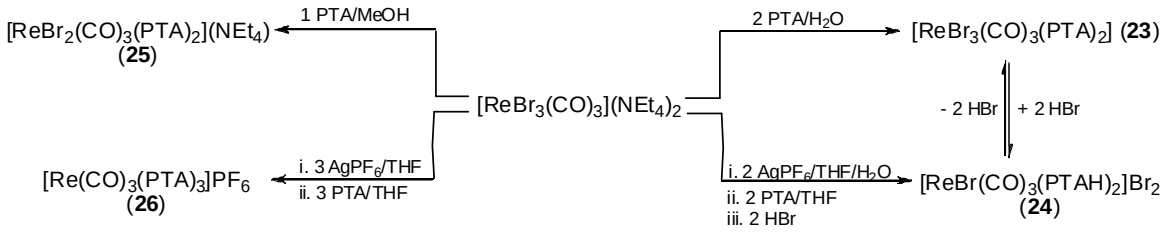


**Scheme 1.3.** Synthesis of some Re-PTA complexes. Adapted from ref. 46.

The number of ruthenium and rhodium complexes with PTA is higher than for other metal-complexes. Indeed they have received much more attention due to their potential use as water-soluble catalysts in hydrogenation and hydroformylation reactions and in the case of ruthenium, rhodium, osmium also for the medicinal properties, the latter being part of a class of compounds spearheaded by the [Ru(arene)(PTA)$Cl_2$] complexes (arene = $\eta^6$-benzene, $\eta^6$-*p*-cymene, $\eta^6$-toluene etc.).[35] Due to their importance in catalysis and being the topic of this thesis work, Ir-, Ru- and Rh-PTA-compounds will be treated in details in Chapters 3, 4 and 5, respectively.

In contrast with what described above, fewer examples of *N*-coordinated PTA complexes are present in literature.[33] Because of the hard nature of manganese(II) and N atoms of PTA, the N-coordinated complexes [$MnX_2$(PTA-$\kappa$N)$_2$($H_2O$)$_2$], X= Cl (**27**) or Br (**28**) (Figure 1.8) have been prepared, for instance, from the straightforward reaction of hydrated $MnX_2$ salts and PTA.[47] The first zinc complex bearing PTA, [$ZnCl_2$(PTA)$_2$] (**29**) was recently obtained by the reaction of $ZnCl_2$ with two equivalents of **13**.[48] The complex is air-stable in the solid state and also in aqueous and methanol solutions. Its structure was authenticated by X-ray diffraction analysis, showing that Zn atom is in a approximately tetrahedral geometry arising from two chloride atoms and two PTA molecules (Figure 1.8). The Zn–Cl distances range from 2.2131(13) to 2.2461(12) Å and the Zn–N distances range from 2.055(3) to 2.101(3) Å.

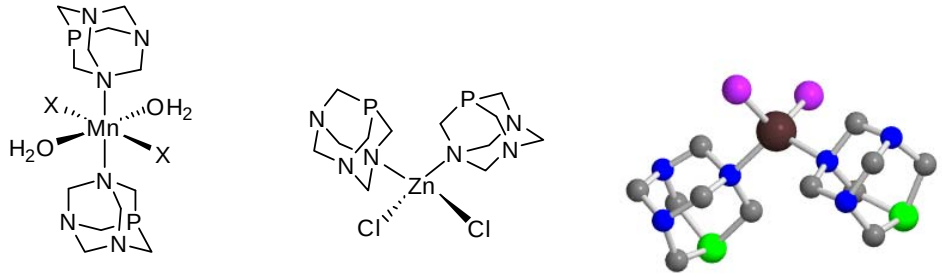


**Figure 1.8.** Two examples of *N*-coordinated PTA complexes and X-ray crystal structure of complex **29** (see atom colour code). Adapted from ref. 48.

## 1.5 Catalytic applications of hydrophilic ligands

Aqueous-phase catalysis and transition metal complexes containing hydrophilic ligands are employed in a large amount of examples to hydroformylation and hydrogenation reactions. In particular, rhodium-PTA complexes were used in olefin hydroformylation reactions, whereas some ruthenium, rhodium and iridium complexes were used for chemoselective hydrogenations and transfer hydrogenations of olefins, aldehydes and ketones.[33] Furthermore, some PTA compounds found use in non-traditional catalytic conversions, such as in the case of the complex [RhCl(PTA)$_3$] (**30**), which was shown to be an active catalyst in the hydrogenation of C=C bonds of unsaturated acyl chains in biomembranes under mild conditions (37 °C, 1 bar $H_2$), giving highest conversion at pH 4.70.[49] Another example of such application was recently reported, showing the use of PTA or [RuCl$_2$(*p*-cymene)(PTA)] (**31**) complex as dendrimer-supported catalysts in allylic alcohol isomerization and in phenylacetylene hydration in water/isopropanol mixtures.[50]

### *1.5.1 Olefin hydroformylation reactions*

The first large-scale industrial process utilizing a water soluble organometallic catalyst is the Rhône-Poulenc process for the hydroformylation of propene.[20a] This continuous aqueous-biphasic process involves the use of a rhodium-based catalytic system stabilized by an excess of the hydrophilic phosphine *m*-TPPTS (**2**) and produces 300.00 tonnes of *n*-butanal per year (Scheme 1.4). Upon completion of the reaction, the Rh-TPPTS complex and the excess of the phosphine can be isolated in water, while the organic layer containing the products aldehydes can be easily recovered by decantation. Additionally, in hydroformylation reactions water works not only just as the solvent but, thanks to the water-gas shift reaction catalyzed by Rh, water can be used also as the hydrogen source.

In addition to *m*-TPPTS, a variety of other mono- and bidentate ligands have been applied to the hydroformylation of propene and some chelating phosphines have shown an improvement in the activity as well as linear selectivity of the Rh catalyst.

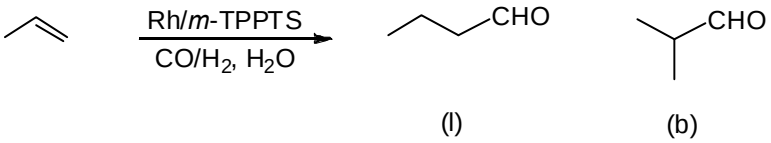


**Scheme 1.4.** Rh-catalyzed hydroformylation of propene.

While the Rhône-Poulenc process works well for propene, the activity is very low when the same system is applied to higher alkenes ($\geq C_6$) due to the very low solubility of these alkenes in water. In the case of 1-hexene, a cobalt complex with TPPTS showed a good activity using very high catalyst loadings and performing the hydroformylation reaction at 100 °C.[51] A possible approach to improve the activity of Rh/TPPTS system for higher olefins is to use a small amount of water-miscible organic co-solvent to increase the solubility of the alkene in the aqueous phase or that of the catalyst in the organic phase. Otherwise it is possible to use surfactants to form micelles which can sequestrate the hydrophobic substrate increasing the water/organic interfacial area. Interestingly, the carboxylate analog of *m*-TPPTS, *m*-

TPPTC (**4**) is a much more active catalyst for hydroformylation of higher olefins in water. In the case of 1-octene, for example, the conversion is only 2% with *m*-TPPTS and 94% with *m*-TPPTC under the same conditions.[52] An alternative strategy to solubilize higher olefins in water is the employment of cyclodextrins (CDs) as inverse phase mass transfer catalysts. Cyclodextrins are able to form inclusion complexes with hydrophobic substrates and carry them into the aqueous phase to react with the water-soluble catalyst. It has been shown that the presence of permethylated β-CD increases the rate of hydroformylation of hydrophobic aldehydes, such as 1-decene,[53] and the randomly methylated β-CD (RAME-β-CD) was found to be a highly effective promoter for hydroformylation of higher olefins catalyzed by Rh/TPPTS complexes. The efficiency of RAME-β-CD is believed to be due to its surface-active behavior and the lower stability of the formed aldehyde inclusion complex.[54] The use of RAME-β-CD in the hydroformylation of 1-decene using a Rh(I) precursor in the presence of the phosphines PTA has been tested and is part of this study (Chapter 5). Generally, rhodium-PTA systems have received great attention due to their potential catalytic activity, but only few examples of complexes found applications in biphasic olefin hydroformylation reactions. Complexes containing the *N*-methylated PTA derivative, [mPTA]I (**32**), i.e. $[RhI_4(mPTA)_2]I$ (**33**), was found to be active for the hydroformylation of 1-hexene under 3.5 MPa total pressure of $CO/H_2$ (1:1) at 60 °C using 0.01 mmol catalyst.[55] The final conversion was of 93% but the regioselectivity was very modest with a linear to branched ratio (l/b) of 1.7. $[RhI(CO)(mPTA)_2]I_2$ (**34**) and $[RhI(CO)(mPTA)_3]I_3 \cdot 4H_2O$ (**35**) were also tested in the hydroformylation of 1-hexene under biphasic conditions.[56] With these systems, the l/b ratio was found to be *ca*. 1 in the presence of **34** with a significant amount of isomerization products and although reaction rates were very high, the activity of both **34** and **35** was about two times lower than the corresponding TPPTS analogs. Furthermore, the use of **35** with an excess of the free ligand [mPTA]I increased the conversion (from 70% to 91%) but did not improve the selectivity and favored hydrocarboxylation and hydrogenation as side reactions. The complex [Rh(acac)(CO)(PTA)] (**36**) (acac= acetylacetonate) also hydroformylated 1-hexene

using $10^{-5}$ mol of catalyst at 60 °C under a $CO/H_2$ total pressure of 3.0 MPa, but the maximum conversion reached was 64.9% with a poor selectivity (2.5 l/b ratio) including a big amount of isomerization products.[57]

### *1.5.2 Hydrogenation reactions*

The selective homogeneous hydrogenation of the carbonyl groups of organic compounds is an important approach for the synthesis of alcohols, especially if the reduction can be done with control of stereochemistry when a prochiral substrate is used. If selective for C=O bond, the hydrogenation can be achieved also in the presence of other functionalities such as C=C double bonds. The hydrogenation protocols used for these reactions, include both hydrogen gas pressure and *transfer hydrogenation* conditions using hydride sources such as formate or isopropanol in presence of a base, thus allowing the use of very mild reaction conditions. Water is an attractive solvent especially for *transfer hydrogenation* processes. Some interesting examples will be shown in the next paragraph.

Ruthenium complexes of *m*-TPPTS provided to be selective catalysts for the reduction of aldehydes and unsaturated aldehydes using formate as reducing agent.[58] Complex $[RuCl_2(PTA)_4]$ (**37**) resulted to selectively hydrogenate benzaldehyde to benzyl alcohol with a 95.1% conversion at 80 °C under biphasic conditions and using sodium formate as hydrogen source. The proposed catalytic mechanism is shown in Scheme 1.5.[59] On the contrary, long chain aldehydes were not hydrogenated by this complex. Under the same conditions the corresponding *m*-TPPTS complex was more active giving a complete conversion after 1.5h, but **37** was more selective. Deuterium-exchange experiments showed that in the presence of **37**, the source of hydrogen is sodium formate instead of water,[59] and *transfer hydrogenation* was the best protocol for this kind of catalyst. In fact, using 14 psi of $H_2$ the conversion of benzaldehyde was only of 2.6% and to enhance the conversion to 45.9%, the $H_2$ pressure had to be increased to 400 psi.

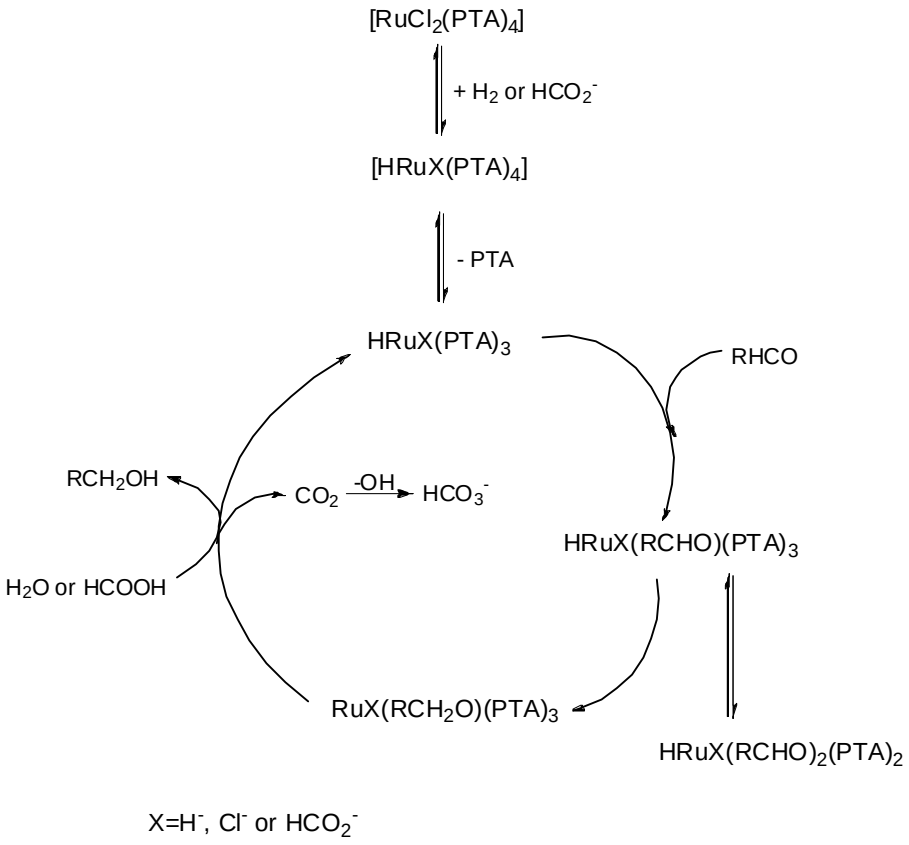


**Scheme 1.5.** Proposed mechanism for the hydrogenation of benzaldehyde to benzyl alcohol catalyzed by **37**.[7]

Some ruthenium(II) and rhodium(III) complexes containing the *N*-alkylated PTA derivative [mPTA]I were found to be active catalysts for the hydrogenation of cinnamaldehyde (CNA, Scheme 1.6). In particular, under biphasic water/toluene or cholorobenzene mixtures and $H_2$ pressure, $[RuI_4(mPTA)]$ (**38**) and *mer*-$[RuI_2(mPTA)_3(H_2O)]I_3$ (**39**) selectively hydrogenated C=O bond giving cinnamyl alcohol, while $[RhI_4(mPTA)_2]I$ (**33**) gave selective reduction of C=C double bond, producing the corresponding saturated aldehyde, hydrocinnamaldehyde.[55]

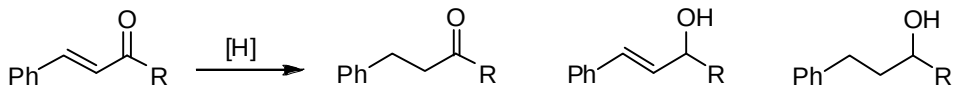


R= H, CNA
R= $CH_3$, BZA

**Scheme 1.6.** Products of the hydrogenation of cinnamaldehyde and benzylidene acetone.

Ruthenium complexes are also effective for the reduction of C=O bond of ketones. The complex [RuCl(*p*-cymene)L(PTA)]Cl (L= 1-butyl-3-methylimidazol-2-ylidene) (**40**, Figure 1. 9) gave good activity for the hydrogenation of acetone and acetophenone (98.2% and 46.1%, respectively) under $H_2$ pressure in pH 6.9 buffer.[60]

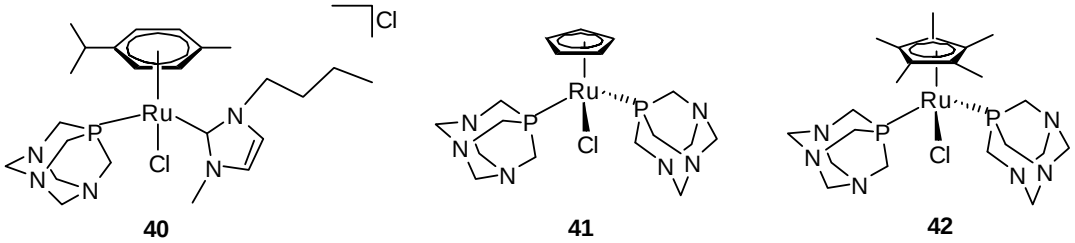


**40** **41** **42**

**Figure 1.9.** Ru-PTA complexes **40**, **41**, **42**.

Complexes [CpRuCl(PTA)$_2$] (**41**) and [Cp*RuCl(PTA)$_2$] (**42**) (Figure 1.9) were active catalysts for the chemoselective hydrogenation of C=C bond of benzylidene acetone (BZA, Scheme 1.4), giving under moderate $H_2$ pressure (450 psi) in a biphasic system water/octane mixture at 130 °C, conversions ranging from 39.1% (after 3h) to 99.7% (after 21h).[61] By using transfer hydrogenation conditions with the system $HCO_2Na$ in methanol/water (1:1 ratio) solvent mixture, the C=C bond hydrogenation of BZA resulted in a 36% conversion with catalyst **41** and 97% with catalyst **42** after 6h at 90 °C.[34a]

Also Rh(I)-PTA complexes were tested in the C=C double bond hydrogenation of allyl alcohols and alkenes. Complex [Rh(acac)(CO)(PTA)] (**36**) was tested under biphasic conditions water/substrate and $H_2$ pressure giving high selectivity (90%) for hydrogenation of allyl alcohol into *n*-propanol, while the hydrogenation of 1-hexene caused also isomerization side reactions as evidenced by the formation of

substantial amounts of 2-hexene and 3-hexene. [57] Under biphasic conditions, using sodium formate as the hydrogen source, the complex [RhCl(PTAH)(PTA)$_2$]Cl (**43**) containing PTA and its mono *N*-hydrogenated derivative [PTAH], catalyzed the conversion of *trans*-cinnamaldehyde with high selectivity for C=C double bond (93.3%).[62] On the contrary, this complex resulted to be poorly selective as transfer hydrogenation catalyst for allylbenzene giving an extensive isomerization to *cis*- and *trans*-propenylbenzene, which was decreased by replacing sodium formate with $H_2$ pressure.

In comparison with ruthenium and rhodium compounds, fewer iridium complexes have been used as catalysts in hydrogenation reactions, although in recent years there has been a growing interest due to the minor cost of this metal and its major selectivity in many catalytic systems.[63] Recently, the iridium complexes **a** reported in the Figure below (Figure 1.10) resulted to be highly enantioselective for C=C bond hydrogenation of $\alpha,\beta$ unsaturated ketones (>99%),[64] while the two Ir-complexes containing planar chiral ferrocenyl P,S ligands (**b** and **c**, Figure 1.10), have shown to be highly efficient in asymmetric hydrogenation of several alkyl aryl ketones (TOF up to *ca*.250 h$^{-1}$, conversions >99% and *ee* up to 99%).[65]

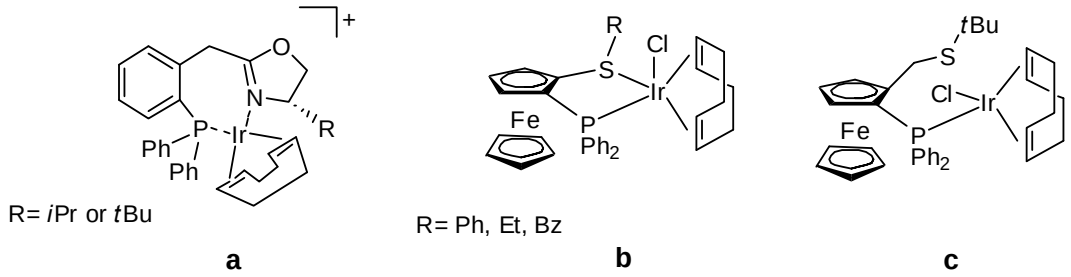


**Figure 1.10.** Examples of Ir complexes active in hydrogenations.[64,65]

Moreover, complexes of formula [IrCl(cod)(L)] (L= phosphine) were found to be active catalysts in the hydrogenation of $\alpha,\beta$-unsaturated aldehydes or ketones.[66] Until now, the unique Ir-PTA complexes reported in the literature which have been used in catalytic hydrogenation are the water-soluble iridium(III) complexes [Cp*IrCl$_2$(PTA)] (**44**) and [Cp*IrCl(PTA)$_2$]Cl (**45**) (Cp*= $\eta^5$-C$_5$Me$_5$).[67] These complexes were tested as catalyst precursors for the reduction of hydrogen carbonate to

formate in aqueous solution showing the highest activity at high temperature (80 °C) and in slightly basic conditions (pH 9).

## 1.6 Aim of the work

Based on all the advantages described above from the use of aqueous homogeneous or aqueous-biphasic catalytic systems incorporating a water-soluble catalyst, this PhD thesis work has been focused on the preparation of water-soluble catalysts containing new derivatives of the neutral water-soluble phosphine PTA (**13**, Figure 1.5). As it has been already highlighted the interest on this phosphine is due not only to its water-solubility , but also to its capability to form transition metal complexes stable in water, together with relatively easy access to various functionalizations which can be of use in several fields of application.

The first step of this work has been the design and synthesis of new ligands derived from the functionalization of PTA. Two different sites of functionalization can be considered on this molecule as it is shown in Figure 1.11. Our main interest was focused on the "upper rim" as this derivatization has been investigated only briefly so far although it results to be very interesting because of the proximity of the modifications to the phosphorus donor atom.

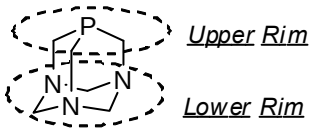


**PTA**

**Figure 1.11.** *Upper* and *lower rim* of PTA phosphine.

The introduction of new functional groups on this side of the molecule can allow to vary the electronic and steric properties of the ligand, to modulate its solubility and to insert in neighbouring position to phosphorus, some donor atoms, such as N, O, S, to form more stable P,X chelating ligands. Furthermore, one or more stereocentres on carbon atoms can be created which would make the new ligands useful for the study of catalytic enantioselective processes in water.

The synthetic procedure to achieve *upper rim* functionalized ligands was reported for the first time by Wong *et al.*,[68] obtaining in only 10% yield the new bidentate chiral phosphine PTA-$PPh_2$ (**46**) not soluble in water (Scheme 1.7). The same method, which provided the initial formation of the lithium salt derivative (PTA-Li, **47**), was extended also to other electrophiles such as $CO_2$, ferrocene carboxaldehyde and benzophenone.[69]

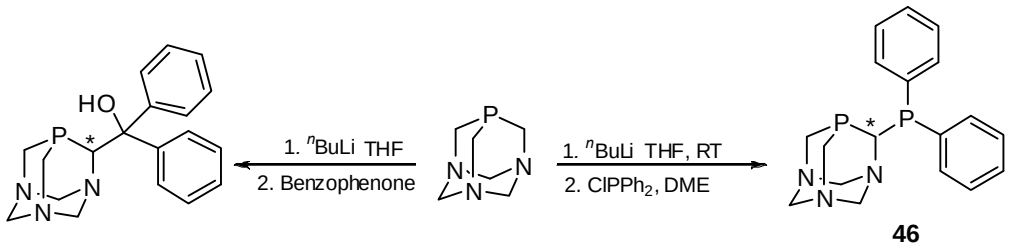


**Scheme 1.7.** Synthesis of some *upper rim* derivatives.[68,69]

These procedures gave not however very good yields and the derivatives obtained were either not stable or not very soluble in water. Therefore our efforts have been initially concentrated on the improvement of this synthetic pathway and on its generalization to different electrophiles (aldehydes and ketons) in order to prepare new ligands.

The water solubility, physical properties and chemical stability of the new ligands, together with the coordination properties towards Ir(I) and Ru(II) precursors have been investigated. The studies related to ligand synthesis will be discussed in Chapter 2, whereas the synthesis and application in catalysis of the new complexes of Ir and Ru (Fig 1.12) will be described in Chapters 3 and 4, respectively.

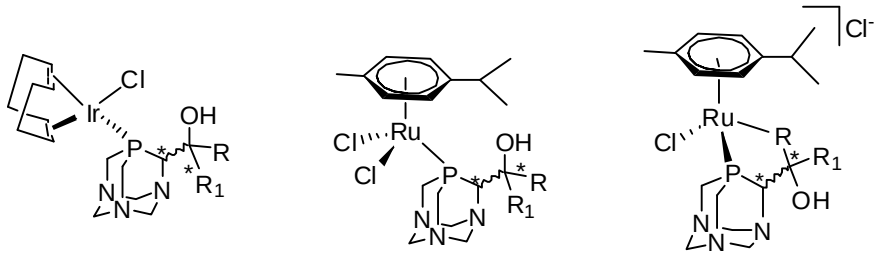


**Figure 1.12.** Ir(I) and Ru(II) complexes bearing upper rim functionalized PTA derivatives.

As we have shown above, synthetic elaboration of PTA can also be achieved by modification of the triazacyclohexane ring (*lower rim*) through an alkylation reaction involving the nitrogen atoms (Figure 1.13).

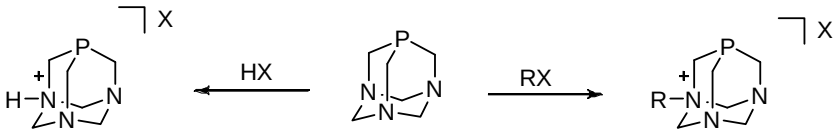


**Figure 1.13.** *Lower rim* derivatization of PTA.

In this part of the work we have been interested in the synthesis of different *N*-benzyl PTA-derivatives aiming at testing their affinity toward cyclodextrins (CDs), in particular the randomly methylated β-cyclodextrin (RAME-β CD). The use of the cyclodextrins as system to improve the mass transfer between the substrate present in the organic phase and the water-soluble catalyst dissolved on the aqueous phase, is well known[15] and our new derivatives have been designed for the application in rhodium-catalyzed hydroformylation reactions of higher olefins. Details of these catalytic studies will be discussed in Chapter 5.

## 1.7 References


[1] Anastas, P. T.; Kirchhoff, M. M. *Acc*. *Chem*. *Res*. **2002**, *35*, 686-694.

[2] Anastas, P. T.; Warner, J. C. *Green Chemistry*: *Theory and Practice*. Oxford University Press, New York, **1998**.

[3] Cornils, B.; Wiebus, E. *Environmental and Safety Aspects*. *In Multiphase Homogeneous Catalysis*. Cornlis, B. Ed. Wiley-VCH Verlag: Weinheim, **2005**.

[4] (a) Breslow, R.; Maitra, U. *Tetrahedron Lett*. **1984**, *25*, 1239-1240. (b) Gajewski, J. J. *Acc*. *Chem*. *Res*. **1997**, *30*, 219-225.

[5] Narayan, S.; Muldoon, J.; Finn, M. G.; Fokin, V. V.; Kolb, H. C.; Sharpless, K. B. *Angew*. *Chem*. *Int*. *Ed*. **2005**, *44*, 3275-3279.

[6] Li, C-J.; Chen, L. *Chem*. *Soc*. *Rev*. **2006**, *35*, 68-82.

[7] Horváth, I. T.; Joó, F. *Aqueous Organometallic Chemistry and Catalysis* Eds. NATO ASI 3/5, Kluwer, Dodrecht, **1995**.

[8] Cornils B. *J*. *Mol*. *Cat*. *A*: *Chem*. **1999**, *143*, 1-10.

[9] Li, J-C. *Acc*. *Chem*. *Res*. **2002**, *35*, 533-538.

[10] Li, C.; Wang, D.; Chen , D. L. *J*. *Am*. *Chem*. *Soc*. **1995**, *117*, 12867-12868.

[11] Deutschmann, O.; Knözinger, H.; Kochloefl, K.; Turek, T. *Heterogeneous Catalysis and Solid Catalysts*. Ed. Wiley-VCH, **2009**.

[12] (a) Herrmann, W. A.; Kohlpaintner, C. W. *Angew*. *Chem*. *Int*. *Ed*. *Engl*. **1993**, *32*, 1524-1544. (b) Joó, F. *Acc*. *Chem*. *Res*. **2002**, *35*, 738-745.

[13] Arhancet, J. P.; Davis, M E.; Merola, J. S.; Hanson, B. E. *Nature* **1989**, *339*, 454-455.

[14] Anderson, M. W.; Shi, J.; Leigh, D. A.; Moody, A. E.; Wade, F. A.; Hamilton, B.; Carr, S. W. *J*. *Chem*. *Soc*. *Chem*. *Commun*. **1993**, 533-536.

[15] Hapiot, F.; Tilloy, S.; Monflier, E. *Chem*. *Rev*. **2006**, *106*, 767-781.

[16] (a) Joó, F.; Tóth, Z. *J*. *Mol*. *Cat*. **1980**, *8*, 369-383. (b) Klack, P.; Monteil, F. *Adv*. *Organometal*. *Chem*. **1992**, *34*, 219-284. (c) Shaughnessy, K. H. *Chem*. *Rev*. **2009**, *109*, 643-710.

[17] Cornils, B.; Hermann, W. A. (Eds) *Aqueous-Phase Organometallic Catalysis*, 2nd ed. Wiley-VCH, Weinheim, **2004**.

[18] Ahrland, S.; Chatt, J.; Davies, N. R.; Williams, A. A. *J. Chem. Soc.* **1958**, 276-288.

[19] Borowski, A. F.; Cole-Hamilton, D. J.; Wilkinson, G. *Nouv*. *J*. *Chem*. **1978**, *2*, 137-144.

[20] (a) Kuntz, E. G. *CHEMTECH* **1987**, *17*, 570-575. (b) Cornlis, B.; Kuntz, E. G. *J*. *Organomet*. *Chem*. **1995**, *502*, 177-186.

[21] Herrmann, W. A.; Kulpe, J. A.; Konkol, W.; Bahrmann, H. *J*. *Organomet*. *Chem*. **1990**, *389*, 85-101.

[22] Peng, Q.; Yang, Y.; Wang, C.; Liao, X.; Yuan, Y. *Catal*. *Lett*. **2003**, *88*, 219-225.

[23] Amengual, R.; Genin, E.; Michelet, V.; Savignac, M.; Genêt, J.-P. *Adv*. *Synth*. *Catal*. **2002**, *344*, 393-398.

[24] Hingst, M.; Tepper, M.; Stelzer, O. *Eur*. *J*. *Inorg*. *Chem*. **1998**, 73-82.

[25] Papp, G.; Kovács, J.; Bényei, A. C.; Laurenczy, G.; Nádasdi, L.; Joó, F. *Can*. *J*. *Chem*. **2001**, *79*, 635-641.

[26] Baskakov, D.; Hermann, W. A. *J*. *Mol*. *Catal*. *A*.: *Chem*. **2008**, *283*, 166-170.

[27] Schull, T. L. ; Brandow, S.L:; Dressik, W. J. *Tetrahedron Lett*. **2001**, *42*, 5373-5376.

[28] Machnitzki, P.; Nickel., T.; Stelzer, O.; Landgrafe, C. *Eur*. *J*. *Inorg*. *Chem*. **1998**, 1029-1034.

[29] Heβler, A.; Kuchen, S.; Stelzer, O.; Blotevogel-Baltronat, J.; Sheldrick, W. S.; *J*. *Organomet*. *Chem*. **1995**, *501*, 293-302.

[30] Dibowski, H.; Schmidtchen, F. P. *Tetrahedron* **1995**, *51*, 2325-2330.

[31] Hessler, A.; Stelzer, O.; Dibowski, H.; Worm, K.; Schmidtchen, F. P.; *J*. *Org*. *Chem*. **1997**, *62*, 2362-2369.

[32] Holz, J.; Heller, D. Stürmer, R.; Börner, A. *Tetrahedron Lett*. **1999**, *40*, 7059-7062.

[33] (a) Phillips, A. D.; Gonsalvi, L.; Romerosa, A.; Vizza, F.; Peruzzini, M. *Coord*. *Chem*. *Rev*. **2004**, *248*, 955-993. (b) Bravo, J.; Bolaño, S.; Gonsalvi, L.; Peruzzini, M. *Coord*. *Chem*. *Rev*. **2010**, *254*, 555-607.

[34] (a) Bolaño, S.; Gonsalvi, L.; Zanobini, F.; Vizza, F.; Bertolasi, V.; Romerosa, A.; Peruzzini, M.; *J*. *Mol*. *Cat*. *A* **2004**, *224*, 61-70. (b) Horváth, H.; Laurenczy, G. ; Katho, A. *J*. *Organomet*. *Chem*. **2004**, *689*, 1036-1045. (c) Korthals, B.; Göttker-Scnetmann, I.; Mecking, S. *Organometallics* **2007**, *26*, 1311-1316.

[35] (a) Ang, W. H.; Daldini, E.; Scolaro, C.; Scopelliti, R.; Juillerat-Jennerat, L.; Dyson, P. *J. Inorg. Chem.* **2006**, *45*, 9006-9013. (b) Scolaro, C.; Bergamo, A.; Brescacin, L.; Delfino, R.; Cocchietto, M.; Laurenczy, G.; Geldbach, T. J.; Sava, G.; Dyson, P. J. *J. Med. Chem.* **2005**, *48*, 4161-4171. (c) Casini, A.; Edafe, F.; Erlandsson, M.; Gonsalvi, L.; Marrone, A.; Ciancetta, A.; Re, N.; Ienco, A.; Messori, L.; Peruzzini, M.; Dyson, P. J. *Dalton Trans.* **2010**, *39*, 5556-5563.

[36] Gutkin, V.; Gun, J.; Prikhodchenko, P. V.; Lev, O.; Romerosa, A.; Campos Malpartida, T.; Lidrissi, C.; Gonsalvi, L.; Peruzzini, M. *J. Electrochem. Soc.* **2007**, *154*, F7-F15.

[37] Daigle, D. J.; Pepperman Jr., A. B.; Vail, S. L. *J. Hetrocycl Chem.* **1974**, *11*, 407-408.

[38] (a) Daigle, D. J. *Inorg. Synth.* **1998**, *32*, 40-42. (b) Caporali, M.; Gonsalvi, L.; Peruzzini, M.; Zanobini, F. *e-EROS Encyclopedia of Reagents for Organic Synthesis*, John Wiley & Sons, Ltd. **2010** and unpublished results.

[39] Darensbourg, D. J.; Robertson, J. B.; Larkins, D. L.; Reibenspies, J. H. *Inorg. Chem.* **1999**, *38*, 2473-2481.

[40] Fluck, E.; Förster, J. E.; Weidlein, J.; Hädicke, E. *Z. Naturforsch.* **1997**, *32b*, 499-506.

[41] Darensbourg, M. Y.; Daigle, D. *Inorg. Chem.* **1975**, *5*, 1217-1218.

[42] Ruiz, J.; Cutillas, N.; López, F.; López, G.; Bautista, D. *Organometallics* **2006**, *25*, 5768-5773.

[43] Brgamini, P.; Bertolasi, V.; Marvelli, L.; Canella, A.; Gavioli, R.; Mantovani, N.; Mañas, S.; Romerosa, A. *Inorg. Chem.* **2007**, *46*, 4267-4276.

[44] Shaik, N.; Martínez, I.; Augustin, H.; Giovinazzo, A.; Varela-Ramírez, A.; Sanaú, M.; Aguilera, R. J.; Contel, M. *Inorg. Chem.* **2009**, *48*, 1577-1587.

[45] Assefa, Z.; McBurnett, B. G.; Staples, R. J.; Fackler, J. P.; Assmann, B.; Angermaier, K.; Schmidbaur, H. *Inorg. Chem.* **1995**, *34*, 75-83.

[46] Schibli, R.; Katti, K. V.; Volkert, W. A.; Barnes, C. L. *Inorg. Chem.* **1998**, *37*, 5306-5312.

[47] Frost, B. J.; Bautista, C.M.; Huang, R.; Shearer, J. *Inorg. Chem.* **2006**, *45*, 3481-3483.

[48] Smoleński, P.; Benisvy, L.; Guedes da Silva, M. F. C.; Pombeiro, A. J. L. *Eur. J. Inorg. Chem.* **2009**, 1181-1186.

[49] Nádasdi, L.; Joó, F. *Inorg. Chim. Acta* **1999**, *293*, 218-222.

[50] Servin, P.; Laurent, R.; Gonsalvi, L.; Tristany, M.; Peruzzini, M.; Majoral, J-P.; Caminade, A-M. *Dalton Trans.* **2009**, 4432-4434.

[51] Parmar, D. U.; Bajaj, H. C.; Jasra, R. V.; Moros, B. M.; Likholobov, V. A. *J. Mol. Catal. A: Chem.* **2004**, *211*, 83-87.

[52] Li, M.; Fu, H.; Yang, M.; Zheng, H.; He, Y.; Chen, H.; Li, X. *J. Mol. Catal. A: Chem.* **2005**, *235*, 130-136.

[53] Monflier, E.; Tilloy, S.; Fremy, G.; Cstanet, Y.; Mortreux, A. *Tetrahedron Lett.* **1995**, *36*, 9481-9484.

[54] Leclercq, L.; Sauthier, M.; Castanet, Y.; Mortreaux, A.; Bricout, H.; Monflier, E. *Adv. Synth. Catal.* **2005**, *347*, 55-59.

[55] Smolenski, P.; Pruchnik, F. P.; Ciunik, Z.; Lis, T. Inorg. Chem. **2003**, *42*, 3318-3322.

[56] Pruchnik, F. P.; Smolenski, P.; Galdecka, E.; Galdecki, Z. *New J. Chem.* **1998**, *22*, 1395-1398.

[57] Pruchnik, F. P.; Smolenski, P.; Wajida-Hermanowicz, K. *J. Organomet. Chem.* **1998**, *570*, 63-69.

[58] Béneyei, A.; Joó, F. *J. Mol. Catal.* **1990**, *58*, 151-163.

[59] Darensbourg, D. J.; Joó, F.; Kannisto, M.; Kathó, A.; Reibenspies, J. H. *Organometallics*, **1992**, *11*, 1990-1993.

[60] Csabai, P.; Joó, F. *Organometallics*, **2004**, *23*, 5640-5643.

[61] Akbayeva, D. N.; Gonsalvi, L.; Oberhauser, W.; Peruzzini, M.; Vizza, F.; Brügeller, P.; Romerosa, A.; sava, G.; Bergamo, A. *Chem. Comm.* **2003**, 264-265.

[62] Darensbourg, D. J.; Stafford, N. W.; Joó, F.; Reibenspies, J. H. *J. Organomet. Chem.* **1995**, *488*, 99-108.

[63] Malacea, R.; Poli, R.; Manoury, E. *Coord. Chem. Rev.* **2010**, *254*, 729-752.

[64] Lu, W-J-; Chen, Y-W.; Hou, X-L. *Angew. Chem. Int. Ed.* **2008**, *47*, 1-5.

[65] Le Roux, E.; Malacea, R.; Manoury, E.; Poli, R.; Gonsalvi, l.; Peruzzini, M. *Adv. Synth. Catal.* **2007**, *349*, 309-313.

[66] (a) Spogliarich, R.; Tencich, A.; Kaspar, J.; Graziani, M. *J. Organomet. Chem.* **1982**, *240*, 453-459. (b) Visintin, M.; Spogliarich, R.; Kaspar, J.; Graziani, M. *J. Mol. Cat.* **1985**, *32*, 349-351.

[67] Erlandsson, M.; Landaeta, V. R.; Gonsalvi, L.; Peruzzini, M.; Phillips, A. D.; Dyson, P. J.; Laurenczy, G. *Eur*. *J*. *Inorg*. *Chem*. **2008**, 620-627.
[68] Wong, G. W.; Harkreader, J. L.; Mebi C. A.; Frost, B. J. *Inorg*. *Chem*. **2006**, *45*, 6748-6755.
[69] Wong, G. W.; Lee, W-C.; Frost, B. J. *Inorg*. *Chem*. **2008**, *47*, 612-620.

# *Chapter 2*

# Synthesis of PTA and its functionalized derivatives

## 2.1 Overview

In this chapter, the syntheses of the water-soluble phosphine PTA and its derivatives are described. The chapter begins with the description of some PTA analogs either protected at the phosphorus atom or obtained by selective opening of the adamantane cage. Then, modifications to the triazacyclohexane ring (*lower rim*), involving in particular alkylation of the nitrogen atoms are presented. The chapter continues with the description of our initial results on *upper rim* functionalization reactions and the synthesis of our new water-soluble chiral ligands obtained by introduction of a binding arm on a methylene group close to the P atom. In the last part, all synthetic procedures and characterizations of these new products are reported.

## 2.2 Introduction

The water-soluble aminophosphine PTA (**13**) was synthesized for the first time by Daigle et *al*.[1] and modified later by Fluck and Forster.[2] These early synthetic procedures reported the use of ammonia hexamethylenetetramine (urotropine) or ammonium acetate as nitrogen source and *tris*-(hydroxymethyl)phosphine (THP) as phosphorus reagent. The reactions were carried out on air and the final yield was not above 40%. Later on, Daigle elaborated an optimized synthesis by a one-pot approach, generating THP *in situ* reacting the commercially available *tetrakis*-(hydroxymethyl)phosphonium chloride (THPC) with an excess of sodium hydroxide and using urotropine as nitrogen source (Scheme 2.1).[3] PTA was obtained in 65% yield and a purity of higher than 97%. In this last procedure, the main by-product was found to be the oxide PTA(O) (**48**), probably formed by carrying out the reaction in the air. Further improvements in yields (up to 70%) and purity (> 90%) were achieved treating THPC with an equimolar amount of sodium hydroxide, and adding formaldehyde and hexamethylenetetramine under an atmosphere of nitrogen.[4]

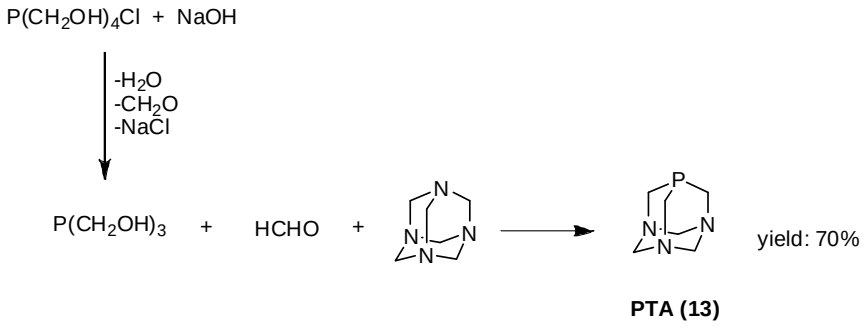


**Scheme 2.1.** Synthesis of PTA.[3]

Oxidation of PTA to PTA(O) (**48**) could be accomplished using mild to strong oxidants such as hydrogen peroxide,[5] nitric acid,[6] or nitrogen tetraoxide under reflux conditions.[7] Protection on the phosphorus atom, could be also obtained refluxing PTA with elemental sulfur[8] or selenium[9] resulting in PTA(S) (**49**) and PTA(Se) (**50**), respectively (Scheme 2.2).

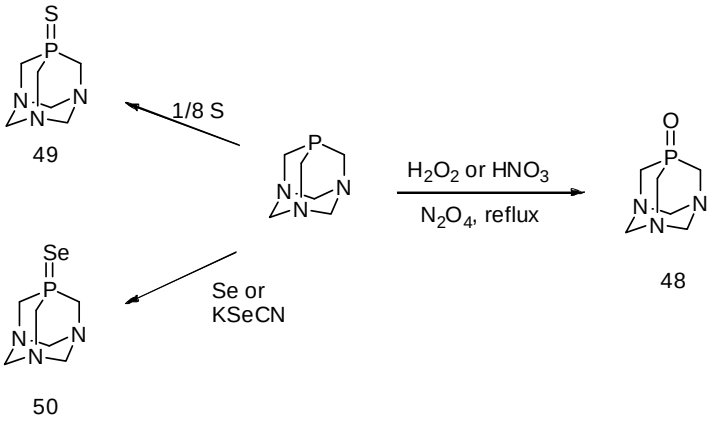


**Scheme 2.2**. Synthesis of PTA(X) derivatives.

PTA(Se) could be also synthesized by reacting directly PTA with KSeCN in methanol and its crystals, obtained upon slow evaporation of the solvent and analysed by X-ray diffraction, showed that PTA retains its highly symmetrical rigid cage-like character with close to ideal tetrahedral angles around all atom (Figure 2.1).[10] Both compounds **49** and **50** are thermally stable (T dec. > 260 °C) and show reduced general solubility properties compared to PTA.

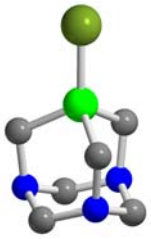

**Figure 2.1.** X-ray crystal structure of PTA(Se) (see atom colour code). Selected bond lengths (Å): P-Se=2.0991(19); P-C1=1.823(4). Adapted from ref. 10.

PTA also reacts with ethyl or phenyl azide to give P=NR protection at phosphorus, yielding the corresponding iminophosphoranes. By reacting **13** with 1,2-diols and orthoquinones such as 3,5-di-*tert*-butyl-*o*-benzoquinone and phenanthroquinone, PTA-based spirophosphoranes were obtained by nucleophilic attack of the PTA phosphorus atom on the oxygen atoms of the diketone (Scheme 2.3).[11]

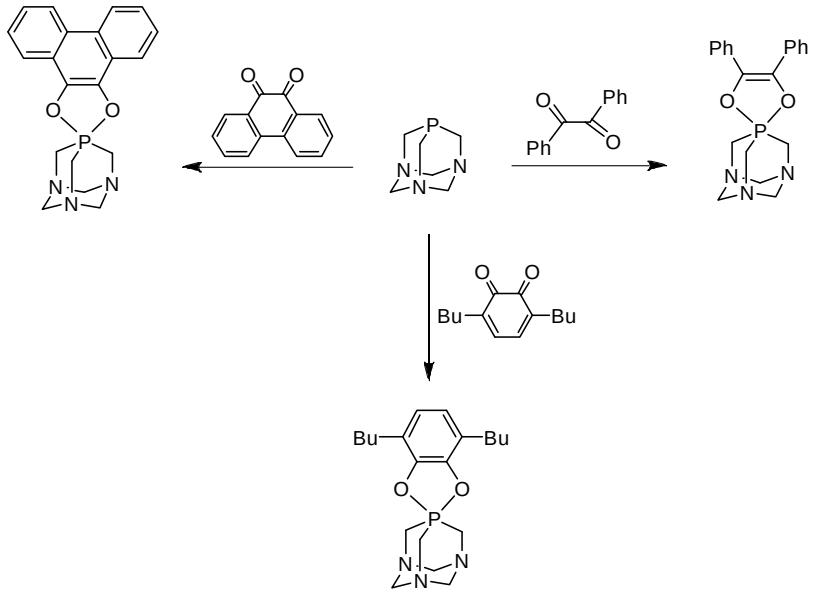

**Scheme 2.3.** Some examples of P protected PTA derivatives.[11]

## 2.3 Triazacyclohexane (*lower rim*) functionalization reactions.

Most of the modifications involving PTA have concerned so far the triazacyclohexane ring known as *lower rim* and in particular the nitrogen atoms (Figure 2.2).

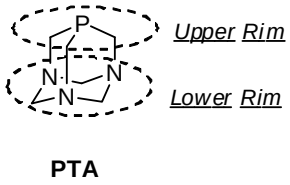


**Figure 2.2.** *Upper* and *lower rim* of PTA.

First of all, due to the basicity of **13** (p$K_a$= 5.70), in water solution at pH lower than 6.5, PTA can be *N*-protonated giving the corresponding ammonium-phosphine [PTAH]X (Scheme 2.4). Further N-protonation is disfavoured as demonstrated by a combined study involving experimental data and *ab initio* calculations which shows that the increase in cage strain of PTA determines the decrease of its stability due to a change in hybridization of the nitrogen centres.[12]

PTA can also be alkylated at one nitrogen atom using several electrophiles such as MeI,[13] EtI,[14] $PhCH_2Cl$,[15] or $I(CH_2)_4I$[16] and performing the reactions either in acetone or in methanol under reflux conditions (Scheme 2.4).

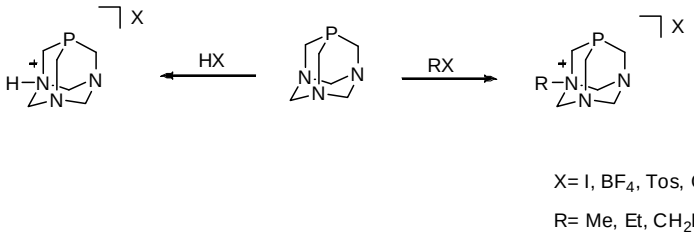


**Scheme 2.4**. *N*-protonation and *N*-alkylation reactions.

The *N*-methylated species [mPTA]I (**32**)[13] was recrystallized from a mixture of methanol and ethyl acetate and as the other R-PTA (R= alkyl, benzyl) derivatives, showed elevated stability in air and high solubility in water and DMSO, but low solubility in organic solvents. Both *N*-protonated and *N*-alkylated PTA salts have shown to be poorer nucleophiles than PTA and this can be used as strategy for functional group protection of the nitrogen centres. Reactivity of *N*-alkylated derivatives differs from that of PTA. For example, oxidation of [mPTA]I (**32**) with $H_2O_2$ does not proceed and it is necessary to synthesize PTA(O) (**48**) before the alkylation. On the contrary, [mPTA(S)]I (**51**) is readily obtained by refluxing **32** with elemental sulfur in benzene,[7] but it can be also synthesized by treating the phosphine sulfide **49** with methyl iodide.[7] Both ligands PTA(S) and [mPTA(S)]I are reported to have limited solubility in water and chloroform.

Terafluoroborate ($BF_4$), tosylate (Tos= *p*-toluensolfonate), and triflate (OTf= $OSO_2CF_3$) salts of $[mPTA]^+$ can be obtained by anion exchange of an aqueous solution of [mPTA]I[17] or by reaction of MeOTf with PTA in $CHCl_3$ solution (Scheme 2.5).[18] $[mPTA]BF_4$ (**52**)[19] together with the oxide $[mPTA{=}O]I_3$ (**53**)[20] have been crystallographically investigated, showing that most of the bonding parameters are comparable with those reported for related compounds bearing the PTA core.

In contrast to the behaviour of PTA, which is easily converted to PTA(Se)(**50**)[10] by using $SeCN^-$, its methylated analogue **32** reacts significantly more slowly with KSeCN

under similar conditions and [mPTA=Se]I (**54**) was obtained by the reaction of Se powder with [mPTA]I in a refluxing methanol/toluene (1:1) mixture.[10]

Bis-methylation on the *lower rim* of PTA can be accomplished by reacting **13** with two equivalents of MeOTf in refluxing acetone,[21] obtaining the dicationic derivative *N*,*N*'-dimethyl-1,3,5-triaza-7-phosphadamantane [dmPTA] as triflate salt [dmPTA](OTF)$_2$ (**55**) (Scheme 2.5). **55** has cone angle and electronic properties similar to PTA and shows a good water solubility ($S_{25°C}$= 12 mg/mL). Reaction of **55** with two equivalents of $NaBF_4$ in acetone led to the synthesis of [dmPTA]($BF_4$)$_2$ (**56**) as a white precipitate with the same spectroscopic features of [dmPTA](OTF)$_2$ except those belonging to the anion (Scheme 2.5). Easy substitution of the counterion confirmed that there are not important interactions between the dication $[dmPTA]^{2+}$ and the anion $(OTF^-)_2$ in solution.[21] **56** can also be obtained by reacting [dmPTA](OTF)$_2$ with $HBF_4 \cdot Et_2O$ in $D_2O$. However, if [dmPTA](OTF)$_2$ is reacted with KOH, a new open-cage ligand 3,7-dimethyl-1,3,7-triaza-5-phosphabicyclo[3.3.1]nonane, [dmoPTA] (**57**) is achieved by elimination of one $CH_2$ group of the *lower rim* of the PTA-cage (Scheme 2.5). Additionally, if [dmoPTA] is treated with 1 equivalent of $HBF_4 \cdot Et_2O$ in water, a new compound tentatively formulated as 3,7-H-3,7-dimethyl-1,3,7-triaza-5-phosphabicyclo[3.3.1]nonane tetrafluoroborate [HdmoPTA]$BF_4$ (**58**) is obtained and the $H^+$ is supposed to bridge both *N*-methylated atoms (Scheme 2.5).[21]

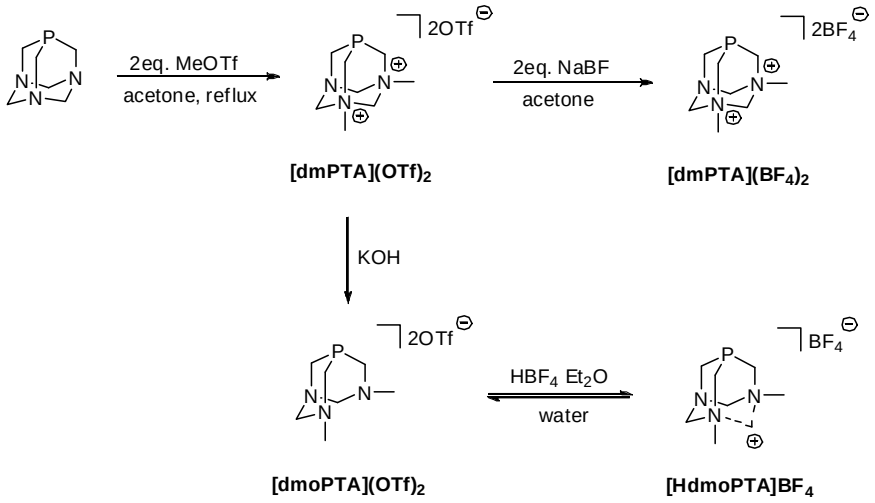


**Scheme 2.5.** Synthesis and reactivity of some *N*-alkylated PTA-derivatives.[21]

*N*-alkyl-PTA halides [R-PTA]X (R= $^{n}$Bu, $^{n}$Pr, Et; X= $I^-$, $Br^-$) undergo an unprecedent α-C-C bond cleavage within the pendant alkyl arm of [R-PTA]X, generating [mPTA]X and the corresponding aldehyde (Scheme 2.6). The reaction can be run in water at ambient temperature but it is accelerated by heating, having a quantitative conversion after 5h reflux.[22] On the contrary, prolonged reaction times (20h reflux) promote the C–N bond cleavage as a side reaction, resulting in the complete elimination of the *N*-alkyl arm.

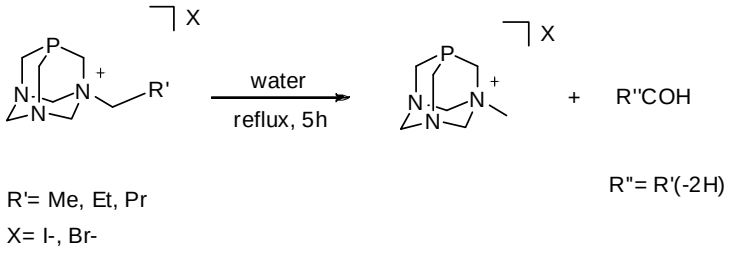


**Scheme 2.6.** N-alkyl-PTA halides.[22]

The *N*-methylpyridyl derivative of PTA [pymePTA]Br (**59**)[23] was prepared by deprotonating 2-bromomethylpyridine hydrobromide and refluxing the resulting amine with an acetone solution of **13**. After 30 min reflux, **59** precipitated as a white air-stable solid in good yield (Scheme 2.7). This derivative was found to be soluble in

halogenated hydrocarbons, in alcohols and more soluble in water ($S_{25°C}$= 2.4 M) than PTA ($S_{25°C}$= 1.5 M). Some examples of bis-phosphine derivatives linking two PTA molecules *via* the N atoms have been prepared by reaction of **13** with differently substituted dibenzyl bromides (Scheme 2.7).[24] Depending on the position of the substituents on the aromatic ring, the *ortho*, *para* and *meta* substituted compounds presented a remarkable difference in water solubility. The *ortho* derivative was found to be the most water-soluble ($S_{25°C}$= 2000 mg/mL). The *meta* phosphine also showed high water-solubility ($S_{25°C}$= 810 mg/mL), while the solubility of the *para* analogue was determined to be very low compared to the others ($S_{25°C}$= 12.5 mg/mL).

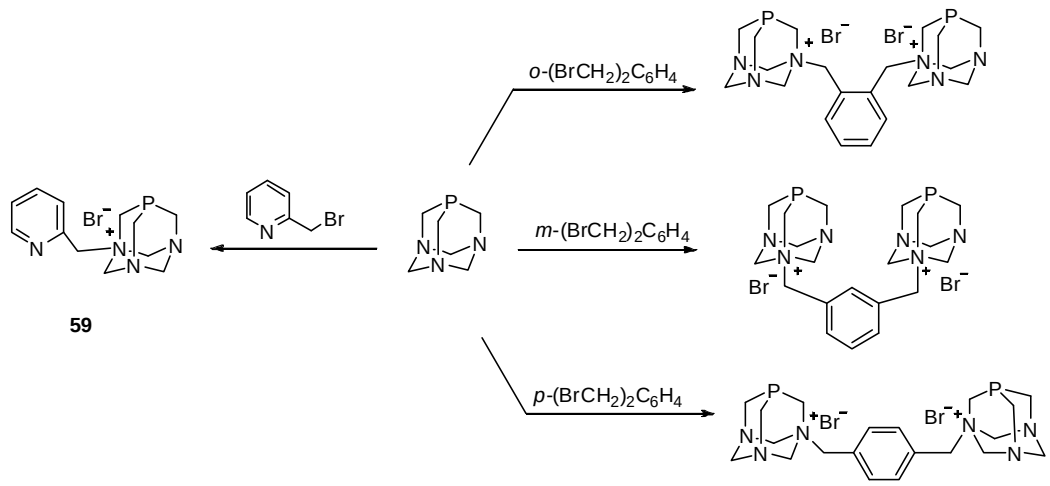


**Scheme 2.7.** Synthesis of [pymePTA]Br[23] and bis-phosphine derivatives.[24]

The preparation of the borane N-adduct of **13,** namely PTA-*N*-$BH_3$ was recently reported.[25,26] Addition of 1.1 equivalents of $BH_3$·THF solution (1 M in THF) gave after work-up a white air-stable solid, of formula 1-boranyl-1,3,5-triaza-7-phosphaadamantane, *N*-*B*-PTAB$H_3$ (**60**).[25] Adding more than one equivalent of borane to a THF solution of PTA, the bis-boranyl species and tris-boronated PTA isomers formed in solution as shown in Scheme 2.8. While the first equivalent of borane was transferred to the phosphaadamantane cage with complete regioselectivity preferring one of the N atoms, the bis and tris-boranyl adducts were formed without regioselective control.[25] All attempts to isolate these derivatives

failed and only the monoboranyl adduct **60** could be isolated as a solid. Although **60** was found to be very stable to oxidation as solid, it gave the corresponding phosphine oxide O=PTA-*N*-$BH_3$ (**61**) after several days in solution. The latter can be directly obtained by adding $BH_3$·THF to a solution of PTA(O) and $BH_3$ may be easily removed either from **60** or **61** by the addition of an excess of diazobicylooctane (DABCO) to an acetone solution of the boronated ligands.[26]

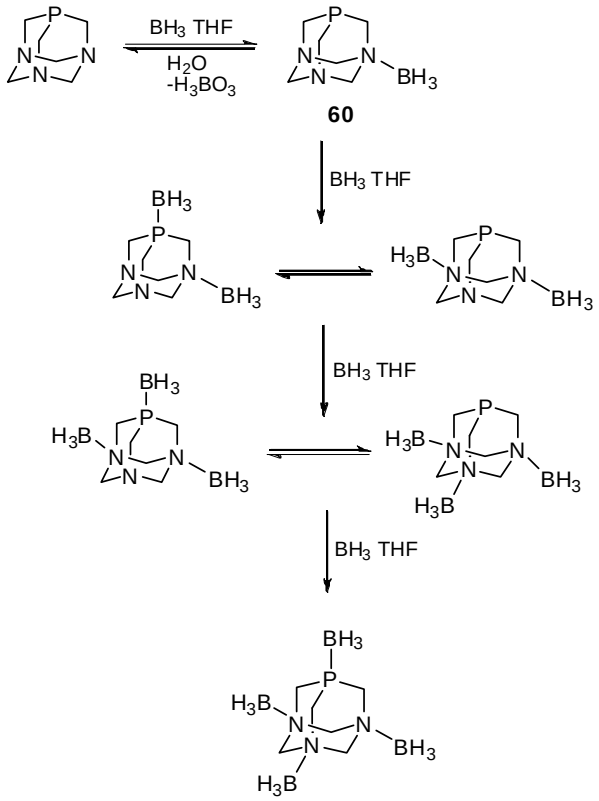


**Scheme 2.8.**Stepwise boronation of PTA. Adapted from ref. 25.

In spite of what described above, *P*-alkylation of PTA does not occur by reacting directly alkylating agent with **13**. By refluxing compounds such as $[RP(CH_2OH)_3]Cl$ (R= Me, Et, Ph, Bz, Cy) in an acetone solution containing ammonium acetate and formaldehyde, the corresponding phosphonium salts [R-*P*-PTA]Cl were obtained in yields from poor to moderate.[27]

To conclude this overview on PTA-*lower rim* modifications, it should be mentioned that also analogs of **13** bearing aryl substituents on the carbon atoms of the triazacyclohexane ring have been reported. By treating $P(CH_2NH_2)_3$ with different

aldehydes under acidic conditions, condensation was followed by nucleophilic attack and ring closure, yielding the heterocyclic ring triazaphosphaadamantane PTA-$R_3$ (R= $C_6H_5$, $C_6H_4OMe$, $C_6H_4$-CN) (Scheme 2.9).[28]

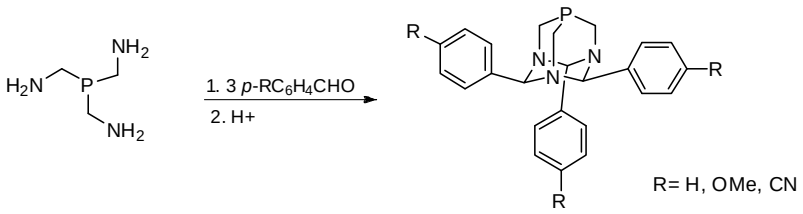


**Scheme 2.9.** PTA-$R_3$ derivatives.[28]

## 2.4. Selective cage-opening reactions.

Open-cage derivatives of PTA can be obtained by cleaving a C–N bond of the triazacyclohexane ring, as seen above in the synthesis of [dmoPTA] (**57**) (par. 2.3).[21] Reaction of water solutions of PTA and PTA(O) with acetic anhydride at 0 °C provided the corresponding acylated products 3,7-diacetyl-1,3,7-triaza-5-phosphabicyclo-[3.3.1]nonane (DAPTA, **62**) and its oxide DAPTA=O (**63**) (Scheme 2.10).[29] Curiously, the water solubility of **62** was found to be excellent ($S_{25°C}$= 7.4 M) and its binding ability toward a variety of metal centres was shown to be comparable to that of PTA. The formyl analog of **62**, 3,7-diformyl-1,3,7-triaza-5-phosphabicyclo-[3.3.1]nonane (DFPTA, **64**) (Scheme 2.10) was synthesized by producing formic anhydride *in situ* and reacting it with an aqueous solution of PTA at -5 °C.[23] After removal of the solvent and work-up in EtOH, **64** was obtained in good yields as an air-stable solid. Surprisingly, its solubility in all solvents, including water, was far less than that of its acetyl analog DAPTA.

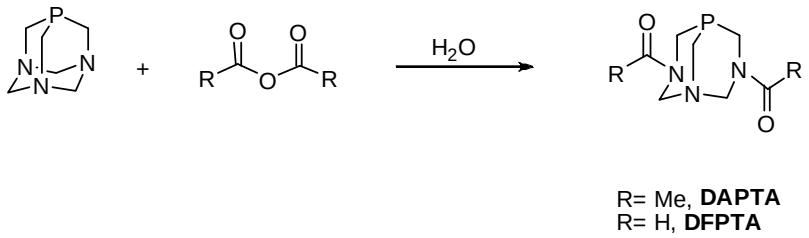


**Scheme 2.10.** Synthesis of DAPTA [29] and DFPTA.[23]

An open-cage version of PTA can also be synthesized through cleavage of an *endo* rather than an *exo* C–P bond of the corresponding phosphonium salt by using sodium amide in liquid ammonia (Scheme 2.11). The final product (RO-PTA, also known as PTN, **65**) was obtained through sublimation of the crude reaction product and it behaved as a *P*,*N*-bidentate ligand. The cleavage of two C–N bonds could be also accomplished by reacting PTA with acetic anhydride.[27c] Likewise, both PTA(O) and PTA(S) undergo identical cage breaking with $Ac_2O$.

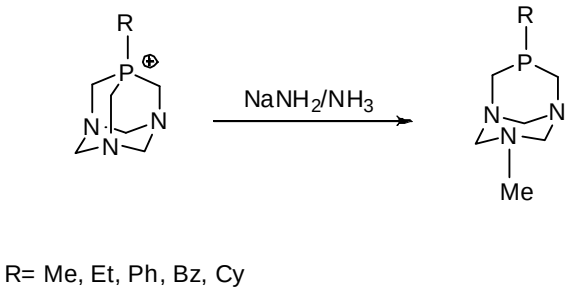


**Scheme 2.11.** Synthesis of some open-cage derivatives PTN(R).

Finally, the treatment of PTA with a large excess of HBr resulted in acidic hydrolysis of C–N bonds with consequent cage disruption and formation of *tris*-(amoniomethyl)-phosphine tribromide, $[(NH_3CH_2)_3P]Br_3$, in 74% yield.[30] Similarly, treatment of PTA(O) with either HBr or HCl, forms white stable solids of formula $[(NH_3CH_2)_3P(O)]X_3$ (X= Br or Cl) in high yields.

## 2.5. *Upper rim* functionalization reactions

The introduction of functional groups on the carbon atoms adjacent to the phosphorus (6-position) is a fundamental target to obtain potentially multidentate ligands for transition metal complexes and to create one or more stereogenic centres close to the P donor atom. The first report on the derivatization of the *upper rim* of PTA-cage was published by Wong *et al*. in 2006, introducing a binding arm and a chiral centre on the $C_\alpha$ bond to the phosphorus (Scheme 2.12).[31] The functionalization reaction provided the initial selective $\alpha$-C lithiation of PTA with $^n$BuLi, yielding the intermediate PTA-Li salt (**47**), which was then reacted with chlorodiphenylphosphine, $ClPPh_2$, resulting in the bidentate phosphine PTA-$PPh_2$ (**46**). The lithiation step was carried out by adding a slight excess of $^n$BuLi to a suspension of PTA in THF and PTA-Li was isolated as an off-white highly pyrophoric powder in *ca*. 90% yield. Because of its insolubility in common organic solvents and its extreme pyrophoric nature, the yield of the reaction and the characterization of **47** were obtained based on the reaction of PTA-Li with $D_2O$ and measuring the ratio of PTA-D/PTA by $^{31}$P NMR spectroscopy ($^{31}$P NMR: $\delta$ -102.5 ppm for PTA-D; $\delta$ -102.1 ppm for PTA). Deuteration occurred regioselectively at an $\alpha$-phosphorus methylene, as confirmed by $^{13}$C NMR spectrum of PTA-D, containing three sets of resonances in the region of 50 ppm: two signals corresponding on the two inequivalent P*C*$H_2$N and one signal for the P*C*HDN group. On the contrary, $^{13}$C NMR spectrum of PTA contains only a single P*C*$H_2$N methylene resonance appearing as a doublet due to the C-P coupling.

The racemic bidentate phosphine PTA-$PPh_2$ was obtained by reaction of PTA-Li with $ClPPh_2$ in 1,2-dimethoxyethane (DME). Other than PTA, the major byproducts of the reaction were due to the products of coupling of $ClPPh_2$ ($Ph_2P$-$PPh_2$, $Ph_2P(O)PPh_2$ and $Ph_2P(O)$-$(O)PPh_2$). For this reason, **46** was purified by column chromatography yielding the final product in 10% yield. PTA-$PPh_2$ resulted to be insoluble in water and more sensitive to oxidation on air than PTA, giving preferentially oxidation on the PTA phosphorus, (O)PTA-$PPh_2$.[31]

Other electrophiles such as $CO_2$, ketones and aldehydes have been reacted with PTA-Li to produce a series of carboxylates and water-soluble β-phosphino alcohols, PTA-$CO_2$X and PTA-CR-R′OH, respectively (Scheme 2.12).[32] Insertion of $CO_2$ into the C-Li bond was obtained by bubbling $CO_2$ through a THF suspension of PTA-Li, resulting in the highly water-soluble compound PTA-$CO_2$Li (**66**) ($S_{25°C}$= *ca*. 800 mg/mL). The esterification of **66** was accomplished by the addition of $Me_3SiCl/NEt_3$ to a methanol solution of the carboxylate, giving PTA-$CO_2$Me (**67**) (Scheme 2.12). The latter also showed high solubility in water but it resulted to be rather air-sensitive in solution, producing the corresponding oxide (O)PTA-$CO_2$Me.

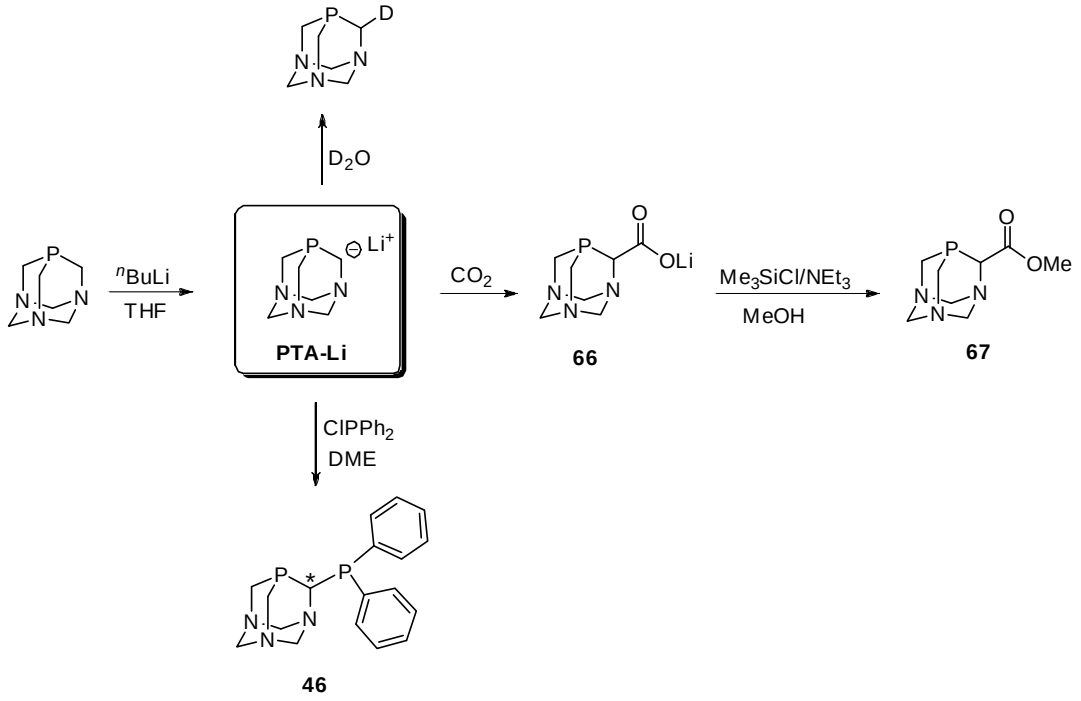


**Scheme 2.12.** Some *upper rim* functionalization reactions.

The β-phosphino alcohols were synthesized by the reaction of a THF suspension of PTA-Li salt with aromatic ketones and aldehydes. In particular, benzophenone, bis-*p*-methoxybenzophenone, *p*-anysaldehyde and ferrocene carboxaldehyde, were used to get compounds **68**, **69**, **70** and **71** respectively (Scheme 2.13).[32] In the first two cases, only one stereogenic centre was introduced and the final products resulted as a racemic mixture of two enantiomers as confirmed by $^{31}P\{^{1}H\}$ NMR

spectrum showing one singlet resonance. Unlike ketones, the addition of the aldehydes to PTA-Li led to the creation of two contiguous chiral centres and, therefore, to the racemic mixture of two diastereoisomers. In this last case, the $^{31}P\{^{1}H\}$ NMR spectrum contained two clearly distinguishable singlets.

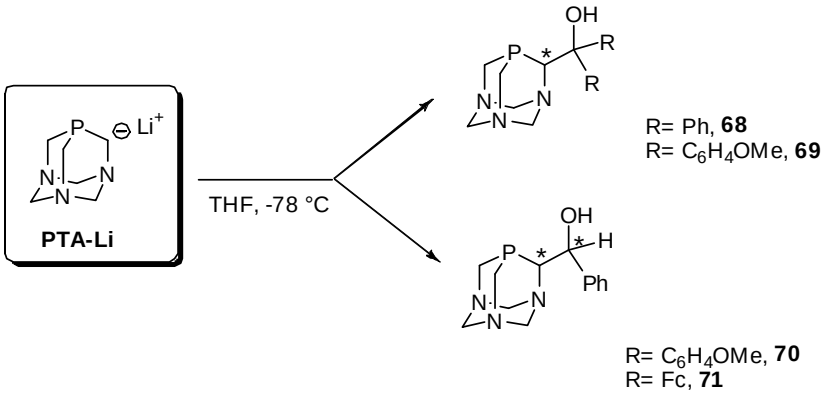


**Scheme 2.13.** Synthesis of β-phosphino alcohols.[32]

Some of these ligands were used to coordinate Ru(II) arene moieties, and the resulting complexes, in which the ligands show a $\eta^1$-P binding mode, possess modest water solubility.

## 2.6. Synthesis of new *lower-* and *upper rim*-PTA derivatives

On the basis of the structural modifications described above, a new *N*-alkylated PTA derivative [*tert*-butylBzPTA]Br (**72**)[33] was synthesised in quantitative yield by reacting a benzene solution of PTA with 4-*tert*-butylbenzylbromide (Scheme 2.14).
The reaction was left stirring at 70 °C for 30 minutes and the resulting white precipitate collected by filtration. As expected, alkylation involved only one nitrogen as confirmed by $^{31}P\{^{1}H\}$ NMR spectrum in $D_2O$ showing a singlet at -83.09 ppm, corresponding to the $^{31}P$ NMR value observed for the analog [BzPTA]Cl ($\delta$ -83.1 ppm).[15] Also $^{1}H$ NMR and $^{13}C\{^{1}H\}$ NMR spectra confirm the proposed formula and the loss of symmetry of the PTA cage due to the functionalization on one nitrogen atom. In fact, all protons and all carbons of the cage resulted to be chemically and magnetically inequivalent. Despite the introduction of the *tert*-butylbenzyl moiety, **72** showed some solubility in water at room temperature with a value of *ca*. 10

mg/mL. Ligand [*tert*-butylBzPTA]Br together with the analog [*N*-BzPTA]Cl (**73**) were used to bind Rh(I) precursors and the resulting complexes were tested in biphasic catalytic hydroformylation reactions in the presence of randomly mehylated β-cyclodextrin (RAME-β-CD) which behaves as mass transfer promoter (as discussed in Chapter 5).

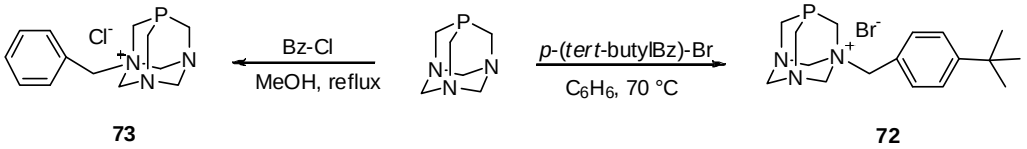


**73** **72**

**scheme 2.14.** Synthesis of [*N*-BzPTA]Cl[15] and the new *N*-alkylated derivative [*tert*-butylBzPTA]Br.[33]

As already discussed, unlike for *lower rim* functionalizations, structural modifications close to the phosphorus atom in PTA cage allows to impart significant stereoelectronic effects often required for chemoselective catalytic applications and for fine-tuning of biological effects in the design of hydrosoluble metal-based drugs. Moreover, they allow to create one or more stereogenic centres close to the P donor atom allowing to address important studies in the topic of enantioselective catalysis. For these reasons we have been interested in the synthesis of new modified *upper rim* derivatives.

According to the syntheses described in the literature[31,32] and following our interest in *upper rim* PTA derivatization, we considered PTA-Li as a valuable intermediate to obtain multidentate, water-soluble, enantiomerically enriched ligands for transition metal complexes. In order to improve on the yields and purity of PTA-Li, we have introduced slight but important changes in the synthetic protocol previously described.[31] In fact, due to the limited solubility of PTA in THF, the reaction suffered from the main disadvantages of being carried out in heterogeneous conditions and workup was needed to separate the unreacted PTA from the final product. Thus, we decided to screen for different solvents and reaction conditions in order to improve the final yield. We were able to find optimal conditions by carrying out the lithiation reaction in warm benzene.[34] At *ca*. 30 °C, PTA completely dissolves and the

following addition of $^{n}$BuLi leads to the precipitation of the lithium derivative (**47**) as an analytically pure microcrystalline powder (Scheme 2.15). The solid is then recovered by filtration under nitrogen, washed with dry *n*-pentane and dried under reduced pressure. Because of its susceptibility to moisture, PTA-Li must be stored in an inert atmosphere of $N_2$ and used within few days to ensure highest purity.

Due to its highly pyrophoric feature as solid, we thought to avoid the isolation of the salt making the derivatization reaction in one pot-synthesis. Several reactions were carried out using benzaldehyde as electrophile and varying conditions such as the lithiation agent ($^{n}$BuLi, $^{s}$BuLi, $^{t}$BuLi, lithium diisopropylamide, LDA), the solvent (benzene, THF, benzene/THF mixtures), reaction time (from 3h to 24h) and temperature. At the end of the reactions, after quenching with water, $^{31}$P NMR analysis of the solid has shown in all experiments the presence of PTA as the only or main product of the reaction. Due to these results, all derivatization reactions have been therefore repeated after isolation of PTA-Li salt.

By reacting a PTA-Li suspension in THF with several aromatic aldehydes at low temperature, ligands phenyl(1,3,5-triaza-7-phosphatricyclo-[3.3.1.1]dec-6-yl) methanol, PZA (**74**),[35] its *p*-dimethylamino analog PZA-$NMe_2$ (**75**)[34] and the imidazole derivative 1-methylimidazolyl-(1,3,5-triaza-7-phosphatricyclo-[3.3.1.1]dec-6-yl)methanol, PTA-CH(1-MeIm)OH (**76**)[36] were synthesized (Scheme 2.15).

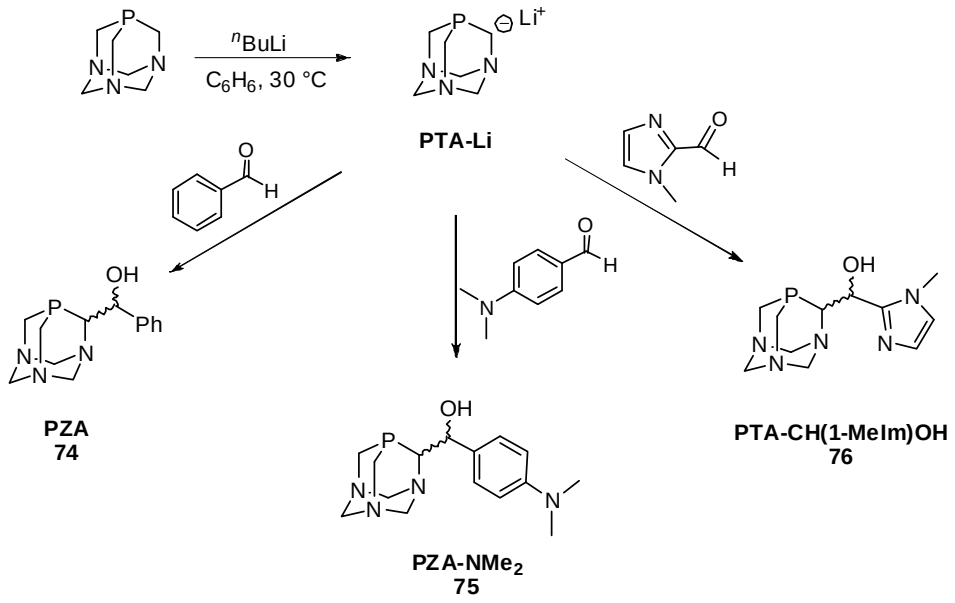


**Scheme 2.15.** Synthesis of PTA-Li and ligands **74**, **75** and **76**.

PZA was prepared by adding distilled benzaldehyde to the suspension of PTA-Li in THF. After quenching with water, the product resulted in a racemic mixture 1:1 ratio of two diastereoisomers, as expected from the presence of two chiral centres and as confirmed by $^{31}P\{^{1}H\}$ NMR spectrum in $D_2O$, which consisted in two singlets at -103.4 and -106.6 ppm. To obtain an analytically pure compound, the crude product was purified by column chromatography, causing the decrease of the yield to an overall *ca*. 20%. PZA showed remarkably high solubility in water ($S_{20°C}$= 1.05 g/mL) and dissolved also in MeOH, EtOH and chlorinated solvents. The corresponding sulfide derivative, PZA(S) (**77**),[35] was obtained by reacting PTA(S) with $^{n}$BuLi for 3h and by subsequent addition of benzaldehyde to the reaction mixture (Scheme 2.16). Also in this case, the formation of a pair of diastereoisomers was confirmed by $^{31}P\{^{1}H\}$ NMR spectrum in DMSO-$d_6$ showing two singlets at -10.5 and at -14.1 ppm (1:4 ratio), in a similar range to PTA(S) ($\delta$ -20.0 ppm).[8] Additionally, IR spectroscopy showed the presence of the P=S group with stretching band at 610 $cm^{-1}$. On the other side, oxidation of PZA was accomplished by treatment of PZA ligand with $H_2O_2$ in methanol (Scheme 2.16). In this last case, one of the two diastereoisomers of

PZA(O) (**78**)[35] separated from the diastereomeric mixture (1:1 ratio) simply by crystallization in water.

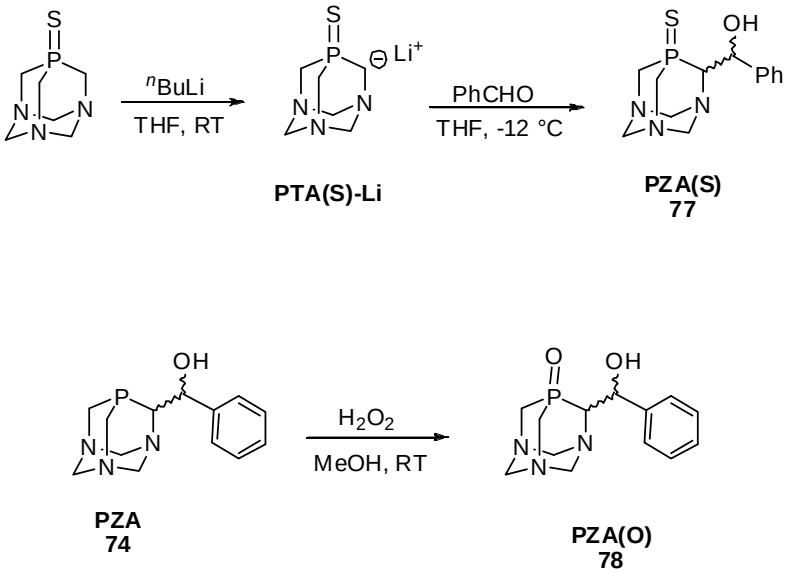


**Scheme 2.16.** Synthesis of PZA(S) and PZA(O). Adapted from ref. 35.

Crystals of PZA(O) were also obtained by slow concentration of a methanol solution of PZA in air, suggesting that **74** is more sensitive to oxidation than PTA as observed for the other *upper rim* derivatives. The X-ray crystal analysis of **78** showed that only the (*R*,*S S*,*R*)-diastereoisomer (Figure 2.3) was present in the solid state and that the P=O oxygen atom formed a strong intermolecular hydrogen bond with the hydroxyl group of a neighboring PZA(O) molecule [P=O···OH distance 2.717(6) Å], giving a monodimensional infinite chain in the solid state (Figure 2.4). Thus could account for the poor solubility of the (*R*,*S S*,*R*)-diastereoisomer.

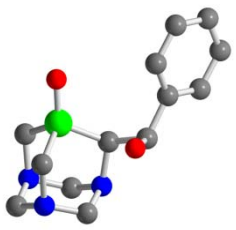

**Figure 2.3**. X-ray crystal structure of *R*,*S S*,*R* diastereoisomer of **78** (see atom colour code).[35]

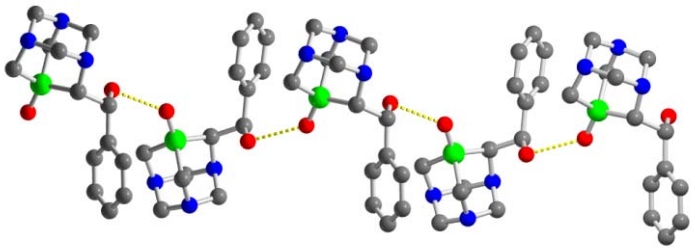

**Figure 2.4.** Monodimensional infinite chain of *R,S S,R* diastereoisomer of **78** (see atom colour code).[35]

The β-phosphino alcohol ligand PZA-$NMe_2$ (**75**) was synthesized in a similar way by replacing benzaldehyde with 4-(dimethylamino)benzaldehyde (Scheme 2.15). After column chromatography, the $^{31}P\{^1H\}$ NMR spectrum in $CDCl_3$ showed the presence of two singlets in 3:1 ratio at -102.7 (major, **75a**) and -106.7 ppm (minor, **75b**). As for PZA(O), it was possible to isolate the major diastereoisomer **75a** through fractional crystallization in $CH_2Cl_2$ and crystals suitable for X-ray analysis were obtained by slow evaporation under nitrogen of a $CH_2Cl_2$/EtOH solution, showing that **75a** corresponded to the (*S*,*R R*,*S*)-diastereoisomer (Figure 2.5).[34]

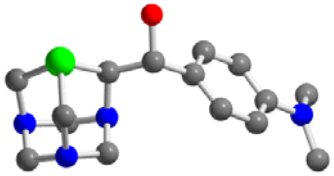

**Figure 2.5.** X-ray crystal structure of ligand (*S*,*R R*,*S*)PZA-$NMe_2$ (see atom colour code). Adapted from ref. 34.

X-ray analysis of **75a** showed that in the solid state, (*S*,*R R*,*S*)PZA-$NMe_2$ molecules were connected by hydrogen bonding between the hydroxyl of the alcohol group and one of the N atoms of the adamantane cage belonging to a neighboring molecule (Figure 2.6). This behaviour could be responsible of the minor water solubility showed by ligand (*S*,*R R*,*S*)PZA-$NMe_2$ ($S_{20°C}$= 1.9 g/L) in comparison with PZA ($S_{20°C}$= 1.05 g/mL).

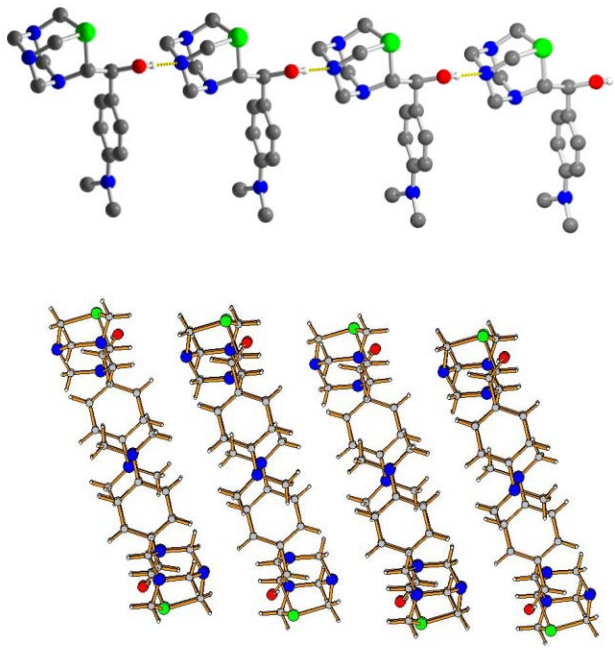

**Figure 2.6.** Intermolecular OH···N hydrogen bonding view along a axis (up) and packing of **75a** within the asymmetric unit, view along b axis parallel to hydrogen bonds (down) (see atom colour code). Adapted from ref. 34.

In solution, the loss of symmetry of the PTA cage due to the functionalization of the 6-position was demonstrated from the magnetic inequivalence of the methylene protons in the $^{1}$H NMR spectrum of **75a** with an AB multiplet centred at 4.85 ppm ($^{2}J_{HAHB}$= 13.4 Hz) corresponding to two NC*H*$_2$N protons and a multiplet in the range 4.57-4.37 ppm corresponding to the remaining four NC*H*$_2$N protons. A similar behaviour was observed for the methylene protons bound to phosphorus, appearing as three overlapped groups of signals between 4.29 and 3.80 ppm. The loss of the adamantane symmetry was also confirmed by $^{13}$C{$^{1}$H} NMR spectrum presenting two signals at 74.20 and 67.78 ppm for N*C*H$_2$N carbon atoms and three doublets at 65.75 (P*C*HN), 51.55 and 48.43 ppm (P*C*H$_2$N) with $^{1}J_{CP}$ ranging from 19.9 to 24.0 Hz.

The corresponding sulfide and oxide of **75a**, (*S*,*R R*,*S*) S=PZA-NMe$_2$ (**79**) and (*S*,*R R*,*S*) O=PZA-NMe$_2$ (**80**) respectively, were also prepared straightforwardly by reacting **75a** with either S$_8$ under reflux conditions or aqueous H$_2$O$_2$ at room temperature.[34] Selective oxidation of the P atom was achieved in both cases, as evidenced by a

singlet in the $^{31}P\{^{1}H\}$ NMR spectra at -14.1 and 2.1 ppm respectively, as expected by comparison with PTA[8] and PZA.[35] IR spectroscopy also evidenced the presence of P=S (band at 646 $cm^{-1}$) for **79** and P=O (band at 1155 $cm^{-1}$) for **80**. (*S*,*R R*,*S*) S=PZA-$NMe_2$ shows very low water solubility, while (*S*,*R R*,*S*) O=PZA-$NMe_2$ has a good solubility in water ($S_{20°C}$= 12.5 mg/mL).

Both new ligands PZA and (*S*,*R R*,*S*)PZA-$NMe_2$ have been used to prepare Ir(I) and Ru(II) arene complexes which have been tested as catalysts in several catalytic hydrogenation reactions as will be discussed in details in the following Chapter 3 and Chapter 4, respectively.

The imidazole derivative PTA-CH(1-MeIm)OH (**76**)[36] was prepared according to the synthetic methodology already described for **74** and **75** (Scheme 2.15). Thus, 1-methyl-2-imidazolecarboxaldehyde was added at low temperature to the PTA-Li suspension in THF and left stirring at room temperature overnight. After quenching with $H_2O$ and removing the solvent, the remaining product was purified by column chromatography and isolated as a white solid in 41% yield. Also in this case, the presence of two diastereoisomers was confirmed by $^{31}P\{^{1}H\}$ NMR in $CDCl_3$ spectrum, showing as expected two singlets at -103.4 and -104.7 ppm. After crystallization from hot acetone, the diastereomeric mixture was enriched to a final 15:1 ratio based on $^{31}P$ NMR. The interpretation of the $^{1}H$ NMR was quite difficult but gave important information. The presence of the imidazole fragment was evident from the two doublets at 6.84 and 6.81 ($^{1}J_{HH}$= 1.1 Hz) and the broad singlet at 3.84 corresponding to the N-*Me* group. The imidazole moiety was also confirmed by $^{13}C\{^{1}H\}$ NMR where the signals at 148.2, 126.6 and 122.2 ppm were attributed to the carbon atoms of the ring and the peak at 33.2 ppm belonged to the N-*Me* group. Phosphine **76** was found to be highly soluble in water ($S_{25°C}$= 320 g/L) and, as observed for the other *upper rim* derivatives, it was an air-stable solid which slowly oxidized in air when in solution as the corresponding oxide after several days. The oxide derivative, O=PTA-CH(1-MeIm)OH (**81**) was also obtained by reacting **76** with an aqueous solution $H_2O_2$ (35%) (Scheme 2.17) and confirmed by IR spectroscopy showing the P=O stretching at 1152 $cm^{-1}$.

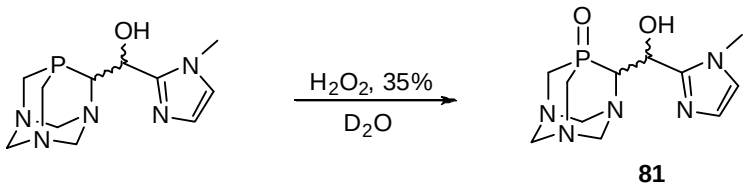


**Scheme 2.17.** Synthesis of O=PTA-CH(1-MeIm)OH.[36]

Finally, a *bis*-*N*-methylimidazolyl PTA derivative was prepared by reacting PTA-Li with *bis*-(*N*-methylimidazole-2-yl)ketone in THF (Scheme 2.18).[36] Thus, ligand PTA-C(1-MeIm)$_2$OH (**82**) was obtained after purification of the crude product through extraction and recrystallization in $Et_2O$.

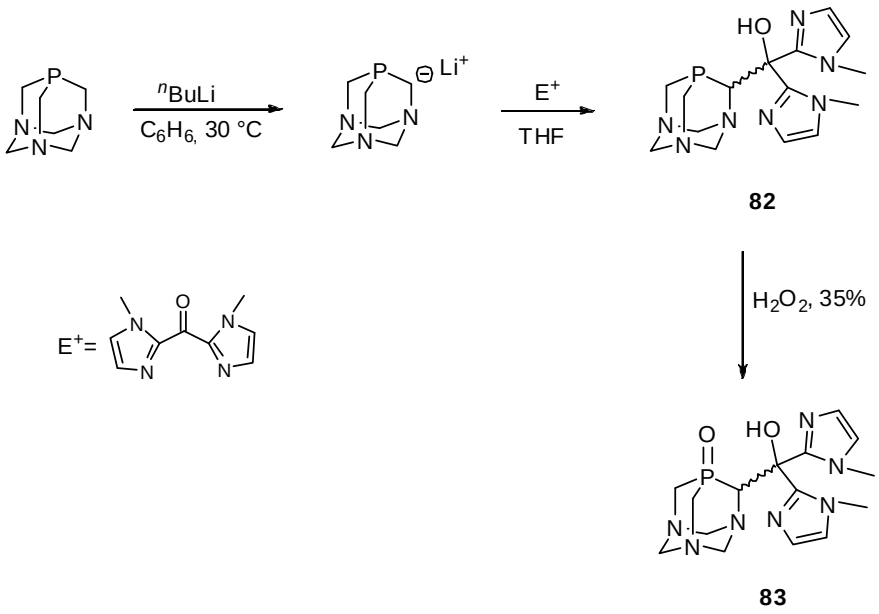


**Scheme 2.18.** Synthesis of PTA-C(1-MeIm)$_2$OH and its oxide.[36]

Compound **82** was obtained as a racemic mixture of the two enantiomers as proven from the $^{31}P\{^1H\}$ NMR in $CD_2Cl_2$ spectrum, where only one singlet at -97.6 ppm was present. $^1H$ NMR confirmed the hypothesized formula, showing two singlets at 3.35 and 3.49 ppm due to the C*H*$_3$ groups of the imidazole moieties and four doublets resonated at 6.94, 6.90, 6.87 and 6.83 ppm ($^1J_{HH}$= 1.1 Hz) due to the C*H*=C*H* imidazole protons. This distinct sets of signals indicated that the two imidazoles

were not equivalent as diastereotopic. The inequivalence of imidazoles was also confirmed by $^{13}C\{^1H\}$ NMR, in which two singlets at 34.4 and 33.2 ppm corresponding to *C*$H_3$ groups, were observed. Water-solubility of PTA-C(1-MeIm)$_2$OH was still high ($S_{25°C}$= 78 g/L) but lower comparing with that of PTA-CH(1-MeIm)OH. As expected, when in solution **82** easily oxidized in air to the corresponding oxide O=PTA-C(1-MeIm)$_2$OH (**83**). This compound was also synthesized as usual by reaction of **82** with $H_2O_2$ (35%) (Scheme 2.18). Oxidation on phosphorus atom was confirmed by the singlet at -0.2 ppm in the $^{31}P\{^1H\}$ NMR and by the band at 1146 cm$^{-1}$ in the IR spectrum corresponding to P=O stretching.

The mono- and bis-imidazolyl-PTA derivatives, **76** and **82**, were used as ligands for the synthesis of two ruthenium(II) arene complexes, which will be discussed in Chapter 4.

## 2.7. Experimental Section

### 2.7.1. Synthetic procedures

All synthetic procedures were carried out using standard Schlenk techniques under an inert atmosphere of dry nitrogen. All glassware was dried overnight in the oven. PTA,[3,4] [*N*-BzPTA]Cl,[15] PZA,[35] the oxides[5] and sulfides[8] derivatives and *bis*-(*N*-methylimidazole-2-yl)ketone[37] were prepared as described in the literature. *Bis*-(*N*-methylimidazole-2-yl)ketone was purified by recrystallization from THF under a nitrogen atmosphere before use. All solvents were distilled and degassed prior to use according to standard procedures.[38] Doubly distilled water was used. Deuterated solvents and other reagents were bought from commercial suppliers and used without further purification. Column chromatography purification was performed using glass columns (10-50 mm wide) and silica gel (230-400 mesh particle size). The $^1H$, $^{13}C\{^1H\}$ and $^{31}P\{^1H\}$ NMR were recorded on a Bruker Avance II 300 spectrometer (operating at 300.13, 75.47 and 121.50 MHz, respectively) and a Bruker Avance II 400 spectrometer (operating at 400.13, 100.61 and 161.98 MHz, respectively). Peak positions are relative to tetramethylsilane and were calibrated against the residual solvent resonance ($^1H$) or the deuterated solvent multiplet ($^{13}C$).

$^{31}P\{^{1}H\}$ NMR were referenced to 85% $H_3PO_4$ with the downfield shift taken as positive. All of the NMR spectra were recorded at room temperature (20 °C). In the case of compound O=PZA and PZA-$NMe_2$ and its oxide and sulfide derivatives, the spectroscopic data are referred to the (*S*,*R R*,*S*)-diastereoisomers. IR spectra (KBr pellets or $CH_2Cl_2$ solution) were recorded on a Perkin-Elmer Spectrum BX II Series FT-IR spectrophotometer in the range 4000-400 $cm^{-1}$. ESI-MS spectra were measured on a LCQ Orbitrap mass spectrometer (ThermoFischer, San Jose, CA, USA) equipped with a conventional ESI source by direct injection of the sample solution and are reported in the form *m/z* (intensity relative to base = 100). Elemental analyses were performed on a Perkin-Elmer 2400 series II elemental analyzer. The water-solubility of the new compounds was quantified by the slow addition of water by using a 100 μL syringe to a 5 mg sample of the products at room temperature.

### *Synthesis of 1,3,5-triaza-7-phosphatricyclo[3.3.1.1]decane, PTA* (**13**)

Under a nitrogen atmosphere, a three-necked flask was charged with a commercially available 80% water solution of *tetrakis*-(hydroxymethyl)phosphonium chloride (THPC, 268.0 g, 1.13 mol) and grinded ice (*ca*. 110 g). The flask was put in an ice-cold bath (ca. 15 °C) and a freshly prepared NaOH solution (1.14 g, 1.14 mol, 1equiv) in degassed water (70 mL) was added dropwise over 30 min. The reaction mixture was additionally stirred for 15 min and then a degassed 37% water solution of formaldehyde (405 g, 5.6 mol, 5 equiv) was added dropwise over 30 min. Then, hexamethylenetetramine (126.0 g, 0.9 mol) was added as solid in small portions of *ca*. 10 g each and the reaction mixture was left stirring overnight at room temperature under a nitrogen atmosphere. The resulting white suspension was filtered on a Bückner funnel and the solution concentrated in air in a crystallizer over a *ca*. 8 days period, producing white crystals collected by filtration. In order to eliminate any residue of NaCl, PTA was dissolved in hot $CHCl_3$ and then in hot EtOH and the solutions concentrated by means of a rotary evaporator. PTA was so obtained as a white crystalline solid in 66% yield.

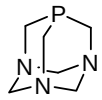

**13:** ***S*(H$_2$O)$_{20\ °C}$** = 235 mg·mL$^{-1}$. **$^1$H NMR** (400.13 MHz, $D_2O$): $\delta$ 4.42 (AB system, $^1J_{HAHB}$=12.5 Hz, 6H, NC*H*$_2$N); 3.89 (d, $^1J_{HP}$= 9.0 Hz; 6H, PC*H*$_2$N). **$^{31}$P{$^1$H} NMR** (161.98 MHz, $D_2O$): $\delta$ -98.61 (s). **Anal**. Calcd for $C_6H_{12}N_3P$ (157.15 gmol$^{-1}$) Found: (calc.) C, 45.77 (45.86); H, 7.73 (7.70): N, 26.65 (26.74).

*Synthesis of 1,3,5-triaza-7-phosphatricyclo[3.3.1.1]decane 7-oxide, PTA(O)* (**48**)

In a one-necked flask, PTA (1.5 g, 9.6 mmol) was completely dissolved in methanol (75 mL) and a 35% water solution of $H_2O_2$ (1.9 mL, 19.1 mmol) diluted in ethanol (30 mL) was added dropwise. The reaction mixture was left under stirring for 30 min, after which a white precipitate appeared. The solid was collected by filtration, recrystallized from hot EtOH and washed once with $Et_2O$ (1 x 5 mL). The product was dried under vacuum producing 1.16 g of PTA(O) (70% yield).

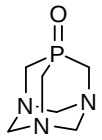

**48:** **$^1$H NMR** (400.13 MHz, $D_2O$): $\delta$ 4.31 (AB system, $^1J_{AB}$= 13.2 Hz, 3H, NC*H*$_2$N), 4.17 (AB system, $^1J_{AB}$ =13.2 Hz, 3H, NC*H*$_2$N), 3.95 (d, $^1J_{HP}$=10.3 Hz, 6H, PC*H*$_2$N). **$^{31}$P{$^1$H} NMR** (161.98 MHz, $D_2O$): $\delta$ -2.92 (s). **Anal**. Calcd for $C_6H_{12}N_3OP$ (173.15 gmol$^{-1}$) Found: (calc.) C, 41.70 (41.62); H, 7.71 (6.99): N, 24.62 (24.27).

*Synthesis of 1,3,5-triaza-7-phosphatricyclo[3.3.1.1]decane 7-sulfide, PTA(S)* (**49**)

In a three-necked flask, PTA (2 g, 12.7 mmol) was dissolved in 50 mL. of degassed water. Elemental sulfur (1 g, 31.8 mmol) was added and the reaction mixture was refluxed under stirring for *ca*. 40 min. The suspension was then filtered and the yellow solid washed with hot $CCl_4$ (1 x 20 mL), yielding 1.2 g of product (50% yield).

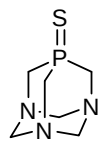

**49:** **$^1$H NMR** (400.13 MHz, DMSO-$d_6$): $\delta$ 4.28 (s, 6H, NC*H*$_2$N), 3.97 (d, $^1J_{HP}$=7.0 Hz, 6H, PC*H*$_2$N). **$^{31}$P{$^1$H} NMR** (161.98 MHz, DMSO-$d_6$): $\delta$ -19.99 (s). **Anal**. Calcd for $C_6H_{12}N_3SP$ (189.22 gmol$^{-1}$) Found: (calc.) C, 39.22 (38.09); H, 6.57 (6.39): N, 22.26 (22.21).

*Synthesis of 1-benzyl-1-azonia-3,5-diaza-7-phosphaadamantane chloride, [N-BzPTA]Cl* (**73**)

In an inert atmosphere of nitrogen, to a solution of PTA (2,17 g, 13.8 mmol) in dried degassed methanol (70 mL), benzylchloride (1,75 g, 13.8 mmol) was added. After 2h reflux, the volume of the solvent was reduced to *ca*. 10 mL and diethyl ether (15 mL) was added to give a white precipitate. The solid was washed with methanol (2 x 3 mL) and diethyl ether (2 x 3 mL) and then recrystallized from methanol, yielding 1.2 g of pure product (30% yield).

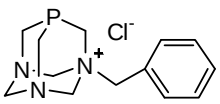

**73: $^{1}$H NMR** (300.13 MHz, $D_2O$): $\delta$ 7.47-7.37 (m, 5H, Ar); 4.83 (AB system, $^{1}J_{AB}$= 11.8 Hz, 4H, NC*H*$_2$N); 4.47 (d, $^{1}J_{HH}$= 13.7 Hz, 1H, NC*H*$_2$N); 4.31 (d, $^{1}J_{HH}$= 13.7 Hz, 1H, NC*H*$_2$N); 4.13 (d, $^{1}J_{HP}$= 6.3 Hz, 2H, PC*H*$_2$N$^+$); 4.04 (s, 2H, PhC*H*$_2$N$^+$); 3.85-3.75 (m, 2H, PC*H*$_2$N); 3.66-3.63 (m, 2H, PC*H*$_2$N). **$^{31}$P{$^{1}$H} NMR** (121.50 MHz, $D_2O$): $\delta$ -83.05 (s). **Anal**. Calcd for $C_{13}H_{19}N_3ClP$ (283.74 gmol$^{-1}$) Found: (calc.) C, 54.97 (55.03); H, 6.61 (6.75): N, 15.02 (14.81).

*Synthesis of 1-(4-tert-butyl)-benzyl-1-azonia-3,5-diaza-7-phosphaadamantane bromide, [tert-butylBzPTA]Br* (**72**)

In a 3-necked round-bottomed flask, PTA (0.86 g, 5.5 mmol) was dissolved in 80 mL of dried and degassed benzene at 70 °C. To this solution, 1-(bromomethyl)-4-*tert*-butylbenzene (1.2 g, 5.5 mmol) was added dropwise and after few drops a white precipitate appeared. The reaction mixture was stirred at 70 °C for 30 min, cooled to room temperature and the precipitate filtered on a Bückner funnel. After washing with petroleum ether (1 x 8 mL), the solid was dried under vacuum, to yield 1.85 g of pure product (88% yield).

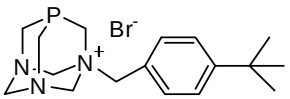

**72: *S*(H$_2$O)$_{20°C}$**= 10 mg·mL$^{-1}$. **$^{1}$H NMR** (300.13 MHz, $D_2O$): $\delta$ 7.50 (d, $^{3}J_{HH}$= 8.1 Hz, 2H, Ar); 7.33 (d, $^{3}J_{HH}$= 8.1 Hz, 2H, Ar); 4.81 (d, AB system, $^{1}J_{AB}$= 11.8 Hz, 4H, NC*H*$_2$N); 4.48 (d, AB system, $^{1}J_{AB}$= 13.7 Hz, 1H, NC*H*$_2$N); 4.31 (d, AB system, $^{1}J_{AB}$= 13.7 Hz, 1H, NC*H*$_2$N); 4.10 (d, $^{1}J_{HP}$= 6.2 Hz, 2H, PC*H*$_2$N$^+$); 4.01 (s, 2H, PhC*H*$_2$N$^+$); 3.85-3.80 (m, 2H, PC*H*$_2$N); 3.65-3.57 (dd, ABX system, $^{1}J_{AB}$= 15.3 Hz, $^{1}J_{HP}$= 8.9 Hz, 2H, PC*H*$_2$N); 1.19 (s, 9H, *tert*-

C*H*$_3$). **$^{31}$P{$^1$H} NMR** (121.50 MHz, $D_2O$): $\delta$ -83.09 (s). **$^{13}$C {$^1$H}NMR** (75.47 MHz, $D_2O$): $\delta$ 154.69 (s, Ar); 132.70 (s, Ar); 128.44 (s, Ar); 126.27 (s, Ar); 78.43 (s, Ph*C*H$_2$N$^+$); 69.29 (s, 2 x N*C*H$_2$N); 66.37 (s, N*C*H$_2$N); 52.66 (d, $^1J_{CP}$= 33.3 Hz, P*C*H$_2$N$^+$); 45.50 (d, $^1J_{CP}$= 21.1 Hz, 2 x P*C*H$_2$N); 34.19 (s, *C*-Me$_3$); 30.27 (s, 3 x *C*H$_3$). **MS** (nESI$^+$), *m/z*: 304.17 (100) [M$^+$]. **Anal**. Calcd for $C_{17}H_{27}N_3BrP$ (384.29 gmol$^{-1}$) Found: (calc.) C, 53.58 (53.13); H, 7.16 (7.08): N, 10.89 (10.93).

*Synthesis of 1,3,5-triaza-7-phosphadamantane-6yl lithium, PTA-Li* (**47**)

In an inert atmosphere of nitrogen, PTA (1.57 g, 10.0 mmol) was completely dissolved in dry degassed benzene (160 mL) at 50 °C under vigorous stirring. The solution was then allowed to cool to approximately 30 °C and *n*-butyllithium solution (1.6 M solution in hexanes, 10 mL, 16 mmol) was slowly added by syringe. After a few minutes a white solid appeared and the reaction was stirred at room temperature for 2 h. The solid was filtered on a frit under nitrogen and washed with dry *n*-pentane (3 x 30 mL), yielding PTA-Li in quantitative yield (1.63 g). Due to its highly pyrophoric nature and sensitivity to atmospheric moisture, the solid had to be stored under nitrogen and the batch consumed within a few days.

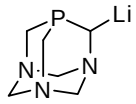


*Synthesis of phenyl-(1,3,5,-triaza-7-phosphatricyclo[3.3.1.1]dec-6-yl) methanol, PZA* (**74**)

PTA-Li (1.0 g, 6.1 mmol) was suspended in dry degassed THF (20 mL) and maintained at -78 °C by means of a liquid nitrogen/acetone bath. After 10 min, freshly distilled benzaldehyde (0.68 mL, 6.71 mmol) cooled to -78 °C was added and the resulting yellow suspension left at low temperature for 15 min. The suspension was then allowed to warm to room temperature and left under stirring additionally for 2h. Degassed and doubly distilled water (0.3 mL) was added and the solvent removed under reduced pressure, to give an orange solid. After washing with

acetone (1 X 8 mL), the crude product was purified through silica gel flash column chromatography ($R_f$= 0.24, eluent: MeOH) (0.335 g, 20% yield). White solid.

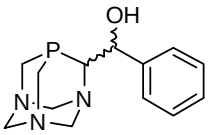

**74: *S*($H_2O$)$_{20°C}$**= 1.05 mg·mL$^{-1}$. **$^1$H NMR** (400.13 MHz, CDCl3): $\delta$ 7.28-7.49 (m, 10 H, Ar); 5.20 (dd, $^3J_{HH}$= 8.9 Hz, $^2J_{HP}$= 4.6 Hz, 1H, C*H*OHPh); 5.15 (dd,$^2J_{HH}$= 10.9 Hz, $^4J_{HH}$= 3.6 Hz, 1H, NC*H*$_2$N); 5.02 (dt, $^2J_{HH}$= 13.4 Hz, $^4J_{HH}$= 2.4 Hz, 1H, NC*H*$_2$N); 4.75 (dt, $^2J_{HH}$= 13.7 Hz, $^4J_{HH}$= 2.4 Hz, 1H, NC*H*$_2$N); 4.65 (brd, $^3J_{HH}$= 13.0 Hz, 1H, C*H*Ph); 4.22-4.60 (m, 8H, NC*H*$_2$N); 3.65-4.12 (m, 9 H, PC*H*$_2$N + NC*H*$_2$N); 3.81 (m, 1H, PC*H*N); 3.58 (dd, $^3J_{HH}$= 13.0 Hz, $^2J_{HP}$= 5.4 Hz, 1H, PC*H*N); **$^{31}$P{$^1$H} NMR** (161.98 MHz, $CDCl_3$):$\delta$-103.42 (s), -106.58 (s). **$^{13}$C{$^1$H} NMR** (100.03 MHz, $CDCl_3$):$\delta$ 143.24 (s, Ar); 140.40 (s, Ar); 128.47 (s, Ar); 128,37 (s, Ar); 128.31 (s, Ar); 128.02 (s, Ar); 127.51 (s,Ar); 126.35 (s, Ar); 77.94 (d, $^2J_{CP}$= 6.3 Hz, *C*HPh); 76.79 (d, $^2J_{CP}$ = 6.1 Hz, *C*HPh); 76.11 (s, NCH$_2$N); 74.06 (s, NCH$_2$N); 71.58 (s, NCH$_2$N); 71.42 (s, NCH$_2$N); 67.82 (s, NCH$_2$N); 66.37(s, NCH$_2$-N); 65.81 (d, $^1J_{CP}$= 23.7 Hz, NCHP); 65.53 (d, $^1J_{CP}$= 21.9 Hz, NCHP); 51.53 (d, $^1J_{CP}$= 20.0 Hz, NCH$_2$P); 50.78 (d, $^1J_{CP}$= 21.5 Hz, NCH$_2$P); 48.91(d, $^1J_{CP}$= 24.2 Hz, NCH$_2$P); 47.26 (d, $^1J_{CP}$= 24.2 Hz,NCH$_2$P). **GC-MS** *m/z* (%): 263.01 (10) [M$^+$], 156.02 (100) [$C_6H_{11}N_3P^+$]. **Anal**. Calcd. for $C_{13}H_{18}N_3OP$ (263.28 gmol$^{-1}$). Found (calcd): C, 59.12 (59.31); H, 6.99 (6.89); N, 15.87 (15.96).

*Synthesis of phenyl-(1,3,5,-triaza-7-phosphatricyclo[3.3.1.1]dec-6-yl) methanol oxide, PZA(O)* (**78**)

PZA (0.09 g, 0.4 mmol) was dissolved into doubly distilled water (10 mL) and an excess of 35% $H_2O_2$ (50 µL) was added. The reaction was left stirring at room temperature and after 20 min a precipitate separated out. This was filtered, washed with EtOH and dried under vacuum resulting in a white solid containing the (*S*,*R R*,*S*)-diastereoisomer (24.5 mg, 24.4% yield).

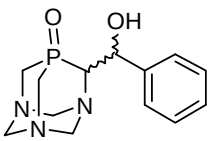

**78**: *S*,*R R*,*S* diastereoisomer. **$^1$H NMR** (400.13 MHz, DMSO-$d_6$): $\delta$ 7.20-7.47, (m, 5H, Ar); 5.20 (dd, $^3J_{HH}$= 13.1 Hz, $^2J_{HP}$= 4.8 Hz, 1H, C*H*Ph); 4.49 (dt, $^2J_{HH}$= 13.7 Hz, $^4J_{HH}$= 4.6Hz, 1H, NC*H*$_2$N); 3.63-4.27 (m, 10 H, NC*H*$_2$P + NC*H*$_2$N + NC*H*P). **$^{31}$P{$^1$H} NMR** (161.98 MHz, DMSO-$d_6$):$\delta$-3.38 (s).

**$^{13}C\{^{1}H\}$ NMR** (100.61 MHz, DMSO-$d_6$): $\delta$ 143.85 (d, $^{3}J_{CP}$= 4.1 Hz, Ar); 128.38 (s, Ar); 127.38 (s, Ar); 126.66 (s, Ar); 76.26 (d, $^{2}J_{CP}$ = 2.2 Hz, *C*HPh); 73.89 (d, $^{2}J_{CP}$= 5.6 Hz, N*C*$H_2$N); 71.95 (d, $^{2}J_{CP}$= 8.9 Hz, N*C*$H_2$N); 70.54 (d, $^{1}J_{CP}$= 48.5 Hz, N*C*HP); 66.25 (d, $^{2}J_{CP}$= 12.2 Hz, N*C*$H_2$N); 55.60 (d, $^{1}J_{CP}$= 50.4 Hz, N*C*$H_2$P); 53.67 (d, $^{1}J_{CP}$= 50.4 Hz, N*C*$H_2$P). ). **GC-MS:** *m/z* (%) 279 (11) [$M^+$] 172 (100) [$C_6H_{11}N_3OP^+$]. **IR** (KBr, $cm^{-1}$): $\nu_{(P=O)}$ 1153 (m). **Anal**. Calcd. for $C_{13}H_{18}N_3O_2P$ (279.28 $gmol^{-1}$). Found (calcd): C, 55.91 (55.78); H, 6.50 (6.45): N, 15.05 (14.89).

*Synthesis of phenyl-(1,3,5,-triaza-7-phosphatricyclo[3.3.1.1]dec-6-yl) methanol sulfide, PZA(S)* (**77**)

To a stirred suspension of PTA(S) (1.0 g, 5.3 mmol) in THF (15 ml), *n*-butyllithium solution (1.6 M solution in hexanes, 3.6 ml, 5.8 mmol) was added dropwise over a period of 5 min at room temperature and then left to stir for 3h. After this time, the reaction mixture was cooled to -12 °C and freshly distilled benzaldehyde (0.67 ml, 6.3 mmol) in THF (10 ml) was added. The reaction mixture was left to stir for 3h at -12 °C. $HCl_{(aq)}$ (1 M, 10 ml) was then added and the aqueous solution extracted with ethyl acetate (3 x 10 ml), then with diethylether (3 x 10 ml), and finally neutralized with $NaOH_{(aq)}$ (2%), to give the precipitation of a solid. This was filtered, washed with cold water and dried under vacuum, to give 1.03g of the pure product (yield 65.4%). White solid.

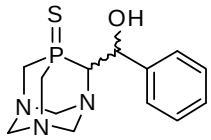


**77**: **$^{1}$H NMR** (400.13 MHz, DMSO-$d_6$): $\delta$ 7.19-7.52, (m, 5H(major) + 5H(minor),Ar); 6.17 (d, $^{3}J_{HH}$= 3.9 Hz, 1H(minor), C*H*Ph); 5.51 (dt, $^{2}J_{HH}$= 7.6 Hz, $^{4}J_{HH}$= 3.8 Hz, 1H(minor), NC*H*$_2$N); 5.39 (ddd, $^{2}J_{HH}$= 12.8 Hz, $^{4}J_{HH}$= 5.8, 2.7 Hz, 1H(major), NC*H*$_2$N); 5.31 (d, $^{3}J_{HH}$= 3.1 Hz, 1H(major), C*H*Ph); 4.99(brd, $^{2}J_{HH}$= 13.0 Hz, 1H(minor), NC*H*$_2$N); 3.81-4.52 (m, 10 H(major) + 9 H(minor), NC*H*$_2$P, NC*H*$_2$N, PC*H*N). **$^{31}P\{^{1}H\}$ NMR** (161.98 MHz, DMSO-$d_6$):$\delta$ -10.49 (s), -14.12 (s). **$^{13}C\{^{1}H\}$ NMR** (100.61 MHz, DMSO-$d_6$): $\delta$ 143.40 (d, $^{2}J_{CP}$= 11.5 Hz, Ar); 143.24 (d, $^{2}J_{CP}$ = 5.55 Hz, Ar); 128.22 (s, Ar); 127.74 (s, Ar); 127.64 (s, Ar); 127.06 (s, Ar); 126.81 (s, Ar); 75.74, (s, *C*HPh); 75.05 (d, $^{2}J_{CP}$= 5.2 Hz, N*C*$H_2$N); 73.81 (d, $^{2}J_{CP}$= 5.9 Hz, N*C*$H_2$N); 71.98 (d, $^{2}J_{CP}$= 8.9 Hz, N*C*$H_2$N); 71.72 (d, $^{2}J_{CP}$= 9.2 Hz, N*C*$H_2$N); 70.17 (d, $^{1}J_{CP}$= 32.2 Hz,

NCHP); 69.13 (d, $^{1}J_{CP}$= 34.5 Hz, NCHP); 67.88 (d, $^{2}J_{CP}$= 13.0 Hz, N*C*$H_2$N); 66.01 (d, $^{2}J_{CP}$= 13.0 Hz, N*C*$H_2$N); 58.42 (d, $^{1}J_{CP}$= 36.3 Hz, N*C*$H_2$P); 58.25 (d, $^{1}J_{CP}$= 35.9 Hz, N*C*$H_2$P); 56.58, (d, $^{1}J_{CP}$= 34.4 Hz, N*C*$H_2$P); 55.67, (d, $^{1}J_{CP}$= 34.8 Hz, N*C*$H_2$P). **GC-MS:** *m/z* (%): 295 (10) [$M^+$], 188 (100) [$C_6H_{11}N_3SP^+$]. **IR** (KBr, $cm^{-1}$): $\nu_{(P=S)}$ 610 (m). **Anal**. Calcd. for $C_{13}H_{18}N_3OPS$ (295.34 $gmol^{-1}$). Found (calcd): C, 52.87 (52.76); H, 6.14 (6.22); N, 14.23 (14.14).

*Synthesis of 4'-(dimethylamino)phenyl-(1,3,5,-triaza-7-phosphatricyclo[3.3.1.1]dec-6-yl) methanol, (PZA-NMe$_2$)* (**75**)

In a 100 mL Schlenk flask, PTA-Li (1.80 g, 11.0 mmol) was suspended in 30 mL of dry THF and maintained in a liquid nitrogen/acetone bath at -78 °C under an inert atmosphere of nitrogen. 4-(dimethylamino)benzaldehyde (1.80 g, 12.1 mmol) was dissolved in 10 mL of dry THF, cooled to 0 °C and transferred *via* cannula to the slurry. The resulting yellow mixture was left at -78 °C for 15 min, then allowed to reach room temperature and stirred for an additional 2h. Then, 0.5 mL of doubly distilled water was added to quench the reaction and the solvent was removed under reduced pressure. The resulting solid was washed with acetone (10 mL) to give a pale yellow powder (2.10 g, 62% yield) containing a mixture of the two diastereoisomers. Silica gel flash column chromatography gave pure product **75** (1.40 g, 41% yield) ($R_f$= 0.23, eluent: MeOH). After fractional crystallization from $CH_2Cl_2$, the pure major diastereoisomer **75a** was obtained (0.77 g, white powder, 23% yield) and fully characterized. Crystals suitable for X-ray diffraction were obtained by the slow evaporation under nitrogen of a solution of **75a** in $CH_2Cl_2$ and EtOH.

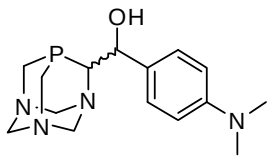


**75: *S*($H_2O$)$_{20°C}$**= 1.9 mg·$mL^{-1}$. Major diastereoisomer (*SR, RS*) (**75a**): **$^1$H NMR** ($CDCl_3$, 400.13 MHz): $\delta$ 7.35 (d, $^{3}J_{HH}$ = 8.6 Hz, 2H, Ar); 6.74 (d, $^{1}J_{HH}$ = 8.6 Hz, 2H, Ar); 5.16 (dd, $^{3}J_{HH}$ = 3.7 Hz, $^{3}J_{HP}$ = 8.4 Hz, 1H, C*H*OH); 4.85 (AB system, $^{2}J_{H_AH_B}$ = 13.4 Hz, 2H, NC*H*$_2$N); 4.57-4.37 (m, 4H, NC*H*$_2$N); 4.29-4.24 (m, 1H, PC*H*$_2$N); 4.15-4.08 (m, 1H, PC*H*$_2$N); 3.90-3.80 (m, 3H, PC*H*$_2$N + PC*H*N); 2.97 (s, 6H, N*Me*$_2$). **$^{31}$P{$^1$H} NMR** ($CDCl_3$, 161.98 MHz): $\delta$ -102.72

(s); ($D_2O$, 121.50 MHz): $\delta$ -99.07 (s). **$^{13}C\{^1H\}$ NMR** (100.61 MHz, $CDCl_3$): $\delta$ 150.42 (s, Ar); 130.51 (s, Ar); 127.24 (s, Ar); 112.30 (s, Ar); 77.64 (d, $^2J_{CP}$ = 6.5 Hz, *C*HOH); 74.20 (s, N*C*$H_2$N); 67.78 (s, N*C*$H_2$N); 65.75 (d, $^1J_{CP}$ = 23.1 Hz, P*C*HN); 51.55 (d, $^1J_{CP}$ = 19.9 Hz, P*C*$H_2$N); 48.43 (d, $^1J_{CP}$ = 24.0 Hz, P*C*$H_2$N); 40.54 (s, N*Me*$_2$). **MS** (nESI$^+$), *m/z* (%): 307.06 (7) [$M^+$], 246.02 (100) [$C_{13}H_{17}N_3P^+$]. **IR** (KBr, $cm^{-1}$): $\nu_{(OH)}$ 3401 (br, s); $\nu_{(arom)}$ 1612 (s), 1525 (s). **Anal**. Calcd. for $C_{15}H_{23}N_4OP$ (306.34 $gmol^{-1}$). Found (calcd): C, 58.67 (58.81); H, 7.55 (7.57); N, 18.58 (18.29).

*Synthesis of (S,R R,S)-4'-(dimethylamino)phenyl-(1,3,5,-triaza-7-phospha-tricyclo[3.3.1.1]dec-6-yl)methanol oxide (O=PZA-NMe$_2$)* (**80**)

In a one-necked round bottomed flask containing ligand **75a** (0.55 g, 1.8 mmol), methanol (140 mL) was added and slightly heated to dissolve the solid. The solution was cooled to room temperature and an excess of aqueous $H_2O_2$ (35%, 260 µL) diluted in ethanol (8 mL) was slowly added. The reaction mixture was stirred at room temperature for 1h when a small amount of a white precipitate appeared. The solvent was then removed by rotary evaporation yielding 0.52 g (90%) of pure product.

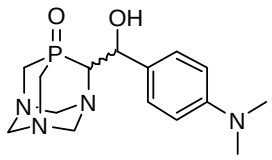


**80: *S*(H$_2$O)$_{20°C}$**= 12.5 mg·mL$^{-1}$. **$^1$H NMR** (400.13 MHz, $D_2O$): $\delta$ 7.33 (d, $^3J_{HH}$ = 8.2 Hz, 2H, Ar); 6.94 (d, $^3J_{HH}$ = 8.2 Hz, 2H, Ar); 5.34 (dd, $^3J_{HP}$ = 10.9 Hz, $^3J_{HH}$ = 3.4 Hz, 1H, C*H*OH); 4.19 (AB system, $^2J_{H_AH_B}$ = 14.0 Hz, 2H, NC*H*$_2$N); 4.31-4.10 (m, 6H, NC*H*$_2$N + PC*H*$_2$N); 3.89-3.77 (m, 3H, PC*H*$_2$N + PC*H*N); 2.79 (s, 6H, N*Me*$_2$). **$^{31}P\{^1H\}$ NMR** (161.98 MHz, $D_2O$): $\delta$ 2.09 (s). **$^{13}C\{^1H\}$ NMR** (100.61 MHz, $D_2O$): $\delta$ 151.44 (s, Ar); 131.44 (d, $^3J_{CP}$ = 7.1 Hz, Ar); 127.57 (s, Ar); 115.52 (s, Ar); 72.97 (d, $^2J_{CP}$ = 2.3 Hz, *C*HOH); 72.44 (d, $^3J_{CP}$ = 6.1 Hz, N*C*$H_2$N); 70.45 (d, $^3J_{CP}$ = 8.4 Hz, N*C*$H_2$N); 68.50 (d, $^1J_{CP}$ = 50.7 Hz; P*C*HN); 64.89 (d, $^3J_{CP}$ = 11.6 Hz, N*C*$H_2$N); 53.31 (d, $^1J_{CP}$ = 52.7 Hz, P*C*$H_2$N); 50.79 (d, $^1J_{CP}$ = 52.0 Hz, P*C*$H_2$N); 40.96 (s, N*Me*$_2$). **IR** (KBr, $cm^{-1}$): $\nu_{(OH)}$ 3227 (br, m); $\nu_{(arom)}$ 1613 (s), 1525 (s); $\nu_{(P=O)}$ 1155 (m). **Anal**. Calcd. for $C_{15}H_{23}N_4O_2P$ (322.34 $gmol^{-1}$). Found (calcd): C, 56.24 (55.89); H, 7.88 (7.19); N, 17.67 (17.38).

*Synthesis of (S,R R,S)-4'-(dimetylamino)phenyl-(1,3,5,-triaza-7-phospha-tricyclo[3.3.1.1]dec-6-yl)methanol sulfide (S=PZA-NMe$_2$)* (**79**)

In a three-necked round bottomed flask equipped with a reflux condenser, ligand **75a** (0.50 g, 1.6 mmol) was dissolved in degassed water (150 mL) and heated to 90 °C to dissolution. An excess of elemental sulfur (0.13 g, 4.1 mmol of S) was added and the suspension refluxed for 90 min under vigorous stirring. The reaction mixture was cooled to room temperature and the precipitate filtered on a Bückner funnel. The solid was washed with hot $CCl_4$ (2 x 3 mL) and dried under vacuum, yielding 0.35 g of pure product as a white solid (65% yield).

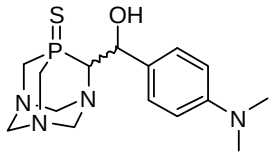

**79**: ***S*(H$_2$O)$_{20°C}$** = 0.5 mg·mL$^{-1}$. **$^1$H NMR** (400.13 MHz, DMSO-$d_6$): $\delta$ 7.30 (d, $^3J_{HH}$ = 8.5 Hz, 2H, Ar); 6.66 (d, $^3J_{HH}$ = 8.5 Hz, 2H, Ar); 5.32 (dd, $^3J_{HP}$ = 10.1 Hz, $^3J_{HH}$ = 3.6 Hz, 1H, C*H*OH); 4.39-4.18 (m, 7H, NC*H*$_2$N + PC*H*$_2$N); 4.00- 3.84 (m, 4H, PC*H*$_2$N + PC*H*N); 2.87 (s, 6H, N*Me*$_2$). **$^{31}$P{$^1$H} NMR** (161.98 MHz, DMSO-$d_6$): $\delta$ -14.07 (s). **$^{13}$C{$^1$H} NMR** (100.61 MHz, DMSO-$d_6$): $\delta$ 150.26 (s, Ar); 130.43 (d, $^3J_{CP}$ = 6.8 Hz, Ar); 128.48 (s, Ar); 112.27 (s, Ar); 74.85 (s, *C*HOH); 73.82 (d, $^3J_{CP}$ = 5.8 Hz, NCH$_2$N); 71.71 (d, $^3J_{CP}$ = 9.2 Hz, NCH$_2$N); 70.17 (d, $^1J_{CP}$ = 31.4 Hz, P*C*HN); 65.92 (d, $^3J_{CP}$ = 12.6 Hz, NCH$_2$N); 58.11 (d, $^1J_{CP}$ = 35.4 Hz, PCH$_2$N); 55.36 (d, $^1J_{CP}$ = 34.5 Hz; PCH$_2$N); 40.73 (s, N*Me*$_2$). **IR** (KBr, cm$^{-1}$): $\nu_{(OH)}$ 3360 (vs); $\nu_{(arom)}$ 1615 (s), 1529 (s); $\nu_{(P=S)}$ 646 (m). **Anal**. Calcd. for $C_{15}H_{23}N_4OPS$ (338.41 gmol$^{-1}$). Found (calcd): C, 53.71 (53.24); H, 6.93 (6.85); N, 16.71 (16.56).

*Synthesis of 1-methylimidazolyl-(1,3,5,-triaza-7-phospha-tricyclo[3.3.1.1]dec-6-yl)methanol (PTA-CH(1-MeIm)OH)* (**76**)

In a Schlenk flask, PTA-Li (2.10 g, 12.9 mmol) was dissolved under nitrogen in dry degassed THF (20 mL) and cooled at -78 $^oC$ by using an alcohol/liquid $N_2$ bath. A separate Schlenk flask was charged with 1-methyl-2-imidazolecarboxaldehyde (1.71 g, 15.4 mmol) dissolved in THF (15 mL) and cooled to -78 °C. The aldehyde solution was added dropwise to the PTA-Li slurry under $N_2$ over a 3 min period. The reaction mixture was stirred at -78 °C for 30 min and then allowed to warm to room temperature. After 12h, the dark orange reaction mixture was quenched by adding

$H_2O$ (3.0 mL) and an orange slurry was obtained. The solvents were removed *in vacuo*, the product was extracted with $CHCl_3$ and the resulting slurry filtered through Celite. The $CHCl_3$ solution was evaporated to dryness and the residue purified by column chromatography on silica ($R_f$ value = 0.17, eluent: MeOH). to give a pale yellow solid. This was washed with THF (10 mL) and benzene (20 mL), and collected on a frit under $N_2$ and finally washed with pentane (25 mL). After drying *in vacuo,* 1.40 g of the product were obtained as an off-white solid (yield 40.7% calculated for PTA-Li). The mixture may be diastereomerically enriched as follows: 300 mg of the off-white powder was dissolved in hot acetone (35 mL) under $N_2$ and filtered while still hot. The resulting solution was put into the freezer at -20 $^{o}$C for 12 h, after which the mother liquor was decanted off leaving 122 mg of a white powder.

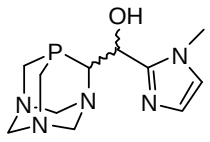


**76**: ***S*(H$_2$O)$_{20°C}$**= 320 mg·mL$^{-1}$. Enriched diastereoisomer: **$^{1}$H NMR** (400.13 MHz, $CDCl_3$): $\delta$ 6.84 (d, $^{3}J_{HH}$= 1.1 Hz, 1H, NCHC*H*NMe-Im); 6.81 (d, $^{3}J_{HH}$= 1.1 Hz, 1H, NC*H*CHNMe-Im); 6.3 (br s, 1H, O*H*); 5.29 (at, *J*= 7.7 Hz, 1H, C*H*ImOH); 4.75 (br d, *J* = 13.7 Hz, 1H, PC*H*CHImOH); 4.62 (br d, $^{1}J_{HH}$= 13.2 Hz, 1H, NC$H_2$N); 4.4-4.5 (m, 3H, NC$H_2$N); 4.20-4.26 (m, 2H, NC$H_2$N); 4.0-4.15 (m, 2H, PC$H_2$N); 3.8-3.9 (m, 2H, PC$H_2$N); 3.74 (s, 3H, N*Me*-Im). **$^{31}$P{$^{1}$H} NMR** (161.98 MHz, $CDCl_3$): $\delta$ -103.39 (s); -104.65 (s). **$^{13}$C{$^{1}$H} NMR** (100.61 MHz, $CDCl_3$): $\delta$ 148.24 (d, $^{3}J_{CP}$= 4.1 Hz, N*C*NMe-Im); 126.56 (s, N*C*=CNMe-Im); 122.22 (s, NC=*C*NMe-Im); 76.33 (s, N*C*N); 74.02 (s, N*C*N); 69.05 (d, $^{2}J_{CP}$= 9.3 Hz, **C*HOH); 67.52 (d, $^{3}J_{CP}$= 2.2 Hz, N*C*N); 63.32 (d, $^{1}J_{CP}$= 21 Hz, P**C*N); 51.25 (d, $^{1}J_{CP}$= 20 Hz, P*C*N); 47.63 (d, $^{1}J_{CP}$= 25 Hz, P*C*N); 33.21 (s, N*Me*-Im). ). **MS** (nESI$^{+}$), *m/z* (%): 268.19 (100) [M$^{+}$]. **IR** ($CH_2Cl_2$, cm$^{-1}$): $\nu_{(OH)}$ 3375 (sh); $\nu_{(C=N)}$ 1604. **Anal**. Calcd. for $C_{11}H_{18}N_5OP$ (267.27 gmol$^{-1}$) Found (calcd): C, 46.41 (49.43); H, 6.98 (6.79); N, 23.26 (26.21).

*Synthesis of 1-methylimidazolyl-(1,3,5,-triaza-7-phospha-tricyclo[3.3.1.1]dec-6-yl)methanol oxide (O=PTA-CH(1-MeIm)OH)* (**81**) – *NMR tube scale*

Ligand PTA-CH(1-MeIm)OH (0.040 g, 0.15 mmol) was dissolved in 1 mL $D_2O$ in the air. The resulting clear solution was then combined with a $H_2O_2$ water solution

(35%, 20 μL) and the system analyzed by $^{31}$P NMR, showing that the phosphine was quantitatively converted into its oxide. The solvent was then removed under vacuum at 30°C and the resulting white residue washed with acetone (3 x 5 mL) and finally dried *in vacuo*, yielding 23.6 mg of pure product (60 % yield).

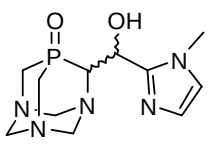

**81**: (enriched diastereoisomer). **$^{1}$H NMR** (400.13 MHz, $D_2O$): $\delta$ 6.94 (d, $^{3}J_{HH}$= 1.1 Hz, 1H, NCHC*H*NMe-Im); 6.81 (d, $^{3}J_{HH}$= 1.2 Hz, 1H, Im, NC*H*CHNMe-Im); 5.57 (at, *J*= 9.0 Hz 1H, PCHC*H*ImOH); 4.62 (m, *J*= 9.0 Hz, 1H, PC*H*CHImOH); 4.1-4.3 (m, 6H, NC$H_2$N); 3.95 (br d, *J*= 14.2 Hz 1H, PC$H_2$N); 3.83 (m, 3H, PC$H_2$N); 3.64 (s, 3H, N*Me*-Im). **$^{31}$P{$^{1}$H} NMR** (161.98 MHz, $D_2O$): $\delta$ 0.59 (s); -0.48 (s). **$^{13}$C{$^{1}$H} NMR** (100.03 MHz, $D_2O$): $\delta$ 145.42 (d, $^{3}J_{CP}$= 10.0 Hz, N*C*NMe-Im); 126.28 (s, N*C*=CNMe-Im); 123.62 (s, NC=*C*NMe-Im); 72.44 (d, $^{3}J_{CP}$= 5.6 Hz, N*C*N); 70.31 (d, $^{3}J_{CP}$= 8.9 Hz, N*C*N); 66.10 (d, $^{1}J_{CP}$= 52 Hz, P***C*N); 65.03 (d, $^{2}J_{CP}$= 11.5 Hz, **C*HOH); 64.65 (s, N*C*N); 53.19 (d, $^{1}J_{CP}$= 54 Hz, P*C*N); 50.41 (d, $^{1}J_{CP}$= 52 Hz, P*C*N); 33.74 (s, N*Me*-Im). **MS** (nESI$^{+}$), *m/z* (%): 284.25 (100) [$M^{+}$]; 306.17 (45)[ $MNa^{+}$]. **IR** (KBr, $cm^{-1}$): $\nu_{(OH)}$ 3367 (sh); $\nu_{(C=N)}$ 1597; $\nu_{(P=O)}$ 1152 (m). **Anal**. Calcd. for $C_{11}H_{18}N_5O_2P$ (283.27 $gmol^{-1}$): C, 46.35 (46.64); H, 5.97 (6.40); N, 23.90 (24.72).

*Synthesis of bis(1-methylimidazolyl)-(1,3,5,-triaza-7-phospha-tricyclo[3.3.1.1]dec-6-yl)methanol (PTA-C(1-MeIm)$_2$OH)* (**82**)

A 100 mL Schlenk flask was charged with PTA-Li (0.49 g, 3.0 mmol) and 15 mL THF and put into a -78 °C alcohol/liquid nitrogen bath. *Bis*-(*N*-methylimidazole-2-yl)ketone (0.65 g, 3.4 mmol) was dissolved in 15 mL of dry degassed THF cooled to -78 °C and added to the PTA-Li slurry under $N_2$. After 30 min at -78 °C, the reaction was allowed to warm to room temperature and left to stir for 12 h. The reaction was then quenched by the addition of doubly distilled $H_2O$ (1 mL) to give an orange slurry. The solvents were removed *in vacuo* and the product extracted with $CHCl_3$. The organic phase was filtered through Celite and evaporated to dryness, obtaining an orange residue. This was extracted with $Et_2O$ under $N_2$ (5 x 50 mL) and the combined solutions were evaporated leaving a pale yellow solid (0.62 g, 59.7 %

yield). The product can be recrystallized from hot $Et_2O$ under $N_2$ to produce white microcrystals after sitting overnight at -20 °C temperature.

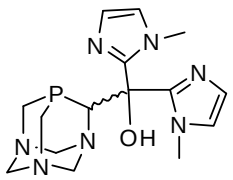

**82**: ***S*(H$_2$O)$_{20°C}$**= 78 mg·mL$^{-1}$. **$^1$H NMR** (400.13 MHz, $CD_2Cl_2$): $\delta$ 6.94 (d, $^3J_{HH}$= 1.1 Hz, 1H, NCHC*H*NMe-Im); 6.90 (d, $^3J_{HH}$= 1.1 Hz, 1H, NCHC*H*NMe-Im); 6.87 (d, $^3J_{HH}$= 1.1 Hz, 1H, NC*H*CHNMe-Im); 6.83 (d, $^3J_{HH}$= 1.1 Hz, 1H, NC*H*CHNMe-Im); 6.24 (br s, 1H, O*H*); 5.55 (br d, *J*= 1.3 Hz 1H, NC*H*$_2$N); 4.77 (br d, *J*= 13.6 Hz, 1H, PC*H*N); 4.63 (AB quartet, *J*= 13.2 Hz, 2H, NC*H*$_2$N); 4.4-4.5 (m, 3H, NC*H*$_2$N); 4.0-4.15 (m, 3H, PC*H*$_2$N); 3.83 (at, *J* = 13.7 Hz, 1H, PC*H*$_2$N); 3.49 (s, 3H, N*Me*$_2$-Im); 3.35 (s, 3H, N*Me*$_2$-Im). **$^{31}$P{$^1$H} NMR** (161.98 MHz, $CD_2Cl_2$): $\delta$ -97.55 (s). **$^{13}$C{$^1$H} NMR** (100.61 MHz, $CD_2Cl_2$): $\delta$ 147.48 (d, $^3J_{CP}$= 4.1 Hz, N*C*NMe-Im); 145.26 (s, N*C*NMe-Im); 125.44 (s, N*C*=CNMe-Im); 124.55 (s, N*C*=CNMe-Im); 124.20 (s, NC=*C*NMe-Im); 124.11 (s, NC=*C*NMe-Im); 78.49 (d, $^2J_{CP}$= 8.1 Hz, C**C*OHIm$_2$); 77.77 (s, N*C*N); 74.24 (d, $^3J_{CP}$= 1.5 Hz, N*C*N); 67.49 (d, $^3J_{CP}$= 3.3 Hz, N*C*N); 62.30 (d, $^1J_{CP}$= 24.4 Hz, P**C*N); 51.94 (d, $^1J_{CP}$= 19.6 Hz, P*C*N); 49.13 (d, $^1J_{CP}$= 23.7 Hz, P*C*N); 34.40 (s, N*Me*-Im); 33.18 (s, N*Me*-Im). ). **MS** (nESI$^+$), *m/z* (%): 348.14 (100) [M$^+$]. **IR** ($CH_2Cl_2$, cm$^{-1}$): $\nu_{(OH)}$ 3358 (sh); $\nu_{(C=N)}$ 1602. **Anal**. Calcd. for $C_{15}H_{22}N_7OP$ (347.37 gmol$^{-1}$). Found (calcd): C, 49.04 (51.87); H, 6.51 (6.38); N, 26.39 (28.23).

*Synthesis of bis(1-methylimidazolyl)-(1,3,5,-triaza-7-phospha-tricyclo[3.3.1.1]dec-6-yl)methanol oxide (O=PTA-C(1-MeIm)$_2$OH)* (**83**) – *NMR tube scale*

Following the same procedure described previously, PTA-C(1-MeIm)$_2$OH (0.033 g, 0.09 mmol) was quantitatively converted into its oxide according to $^{31}$P NMR. After evaporation and washing with absolute ethanol, the pure product was obtained as a white powder ( 26.1 mg, 76.7% yield).

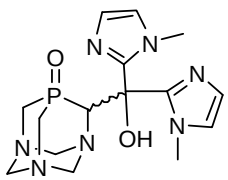

**83**: **$^1$H NMR** (400.13 MHz, $D_2O$): $\delta$ 6.92 (s, 1H, NCHC*H*NMe-Im); 6.90 (s, 1H, NCHC*H*NMe-Im); 6.84 (s, 1H, NCHC*H*NMe-Im); 6.79 (s, 1H, NC*H*CHNMe-Im); 5.57 (br d, *J*= 14.0 Hz, 1H, NC*H*$_2$N); 4.47 (br d, *J*= 14.0 Hz, 1H, PC*H*ClIm$_2$OH); 4.34 (at, *J*= 12.2 Hz, 1H, NC*H*$_2$N); 4.19 (m, 3H, NC*H*$_2$N); 4.08 (br d, *J* = 13.6 Hz, 1H, NC*H*$_2$N); 3.75-3.95 (m, 2H, PC*H*$_2$N); 3.65-3.75 (m, 2H, PC*H*$_2$N); 3.10 (s, 3H, N*Me*-Im); 2.90 (s, 3H, N*Me*-Im).

**$^{31}$P{$^{1}$H} NMR** (161.98 MHz, $D_2O$): $\delta$ -0.20 (s). **$^{13}$C{$^{1}$H} NMR** (100.03 MHz, $D_2O$): $\delta$ 144.64 (d, $^{3}J_{CP}$= 6.7 Hz, N*C*NMe-Im); 143.99 (s, N*C*NMe-Im); 125.43 (s, N*C*=CNMe-Im); 125.17 (s, N*C*=CNMe-Im); 125.14 (s, NC=*C*NCMe-Im); 125.04 (s, NC=*C*NCMe-Im); 75.78 (d, $^{3}J_{CP}$= 2.2 Hz, N*C*N); 74.03 (d, $^{3}J_{CP}$= 4.4 Hz, N*C*N); 70.40 (d, $^{3}J_{CP}$= 8.1 Hz, N*C*N); 68.34 (d, $^{1}J_{CP}$= 53 Hz, P**C*N**);** 65.17 (d, $^{2}J_{CP}$= 13.7 Hz, C**C*OHIm$_2$); 53.92 (d, $^{1}J_{CP}$= 52 Hz, P*C*N); 52.74 (d, $^{1}J_{CP}$= 56 Hz, P*C*N); 33.17 (s, N*Me*-Im); 32.67 (s, N*Me*-Im). **MS** (nESI$^+$), *m/z* (%): 364.17 (100) [M$^+$]; 386.17 (18) [MNa$^+$]. **IR** ($CH_2Cl_2$, cm$^{-1}$): $\nu_{(OH)}$ 3389 (sh); $\nu_{(C=N)}$ 1597; $\nu_{(P=O)}$ 1146 (m). **Anal**. Calcd. for $C_{15}H_{22}N_7O_2P$ (363.35 gmol$^{-1}$). Found (calcd): C, 45.85 (49.58); H, 6.32 (6.10); N, 25.05 (26.98).

### 2.7.2. X-ray diffraction data collection

X-ray data collections for compounds **78** and **75a** were carried out at room temperature by using a CCD diffractometer equipped with the Mo-$K_\alpha$ radiation (0.71073 Å). The program CrysAlis CCD[39] and CrysAlis RED[40] were used for data collection and reduction respectively. Absorption correction was applied through the program ABSPACK.[40] The structure solution obtained by using the direct methods in Sir97.[41] Structure refinement was performed with SHELXL[42] by using the full-matrix least squares method for all the available $F^2$ data. All of the non-hydrogen atoms were refined anisotropically and the H atoms bonded to the Carbon atoms were fixed in calculated positions and refined isotropically with thermal factors 20% larger (50% for the H of the methyl groups) than the atom to which they are bound. The hydrogen atoms of the OH were located in the Fourier difference map and its coordinates were free refined. All calculations were performed under the WINGX package.[43] The molecular drawings were made by using both ORTEP-III for Windows[44] and SCHAKAL97.[45]

*X-ray crystal structure of phenyl-(1,3,5,-triaza-7-phosphatricyclo[3.3.1.1]dec-6-yl) methanol oxide, PZA(O)* (**78**)

The X-ray crystal structure of PZA(O) shows that only the (*R*,*S S*,*R*)-diastereoisomer is present in the asymmetric unit. In the molecular structure, the P atom is tetrahedrally bound to three C atoms and one O atom with O–P–C angles [ave 116.8(3)°] larger than the C–P–C ones [ave 101.2(3)°] (Figure 2.7). The P=O oxygen forms a strong intermolecular hydrogen bond with the OH group of a neighboring PZA(O) molecule [O(1)···O(2) distance= 2.717(6) Å], forming a 1D infinite chain parallel to *b* axis (Figure 2.7). This weak solid-state interaction extends the P(1)–O(2) distance of *ca*. 0.02 Å more than the P–O distance of oxides of PTA.[27a] The P(1)–C(1) and C(1)–N(1) [1.833(6) Å and 1.502(6) Å, respectively] bonds belonging to the upper rim of PZA(O) are slightly longer than the corresponding P(1)–C(2), P(1)–C(3), C(2)–N(2) and C(3)–N(3) bonds of PTA [ave 1.813(6) and 1.489(7) Å, respectively].[46]

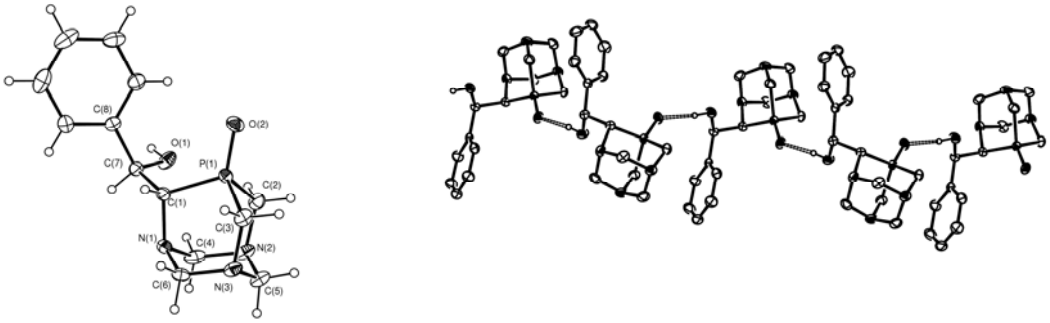


**Figure 2.7.** Asymmetric units of (*R*,*S S*,*R*) PZA(O) (left) and view of 1D infinite chain of **78** parallel to axis b (right). Adapted from ref. 35.

*X-ray crystal structure of (S,R R,S)-4'-(dimethylamino)phenyl-(1,3,5,-triaza-7-phospha-tricyclo[3.3.1.1]dec-6-yl)methanol* (**75a**).

The X-ray structure of **75a** contains both enantiomers *S*,*R* and *R*,*S* in the unit cell. Figure 2.8 shows the ORTEP drawing with selected distances and angles in the caption. As previously noted for other *upper rim* PTA derivatives,[32,35] the P1-C1

bond [1.8695(16) Å] is slightly longer than the other two P-C bonds [P1-C2= 1.859(2) Å, P1-C3= 1.8503(19) Å], while the C-N bonds of the adamantane cage do not differ significantly.

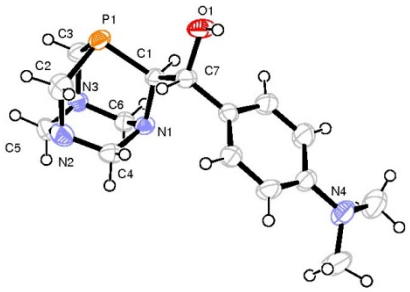


**Figure 2.8.** ORTEP view of **75a**. Ellipsoids drawn at 50% probability level. Selected bond lengths (Å) and angles (°) for **75a**: P1-C1=1.8695(16); P1-C2=1.859(2); P1-C3=1.8503(19); C1-N1=1.476(2); C2-N2=1.476(3); C3-N3=1.470(2); C7-O1=1.420(2); C1-C7=1.531(2); C7-C1-P1=111.62(11); N1-C1-C7=112.86(13). Adapted from ref. 34.

The hydroxyl group forms a strong intramolecular hydrogen bond with a nitrogen atom of a neighbouring molecule [O1···N3#1 = 2.7821(19) Å, where the symmetry transformation used to generate the equivalent atom is: *x*, -1+*y*, *z*]. A 1D infinite chain can be recognized along the *b* axis as previously shown in Figure 2.4. The π···π stacking of the (dimethylamino)phenyl groups holds together two of the 1D chains. The latter supramolecular units arrange themselves in the space as seen from the packing diagram (Figure 2.6) along the *b* axis. The existence of a hydrogen bond 1D chain was also found in O=PTA-CH($C_6H_4OCH_3$)OH[32] and PZA(O)[35] while two O=PTA-C($C_6H_4OCH_3$)$_2$OH and four PTA-C($C_6H_4OCH_3$)$_2$OH units forms an hydrogen bonded dimer and tetramer, respectively. Interestingly, while the intermolecular hydrogen bonding network is established between the P=O oxygen and the hydroxyl group of a neighboring PZA(O) molecule, for **75a** this occurs by connecting the hydroxyl OH group with a N atom of the adamantane cage.

## 2.8. References


[1] Daigle, D. J.; Pepperman Jr., A. B.; Vail, S. L. *J. Hetrocycl Chem*. **1974**, *11*, 407-408.
[2] Fluck, E.; Forster, J. E. *Chem Z*. **1975**, *99*, 246
[3] Daigle, D. J. *Inorg*. *Synth*. **1998**, *32*, 40-42.
[4] Caporali, M.; Gonsalvi, L.; Peruzzini, M.; Zanobini, F. *e-EROS Encyclopedia of Reagents for Organic Synthesis*, John Wiley & Sons, Ltd. **2010** and unpublished results.
[5] Daigle, D. J. *Inorg*. *Synth*. **1998**, *32*, 42-43.
[6] Siele, V. I. *J. Heterocycl*. *Chem*. **1977**, *14*, 337-339.
[7] Daigle, D. J.; Pepperman, A. B. Jr. *J. Heterocycl*. *Chem*. **1975**, *12*, 579-580.
[8] Fischer, K. J.; Alyea, E. C.; Shahnazarian, N. *Phoshorus*, *Sulfur and Silicon* **1990**, *48*, 37-40.
[9] Cowley, A. H.; Lattman, M. ; Striklen, P.M.;Verkade, J. G. *Inorg*. *Chem*. **1982**, *21*, 543-549.
[10] Otto, S. ; Ionescu, A.; Roodt, A. *J. Organomet*. *Chem*. **2005**, *690*, 4337-4342.
[11] Benhammou, M. ; Kraemer, R. ; Germa, H.; Majoral, J. P.; Navech, J. *Phosphorus Sulfur* **1982**, *14*, 105-119.
[12] Darensbourg, D. J.; Decuir, R. J.; Reibenspies, J. H. In *Aqueous Organometallic Chemistry and Catalysis*. Horvart, I. T.; Joó, F. Eds.; Kluwer, Dordrecht: **1995**, p 61.
[13] Daigle, D. J. *Inorg*. *Synth*. **1998**, *32*, 43-45.
[14] Forward, J. M.; Staples, R. J.; Liu, C. W.; Fackler, J. P. *Acta Crystallogr* C **1997**, *53*, 195-197.
[15] Fluck, E.; Förster, J. E.; Weidlein, J.; Hädicke, E. *Z. Naturforsch*. **1997**, *32b*, 499-506.
[16] Forward, J. M.; Staples, R. J.; Fackler, J. P. Jr. *Z. Kristallogr*. **1996**, *211*, 129.
[17] Kovács, J.; Joó, F.; Bényei, A. C.; Laurenczy, G. *Dalton Trans*. **2004**, 2336-2340.
[18] Romerosa, A.; Campos-Malpartida, T.; Lidrissi, C.; Saoud, M.; Serrano-Ruiz, M.; Peruzzini, M.; Garrido-Cárdenas, J. A.; García-Maroto, F. *Inorg*. *Chem*. **2006**, *45*, 1289-1298.
[19] Smoleński, P.; Kirillov, A. M.; Guedes da Silva, M. F. C.; Pombeiro, A. J. L. *Acta Cryst*. E64, **2008**, o556.
[20] Kirillov, A. M.; Smoleński, P.; Guedes da Silva, M. F. C.; Pombeiro, A. J. L. *Acta Cryst*. E64, **2008**, o496-o497.
[21] Mena-Cruz, A.; Lorenzo-Luis, P.; Romerosa, A.; Saoud, M.; Serrano-Ruiz, M. *Inorg*. *Chem*. **2007**, *46*, 6120-6128.
[22] Kirillov, A. M.; Smoleński, P.; Haukka, M.; Guedes da Silva, M. F. C.; Pombeiro, A. J. L. *Organometallics* **2009**, *28*, 1683-1687.
[23] Krogstad, D. A.; Ellis, G. S.; Gunderson, A. K.; Hammirich, A. J.; Rudolf, J. W.; Halfen, J. A. *Polyedron*, **2007**, *26*, 4093-4100.
[24] Krogstad, D. A. ; Gohmann, K. E.; Sunderland, T. L.; Geis, A. L.; Bergamini, P.; Marvelli, L.; Young, V. G. Jr. *Inorg*. *Chim*. *Acta* **2009**, *362*, 3049-3055.
[25] Bolaño, S.; Albinati, A.; Bravo, J.; Gonsalvi, L.; Peruzzini, M. *Inorg*. *Chem*. *Comm*. **2006**, *9*, 360-363.
[26] Frost, B. J.; Mebi, C. A.; Gingrich, P. W. *Eur*. *J*. *Inorg*. *Chem*. **2006**, 1182-1189.
[27] (a) Fluck, E.; Weissgraber, H. J. *Chem.-Ztg*. **1977**, *101*, 304. (b) Assman B.; Angermaier, K.; Schmidbaur, H. *J. Chem*. *Soc*. *Chem*. *Comm*. **1994**, 941-942. (c) Assman, B.; Angermaier, K.; Paul, M.; Riede, H.; Schmidbaur, H. *Chem*. *Ber*. **1995**, *128*, 891-900.
[28] Huang, R.; Frost, B. J. *Inorg*. *Chem*. **2007**, *46*, 10962-10964.
[29] Darensbourg, D. J.; Ortiz. C. G.; Kamplain, J. W. *Organometallics* **2004**, *23*, 1747-1754.
[30] Frank, A. W.; Daigle, D. J. *Phosphorus Sulfur* **1981**, *10*, 255-259.
[31] Wong, G. W.; Harkreader, J. L.; Mebi, C. A.; Frost, B. J. *Inorg*. *Chem*. **2006**, *45*, 6748-6755.
[32] Wong, G. W.; Lee, W-C.; Frost, B. J. *Inorg*. *Chem*. **2008**, *47*, 612-620.
[33] Six, N.; Guerriero, A.; Landy, D.; Peruzzini, M.; Gonsalvi, L.; Hapiot, F. Monflier, E. manuscript in preparation.
[34] Guerriero A.; Erlandsson, M.; Ienco, A.; Krogstad, D. A.; Peruzzini, M.; Reginato, G.; Gonsalvi, L. submitted for publication.
[35] Erlandsson, M.; Gonsalvi, L.; Ienco, A.; Peruzzini, M. *Inorg*. *Chem*. **2008**, *47*, 8-10.
[36] Krogstad, D. A.; Guerriero A.; Ienco, A.; Peruzzini, M.; Bosquain, S. S.; Reginato, G.; Gonsalvi, L. manuscript in preparation.
[37] Chen, X-M.; Xu, Z-T. Polyhedron **1995**, *14*, 319-322.

[38] Perrin, D.D; Armarego, W. L. F. *Purification of Laboratory Chemicals*, 3rd ed. **1988**.
[39] CrysAlys CCD, Oxford Diffraction Ltd., Version 1.171.31.2 (release 07-07-2006 CrysAlis171.NET).
[40] CrysAlys RED, Oxford Diffraction Ltd., Version 1.171.31.2 (release 07-07-2006 CrysAlis171.NET).
[41] Altomare, A.; Burla, M. C.; Camalli, M.; Cascarano, G. L.; Giacovazzo, C.; Guagliardi, A.; Moliterni, A. G. C.; Polidori, G.; Spagna, R. *J. Appl. Crystallogr.* **1999**, *32*, 115-119.
[42] Scheldrick, G. M. *SHELX97*. University of Göttingen: Göttingen, Germany, **1997**.
[43] Farrugia, L. J. *J. Appl. Crystallogr*. **1999**, *32*, 837-838.
[44] Burnett, M. N.; Johnson, C. K. ORTEP-III; Oak Ridge National Laboratory, Oak Ridge, TN, **1996**.
[45] Keller, E. *SCHAKAL97*, University of Freiburg, Germany, **1997**.
[46] Jogun, K. H.; Stezowski, J. J.; Fluck, E.; Weidlein, J. *Phosphorus Sulfur Relat. Elem*. **1978**, *4*, 199-204.

# *Chapter 3*

# Iridium complexes containing PTA and its "*upper rim*" derivatives

## 3.1 Overview

This chapter describes the coordination chemistry of PTA and two new *upper-rim* modified derivatives, PZA (**74**) and PZA-$NMe_2$ (**75**), to iridium. In the first part, the literature data regarding the syntheses of water-soluble Ir-PTA complexes and their use as catalysts are reviewed. In the second part, the syntheses of two new Ir(I) complexes containing PZA and PZA-$NMe_2$ are described together with the results of the test catalytic hydrogenations of selected substrates using the abovementioned complexes under different mild catalytic protocols. The chapter ends with the experimental section related to the synthesis and characterization of the complexes and the description of catalytic tests.

## 3.2 Introduction

The coordination chemistry of PTA and its derivatives to iridium has been less investigated than other late transition metals such as ruthenium, rhodium and palladium.[1] This is due to the generally believed minor catalytic activity of iridium complexes in comparison to the other platinum group transition metals.

The iridium carbonyl cluster $Ir_4(CO)_7(PTA)_5$ is the first example of Ir(0) water-soluble PTA complex appeared in the literature.[2] This was synthesized by refluxing $Ir_4(CO)_{12}$ with an excess of PTA in toluene. The product was isolated as a red-orange solid and characterized by X-ray diffraction analysis (Figure 3.1).

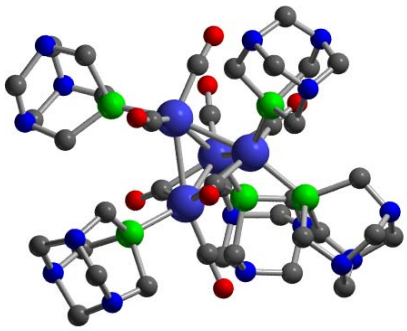

**Figure 3.1.** X-ray crystal structure of $Ir_4(CO)_7(PTA)_5$. Selected bond distances (Å): Ir-Ir= 2.757; Ir-C= 2.10; Ir-P= 2.290 (see atom colour code).

The complex *trans*-$[IrCl(CO)(PTA)_2]$[3] represents an important water-soluble analogue of Vaska's complex $[IrCl(CO)(PPh_3)_2]$,[4] which was tested as a catalyst for a large variety of reactions, including hydrogenation of $\alpha,\beta$-unsaturated ketones.[5] *Trans*-$[IrCl(CO)(PTA)_2]$ was prepared from the reaction of $[Ir(cod)Cl]_2$[6] (cod = 1,5-cyclooctadiene) with an excess of PTA in hexane/$CH_2Cl_2$ under an atmosphere of carbon monoxide. This compound is insoluble in common organic solvents and only moderately soluble in DMSO. Two related compounds, i.e. $[IrCl(CO)(PTA)_3]$ and $[Ir(CO)(PTA)_4]Cl$ were also synthesized by Krogstad *et al*.[3a] The first complex was obtained in 54% yield by refluxing *trans*-$[IrCl(CO)(PPh_3)_2]$ with three equivalents of PTA in absolute ethanol. Doubling the amount of the phosphine, the same experiment gave an increase of the yield to 77%. The lower yield was due to the formation of mixed $PPh_3$/PTA complexes. It was shown that the formation of these

side-products can be avoided by reacting $[Ir(cod)Cl]_2$ under an atmosphere of CO with six equivalents of PTA. The resulting air-stable green product showed low solubility in DMSO and it was insoluble in other organic solvents, such as alcohols and ethers. Interestingly, the reaction between $[Ir(cod)Cl]_2$ and two equivalents of PTA led to a mixture of *trans*-$[IrCl(CO)(PTA)_2]$ and $[IrCl(CO)(PTA)_3]$ as confirmed by IR spectroscopy showing two CO stretching frequencies at 1939 and 1950 $cm^{-1}$ respectively. The complex *trans*-$[IrCl(CO)(PTA)_2]$ is moderately soluble in DMSO and gives a singlet at -58.1 ppm in the corresponding $^{31}P$ NMR spectrum, whereas $[IrCl(CO)(PTA)_3]$ was separated as insoluble solid from the mixture in this solvent. It was suggested that in solution both compounds are in equilibrium with free PTA (Scheme 3.1). In aqueous solution, the tris-PTA derivative rapidly converted into the ionic tetrakis-PTA complex $[Ir(CO)(PTA)_4]Cl$. This compound could also be formed by reaction of $[IrCl(CO)(PTA)_3]$ with one equivalent of PTA in 95% ethanol or by refluxing Vaska's complex with excess PTA in 95% ethanol. In contrast to the tris-PTA related compound, $[Ir(CO)(PTA)_4]Cl$ has an appreciable solubility in water (6 x $10^{-2}$ M), while it is only sparingly soluble in DMSO and methanol and insoluble in other organic solvents. Scheme 3.1 summarizes the synthetic routes to these iridium(I) PTA complexes. Some iridium PTA complexes were protonated at N-PTA atoms in aqueous solutions by reaction with aqueous HCl. In the case of $[IrCl(CO)(PTA)_3]$, the reaction with 0.1 M HCl gave a mixture of two new compounds, *cis*-$[IrCl_2(PTAH)_2(PTA)_2]Cl_3$ and *cis*-$[Ir(H)_2(PTAH)_4]Cl_5$, which could be readily separated in the solid state by fractional crystallization. The latter was also synthesized by direct acidification of $[Ir(CO)(PTA)_4]Cl$ (Scheme 3.1). The behaviour showed by these iridium complexes is somehow in contrast with previous reports which have shown that the treatment of Pd,[7] Pt,[8] Ru and Rh[9] PTA complexes with strong acids led to the rapid protonation of the nitrogen atoms of the ligand inhibiting protonation of the metal centre, that could be achieved[8] in the case of $Pt(PTA)_4$ only when 1 equivalent of aqueous HCl was slowly added dropwise to the solution of the complex in water. The protonation mechanism proposed by the authors[3a] entails CO dissociation from the axial coordination site and replacement

by free PTA present in solution from the dissociative equilibrium involving $[IrCl(CO)(PTA)_3]$ and *trans*-$[IrCl(CO)(PTA)_2]$. The transient 16-electron $[Ir(PTA)_4]^+$ cation reacts with HCl to form the hydride intermediate $[Ir(H)Cl(PTA)_4]^+$ from which the two final complexes originate.

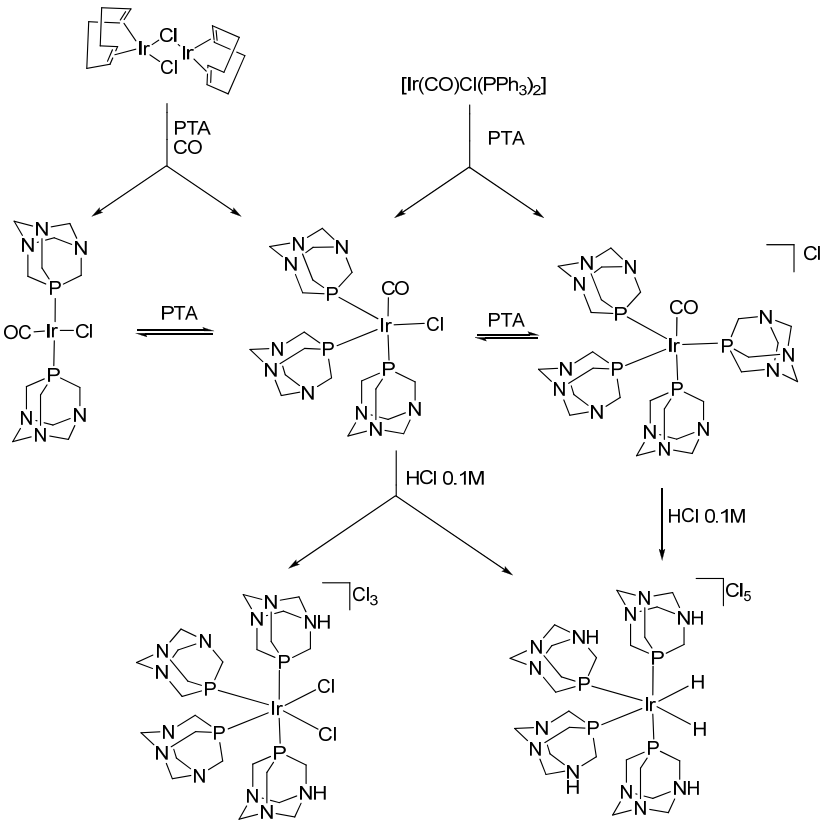


**Scheme 3.1.** Syntheses of higher substituted iridium PTA complexes. Adapted from ref.1a.

Another recent example[10] of Ir(I) PTA complex reported in the literature is $[Ir(cod)(PTA)_3]Cl$. This was synthesized in high yield (83%) reacting $[Ir(cod)Cl]_2$ with six equivalents of PTA in $CH_2Cl_2$. The complex readily precipitated from the solution as an air-stable solid. The slow diffusion of ethanol in the aqueous solution of the complex gave crystals suitable for X-ray analysis that showed a distorted square-pyramidal geometry around the metal centre (Figure 3.2). This structure shows similar geometry[11] to $[Ir(cod)(PMe_3)_3]Cl$ and both represent the only examples of square pyramid for five-coordinate $[Ir(cod)(phosphine)_3]^+$ complexes, whereas all the others are trigonal bypiramidal.[12]

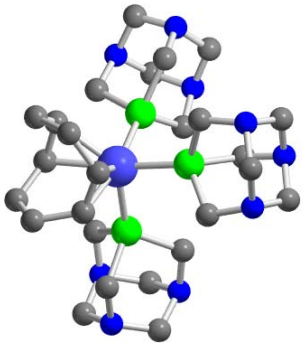

**Figure 3.2.** X-ray crystal structure of $[Ir(cod)(PTA)_3]Cl$. Selected bond lengths (Å): Ir-P1= 2.349(2); Ir-P2= 2.3007(18); Ir-P3= 2.3022(18); Ir-C1= 2.208(7); Ir-C2= 2.194(7); Ir-C5= 2.226(7); Ir-C6= 2.236(7). Adapted from ref. 10 (see atom colour code).

$[Ir(cod)(PTA)_3]Cl$, $[IrCl(CO)(PTA)_3]$ and $[Ir(CO)(PTA)_4]Cl$ were tested as catalysts for the intramolecular hydroamination of 4-pentyn-1-amine in water at 50 °C (Scheme 3.2).[10]

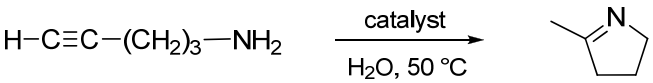


**Scheme 3.2.** Intramolecular hydroamination of 4-pentyn-1-amine.[10]

All three compounds catalyzed the cyclization to the same degree suggesting the formation of similar four-coordinate active catalytic species in solution. While the carbonyl complexes are known[3a] to dissociate a ligand to produce $[Ir(PTA)_3(CO)]^+$ in water, $[Ir(cod)(PTA)_3]Cl$ is thought to dissociate the cod ligand to form $[Ir(PTA)_3]^+$ and to coordinate a solvent molecule resulting in the four-coordinate complex $[Ir(H_2O)(PTA)_3]^+$.[10]

Water-soluble PTA iridium(III) complexes $[Cp^*IrCl_2(PTA)]$ and $[Cp^*IrCl(PTA)_2]Cl$ ($Cp^*$= $\eta^5$-$C_5Me_5$) were prepared[13] in high yields by direct reaction of the iridium dimer $[Cp^*Ir(\mu\text{-}Cl)Cl]_2$[14] with PTA (Scheme 3.3). The former was obtained by reacting two equivalents of the phosphine in $CH_2Cl_2$ at room temperature, the latter by using four equivalents of PTA under reflux in 2-methoxyethanol. Both compounds showed a satisfactory solubility in water ($S_{25\,°C}$= 2.2 and 27.5 mg $cm^{-3}$, respectively) and were tested as catalyst precursors for the reduction of hydrogen carbonate to formate in

aqueous solution.[13] The catalytic tests were carried out under a pressure of 100 bar of $H_2$ in the pH range 5.9-10 and in the temperature range 70-100°C. Under these conditions, [Cp*$IrCl_2$(PTA)] formed quantitatively the dihydride [Cp*$Ir(H)_2$(PTA)] as indicated by the $^1H$ and $^{31}P\{^1H\}$ NMR analyses, but it proved to be essentially inactive as catalyst. On the contrary, the precatalyst [Cp*$IrCl(PTA)_2$]Cl showed to be moderately active, performing best at high temperatures (80 °C) and in slightly basic aqueous solution (pH 9), giving the corresponding monohydride $[Cp^*IrH(PTA)_2]^+$ complex as the catalytically active species.[13]

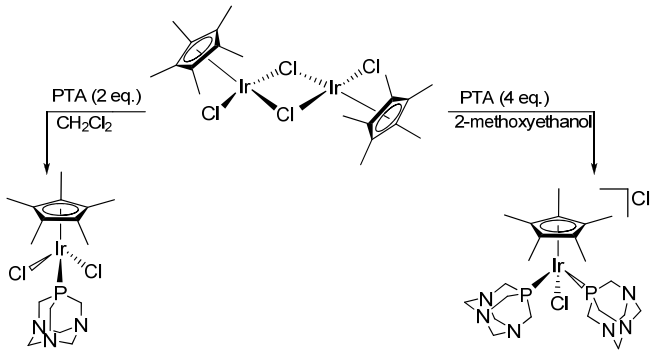


**Scheme 3.3.** Synthesis of water-soluble iridium(III) complexes [Cp*$IrCl_2$(PTA)] and [Cp*$IrCl(PTA)_2$]Cl.[13]

As part of kinetic studies on the mechanism of the selective C-H bond activation within a supramolecular host by an iridium guest, the water-soluble complex [Cp*Ir(Me)($PMe_3$)(PTA)](OTf) was synthesized.[15] The complex was prepared by addition of a stoichiometric amount of PTA to a water solution of [Cp*Ir(Me)(OTf)($PMe_3$)]. When the resulting complex was added to a solution of the host $Na_{12}[Ga_4L_6]$ (L= catechol amide), no encapsulation was observed, indicating that the guest was too large to fit within the host cavity (Scheme 3.4).

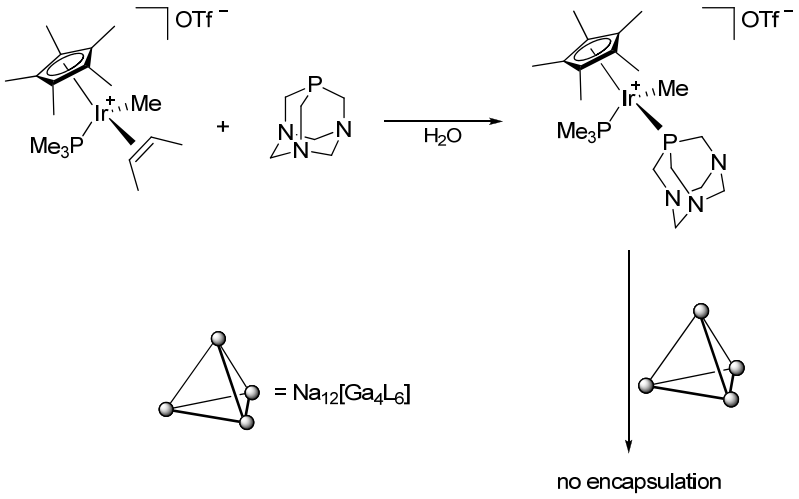


**Scheme 3.4.** Synthesis and kinetic studies on [Cp*Ir(Me)($PMe_3$)(PTA)](OTf). Adapted from ref. 15.

## 3.3 New iridium(I) complexes with PTA "*upper rim*" derivatives

In the literature, the only example of an iridium complex with an "*upper rim*" modified PTA derivative is the iridium(III) complex ($\kappa^1$-P)-[Cp*$IrCl_2$(PZA)] (**84**) prepared in our laboratories[16] in order to test the coordination ability of the new ligand PZA to a transition metal fragment with a piano-stool geometry. The reaction of [Cp*Ir($\mu$-Cl)Cl]$_2$ with the diastereomeric mixture (1:1 ratio) of PZA in $CH_2Cl_2$ led to the formation[14] of [Cp*$IrCl_2$(PZA)] as shown in Scheme 3.5.

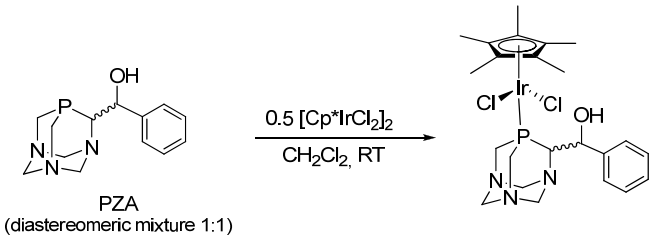


**Scheme 3.5.** Synthesis of complex ($\kappa^1$-P)-[Cp*$IrCl_2$(PZA)]. Adapted from ref.16

The complex showed only a moderate solubility in water ($S_{20\,°C}$= 1.8 mg $mL^{-1}$) in line with the value measured for the corresponding PTA complex [Cp*$IrCl_2$(PTA)] ($S_{20\,°C}$= 2.2 mg·$mL^{-1}$). By slow concentration of a dichloromethane/ethanol solution of [Cp*$IrCl_2$(PZA)], crystals suitable for X-ray analysis were obtained. This revealed as

expected a P-coordination of the PZA ligand to Ir, with the metal octahedral geometry completed by the two chloride ligands and the Cp* ring occupying three contiguous sites of the coordination polyhedron (Figure 3.3). The hydroxyl group is disordered over two sites and forms an intramolecular hydrogen bond with chlorine atoms [O(1a)-Cl(2)= 3.319(6); O(1b)-Cl(2)= 3.112(6) Å]. The $^{31}P\{^{1}H\}$ NMR spectrum showed two singlets of comparable intensity at -59.3 and -72.3 ppm, indicating that both diastereoisomers were present as observed in the solid state.

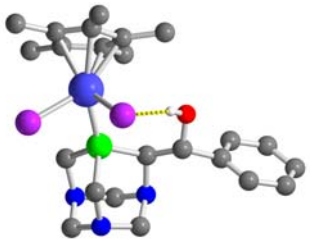

**Figure 3.3.** X-ray crystal structure of the complex ($\kappa^1$-P)-[$Cp^*IrCl_2$(PZA)] (see atom colour code). Adapted from ref.16.

In consideration of these results,[16] we decided to test the coordination ability of both PZA and PZA-$NMe_2$ toward Ir(I), in view of the potential activity in catalysis. Two new Ir(I) complexes have been synthesized (Scheme 3.6).[17] By reacting the diastereomeric mixture (1:1) of PZA with 0.5 equivalents of the dimer $[Ir(cod)Cl]_2$ in a dichloromethane/toluene solution at room temperature, the complex ($\kappa^1$-P)-[IrCl(cod)(PZA)] (**85**) was obtained as a racemic mixture of two diastereoisomers as expected from the diastereomeric nature of the ligand. This was confirmed by the $^{31}P\{^{1}H\}$ NMR spectrum showing two singlets at -64.9 and -58.5 ppm in 1:1 ratio. Remarkably, this complex shows a good solubility in water ($S_{20\,°C}$= 3.4 mg/L).

In the case of PZA-$NMe_2$, the racemic mixture containing only the isolated *S*,*R R*,*S* diastereoisomer (**75a**) was reacted with a $CH_2Cl_2$ solution of $[Ir(cod)Cl]_2$ at room temperature. After the addition of pentane, a yellow solid precipitated from the dichloromethane solution, corresponding to the complex ($\kappa^1$-P)-[Ir(cod)Cl{(*S*,*R R*,*S*)-(PZA-$NMe_2$)}](**86**), which also showed a good solubility in water at room temperature ($S_{20\,°C}$= 1.7 mg $mL^{-1}$).

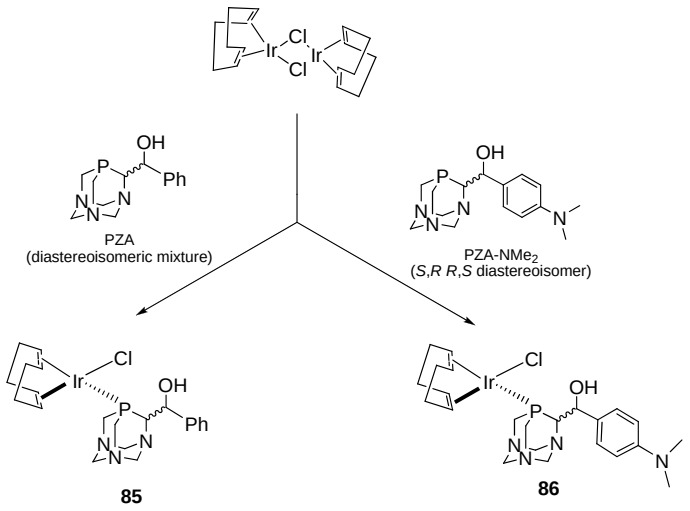


**Scheme 3.6.** Synthesis of ($\kappa^1$-P)-[Ir(cod)(L)] (L= PZA, **85**; PZA-$NMe_2$, **86**).[17]

Complex **86** exhibits a singlet at -64.1 ppm in the $^{31}P\{^1H\}$ NMR spectrum, confirming the presence of a single diastereoisomer. $^{13}C\{^1H\}$ NMR data were diagnostic to confirm the formation of the complex, in particular the CH signals of cod ligand at 98.1 (d, $^2J_{CP}$= 12.8 Hz) and 97.1 (d, $^2J_{CP}$= 13.7 Hz) reflecting the lack of symmetry in the molecule. Failing so far all the attempts to get crystals suitable for the solid-state analysis by X-ray diffraction, elemental analysis and ESI-MS data were useful to establish the formulas of both complexes. ESI-MS spectra for $[Ir(cod)(PZA)]^+$ and $[Ir(cod)\{(S,R\ R,S)\text{-}(PZA\text{-}NMe_2)\}]^+$ ($m/z$= 564.2 and $m/z$= 605.3, respectively), confirmed the lability of chloride ligand which dissociates easily upon ionization. Conductivity measurements were also performed for **86**. These revealed that in $CH_2Cl_2$ the complex is not substantially conductive in nature, probably due to the strong coordination of the chloride ligand to iridium. On the contrary, partial dissociation was noted in polar solvents such as methanol and in water/methanol 2:1 v/v, however giving low conductivity values (0.032 mS/cm and 0.026 mS/cm, respectively).

The lability of the chloride ligand in polar solvents together with the presence of an oxygen donor atom close to phosphorus in PZA and PZA-$NMe_2$, imply that $\kappa^2$-P,O chelate analogues of **85** and **86** in solution are possible. In order to verify this, two different experiments were carried out as shown in Scheme 3.7. Initially, a $CH_2Cl_2$

solution of **86** was reacted at room temperature with a chloride scavenger, thallium(I) hexafluorophosphate ($TlPF_6$). The initial yellow colored solution turned immediately to red and, after removing TlCl by filtration, an aliquot of the solution was analysed by $^{31}P\{^1H\}$ NMR. The spectra showed a singlet at -17.0 ppm and a septet at *ca*. -144 ppm, due to $PF_6$. The low field NMR shift observed from the initial value of -64.1 ppm to -17.0 ppm can be attributed both to the formation of a cationic species such as $[Ir(cod)(PZA\text{-}NMe_2)]^+$ and to the Δ-ring contribution upon $\kappa^2$-P,O coordination.[18] In a second experiment, *S*,*R R*,*S* PZA-$NMe_2$ (**75a**) was reacted in a 1:1 ratio with the Ir(I) precursor[19] $[Ir(cod)_2]PF_6$ in $CH_2Cl_2$ at room temperature. Also in this case, after 2h stirring the $^{31}P\{^1H\}$ NMR analysis of an aliquot of the solution showed the presence of the singlet at -17.0 ppm. Interestingly, when the solution was left standing for 24 h at room temperature, this singlet at -17.0 ppm decreased in intensity and a new signal at -53.4 ppm appeared. This could be explained by a possible equilibrium involving $\kappa^1$-P and $\kappa^2$-P,O species in solution. Considering the relative acidity of the OH proton and the basicity of the N atoms in the triazacyclohexane bottom rim on the PTA skeleton (Scheme 3.7), a protonation-deprotonation intermolecular equilibrium could be responsible for the observed reactivity and consistent with the NMR data reported above. Unfortunately, we have not been able to obtain any isolated pure product. Both precipitation induced by the addition of another solvent and evaporation to dryness of $CH_2Cl_2$ caused the decomposition of the compounds evidenced by the presence of many peaks in the region from -34 to -76 ppm in the $^{31}P\{^1H\}$ NMR spectrum, due to unidentified by-products.

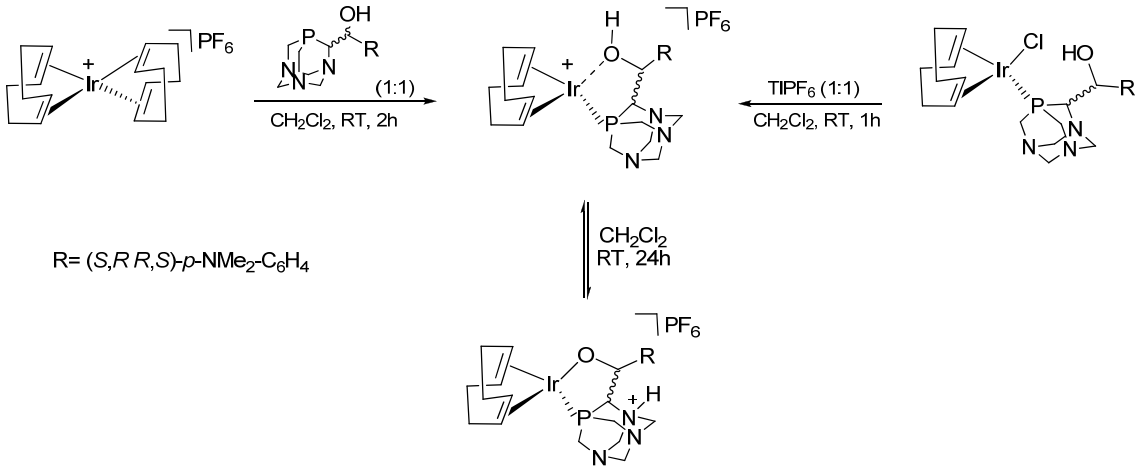


**Scheme 3.7.** Experiments on complex **86**. Adapted from ref. 17.

DFT theoretical calculations were used to verify the possible replacement of Cl with OH group on the ligand for the two complexes **85** and **86**, and the energies associated with a protonation-deprotonation intermolecular equilibrium. The effects of the substituent of the phenyl group on the geometrical parameters was found relatively small. For this reason, only the results relatively to complex **86** were considered.

The theoretical study concerned several models, in particular the structures related to **86a**, a model of **86** with $\kappa^1$-P coordination mode of PZA-$NMe_2$ and **86b**, having a $\kappa^2$-P,O bonding mode of the ligand, were optimized. In all the conformers **86a-86c** reported in Figure 3.4, the Ir atoms are square planar coordinated. Regarding the intermolecular equilibrium, the four nitrogen atoms of the molecule could act as proton acceptors for the hydroxyl deprotonation. Consequently, four different models were studied, but considering the lower basicity of the aromatic substituted amines compared to alkyl ones, probably the protonation involved a nitrogen atom of the cage (model **86c**, Figure 3.4).

From an energetic point of view **86c** model, in which N1 was protonated, resulted to be more stable and in turn, **86b** more stable (11.7 kcal/mol) respect to **86c** These results were consistent with the experimental data and with the protonation-deprotonation equilibrium assumed above (Scheme 3.7).

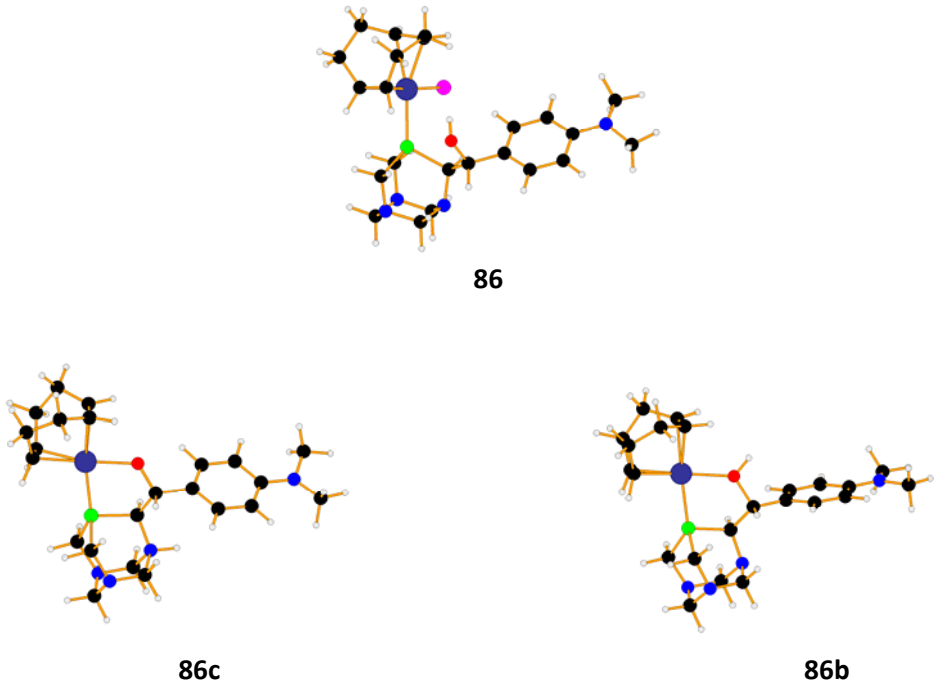


**Figure 3.4.** Optimized structures for the isomers $\kappa^1$-P (86a) and $\kappa^2$-P (86b, 86c). Color code: O= red; N= blue; P= green Cl= pink; Ir= dark blue (large sphere); C= black; H= white. Adapted from ref. 17.

## 3.4 Hydrogenation reactions catalyzed by the new iridium(I) complexes

As already discussed, only few Ir complexes bearing PTA have been tested in catalytic applications. In particular, the compounds $[IrCl(CO)(PTA)_3]$, $[Ir(CO)(PTA)_4]Cl$ and $[Ir(cod)(PTA)_3]Cl$ catalyzed the cyclization of 4-pentyn-1-amine to 2-methyl-pyrroline in water at 50 °C,[10] while the complex $[Cp^*IrCl(PTA)_2]Cl$ was tested as catalyst for $CO_2/HCO_3^-$ reduction to formate under mild conditions.[13]

Nevertheless, many iridium complexes are reported in the literature to catalyze chemo- and enantioselective hydrogenations[20] and transfer hydrogenations[21] of compounds of industrial interest such as alkenes, aldehydes and α,β-unsaturated carbonyl compounds in water or biphasic systems. In most of these complexes, bidentate ligands such as 4,4'-dihydroxy-2,2'-bipyridine,[22] Noyori's (*R*,*R*)-TsDPEN and derivatives, [(*R*,*R*)-TsDPEN= (1*R*,2*R*)-*N*-(*p*-toluenesulfonyl)-1,2-

diphenylethylenediamine)],[23] or other systems such as $[Ir(cod)Cl]_2$ in combination with HSA (HSA= human serum albumin),[24] are used. No examples of Ir-PTA complexes have been reported so far to perform these catalytic transformations. However, many ruthenium and rhodium compounds containing PTA have been extensively used in hydrogenation reactions.[1] For instance, Ru-PTA complexes show relatively high activity in the reduction of C=O bond of aromatic aldehydes such as benzaldeyde using sodium formate[9] or in the chemoselective hydrogenation of benzylidene acetone (BZA) to 4-phenyl-butan-2-one in biphasic system at mild temperatures under hydrogen pressure.[25] Again, both Ru- and Rh-PTA complexes were found to be able to reduce selectively cinnamaldehyde (CNA) at the C=O bond for Ru and at the C=C bond in the case of Rh, giving cinnamyl alcohol and saturated aldehyde, respectively. Rh-PTA compounds were also active catalysts for two-phase hydroformylation of 1-hexene [26]

Therefore, the two new Ir complexes [Ir(cod)Cl(PZA)] (**85**) and [Ir(cod)Cl{(*S*,*R R*,*S*)-(PZA-$NMe_2$)}](**86**) have been tested as catalysts for chemoselective hydrogenations of model substrates.[17] Specifically, the α,β-unsaturated aldehydes cinnamaldehyde (CNA) and benzilidene acetone (BZA), a cyclic ketones (2-cyclohexene-1-one) and a simple aryl alkyl ketone (acetophenone) were used as model substrates (Scheme 3.8). The catalytic tests have been carried out using different reduction protocols. The first experiments were made using sodium formate which is one of the mildest reducing agents and allows for a wide compatibility between functional groups and water solubility. In order to insure the formation of a homogeneous phase at moderate temperatures and due to the poor solubility of some substrates in water, catalytic reactions were often performed in a water/methanol solvent mixture.

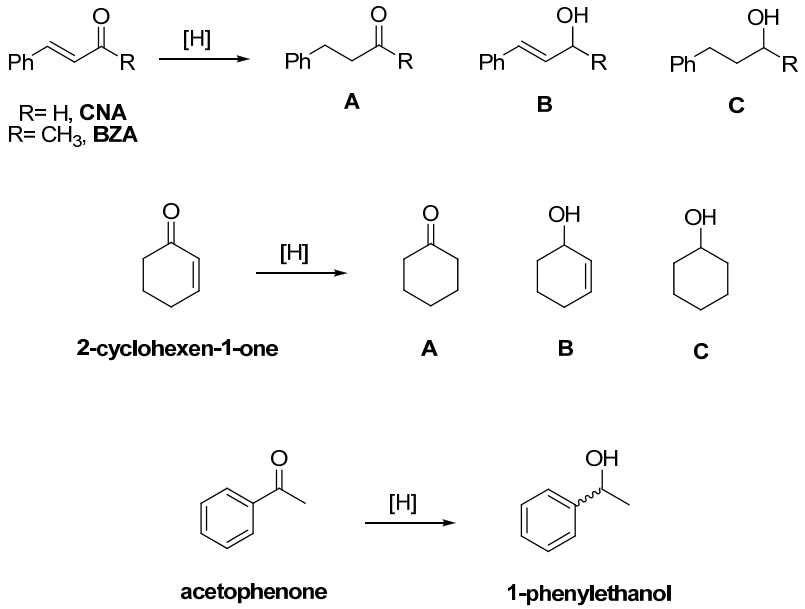


**Scheme 3.8.** Hydrogenation test reactions.[17]

Transfer hydrogenation (TH) of cinnamaldehyde using $HCO_2Na$ in water/methanol was generally carried out at a catalyst/CNA = 1/100 ratio varying parameters such as temperature, reaction time and solvent mixture composition to observe the effects on activity and selectivity. The different conditions and the results of the catalytic tests using **85** and **86** are reported in Tables 3.1 and 3.2.

**Table 3.1.** Transfer Hydrogenation of CNA with catalyst **85** using $HCO_2Na/H_2O$/MeOH. Adapted from ref. 17.

| | | | | yields | | | |
|---|---|---|---|---|---|---|---|
| Cat. | Solvent | % Conv (h) | T (°C) | % A[b] | % B[b] | % C[b] | TON(avg) |
| **85** | MeOH:$H_2O$ (1:2) | 99.1 (6) | 80 | 0.0 | 69.4 | 29.7 | 99 |
| **85** | MeOH:$H_2O$ (1:2) | 94.7 (6) | 60 | 4.4 | 72.9 | 17.4 | 95 |
| **85** | MeOH:$H_2O$ (1:2) | 98.6 (16) | 60 | 0.7 | 72.0 | 25.9 | 99 |
| **85** | MeOH:$H_2O$ (1:2) | 99.4 (8) | 40 | 0.7 | 77.6 | 21.1 | 99 |
| **85**[c] | MeOH:$H_2O$ (1:2) | 96.4 (8) | 40 | 0.6 | 84.7 | 11.1 | 483 |
| **85**[d] | MeOH:$H_2O$ (1:2) | 45.9 (8) | 40 | 5.1 | 39.5 | 1.3 | 459 |
| **$[Ir(cod)Cl]_2$**[e] | MeOH:$H_2O$ (1:2) | 99.9 (8) | 80 | 0.0 | 50.6 | 49.3 | 100 |
| **$[Ir(cod)Cl]_2$**[e] | MeOH:$H_2O$ (2:1) | 99.9 (8) | 60 | 0.0 | 58.2 | 41.7 | 100 |
| **$[Ir(cod)Cl]_2$**[e] | MeOH:$H_2O$ (1:2) | 25.9 (8) | 40 | 3.1 | 22.3 | 0.5 | 26 |

[a] Conditions: CNA, 0.75 mmol; catalyst, 7.5 x $10^{-3}$ mmol; $HCO_2Na$, 7.5 mmol; total volume of solvents, 6 mL
[b] GC values based on pure samples. A = hydrocinnamaldehyde; B = cinnamol; C = 3-phenyl-1-propanol
[c] catalyst/substrate ratio, 1:500; [d] catalyst/substrate ratio, 1:1000
[e] CNA, 1.50 mmol; catalyst, 7.5 x $10^{-3}$ mmol; $HCO_2Na$, 15 mmol

**Table 3.2.** Transfer Hydrogenation of CNA with catalyst **86** using $HCO_2Na/H_2O$/MeOH.Adapted from ref. 17.

| Cat. | Solvent | % Conv (h) | T (°C) | yields | | | TON(avg) |
|---|---|---|---|---|---|---|---|
| | | | | % A[b] | % B[b] | % C[b] | |
| **86** | MeOH:$H_2O$ (1:1) | 60.0 (6) | 80 | 5.1 | 44.0 | 10.9 | 60 |
| **86** | MeOH:$H_2O$ (1:1) | 48.0 (6) | 60 | 8.8 | 32.7 | 6.5 | 48 |
| **86** | MeOH:$H_2O$ (1:1) | 99.5 (16) | 60 | 0.0 | 71.4 | 28.1 | 99 |
| **86** | MeOH:$H_2O$ (2:1) | 15.6 (1) | 60 | 6.0 | 9.1 | 0.5 | 16 |
| **86** | MeOH:$H_2O$ (2:1) | 55.0 (6) | 60 | 8.6 | 40.2 | 6.2 | 55 |
| **86** | MeOH:$H_2O$ (2:1) | 98.7 (16) | 60 | 1.7 | 68.7 | 28.3 | 99 |
| **86**[c] | MeOH:$H_2O$ (2:1) | 49.5 (6) | 60 | 5.4 | 42.6 | 1.5 | 248 |
| **86**[c] | MeOH:$H_2O$ (2:1) | 97.1 (16) | 60 | 1.7 | 80.5 | 14.9 | 486 |
| **86** | MeOH:$H_2O$ (1:2) | 25.0 (6) | 40 | 4.4 | 19.1 | 1.4 | 25 |
| **86** | MeOH:$H_2O$ (1:1) | 33.4 (6) | 40 | 6.3 | 25.6 | 1.5 | 33 |
| **86**[c] | MeOH:$H_2O$ (2:1) | 48.2 (6) | 40 | 4.6 | 43.1 | 0.5 | 241 |
| **86**[c] | MeOH:$H_2O$ (2:1) | 66.7 (16) | 40 | 4.8 | 59.8 | 2.1 | 334 |
| **$[Ir(cod)Cl]_2$**[e] | MeOH:$H_2O$ (1:2) | 99.9 (8) | 80 | 0.0 | 50.6 | 49.3 | 100 |
| **$[Ir(cod)Cl]_2$**[e] | MeOH:$H_2O$ (2:1) | 99.9 (8) | 60 | 0.0 | 58.2 | 41.7 | 100 |
| **$[Ir(cod)Cl]_2$**[e] | MeOH:$H_2O$ (1:2) | 25.9 (8) | 40 | 3.1 | 22.3 | 0.5 | 26 |

[a] Conditions: CNA, 0.75 mmol; catalyst, 7.5 x $10^{-3}$ mmol; $HCO_2Na$, 7.5 mmol; total volume of solvents, 6 mL
[b] GC values based on pure samples. A = hydrocinnamaldehyde; B = cinnamol; C = 3-phenyl-1-propanol
[c] catalyst/substrate ratio, 1:500; [d] catalyst/substrate ratio, 1:1000
[e] CNA, 1.50 mmol; catalyst, 7.5 x $10^{-3}$ mmol; $HCO_2Na$, 15 mmol

The first catalytic tests were carried out with both compounds at high temperature (80 °C), obtaining after 6 hours high conversions (99% for catalyst **85** and 60% for catalyst **86**), yielding a mixture of cinnamol and 3-phenyl-1-propanol (2:1 and 4:1 ratios, respectively). In both cases, the formation of a black precipitate was observed after 1 hour, suggesting that the complexes probably decompose under these conditions. A control test using $[Ir(cod)Cl]_2$ showed that in this case the black precipitate formed at 80 °C after few seconds. This observation suggests that the formation of catalytically active phosphine oxide-stabilized metal nanoparticles cannot be ruled out. This was indirectly evidenced by $^{31}P$ NMR analysis of aliquots of the reaction mixture catalyzed by complex **86**, which showed the presence of the uncoordinated phosphine oxide species (**80**) after 1 hour. When the tests were repeated at 60 °C, the complex **85** showed almost the same conversion after 6h and

16h (95% and 99%, respectively). This result, together with the formation of a small amount of a black solid in the reaction mixture, again suggested a possible dissociation of the precatalyst under the conditions used. As expected, the selectivity was again toward the hydrogenation of C=O bond (final selectivity: 26% in 3-phenyl-1-propanol *vs* 72% for cinnamol) and this selectivity was retained in the catalytic run at 40 °C after 8h. With catalyst **85** (0.5 mol%) a maximum TON of 483 was observed.

At 60 °C, with complex **86** high conversion was achieved after 16 h (>98%) with *ca*. 70% selectivity to cinnamol, either using a solvent mixture MeOH/$H_2O$ 1:1 or MeOH/$H_2O$ 2:1. At this temperature, by monitoring the reaction at 1, 6 and 16h, it was evident that the hydrogenation of the C=C bond was faster than that of the C=O bond and the hydrocinnamaldehyde initially formed was then reduced to the fully hydrogenated product. Also in the case of catalyst **86**, the highest TON of 486 was recorded by using a catalyst load of 0.5% mol, resulting in a maximum conversion of *ca*. 97% after 16h and a 83% selectivity to cinnamol. This selectivity was maintained also at 40 °C, but at this temperature the highest conversion achieved was 67% after 16h using 0.5% mol of catalyst.

By comparing the results obtained using **85** and **86** and those obtained using $[Ir(cod)Cl]_2$ (Tables 3.1 and 3.2), it can be observed that catalysts **85** and **86** allow to use mild catalytic conditions, maintaining high selectivity and high TON values.

As described above, the formation of a black precipitate was observed under catalytic conditions, especially at high temperatures. To avoid this and enhance the stability of the complex, tests were repeated using catalyst **86** and adding 2 equivalents of free ligand PZA-$NMe_2$ (**75a**) to the reaction mixture. The catalytic tests were performed in MeOH/$H_2O$ 1:1 v/v, at 80, 60 and 40 °C and the results obtained are reported in Table 3.3. At all temperatures, complete conversion was achieved after 24h and no formation of black precipitate was noted. However, the selectivity changed if compared to the original tests and, if at 80 °C the selectivity to cinnamol was still higher, it reversed in favor of the formation of 3-phenyl-1-propanol at 60 and 40 °C. These results could suggest the formation of the Ir

bis(phosphine) complexes in the presence of an excess of free ligand, albeit no direct proof for the existence of such derivatives has been obtained so far.

**Table 3.3.** Transfer Hydrogenation of CNA with catalyst **86** using $HCO_2Na/H_2O/MeOH$ in presence of an excess of free ligand.

| Cat. | Solvent | % Conv (h) | T (°C) | yields % A[b] | % B[b] | % C[b] | TON(avg) |
|---|---|---|---|---|---|---|---|
| **86** | MeOH:$H_2O$ (1:1) | 100 (24) | 80 | 0.0 | 56 | 44 | 100 |
| **86** | MeOH:$H_2O$ (1:1) | 99.5 (24) | 60 | 0.0 | 33.6 | 65.9 | 101 |
| **86** | MeOH:$H_2O$ (1:1) | 100 (24) | 40 | 1 | 29.6 | 69.4 | 100 |

[a] Conditions: CNA, 0.75 mmol; catalyst, 7.5 x $10^{-3}$ mmol; PZA-$NMe_2$, 1.5 x $10^{-2}$ mmol; $HCO_2Na$, 7.5 mmol; total volume of solvents, 6 mL
[b] GC values based on pure samples. A = hydrocinnamaldehyde; B = cinnamol; C = 3-phenyl-1-propanol.

Transfer hydrogenation tests with catalyst **86** using the system $HCO_2Na$ in water/methanol were then performed using two different ketones, the α,β-unsaturated ketone benzylidene acetone (BZA) and the cyclic ketone 2-cyclohexen-1-one (Table 3.4). The catalytic runs were carried out by using a catalyst/substrate = 1/100 ratio at 60 °C for BZA and at 80 °C for 2-cyclohexen-1-one. In the first case, the maximum conversion after 24h was *ca* 55%, while for the cyclic ketone the maximum conversion after 24h was *ca* 69%. Contrary to what observed for cinnamaldehyde, in the case of ketones, the hydrogenation was selective for the C=C bond, giving the corresponding saturated ketones as main products of the reaction.

**Table 3.4.** TH of BZA and 2-cyclohexen-1-one with catalyst **86** using $HCO_2Na/H_2O/MeOH$.

| Solvent | Substrate | % Conv (h) | yields T (°C) | % A[b] | % B[b] | % C[b] | TON(avg) |
|---|---|---|---|---|---|---|---|
| MeOH:$H_2O$ (2:1)[a] | BZA | 25.5 (5) | 60 | 21.1 | 4.4 | 0.0 | 26 |
| MeOH:$H_2O$ (2:1)[a] | BZA | 55.1 (24) | 60 | 43.7 | 11.5 | 0.0 | 55 |
| MeOH:$H_2O$ (1:1)[a] | 2-cyclohexen-1-one | 38.3 (5) | 80 | 37.0 | 0.2 | 1.1 | 38 |
| MeOH:$H_2O$ (1:1)[a] | 2-cyclohexen-1-one | 69.3 (24) | 80 | 61.8 | 0.3 | 7.2 | 69 |

[a] Conditions: CNA, 0.75 mmol; catalyst, 7.5 x $10^{-3}$ mmol; $HCO_2Na$, 7.5 mmol; total volume of solvents, 6 mL
[b] GC values based on pure samples. For BZA, A= 4-phenyl-2-butanone; B= 4-phenyl-3-buten-2-ol; C= 4-phenyl-2-butanol. For 2-cyclohexen-1-one, A=cyclohexanone; B=2-cyclohexen-1-ol; C=cyclohexanol.

The more commonly used catalytic protocol using KOH/$^{i}$PrOH was then applied for comparison in the presence of catalyst **86** for the hydrogenation tests of 2-cyclohexen-1-one and acetophenone (Table 3.5). The tests were performed at 80 °C with a catalyst /substrate ratio 1/500.

In the case of 2-cyclohexen-1-one, the use of this stronger reducing agent KOH gave after 24h almost complete reduction (*ca*. 91%) to cyclohexanol with TON = 455. Remarkably, the selectivity was different to that obtained by the system $HCO_2Na$ in water/methanol. Using KOH/$^{i}$PrOH, under the same conditions, acetophenone was also reduced to 1-phenylethanol (*ca*. 95% conversion) with a maximum TON of 475.

**Table 3.5.** TH of 2-cyclohexen-1-one and acetophenone with catalyst **86** using KOH/$^{i}$PrOH.

| | | | yields | | | | |
|---|---|---|---|---|---|---|---|
| Solvent | Substrate | % Conv (h) | T (°C) | % A[b] | % B[b] | % C[b] | TON(avg) |
| $^{i}$PrOH[a] | 2-cyclohexen-1-one | 82.2 (5) | 80 | 23.7 | 0.7 | 57.8 | 415 |
| $^{i}$PrOH[a] | 2-cyclohexen-1-one | 91.3 (24) | 80 | 16.4 | 0.6 | 74.3 | 455 |
| $^{i}$PrOH[a] | acetophenone | 79.2 (5) | 80 | 79.2 | - | - | 395 |
| $^{i}$PrOH[a] | acetophenone | 94.9 (24) | 80 | 94.9 | - | - | 475 |

[a] Conditions: substrate, 4.40 mmol; catalyst, 8.8 x $10^{-3}$ mmol; KOH, 0.88 mmol; $^{i}$PrOH, 8.8 mL.
[b] GC values based on pure samples. For 2-cyclohexen-1-one, A=cyclohexanone; B=2-cyclohexen-1-ol; C=cyclohexanol. For acetophenone, A=1-phenylethanol.

Finally, the reduction of acetophenone, 2-cyclohexen-1-one and cinnamaldehyde was tested using a mixed hydrogenation/transfer hydrogenation protocol based on $^{t}$BuOK/$^{i}$PrOH under hydrogen pressure at room temperature. This procedure already applied to acetophenone in previous studies,[27] was tested using [Ir(cod)Cl{(*S*,*R R*,*S*)-(PZA-$NMe_2$)}](**86**) as catalyst and the results are reported in the following table (Table 3.6).

**Table 3.6.** Hydrogenation of acetophenone, 2-cyclohexen-1-one and CNA with **86** under $H_2$ pressure. Adapted from ref. 17.

| Entry | Substrate | % Conv (h) | yields | | | TON(avg) |
|---|---|---|---|---|---|---|
| | | | % A[b] | % B[b] | % C[b] | |
| 1 | acetophenone[a] | 78.3 (4) | 78.3 | - | - | 195 |
| 2 | acetophenone[a] | 94.1 (6) | 94.1 | - | - | 240 |
| 3 | acetophenone[c] | 19.6 (4) | 19.6 | - | - | 47 |
| 4 | acetophenone[d] | < 1 (4) | < 1 | - | - | 0 |
| 5 | acetophenone[e] | < 1 (4) | < 1 | - | - | 0 |
| 6 | 2-cyclohexen-1-one[a] | 60.1 (4) | 42.5 | 0.9 | 16.7 | 150 |
| 7 | 2-cyclohexen-1-one[d] | 19.8 (4) | 17.1 | 0.0 | 2.7 | 50 |
| 8 | 2-cyclohexen-1-one[e] | 17.1 (6) | 17.1 | 0.0 | 0.0 | 43 |
| 9 | cinnamaldehyde[a] | 96.4 (4) | 1.5 | 85.4 | 9.5 | 240 |
| 10 | cinnamaldehyde[e] | 9.3 (4) | 8.4 | 0.9 | 0.0 | 22 |

[a] Conditions: substrate, 1.75 mmol; catalyst, $7.0 \times 10^{-3}$ mmol; $^t$BuOK , 0.35 mmol; $^i$PrOH, 2 mL. $p(H_2)$, 30 bar, 25 °C. [b] GC values based on pure samples. For acetophenone, A=1-phenylethanol. For 2-cyclohexen-1-one, A=cyclohexanone; B=2-cyclohexen-1-ol; C=cyclohexanol. For cinnamaldehyde: A=hydrocinnamaldehyde; B=cinnamol; C=3-phenyl-1-propanol.
[c] as above, catalyst $[Ir(cod)Cl]_2$. [d] as above, no catalyst. [e] as above, no base.

Under these catalytic conditions, acetophenone gave almost complete conversion already after 6h (*ca*. 94%), but without either the catalyst or the base, the substrate was not reduced as confirmed by blank runs (no catalyst, entry 4; no base, entry 5). $[Ir(cod)Cl]_2$ performed poorly with *ca*. 20% conversion after 4h, whereas catalyst **86** performed fairly better (*ca*. 78% conversion, TON= 195). In the case of 2-cyclohexen-1-one, the control runs showed some conversion in the presence of $[Ir(cod)Cl]_2$ (entries 7 and 8), but it was still lower than that obtained in the presence of **86** (*ca*. 60% conversion at 4h). Under these catalytic conditions, the selectivity was again for the reduction of C=C bond as previously observed using $HCO_2Na/H_2O$/MeOH (Table 3.4), thus the main product of hydrogenation was cyclohexanone. Finally, cinnamaldehyde was efficiently reduced to cinnamol (entry 9, 89% selectivity, TON= 240), with 96% conversion after 4h. Also in this case, the presence of the base was necessary to get high conversion as showed by the blank experiment (entry 10), where the catalytic test performed without base gave only *ca*. 9% conversion.

## 3.5 Conclusions

The two iridium(I) complexes ($\kappa^1$-P)-[IrCl(cod)(PZA)] (**85**) and ($\kappa^1$-P)-[Ir(cod)Cl{(*S*,*R* *R*,*S*)-(PZA-$NMe_2$)}](**86**) have been synthesized and fully characterized in solution. They have shown a good solubility in water and represent the first examples of Ir(I) water-soluble complexes bearing an *upper rim* PTA-derivative as phosphine ligand. Their reactivity and catalytic activity have been investigated. A combination of experimental and theoretical data suggest that in solution the $\kappa^1$-P-[IrCl(cod)(L)] may easily displace the chloride ligand to form the cationic $\kappa^2$-P,O-[Ir(cod)(L)]+, which in turn may be in equilibrium with an isomer containing the ligand L in a zwitterionic $NH^+\cdots O^-$ form. Moreover, water molecules are likely to act as proton shuttles as recently demonstrated for metal hydrides formation from [Cp'RuCl$(PTA)_2$] (Cp'= $\eta^5$-$C_5H_5$, $\eta^5$-$C_5Me_5$) in water.[28] The precatalysts were tested in homogeneous hydrogenation reactions of several $\alpha,\beta$-unsaturated aldehydes and ketones including acetophenone using different mild reduction protocols. In the case of cinnamaldehyde, both complexes showed selective reduction of C=O bond to cinnamol with average TON up to 483 *via* transfer hydrogenation system by using $HCO_2Na$ as reducing agent. On the contrary, in the case of ketones, benzylidene acetone (BZA) and the cyclic ketone 2-cyclohexen-1-one, hydrogenation performed with $HCO_2Na$ was selective for the C=C bond, giving the corresponding saturated ketones as main products of the reaction. A combined hydrogenation/transfer hydrogenation protocol, run at room temperature in $^i$PrOH under a pressure of 30 bar $H_2$ and in the presence of $^t$BuOK as base, gave promising results in the reduction of acetophenone to *rac*-1-phenylethanol, of 2-cyclohexen-1-one to cyclohexanol and also of cinnamaldehyde to cinnamol (max. selectivity 89%). Work is in progress to obtain chirally pure versions of PZA and PZA-$NMe_2$ ligands and then of the Ir(I) corresponding complexes, to extend the scope of the catalytic test to the enantioselective version.

## 3.6 Experimental Section

### 3.6.1 Synthetic procedures

All details about general synthetic procedures and characterization of compounds are reported in the experimental section of Chapter 2. $[Ir(cod)Cl]_2$ was prepared as described in the literature.[6] 1,5-cyclooctadiene (cod) was bought from commercial suppliers and used without purification. In the case of complex [Ir(cod)Cl(PZA)] (**n**), the spectroscopic data are referring to the mixture of two diastereoisomers in 2:1 ratio and when distinguishable, the values for minor isomer are reported in brackets. Conductivities were measured with an Orion model 990101 conductance cell connected to a model 101 conductivity meter. GC analyses were performed on a Shimadzu 2010 gas chromatograph (with polar column) equipped with a flame ionization detector and a VF-WAXms capillary column (30 m, 0.25 mm i.d., 0.25 µm film thickness); on a Shimadzu GC-14A gas chromatograph (with apolar column) equipped with flame ionization detector and a SPB-1 Supelco fused silica capillary column (30 m, 0.25 mm i.d., 0.25 µm film thickness); and on a Shimadzu GC-17A gas chromatograph (with a chiral column Lipodex-E Macherey-Nagel) equipped with a flame ionization detector (50 m, 0.25 mm i.d., 0.40 mm o.d.).

*Synthesis of $[Ir(cod)Cl]_2$,* (**87**)

In a three-necked round-bottomed flask equipped with a condenser, $IrCl_3 \times 3H_2O$ (4.0 g, 11.3 mmol) was dissolved under nitrogen in a mixture of degassed ethanol (68 mL) and water (34 mL). 1,5-cyclooctadiene (cod, 12 mL, 98 mmol) was added by syringe. The reaction mixture was stirred and refluxed for 24h, during which time a red-orange precipitate formed. This was collected by filtration, washed with cold methanol and dried *in vacuo* (2.1 g, 55% yield).

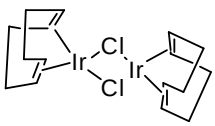


**87: Anal**. Calcd. for $C_{16}H_{24}Cl_2Ir_2$ (671.70 $gmol^{-1}$). Found (calcd): C 28.69 (28.61); H 3.67 (3.60).

*Synthesis of [Ir(cod)Cl(PZA)],* (**85**).

Under an inert atmosphere of nitrogen, a solution of $[Ir(cod)Cl]_2$ (0.26 g, 0.4 mmol) in toluene (5 mL) was added by cannula to a solution of the ligand PZA (**75**) (0.20 g, 0.8 mmol) in $CH_2Cl_2$ (10 mL). The solution was left stirring at room temperature for 1h, after which time the volume was reduced to approximately 5 mL, resulting in the formation of an orange precipitate. This was collected by filtration, washed once with cold toluene and then twice with *n*-pentane. Finally, the solid was dried under vacuum (0.33 g, 74% yield).

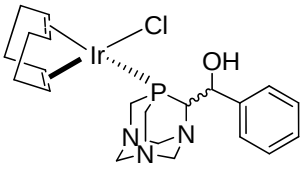


(diastereoisomeric mixture 1:2 ratio)

**85**: ***S*(H$_2$O)**$_{20°C}$= 3.4 mg mL$^{-1}$. **$^1$H NMR** (400.13 MHz, $CD_2Cl_2$): $\delta$ 7.13-7.42 (m, 5H, Ar); 5.32-5.26 (5.68-5.63) (m, 2H, NC*H*$_2$N); 5.18-5.09 (m, 2H, cod + C*H*OH); 5.08-4.84 (m, 3H, cod); 4.62-4.43 (m, 2H, NC*H*$_2$N); 4.38-4.19 (m, 3H, NC*H*$_2$N + PC*H*N); 4.12-3.84 (m, 4H, PC*H*$_2$N); 2.32-2.08 (m, 4H, cod); 1.94-1.64 (m, 4H, cod). **$^{31}$P{$^1$H} NMR** (161.98 MHz, $CD_2Cl_2$): $\delta$ -64.97 (-58.50) (s). **$^{13}$C{$^1$H} NMR** (100.61 MHz, $CD_2Cl_2$): $\delta$ 140.88 (140.97) (s, Ar); 128.26 (128.02) (s, Ar); 127.89 (127.36) (s, Ar); 127.15 (126.91) (s, Ar); 97.93 (d, $^2J_{CP}$ = 16.9 Hz, cod); 97.20 (d, $^2J_{CP}$= 17.5 Hz, cod); 75.65 (s, N*C*H$_2$N); 73.83 (d, $^3J_{CP}$= 7.7 Hz, N*C*H$_2$N); 72.83 (s, N*C*H$_2$N); 67.65 (d, $^1J_{CP}$= 41.9 Hz, P*C*HN); 67.48 (d, $^2J_{CP}$= 28.8 Hz, *C*HOH); 49.59 (49.98) (d, $^1J_{CP}$= 24.4 Hz, P*C*H$_2$N); 44.82 (46.0) (d, $^1J_{CP}$= 23.0 Hz, P*C*H$_2$N); 34.60 (34.26) (s, cod); 33.11 (33.66) (s, cod); 29.58 (28.95) (s, cod); 28.59 (27.98) (s, cod). **MS** (nESI$^+$), *m/z*: 564.2 [Ir(cod)(PZA)]$^+$. **IR** (KBr, cm$^{-1}$): $\nu_{(OH)}$ 3433 (br, s); $\nu_{(arom)}$ 1610 (s), 1524 (s). **Anal**. Calcd for $C_{21}H_{30}ClIrN_3OP$ (599.13 gmol$^{-1}$) Found: (calc.) C, 41.86 (42.10); H, 4.94 (5.05): N, 7.06 (7.01).

*Synthesis of [Ir(cod)Cl{(S,R R,S)-(PZA-NMe$_2$)}]* (**86**).

A Schlenk tube was charged under nitrogen with $[Ir(cod)Cl]_2$ (0.22 g, 0.3 mmol) and ligand **75a** (0.20 g, 0.6 mmol). Dry degassed $CH_2Cl_2$ (15 mL) was added and the resulting yellow solution was stirred at room temperature for 1h 30min. The solution was then concentrated under vacuum to half of the volume and dry *n*-pentane (10 mL) was added. The resulting yellow precipitate was filtered on a frit,

washed with cold *n*-pentane and dried under vacuum yielding 0.26 g of the title complex (67% yield).

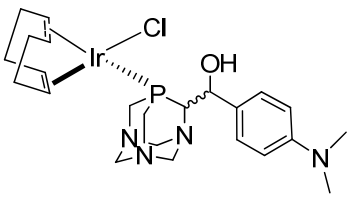


**86**: ***S*(H$_2$O)$_{20°C}$**= 1.7 mg·mL$^{-1}$. **$^1$H NMR** (300.13 MHz, $CDCl_3$): $\delta$ 7.33 (d, $^3J_{HH}$ = 8.6 Hz, 2H, Ar); 6.72 (d, $^3J_{HH}$= 8.6 Hz, 2H, Ar); 5.30-5.16 (br m, 2H, NC*H*$_2$N + cod); 5.04-5.01 (m, 1H, cod); 4.67-4.44 (m, 6H, NC*H*$_2$N + PC*H*N + C*H*OH); 4.35-3.87 (m, 7H, cod + PC*H*$_2$N); 2.95 (s, 6H, N*Me*$_2$); 2.25-1.68 (m, 8H, C*H*$_2$, cod). **$^{31}$P{$^1$H} NMR** (121.50 MHz, $CDCl_3$): $\delta$ -64.09 (s); (121.50 MHz, $D_2O$): $\delta$ -18.12 (s). **$^{13}$C{$^1$H} NMR** (75.47 MHz, $CDCl_3$): $\delta$ 150.36 (s, Ar); 127.91 (s, Ar); 127.56 (d, $^3J_{CP}$= 6.9 Hz, Ar); 112.26 (s, Ar); 98.07 (d, $^2J_{CP}$= 12.8 Hz, cod); 97.13 (d, $^2J_{CP}$= 13.7 Hz, cod); 75.74 (d, $^3J_{CP}$= 4.2 Hz, N*C*H$_2$N); 73.98 (d, $^3J_{CP}$= 6.0 Hz, N*C*H$_2$N); 72.97 (d, $^3J_{CP}$= 3.9 Hz, N*C*H$_2$N); 67.52 (d, $^1J_{CP}$= 17.3 Hz, P*C*HN); 67.32 (d, $^2J_{CP}$= 8.3 Hz, *C*HOH); 49.76 (d, $^1J_{CP}$= 18.2 Hz, P*C*H$_2$N); 44.89 (d,$^1$ $J_{CP}$= 17.3 Hz, P*C*H$_2$N); 40.49 (s, N*Me*$_2$); 34.62 (d, $^3J_{CP}$= 3.6 Hz, cod); 33.09 (d, $^3J_{CP}$= 3.0 Hz, cod); 29.65 (d, $^3J_{CP}$= 2.1 Hz, cod); 27.98 (d, $^3J_{CP}$= 4.2 Hz, cod). **MS** (nESI$^+$) *m/z*: 605.3 [Ir(cod)(PZA-NMe$_2$)]$^+$. **IR** (KBr, cm$^{-1}$): $\nu_{(OH)}$ 3423 (br, s); $\nu_{(arom)}$ 1613 (m), 1524 (m). **Anal**. Calcd. for $C_{23}H_{35}ClIrN_4OP$ (642.19 gmol$^{-1}$). Found (calcd): C 43.48 (43.02); H 5.67 (5.49); N 8.58 (8.72).

### 3.6.2 Transfer hydrogenation test procedures

The reactions were carried out in Schlenk tubes under an inert atmosphere using degassed solvents. For transfer hydrogenation of cinnamaldehyde (CNA) and 2-cyclohexen-1-one, the catalyst and $HCO_2Na$ were placed in two different Schlenk tubes, maintained under vacuum for 5 minutes and then dissolved in 3 mL of a $H_2O$/MeOH mixture (1:1, 1:2 or 2:1 as specified in the tables). The formate solution was added by cannula to the solution of catalyst and the temperature was set. The liquid substrate was directly added by a syringe to the reaction mixture. In the case of benzylidene acetone (BZA), $HCO_2Na$ was dissolved in 2 mL of water and added via cannula to the solution of catalyst in MeOH (2 mL). The temperature was set and

the solution of BZA in MeOH (2 mL) was added to the mixture. At the end of all reactions, an aliquot of the reaction mixture (0.1 mL) was diluted with methanol (0.4 mL) or extracted with dichloromethane and analysed by GC. For hydrogenation of 2-cyclohexen-1-one and acetophenone with KOH/$^{i}$PrOH, the catalyst and the base were placed in a Schlenk tube and dissolved in dry isopropanol (8.8 mL). When the desired temperature was reached, the substrate was slowly added. At the end of the reaction, the mixture was diluted with MeOH and analysed by GC. In the case of acetophenone, the solution was also passed through a plug of silica before the injection. Each test was repeated twice to check for reproducibility.

### 3.6.3 Autoclave experiments procedure

Vials with appropriate size were collocated in a home-build stainless steel autoclave and charged under nitrogen with the catalyst and the base. Dry isopropanol (2 mL) and the substrate were added by using a syringe and after three cycles of purging with hydrogen, the autoclave was pressurized to 30 bar and left for 4 hours at room temperature under magnetic stirring. The pressure was then released and an aliquot of the reaction mixture (0.1 mL) was diluted with methanol (0.4 mL) and analysed by GC. Each test was repeated twice to check for reproducibility.

## 3.7 References


[1] (a) Phillips, A. D., Gonsalvi, L.; Romerosa, A.; Vizza, F.; Peruzzini, M. *Coord*. *Chem*. *Rev*. **2004**, *248*, 955-993. (b) Bravo, J.; Bolaño, S.; Gonsalvi, L.; Peruzzini, M. *Coord Chem Rev*. **2010**, *254*, 555-607.

[2] Darensbourg, D. J.; Beckford, F. A.; Reibenspies, J. H. *J*. *Cluster Sci*. **2000**, *11*, 95-107.

[3] (a) Krogstad, D. A.; Halfen, J. A.; Terry, T. J.; Young Jr., V. G. *Inorg Chem* **2001**, *40*, 463-471. (b) Kovács, J.; Todd, T. D.; Reibenspies, J. H.; Joó, F.; Darensbourg, D. J. *Organometallics*, **2000**, *19*, 3963-3969.

[4] Vaska, L.; DiLuzio, J. W. *J*. *Am*. *Chem*. *Soc*. **1961**, *83*, 2784-2785.

[5] Strohmeier, W.; Michel, M.; Weigelt, L. *Zeit*. *Naturforsc*. *Teil B*: *Anorg Chem*, *Org Chem*. **1980**, *35B*, 648-650.

[6] Herde, J. L.; Lambert, J. C.; Senoff, C. V. *Inorg Synth*. **1974**, *15*, 18-19.

[7] Darensbourg, D. J.; Decuir, T.J.; Stafford, N.W.; Robertson, J.B.; Draper, J.D.; Reibenspies, J.H. *Inorg*. *Chem*. **1997**, *36*, 4218-4226.

[8] Darensbourg, D. J.; Robertson, J. B.; Larkins, D. L.; Reibenspies, J. H. *Inorg*. *Chem*. **1999**, *38*, 2473-2481.

[9] Darensbourg, D. J.; Joó, F.; Kannisto, M.; Katho, A.; Reibenspies, J. H. *Organometallics* **1992**, *11*, 1990-1993.

[10] Krogstad, D. A.; DeBoer, A. J.; Ortmeier, W. J.; Rudolf, J. W.; Halfen, J. A. *Inorg*. *Chem*. *Comm*. **2005**, *8*, 1141-1144.

[11] Frazier, J. F.; Merola, J. S. *Polyhedron* **1992**, *11*, 2917-2927.

[12] (a) Sava, X.; Mezailles, N.; Ricard, L.; Mathey, F.; Le Floch, P. *Organometallics*, **1999**,*18*,807-810. (b) Gull, A. M.; Fanwick, P. E.; Kubiak, C. P. *Organometallics*, **1993**, *12*, 2121-2125.

[13] Erlandsson, M.; Landaeta, V. R.; Gonsalvi, L.; Peruzzini, M.; Phillips, A. D.; Dyson, P. J.; Laurenczy, G. *Eur*. *J*. *Inorg*. *Chem*. **2008**, 620-627.

[14] White, C.; Yates, A.; Maitlis, P. *Inorg Synth*. **1992**, *29*, 228-234.

[15] Leung, D. H.; Bergman, R. G.; Raymond, K. N. *J*. *Am*. *Chem*. *Soc*. **2006**, *128*, 9781-9797.

[16] Erlandsson, M.; Gonsalvi, L.; Ienco, A.; Peruzzini, M. *Inorg*. *Chem*. **2008**, *47*, 8-10.

[17] Guerriero, A.; Erlandsson, M.; Ienco, A.; Krogstad, D. A.; Peruzzini, M.; Reginato, G.; Gonsalvi, L. submitted for publication.

[18] Garrou, P. E. *Chem Rev*. **1981**, *81*, 229-266.

[19] Schenck, T. G.; Downes, J. M.; Milne, C. R. C. ; Mackenzie, P. B.; Boucher, H.; Whelan, J.; Bosnich, B. *Inorg*. *Chem*. **1985**, *24*, 2334-2337.

[20] For comprehensive volumes on hydrogenation reactions: (a) Blaser, H. U.; Schmidt, E. (Eds.) *Asymmetric Catalysis on Industrial Scale: Challenges, Approaches and Solutions*, Wiley-VCH, Weinheim, **2004**. (b) De Vries, J. G. (Eds.) *Handbook of Homogeneous Hydrogenation*, Wiley-VCH, Weinheim, **2007**.

[21] For a recent review on asymmetric transfer hydrogenation (ATH) in water: Wu, X.; Wang, C.; Xiao, J. *Platinum Metals Rev*. **2010**, 54, 3-19.

[22] Himeda, Y.; Onozawa-Kumatsuzaky, N.; Miyazawa, S.; Sugihara, H.; Hirose, T.; Kasuga, K. *Chem. Eur. J*. **2008**,14,11076-11081.

[23] (a) Wu, X.; Li, X.; Zanotti-Gerosa, A.; Pettman, A.; Liu, J.; Mills, A. J.; Xiao, J. *Chem*. *Eur*. *J*. **2008**, *14*, 2209-2222. (b) Wu, X.; Corcoran, C.; Yang, S.; Xiao, J. *ChemSusChem* **2008**, *1*, 71-74. (c) Ikariya, T.; Murata, K.; Noyori, R. *Org*. *Biomol*. *Chem*. **2006**, *4*, 393-406. (d) Fujii, A.; Hashiguchi, S.; Uematsu, N.; Ikariya, T.; Noyory, R. *J*. *Am. Chem*. *Soc*. **1996**, *118*, 2521-2522.

[24] Marchetti, M.; Minello, F.; Paganelli, S.; Piccolo, O. *Appl*. *Catal*. *A*.: *Gen*. **2010**,*373*, 76-80

[25] Akbayeva, D. N.; Gonsalvi, L.; Oberhauser, W.; Peruzzini, M.; Vizza, F.; Brüggeller, P.; Romerosa, A.; Sava, G.; Bergamo, A. *Chem Commun*. **2003**, 264-265.

[26] Smoleński, P.; Pruchnik, F. P.; Ciunik, Z.; Lis, T. *Inorg*. *Chem*. **2003**, *42*, 3318-3322.

[27] Le Roux, E.; Malacea, R. Manoury, E.; Poli, R.; Gonsalvi, L.; Peruzzini, M. *Adv*. *Synth*. *Catal*. **2007**, *349*, 309-313.

[28] (a) Rossin, A.; Gonsalvi, L.; Phillips, A. D.; Maresca, O.; Lledos, A.; Peruzzini, M. *Organometallics* **2007**, *26*, 3289-3296. (b) Kovacs, G.; Rossin, A.; Gonsalvi, L.; Lledos, A.; Peruzzini, M. *Organometallics* **2010,** *29***,** 5121–5131.

# *Chapter 4*

# Ruthenium complexes containing PTA and its "*upper rim*" derivatives

## 4.1 Overview

This Chapter opens with a brief description of selected ruthenium PTA complexes present in the literature, describing their important application in catalysis and in medicinal chemistry. The synthesis of our new Ru(II) arene complexes containing all the new *upper rim* derivatives previously described is also reported, and the results of some preliminary catalytic tests in hydrogenation reactions are summarized here. The Chapter ends with the experimental section reporting the characterization of all the new Ru compounds including an X-ray crystal structure determination and details of the catalytic tests.

## 4.2 Introduction

In the last years, most of the reports appeared in the literature about new transition-metal complexes of PTA and its derivatives concern the use of ruthenium. This is principally due to the catalytic ability and potential medicinal properties of such complexes.

In order to prepare aquo complexes to be used as catalyst precursors in aqueous organometallic catalysis, the reaction of $[Ru(H_2O)_6]^{2+}$ with PTA and its methylated analog [mPTA]X (X = I, *p*-toluenesulfonate) was investigated.[1] To avoid the hydrolysis of $[Ru(H_2O)_6]^{2+}$ ( pH> 6) and the protonation of PTA (pH< 6.5), these studies need to be performed under pH control, thus all measurements were performed around pH 6. Depending on the [L]:[Ru] ratio, mixtures of several compounds were obtained (Scheme 4.1). At [L]:[Ru]= 2:1 ratio, the main species in solution at room temperature was $[Ru(H_2O)_5(PTA)]^{2+}$, while the bis- and tris-phosphine species could be detected only in traces. When the [L]:[Ru] was increased to 15:1 ratio, $[Ru(H_2O)_5(PTA)]^{2+}$ was gradually replaced by $[Ru(H_2O)_4(PTA)_2]^{2+}$, but $[Ru(H_2O)_3(PTA)_3]^{2+}$ was also present in low concentration together with smaller quantities of $[Ru(H_2O)_2(PTA)_4]^{2+}$, $[Ru(H_2O)(OH)(PTA)_4]^{2+}$ and $[Ru(OH)_2(PTA)_4]^{2+}$ species.

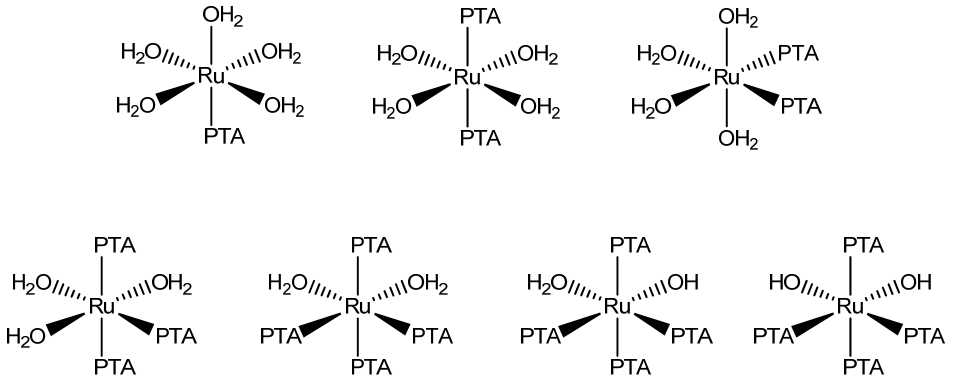


**Scheme 4.1.** Ru(II)-PTA species formed in the reaction with $[Ru(H_2O)_6]^{2+}$. Adapted from ref. 1.

The derivatives, *trans*-$[Ru(H_2O)_4(mPTA)_2](tos)_4 \cdot 2H_2O$ (tos = *p*-toluenesulfonate) and *trans-mer*-$[RuI_2(H_2O)(mPTA)_3]I_3 \cdot 2H_2O$ were obtained by reacting $[Ru(H_2O)_6](tos)_2$ with [mPTA]tos and [mPTA]I/KI, respectively, while the reaction of $[Ru(H_2O)_6](tos)_2$

with $PTAH^+$ in water at pH 4, produced the complex *trans*-$[Ru(H_2O)_4(PTAH)_2](tos)_4 \cdot 2H_2O$.

The aquo complex *trans*-$[RuI_2(H_2O)(mPTA)_3]I_3 \cdot 2H_2O$ was also synthesized by reaction of $RuCl_3$ x $3H_2O$ with excess of [mPTA]I in water in the presence of KI. This complex, together with the analog $[RuI_4(mPTA)_2] \cdot 2H_2O$ were tested in two-phase catalytic hydrogenations of cinnamaldehyde (CNA),[2] showing selectivity toward C=O bond reduction to give cinnamol. Their activity did not diminish after three cycles and because of their strong hydrophilic properties, their concentration in the organic phase was low. For this reason, they resulted to be better catalysts for two-phase reactions in comparison with other PTA analogs.

Most of the initial work on PTA coordination chemistry with ruthenium concentrated on simple chloride complexes. *Cis*-$[RuCl_2(PTA)_4]$ was synthesized in quantitative yield by the addition of 6 equivalents of PTA to hydrate $RuCl_3$ in refluxing ethanol or by extracting toluene or dichlorometane solutions of $[RuCl_2(PPh_3)_3]$ with an aqueous solution of PTA (Scheme 4.2).[3] When the extraction was done with a 0.1 M HCl solution, the diprotonated product $[RuCl_2(PTA)_2(PTAH)_2]Cl_2$ was obtained, while further reaction of $[RuCl_2(PTA)_4]$ with CO in 2-methoxyethanol afforded the carbonyl species $[RuCl_2(CO)(PTA)_3]$ (Scheme 4.2).

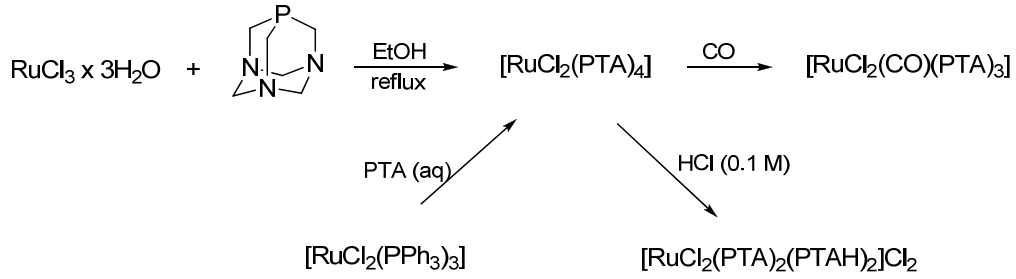


**Scheme 4.2.** Synthesis of some $[RuCl_2(PTA)_n]$ derivatives.[4]

The water-soluble complex $[RuCl_2(PTA)_4]$ was tested as catalyst in the reduction of aldehydes to alcohols using a biphasic system and sodium formate as hydrogen source.[4] The complex resulted to be an effective catalyst for the regioselective hydrogenation of benzaldehyde and cinnamaldehyde to the corresponding alcohols,

while the presence of a strongly coordinating substituent in *ortho* position to the aldehyde functionality, such as in the case of 2-hydroxybenzaldehyde, completely inhibited the catalytic reaction. In addition, hydrogenations of aliphatic aldehydes with $[RuCl_2(PTA)_4]$ showed that the rate of conversion to alcohols was slowed as the hydrocarbon chain length increased.

$[RuCl_2(PTA)_4]$ was also tested for the catalytic hydrogenations of $CO_2$ under $H_2$ pressure.[5] When an alkaline aqueous solution of $[RuCl_2(PTA)_4]$ was pressurized with $H_2$ (60 bar) at room temperature, the *tetrakis*-phosphinoruthenium(II) dihydride complex $[RuH_2(PTA)_4]$ was formed. On the contrary, in acidic solution the monohydride $[RuH(PTA)_4X]$ ($X = H_2O$ or $Cl^-$) was the major hydride species formed. Furthermore, due to the small cone angle of PTA, $[RuH(PTA)_5]^+$ could be obtained for the first time when $[Ru(H_2O)_6](tos)_2$ was reacted with an excess of PTA under hydrogen pressure. In aqueous solution, $[RuCl_2(PTA)_4]$ catalyzed the hydrogenation of aqueous $CO_2$ under mild conditions with low activity. This could be considerably increased if the pH was adjusted to slightly acidic/neutral values and the most of $CO_2$ was present as $HCO_3^-$. A mechanism of the catalytic process was proposed by the authors, suggesting that $[RuH(PTA)_4X]^{n+}$ ($X = Cl, n = 0$; $X = H_2O$, $n = 1$) probably is the active species in the catalytic cycle and bicarbonate replaces X to form $[RuH(PTA)_4(HCO_3)]$, which through an internal rearrangement affords the formate intermediate $[RuH(PTA)_4(HCO_2)]$. This would then release the product $HCOO^-$ with simultaneous coordination of X followed by reaction of $H_2$ to regenerate the catalytically active $[RuH(PTA)_4X]^{n+}$ (Scheme 4.3).

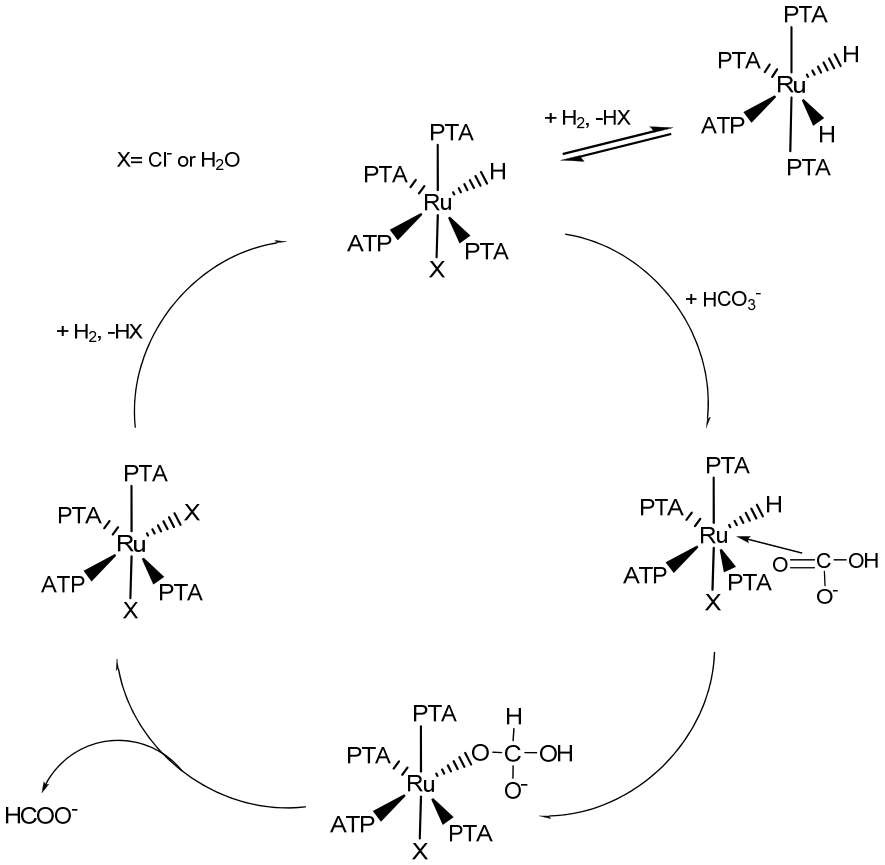


**Scheme 4.3.** Proposed mechanism of hydrogenation of bicarbonate to formate with $[RuCl_2(PTA)_4]$ as precatalyst. Adapted from ref. 5.

The chemistry of $[RuCl_2(PTA)_4]$ was reinvestigated by Mebi and Frost in recent years.[6] In contrast with what previously described,[3] this work showed that the reaction of $RuCl_3$ with PTA does not yield the *cis*-$[RuCl_2(PTA)_4]$ but the *trans* isomer which undergoes isomerisation in solution giving the *cis* isomer. The isomerisation process was studied in different solvents and followed by $^{31}P\{^1H\}$ NMR spectroscopy. In chloroform the equilibrium between both isomers is reached in a week, in water the *trans*-$[RuCl_2(PTA)_4]$ is observed to essentially completely isomerize to *cis* over a period of one week and finally, in acidic solution the *trans* isomer is totally replaced by *cis* over a two-week period.

The isomerization process was further investigated in a photochemical study, which demonstrated that *trans*-$[RuCl_2(PTA)_4]$ can be easily and quantitatively converted into *cis*-$[RuCl_2(PTA)_4]$ by visible light in $CHCl_3$, while in the dark at room temperature the transformation did not occur.[7] In water the *cis* complex could be obtained by

carrying out the synthesis under visible light at room temperature or could be generated by photoirradiation of the *trans* isomer. In this last case, *cis*-[$RuCl_2(PTA)_4$] was formed together with the aquo-complex *cis*-[$RuCl(H_2O)(PTA)_4$]Cl. On the other side, the *cis* complex could isomerize to *trans* with near UV light in $CHCl_3$ but not in water.

When the crude product obtained from the synthesis of *cis*-[$RuCl_2(PTA)_4$] previously described,[3] was recrystallized from water solutions after two weeks standing on air, black crystals were isolated. The X-ray analysis revealed that the new complex formed was [$RuCl_4(PTAH)_2$]·$4H_2O$ (Figure 4.1), in which the phosphine ligands were *trans* to each other and a 3D architectures was mainly governed by the network of hydrogen bonding interactions between water molecules and the N-protonated ligands.[8]

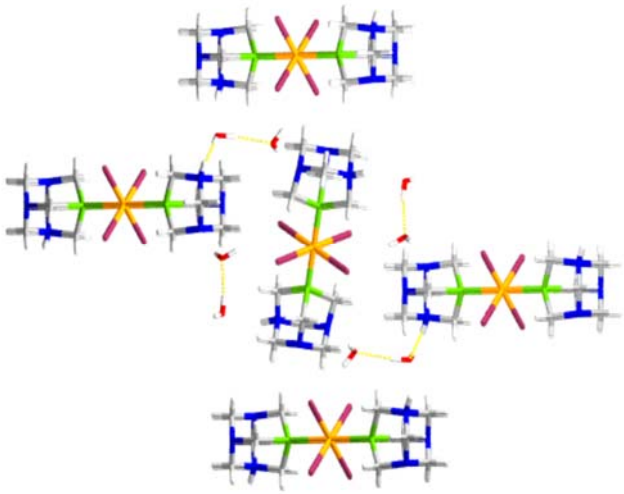

**Figure 4.1.** Wireframe representation of the crystal lattice of [$RuCl_4(PTAH)_2$]·$4H_2O$, showing the hydrogen bonding network. Atom colour code: P, green; C, gray; N, blue; Cl, purple; H, white; Ru, orange. H bonding depicted in yellow. Adapted from ref. 8.

Most of the ruthenium complexes bearing PTA or its derivatives are half-sandwich arene complexes, which have been studied for their catalytic activity and potential applications in medicinal chemistry. Complexes [$CpRuCl(PTA)_2$] (Cp= $\eta^5$-cyclopentadienyl) and [$Cp^*RuCl(PTA)_2$] ($Cp^*$= $\eta^5$-pentamethylcyclopentadienyl) were synthesized according to Scheme 4.4 and obtained in moderate to good yields.[9] Both complexes were tested in catalytic hydrogenation of benzylidene

acetone (BZA) in $H_2O$/*n*-octane biphasic system at 80 °C under $H_2$ pressure (435 psi), showing highly regioselectivity toward the hydrogenation of C=C bond, producing 4-phenyl-butan-2-one as main product of the hydrogenation reaction. In particular, $[CpRuCl(PTA)_2]$ and the complex $[CpRu(MeCN)_2(PTA)]PF_6$ obtained by reacting $[CpRu(MeCN)_3]PF_6$ with PTA,[10] showed high activity under the mild catalytic conditions used, while lower activity was shown by $[Cp^*RuCl(PTA)_2]$.

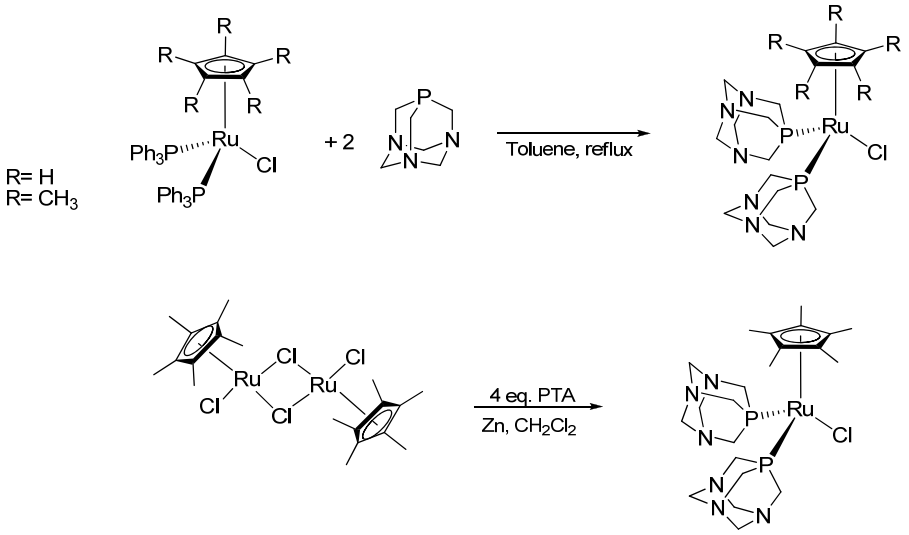


**Scheme 4.4.** Synthesis of $[CpRuCl(PTA)_2]$ and $[Cp^*RuCl(PTA)_2]$.Adapted from ref. 9.

Alternatively, complex $[CpRuCl(PTA)_2]$ can be synthesized by substitution of 1,5-cyclooctadiene (cod) by PTA in [CpRuCl(cod)] precursor.[11] By reacting $[CpRuCl(PTA)_2]$ with KOH in methanol under reflux conditions, the corresponding hydride $[CpRuH(PTA)_2]$ was obtained in good yields (Scheme 4.5). This compound showed high solubility in water ($S_{20°C}$= 20 mg/mL) and stability in deoxygenated water for several weeks, but it decomposed quickly in presence of air.

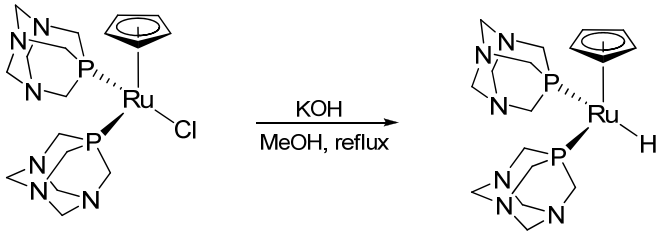


**Scheme 4.5.** Reactivity of $[CpRuCl(PTA)_2]$.[11]

Also the hydride complex $[CpRuH(PTA)_2]$ was tested as catalyst in the hydrogenation of benzylidene acetone (BZA) in a biphasic $H_2O/Et_2O$ solvents system at room

temperature and low pressures of $H_2$ (range= 10-150 psi).[12] The catalytic studies were carried out at different pH values and showed that the hydrogenation of BZA was highly selective toward the reduction of C=C bonds at pH≤ 7.0. The active species in catalysis was proposed to be $[CpRuH(PTA)(PTAH)]^+$, resulting from the protonation of one PTA ligand.

Another class of half-sandwich ruthenium(II) compounds active in catalysis are the complexes $[DpRuCl(PTA)(PPh_3)]$ (Dp= 1,2-dihydropentalenyl) and $[IndRuCl(PTA)(PPh_3)]$ (Ind= indenyl), prepared in refluxing toluene as reported in Scheme 4.6. These were tested as catalysts for the selective transfer hydrogenation of unsaturated substrates, such as BZA and CNA in aqueous media. The catalytic tests revealed that the regioselectivity toward C=C or C=O bonds depended on the ancillary ligand of the catalyst, the substrate and also on the pH of the solution.[13]

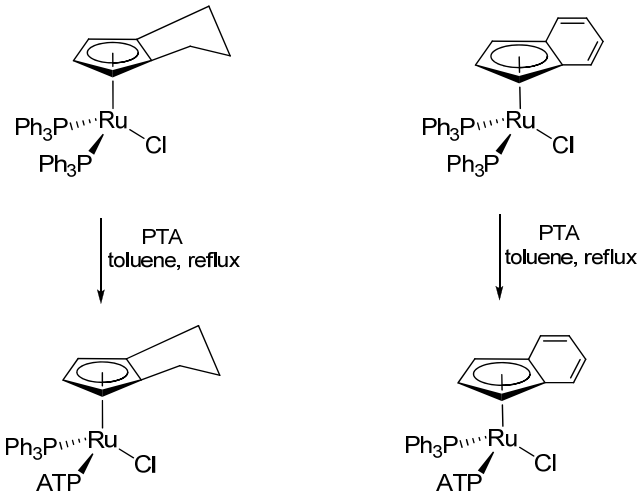


**Scheme 4.6.** Synthesis of complexes $[DpRuCl(PTA)(PPh_3)]$ and $[IndRuCl(PTA)(PPh_3)]$. Adapted from ref. 13.

In order to increase the water solubility, some Ru complexes with *lower rim* PTA derivatives were synthesized. By reacting $[dmPTA](OTf)_2$ (**55**) (dmPTA = = 1,3-dimethyl-1,3,5-triaza-7-phosphatricyclo-[3.3.1.1]decane) with $[CpRuCl(PPh_3)_2]$, the unexpected complex $[CpRuCl(HdmoPTA)(PPh_3)]OTf$ (HdmoPTA = 3,7-H-3,7-dimethyl-1,3,7-triaza-5-phosphabicyclo[3.3.1]nonane) bearing a modification on the triazacyclohexane ring of PTA ligand, i.e. the formation of an open-cage derivative,

was obtained.[14] The formation of this new complex, which could be also directly synthesized in lower yield by the reaction with ligand [dmoPTA]OTf (dmoPTA= 3,7-dimethyl-1,3,7-triaza-5-phosphabicyclo[3.3.1]nonane, Scheme 4.7), was confirmed by NMR spectroscopy and X-ray diffraction analysis. $^{31}P$ $\{^{1}H\}$ NMR studies using different solvents suggested a possible mechanism of the reaction, in which complex [CpRuCl(dmPTA)($PPh_3$)]OTf is firstly formed and then converted into the final complex [CpRuCl(HdmoPTA)($PPh_3$)]OTf with a rate depending on the amount of water in the reaction (Scheme 4.7).

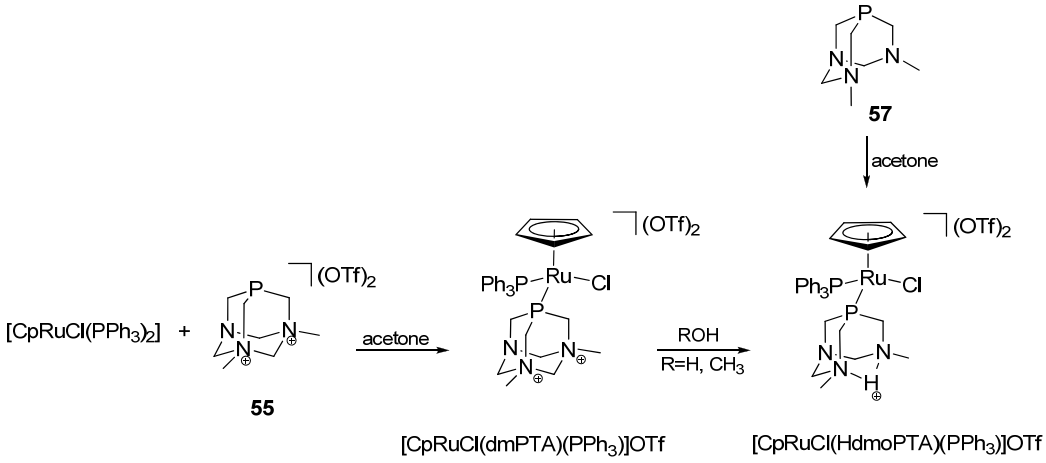


**Scheme 4.7.** Synthesis and reactivity of [CpRuCl(HdmoPTA)($PPh_3$)]OTf complex.[14]

In the design of metal complexes to use as antitumor drugs, ruthenium is so far the most promising metal.[15,16] This is due to its low toxicity and because of its ability to mimic iron in binding serum proteins such as transferrin and albumin. These two proteins are able to solubilise and transport iron, therefore reducing the toxicity of the metal. It has been well demonstrated that cancer cells require high amounts of iron for their metabolism and for this reason they increase the number of transferrin receptors on their surface, hence sequestering high amounts of iron-rich transferrin. Ruthenium, by binding to transferrin, is transported in blood and is accumulated into cells through the binding to the transferrin receptors.[17] For this reasons water soluble Ru(II) complexes are of great interest in the field of biologically active compounds.

The Ru(II)-arene complex [$RuCl_2(\eta^6$-*p*-cymene)PTA] (*p*-cymene= $\eta^6$-$C_{10}H_{14}$), named RAPTA (Figure 4.2), was the first water-soluble ruthenium-PTA complex which showed antitumoral activity causing a pH dependent DNA damage.[18] *In vitro* and *in vivo* biological studies, proved that RAPTA was a highly selective agent for the treatment of secondary cancers (metastasis) with excellent pharmacokinetic properties.[19] Moreover, RAPTA was found also to be active as catalyst in the hydrogenation of several substituted arenes in water.[20]

In order to increase the activity and selectivity of the potential metal-based drugs and to understand the activation mechanism, many RAPTA-type compounds were synthesized, by following the general synthetic approach of direct reaction of [Ru($\eta^6$-arene)(μ-Cl)Cl]$_2$ with PTA or modified PTA ligands (Figure 4.2).[21]

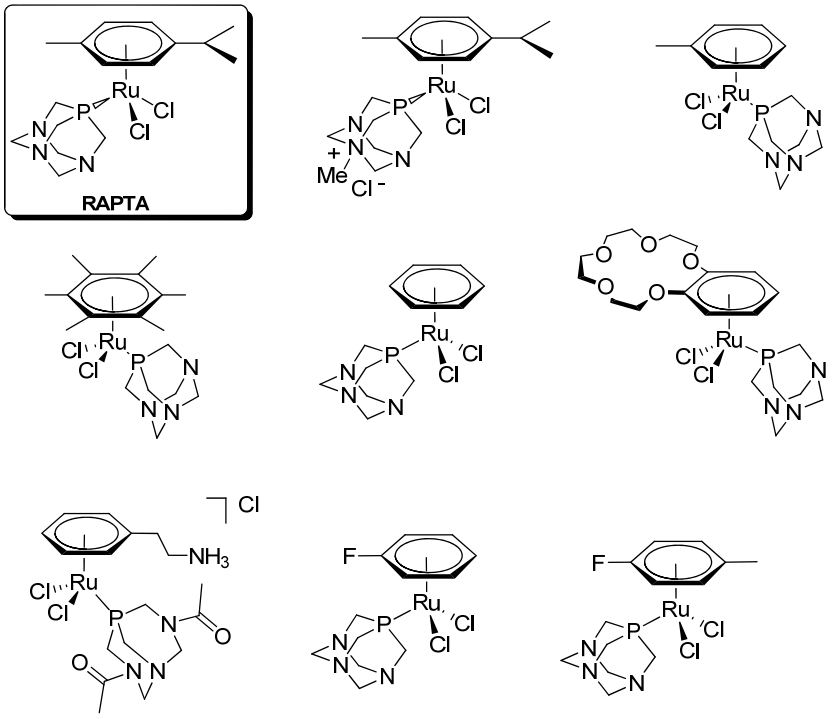


**Figure 4.2.** Some examples of Ru-arene complexes as organometallic anticancer drugs.

Complexes of formula [CpRuX(L)(L')] (X= Cl or I; L=L'= PTA or its derivatives, $PPh_3$) were also synthesized and tested as potential DNA-active drugs. The results of biological tests showed that DNA activity can be modulated by the choice of the phosphine coordinated to the metal.[22]

## 4.3 New Ru(II) complexes bearing "*upper rim*" PTA derivatives

In the literature, a small number of ruthenium complexes containing *upper rim* PTA derivatives have been described. Very recently, the synthesis of some [$RuCl_2(\eta^6$-*p*-arene)(PTA-CRR'OH)] complexes was accomplished in moderate to good yield by adding the opportune *upper rim* PTA-CRR'OH ligand to a $CH_2Cl_2$ solution of [$Ru(\eta^6$-arene)($\mu$-Cl)Cl]$_2$ (Scheme 4.8).[23]

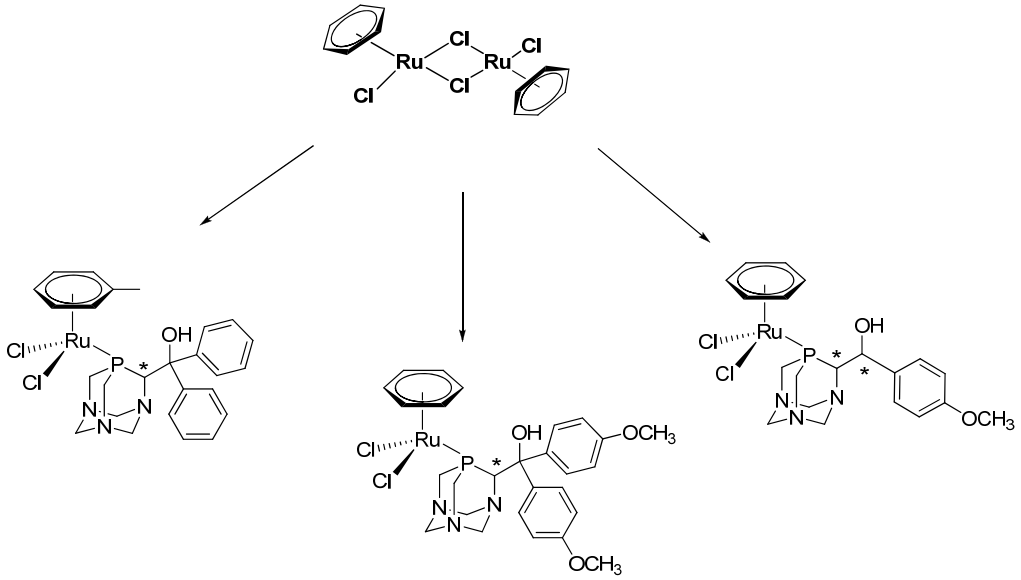


**Scheme 4.8.** Some Ru(II) *upper rim* PTA derivative complexes.[23]

Complexes [$RuCl_2(\eta^6$-*p*-$C_6H_5CH_3$)(PTA-C($C_6H_5$)$_2$OH)] and [$RuCl_2(\eta^6$-*p*-$C_6H_6$)(PTA-C($C_6H_4OCH_3$)$_2$OH)] were obtained in racemic mixture, while complex [$RuCl_2(\eta^6$-*p*-$C_6H_6$)(PTA-CH($C_6H_4OCH_3$)OH)] was obtained in mixture of two diastereoisomers as confirmed by the two singlets at -33.1 ppm (major) and -32.3 ppm (minor) in the $^{31}P\{^1H\}$ NMR spectra. All these compounds exhibited modest water solubility, ranging from 5.4 g/L to 14.1 g/L. The X-ray crystal structures of all the three ruthenium arene complexes were also reported, showing that PTA-CRR'OH ligands bind the metal centre in $\kappa^1$-P mode (Figure 4.3). The addition of either $CsCO_3$ or NaOH to the solution of the complexes produced a shift in the $^{31}P\{^1H\}$ NMR resonance of *ca*. 8-10 ppm, which was attributed by the authors to a deprotonation of the OH functionality and the subsequent formation of the corresponding $\kappa^2$-P,O

chelates. All the attempts made to isolate the $\kappa^2$-P,O complexes were unsuccessful.[23]

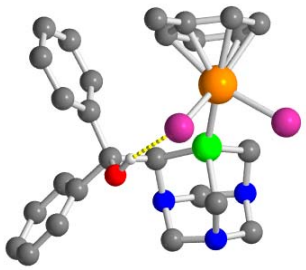

**Figure 4.3.** X-ray crystal structure of the complex $[RuCl_2(\eta^6\text{-}p\text{-}C_6H_5CH_3)(PTA\text{-}C(C_6H_5)_2OH)]$. O–H···Cl hydrogen bonding shown as dotted line (see atom colour code). Adapted from ref. 23.

Following on our interest in the synthesis of new water soluble Ru-arene complexes containing new *upper rim* PTA derivatives, we decided to test the complexation ability of PZA and PZA-$NMe_2$ (see Chapters 2 and 3) toward Ru(II) synthons.[24] In particular we decided to start preparing some [Ru($\eta^6$-*p*-cymene)] complexes as this moiety is known to be a stabilizing ligand for the catalytic applications and also acrive for the potential biological activity of the corresponding complexes as anticancer agents.[25]

First of all the diastereomeric mixture (1:1) of ligand PZA (**74**) was reacted with a $CH_2Cl_2$ solution of [Ru($\eta^6$-*p*-cymene)($\mu$-Cl)Cl]$_2$ at room temperature and the complex ($\kappa^1$-P)-[$RuCl_2$($\eta^6$-*p*-cymene)(PZA)] (**88**) (Scheme 4.9) was obtained in ca. 60% yield. The $^{31}P\{^1H\}$ NMR ($CDCl_3$) of this red complex confirmed the presence of two diastereoisomers in 1:2 ratio as evidenced by the two resonances at -28.7 and -40.3 ppm, for the minor diastereoisomer and the major one, respectively. Also the signals of different intensity in $^{13}C\{^1H\}$ NMR spectrum well evidenced the diastereomeric mixture. The complex **88** shows a good water solubility of 2.7 mg $mL^{-1}$.

In the case of ligand PZA-$NMe_2$ (**75**) only the isolated diastereoisomer *S*,*R R*,*S* (**75a**) was used for the synthesis of the corresponding Ru(II) complex. By reacting two equivalents of (*S*,*R R*,*S*)PZA-$NMe_2$ with the Ru(II) arene precursor at room temperature, complex ($\kappa^1$-P)-[$RuCl_2$($\eta^6$-*p*-cymene){(*S*,*R R*,*S*)-(PZA-$NMe_2$)}] (**89**)

precipitated from the dichloromethane solution after addition of pentane as a pale red powder (Scheme 4.9). Complex **89** exhibits a singlet at -40.4 ppm in the $^{31}P\{^{1}H\}$ NMR spectrum, confirming the presence of a single diastereoisomer and, if compared to the complex **88**, shows lower solubility in water ($S_{20°C}$= 1.4 mg $mL^{-1}$). Contrary to what observed in the case of the corresponding iridium(I) complexes described in Chapter 3, both Ru(II) complexes **88** and **89** proved to be stable on air as solids, and could be stored for indefinite time under an inert atmosphere of nitrogen.

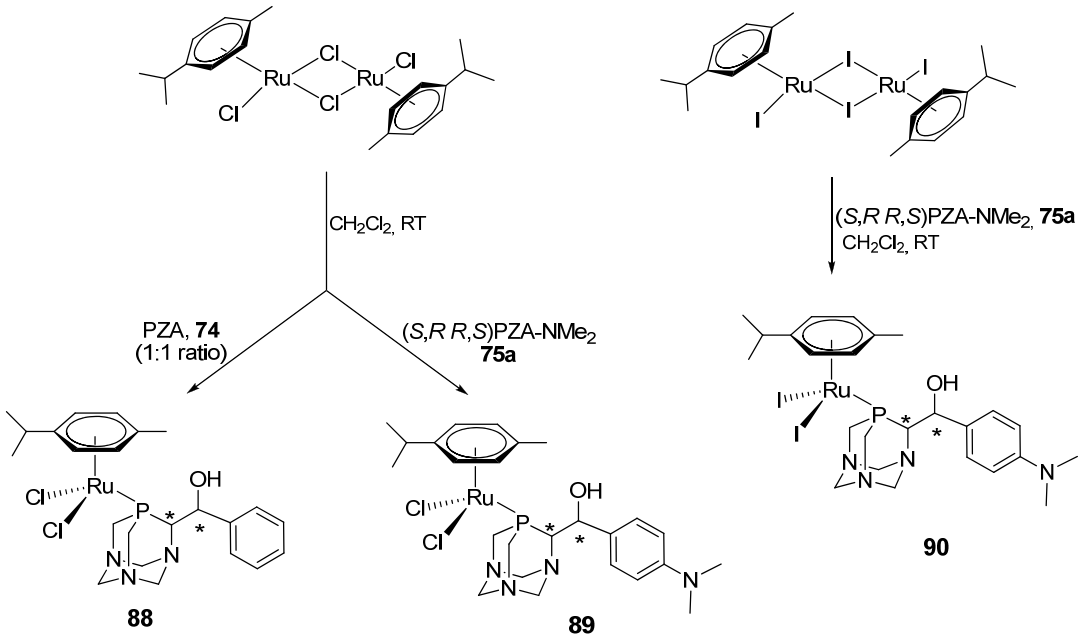


**Scheme 4.9.** Synthesis of the new Ru(II) complexes, **88**, **89** and **90**.[24]

When the reaction was carried out by using [Ru($\eta^6$-*p*-cymene)($\mu$-I)I]$_2$ and (*S*,*R R*,*S*)PZA-NMe$_2$ ligand, the corresponding iodide derivative complex ($\kappa^1$-P)-[RuI$_2$($\eta^6$-*p*-cym){(*S*,*R R*,*S*)-(PZA-NMe$_2$)}] (**90**) was obtained (Scheme 4.9), showing a singlet at -51.9 ppm in the $^{31}P\{^{1}H\}$ NMR spectrum. Red needles of **90** were obtained from the slow diffusion of dry ethanol in a $CH_2Cl_2$ solution of the complex. These were suitable for X-ray crystal diffraction.The X-ray crystal structure shows that the complex crystallizes in a centro-symmetric space group and both the *S*,*R* and *R*,*S* isomers are present in the cell. The geometry around the ruthenium atom in **90** is an octahedron, where *p*-cymene occupies three coordination positions while two

iodine atoms and one PZA-$NMe_2$ ligand occupy the other three. The phosphorus atom binds the ruthenium in $\kappa^1$-P mode and an hydrogen bonding between the iodine atom and the OH group is established (Figure 4.4). Also $^{13}C\{^1H\}$ NMR data of both complexes **89** and **90**, were diagnostic to confirm the formation of the complexes, in particular the CH signals of the *p*-cymene ring which gave three doublets in the range from 89.7 to 83.5 ppm for **89** ($^2J_{HP}$= *ca*. 4.6 Hz) and in the range from 89.3 to 84.8 ppm ($^2J_{HP}$= *ca*. 3.1 Hz) for **90**, reflecting the lack of symmetry in the molecule.

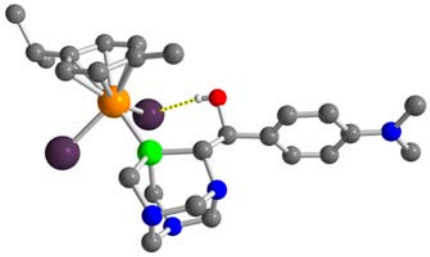

**Figure 4.4.** X-ray crystal structure of complex **90**; O–H···I hydrogen bonding shown as dotted line (see atom colour code).

Finally, the same synthetic procedure used for the complexes described above was applied to the two imidazolyl-PTA ligands, PTA-CH(1-MeIm)OH (**76**) (diastereomeric mixture 1:1 ratio) and PTA-$C(1\text{-MeIm})_2$OH (**82**) (one diastereoisomer). After 2h stirring, the solution was analysed by $^{31}P\{^1H\}$ NMR spectra. Surprisingly four singlets in the case of **76** ($\delta$-39; -35; -26; -23 ppm) and two singlets in the case of **82** ($\delta$-38; -20 ppm) were found. The upfield signals were in the region observed with the compounds **88**, **89**, and **90**, therefore, these resonances were likely due to the corresponding complexes in which the ligands are coordinated in the $\kappa^1$-P mode. Clearly, the presence of a second group of downfield signals is due to the presence of a second species. All attempts either to separate the mixture or to obtain the $\kappa^1$-P species as pure complexes by altering the reaction conditions failed so far.

When the reaction was carried out in chloroform under reflux conditions, only the second species was obtained in both cases. This was attributed to the formation of a $\kappa^2$-P,N ionic complexes, that is ($\kappa^2$-P,N)-[RuCl($\eta^6$-*p*-cymene){PTA-CH(1-

MeIm)OH}]Cl (**91**) and ($\kappa^2$-P,N)-[RuCl($\eta^6$-*p*-cymene){PTA-C(1-MeIm)$_2$OH}]Cl (**92**), respectively.(Scheme 4.10). The formation of these new $\kappa^2$-P,N species was confirmed by the $^{31}$P {$^1$H} NMR spectra which, in the case of complex **91**, contained two singlets at-26.4 and -22.9 ppm, and showed one singlet at -19.8 ppm in the case of complex **92**. These $^{31}$P NMR resonances are in agreement with a similar complexes ($\kappa^2$-P,N)-[RuCl($\eta^6$-*p*-cymene){PTN(Me)}]Cl (Scheme 4.10) recently reported, which was obtained by using the same synthetic conditions.[26]

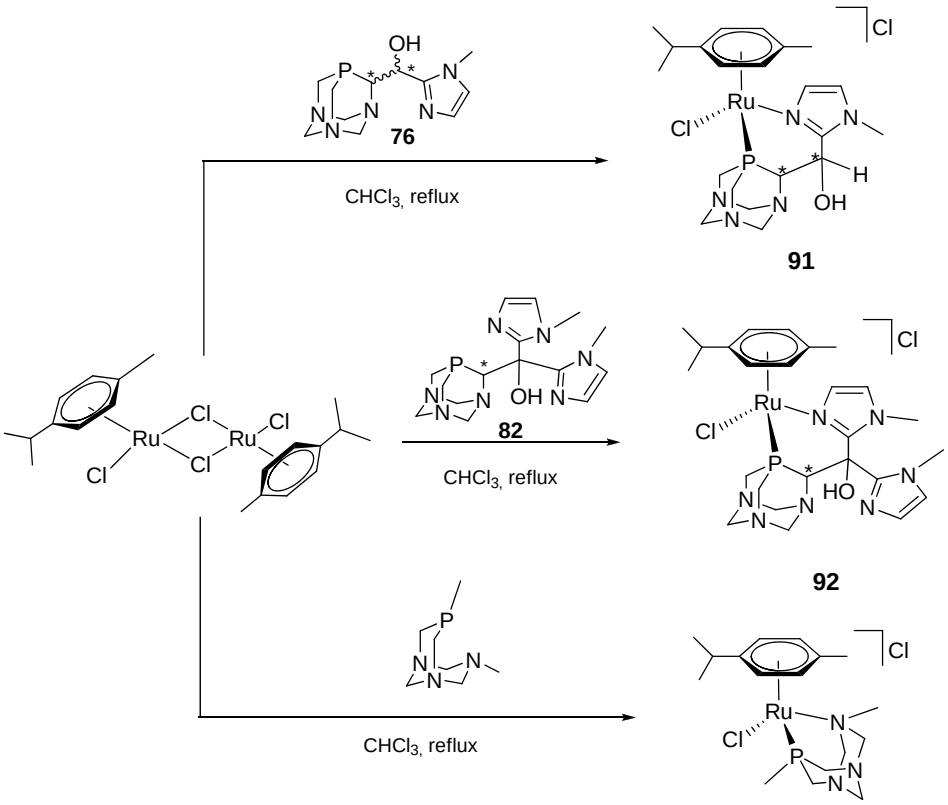


**Scheme 4.10.** Synthesis of the two $\kappa^2$-*P,N* complexes **91**, **92** and ($\kappa^2$-P,N)-[RuCl($\eta^6$-*p*-cymene){PTN(Me)}]Cl.

A diastereomerically enriched sample of compound **91** was obtained by reaction of the diastereomerically enriched (15:1) solution of ligand **76** with the Ru precursor. This and complex **92** were analysed by $^1$H NMR and $^{13}$C {$^1$H} NMR and the spectra obtained were also very important for the structural characterization of the complexes. Both $^1$H NMR spectra showed four resonances for the *p*-cymene ring

protons in the range of 5.5–6.1 ppm. This indicated that the ring was coordinated to a $RuL_1L_2L_3$ moiety, and that the P,N ligands were binding in the $\kappa^2$-P,N mode.[27] The chirality on the ruthenium was further confirmed by the chemical shift values of $CH_3$ protons of the isopropyl group, which appeared as two separate doublets at 1.29 ($^3J_{HH}$= 6.8 Hz) and 1.19 ppm ($^3J_{HH}$= 6.6 Hz) for **91** and at 1.36 ($^3J_{HH}$= 6.9 Hz) and 1.27 ppm ($^3J_{HH}$= 6.8 Hz) for **92**. The presence of two different signals for $CH_3$ indicated that the methyl groups were diastereotopic, hence the complexes were asymmetric about the metal.[28] Also in the $^{13}C$ {$^1H$} NMR spectra of **91** and **92** four resonances for the CH of the arene ring in the range 81-98 ppm were present, evidencing that the Ru atom was bound by four different moieties.

The $^1H$ and $^{13}C$ {$^1H$} NMR data relative to the imidazole rings were also of great significance. In fact, in the free ligand PTA-CH(1-MeIm)OH (**76**) the $H^4$ proton resonance of the imidazole ring (Figure 4.5) was observed at 6.84 ppm (d, $^3J_{HH}$= 1.1 Hz), while in the corresponding complex **91**, this signal was dramatically downfield shifted to 7.76 ppm (br s).

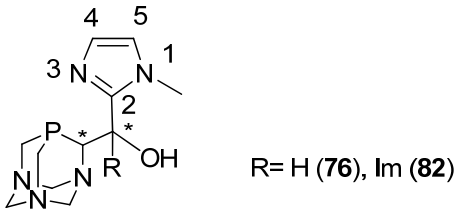


**Figure 4.5.** Structure of the imidazole ligands.

This large shift was likely due to the close proximity of the $H^4$ proton to the N donor atom encountering the greatest $\sigma$-effect. This supports the hypothesis that $N^3$ is bound to the metal centre. Furthermore, only a slight shift is observed for $H^5$ (Figure 4.5). This behaviour is found also in the $^{13}C$ NMR spectrum. While the $C^5$ of the imidazole ring gives a singlet at 122.2 ppm both in the free ligand **76** and in the complex **91**, the resonance of the $C^4$ atom is shifted from 126.6 ppm in the free ligand to 134.6 ppm in the complex. These variations in chemical shift values are in

agreement with what previously observed with other P-imidazole ligands and their $\kappa^2$-P,N complexes.[29]

Similar spectroscopic changes were also observed in the case of the bis-imidazole ligand, PTA-C(1-MeIm)$_2$OH (**82**) and its complex **92**. Since the phosphine **82** contains two diastereotopic imidazoles, the signals of the H$^4$ methylenic protons (Figure 4.5) were splitted into two different doublets at 6.94 and 6.90 ppm ($^3J_{HH}$= 1.1 Hz). In the complex, ($\kappa^2$-P,N)-[RuCl($\eta^6$-*p*-cymene){PTA-C(1-MeIm)$_2$OH}]Cl (**92**), the H$^4$ proton signals were shifted to 7.41 and 6.86 ppm, respectively. This substantial modification in the chemical shift, which involved only one signal, supported again the hypotesis that one of the imidazole moieties was coordinated via N$^3$ atom while the other ring was left as dangling arm. Therefore we can conclude that ligand **82** acts in the $\kappa^2$-P,N mode and not in a tridentate $\kappa^3$-P,N,N mode, as previously seen for other P,N,N ligands.[30]

The two Ru(II)-imidazolyl-PTA complexes **91** and **92** show high solubility in water, 320 mg·ml$^{-1}$ and 170·mg·ml$^{-1}$, respectively. These values are substantially greater than for the related Ru-arene complexes bearing *upper rim* PTA derivatives probably because of a hydrogen bond between the non-coordinating imidazole N atom and water.

## 4.4 Catalytic hydrogenation reactions with the new ruthenium(II) complexes

It is well known from the literature that ruthenium complexes are among the most active hydrogenation catalysts[31] and most of the Ru-PTA complexes previously described have shown good catalytic activity in the hydrogenations of carbonyl compounds. The water-soluble complex [RuCl$_2$(PTA)$_4$], for instance, resulted to be an effective catalyst for the conversion of several aldehydes to alcohols by using a biphasic aqueous-organic medium and sodium formate as hydrogen source.[4] Complexes [CpRuCl(PTA)$_2$] and [Cp*RuCl(PTA)$_2$] were very active in the chemoselective hydrogenation of benzylidene acetone to 4-phenylbutan-2-one (C=C bond reduction) under $H_2$ pressure, forming 4-phenylbutan-2-ol and 4-phenylbut-3-

en-2-ol in small amounts or only in traces.[9] Furthermore, [Cp*RuCl(PTA)$_2$] was also found to be an excellent catalyst for the transfer hydrogenation of cinnalmaldehyde giving a 97% conversion after 6h at 90°C by using $HCO_2Na$ in a water/methanol mixture (1:1).[10] Additionally, complexes [$RuCl_2(\eta^6$-*p*-cymene)(PTA)] and [$RuCl(\eta^6$-*p*-cymene)$(PTA)_2]^+$ catalyzed the hydrogenation of arenes under slightly harsher reaction conditions (90 °C, 870 psi $H_2$).[20] No catalytic applications have been so far investigated for ruthenium complexes containing *upper rim* PTA derivatives.

Therefore, we decided to test our new ruthenium(II) complexes in catalytic hydrogenation reactions by using the same protocols already tested with the two iridium(I) complexes n and n, described in Chapter 3.

Initally the catalytic experiments involved cinnamaldehyde (CNA) (Scheme 4.11), as model substrate to test the chemoselectivity of the catalysts in the hydrogenation of α,β-unsaturated aldehydes under transfer hydrogenation conditions.

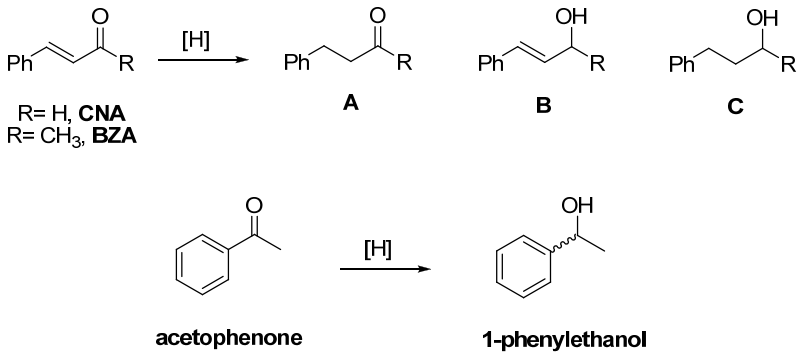


**Scheme 4.11.** Hydrogenation test reactions.

The catalytic experiments were carried out with complexes **88** and **89** at first by using sodium formate as reducing agent in a water/methanol mixture (1:1) and a catalyst/CNA= 1/100 ratio. Some tests were then made by using the more commonly used catalytic protocol KOH/$^i$PrOH, at 80 °C and a catalyst/substrate= 1/500 ratio. The conditions and the results of these catalytic tests using **88** and **89** are reported in Table 4.1.

**Table 4.1.** Transfer Hydrogenation of CNA with catalysts **88** and **89** using $HCO_2Na/H_2O$/MeOH and $^{i}$PrOH/KOH.

| Cat. | Solvent | % Conv (h) | T (°C) | yields % A[b] | % B[b] | % C[b] | TON(avg) |
|---|---|---|---|---|---|---|---|
| **88** | MeOH:$H_2O$ (1:1) | 18.1 (3) | 80 | 7.1 | 8.9 | 2.1 | 18 |
| **88** | MeOH:$H_2O$ (1:1) | 41.2 (24) | 80 | 4 | 30.1 | 7.1 | 41 |
| **89** | MeOH:$H_2O$ (1:1) | 15.3 (3) | 60 | 8.9 | 5.3 | 1.1 | 15 |
| **89** | MeOH:$H_2O$ (1:1) | 32.9 (24) | 60 | 13.6 | 14.9 | 4.4 | 33 |
| **89** | MeOH:$H_2O$ (1:1) | 33.4 (3) | 80 | 17.8 | 13 | 2.6 | 33 |
| **89** | MeOH:$H_2O$ (1:1) | 46.1 (24) | 80 | 7.2 | 29.7 | 9.2 | 46 |
| **89**[c] | MeOH:$H_2O$ (1:1) | 56.8 (24) | 80 | 0.8 | 54 | 2 | 57 |
| **88**[d] | $^{i}$PrOH (10 mL) | 7.2 (3) | 80 | 0.7 | 6.5 | – | 33 |
| **88**[d] | $^{i}$PrOH (10 mL) | 9.7 (24) | 80 | 0.7 | 8.8 | – | 44 |
| **89**[d] | $^{i}$PrOH (10 mL) | 6.4 (3) | 80 | 1.1 | 5.2 | 0.1 | 32 |
| **89**[d] | $^{i}$PrOH (10 mL) | 9.0 (24) | 80 | 1.5 | 7.3 | 0.2 | 41 |

[a] Conditions: CNA, 0.75 mmol; catalyst, 7.5 x $10^{-3}$ mmol; $HCO_2Na$, 7.5 mmol; total volume of solvents, 6 mL
[b] GC values based on pure samples. A = hydrocinnamaldehyde; B = cinnamol; C = 3-phenyl-1-propanol
[c] Test runned with 1.6 x $10^{-2}$ mmol of free ligand (*S*,*R R*,*S*)PZA-$NMe_2$
[d] Conditions: CNA, 4.0 mmol; catalyst, 8.8 x $10^{-3}$ mmol; KOH, 0.16 mmol.

The first catalytic tests were carried out at high temperature (80 °C) with both complexes by using sodium formate in methanol/water mixture, and showed, after 24 h, comparable conversions (41% for **88** and 46% for **89**). The selectivity was in both cases for C=O bond reduction, giving cinnamol as the main product of hydrogenation (selectivities at 24h: 73% for **88** and 64% for **89**). This selectivity was lost when the catalysis was carried out with complex **89** at 60 °C, where the hydrogenation involved both C=O and C=C bond (selectivities at 24h: 41% in hydrocinnamaldehyde *vs* 45% for cinnamol). On the contrary, the selectivity for cinnamol was increased to 95%, when the catalytic test with complex **89**, was performed at 80 °C with the addition of two equivalents of the free ligand (*S*,*R R*,*S*)PZA-$NMe_2$, but still giving a modest final conversion (56.8%). Lower conversions (*ca*. 9% after 24h at 80 °C), but higher TON were obtained with the system KOH/$^{i}$PrOH. The selectivity remained for both complexes for C=O bond hydrogenation (91% for **88** and 81% for **89**).

The system $HCO_2Na/H_2O$/MeOH was then used with complex **91** and **92** for the hydrogenation of CNA (Scheme 4.11) and the results are reported in Table 4.2.

**Table 4.2.** Transfer Hydrogenation of CNA with catalysts **91** and **92** using $HCO_2Na/H_2O$/MeOH.

| | | | | yields | | | |
|---|---|---|---|---|---|---|---|
| Cat. | Solvent | % Conv (h) | T (°C) | % A[b] | % B[b] | % C[b] | TON(avg) |
| **91** | MeOH:$H_2O$ (1:1) | 18.5 (1) | 80 | 8.0 | 9.2 | 1.3 | 18 |
| **91** | MeOH:$H_2O$ (1:1) | 33.5 (5) | 80 | 13.1 | 15.8 | 4.6 | 33 |
| **92** | MeOH:$H_2O$ (1:1) | 20.6 (1) | 80 | 17.9 | 1.3 | 1.4 | 21 |
| **92** | MeOH:$H_2O$ (1:1) | 24.6 (5) | 80 | 18.6 | 2.8 | 3.2 | 25 |

[a] Conditions: CNA, 0.75 mmol; catalyst, 7.5 x $10^{-3}$ mmol; $HCO_2Na$, 7.5 mmol; total volume of solvents, 6 mL
[b] GC values based on pure samples. CNA: A = hydrocinnamaldehyde; B = cinnamol; C = 3-phenyl-1-propanol

The results obtained with catalysts **91** and **92** at 80 °C, showed that these two compounds were more active giving after 5h conversions almost similar to that obtained with the $\kappa^1$-P complexes after 24h under the same reaction conditions. About the selectivity, the results were very different. In fact, complex **91** showed to hydrogenate both C=O and C=C bonds (39% selectivity for C=C bond *vs*. 47% selectivity for C=O bond), but catalyst **92** showed a higher selectivity (76%) toward C=C bond hydrogenation.

The system $HCO_2Na/H_2O$/MeOH was also applied to reduce benzylidene acetone (BZA, Scheme 4.11) in the presence of the various catalysts mentioned above (Table 4.3).

**Table 4.3.** Transfer Hydrogenation of BZA with catalysts **88**, **89**, **91** and **92** using $HCO_2Na/H_2O$/MeOH.

| | | | | yields | | | |
|---|---|---|---|---|---|---|---|
| Cat. | Solvent | % Conv (h) | T (°C) | % A[b] | % B[b] | % C[b] | TON(avg) |
| **88** | MeOH:$H_2O$ (1:1) | 13.7 (5) | 80 | 10.2 | 3.5 | – | 14 |
| **89** | MeOH:$H_2O$ (1:1) | 11.9 (5) | 80 | 9.5 | 2.4 | – | 12 |
| **91** | MeOH:$H_2O$ (1:1) | 24.5(5) | 80 | 20.4 | 4.2 | – | 25 |
| **92** | MeOH:$H_2O$ (1:1) | 25.9(5) | 80 | 25.9 | – | – | 26 |

[a] Conditions: CNA, 0.88 mmol; catalyst, 8.8 x $10^{-3}$ mmol; $HCO_2Na$, 7.5 mmol; total volume of solvents, 6 mL
[b] GC values based on pure samples. For BZA, A= 4-phenyl-2-butanone; B= 4-phenyl-3-buten-2-ol; C= 4-phenyl-2-butanol.

In the hydrogenation of BZA, after 5h at 80 °C, all the complexes showed minor activity compared to the hydrogenation of CNA under same conditions. In all cases, selectivity toward C=C bond hydrogenation was shown as for other Ru-PTA

complexes[10] and, in particular with complex **92** the complete selectivity for 4-phenyl-2-butanone was achieved.

Finally, the new Ru(II) *upper rim* PTA complexes were tested in the reduction of acetophenone (Scheme 4.11), using a mixed hydrogenation/transfer hydrogenation protocol based on $^{t}$BuOK/$^{i}$PrOH under hydrogen pressure at room temperature. All the tests were carried out by using a catalyst/acetophenone/$^{t}$BuOK = 1:250:50 ratio. The results are summerized in the following table (Table 4.4).

**Table 4.4.** Hydrogenation of acetophenone with catalysts **88**, **89** and **91** under $H_2$.

| Cat. | Solvent | % Conv (h) | T (°C) | TON(avg) |
|---|---|---|---|---|
| **88** | $^{i}$PrOH | 26.4 (4) | RT | 66 |
| **89** | $^{i}$PrOH | 2 (4) | RT | 5 |
| **91** | $^{i}$PrOH | >99 (4) | RT | 246 |
| **[Ru(η$^6$-*p*-cym)Cl$_2$]$_2$** | $^{i}$PrOH | 14 (4) | RT | 70 |

[a] Conditions: substrate, 1.75 mmol; catalyst, 7.0 x $10^{-3}$ mmol; $^{t}$BuOK , 0.35 mmol; $^{i}$PrOH, 2 mL. *p*($H_2$), 30 bar, 25 °C.
[b] GC values based on pure samples. For acetophenone, A=1-phenylethanol.

Whereas complexes **88** gave only a 26% conversion after 4h, complex **89** gave poor catalytic activity (2% conversion) for the hydrogenation of acetophenone under the catalytic conditions applied. On the contrary, catalyst **91** resulted to be very active, giving almost complete conversion after 4h with a TON of 246.

## 4.5 Conclusions

Five new ruthenium(II) complexes with all the new *upper rim* PTA derivatives previously described were synthesized. Depending on the phosphine ligand used, the two κ$^1$-P species, [RuCl$_2$(η$^6$-*p*-cymene)(PZA)] and [RuCl$_2$(η$^6$-*p*-cymene){(*S*,*R R*,*S*)-(PZA-NMe$_2$)}] and the two κ$^2$-P,N species [RuCl(η$^6$-*p*-cymene){PTA-CH(1-MeIm)OH}]Cl and [RuCl(η$^6$-*p*-cymene){PTA-C(1-MeIm)$_2$OH}]Cl, have been obtained and fully characterized in solution. Complex (κ$^1$-P)-[RuI$_2$(η$^6$-*p*-cymene){(*S*,*R R*,*S*)-(PZA-NMe$_2$)}] was also synthesized and characterized and the corresponding structure in the solid state was obtained by single-crystal X-ray diffraction analysis. All the complexes have shown long term stability as solids in air and a good

solubility in water, in particular the two imidazolyl-PTA derivatives. Their catalytic activity have been preliminary investigated on different substrates under several reaction conditions. All the compounds have shown modest conversions in the hydrogenation of cinnamaldehyde using the system $HCO_2Na/MeOH/H_2O$. The selectivity is in most cases for C=O bond hydrogenations, except for complex **92** which gave a 76% selectivity toward C=C bond. In the case of benzylidene acetone, the conversions were lower and the selectivity was toward C=C bond hydrogenation. Finally, by using the system $^{i}$PrOH/tBuOK under a pressure of 30 bar $H_2$, complex **91** resulted a very active catalyst for the reduction of acetophenone giving a 99% conversion after 4h and a TON of 246. Work is in progress to optimize the catalytic reaction conditions and to test all the new Ru(II) arene complexes for antitumoral activity.

## 4.6 Experimental Section

### 4.6.1 Synthetic procedures

All details about general synthetic procedures and characterization of compounds are reported in the experimental section of Chapter 2. The information about the GC analyses, transfer hydrogenation procedures and experiments in autoclaves are described in the experimental section of Chapter 3. $[Ru(\eta^6\text{-}p\text{-cymene})(\mu\text{-Cl})Cl]_2$ and $[Ru(\eta^6\text{-}p\text{-cymene})(\mu\text{-I})I]_2$ were prepared as described in the literature.[32] $\alpha$-Phellandrene was bought from commercial suppliers and used without purification. In the case of complex $[RuCl_2(\eta^6\text{-}p\text{-cymene})(PZA)]$ (**88**), the spectroscopic data are referred to the mixture of two diastereoisomers in 1:2 ratio and when distinguishable, the values for minor isomer are reported in brackets.

*Synthesis of $[Ru(\eta^6\text{-}p\text{-cymene})Cl_2]_2$* (**93**)

$RuCl_3$ x $3H_2O$ (2.0 g, 7.7 mmol) was dissolved in ethanol (100 mL) and filtered through a filter paper. In a three-necked round-bottomed flask equipped with a condenser, $\alpha$-phellandrene (50% pure, 10 mL, 30.5 mmol) was added to the ethanol

solution and the reaction mixture was stirred and refluxed under nitrogen for 4h. After reaching room temperature, the flask was put in the fridge and left overnight at low temperature. The red crystals formed were collected by filtration, washed once with cold pentane and dried *in vacuo* (1.9 g, 78% yield).

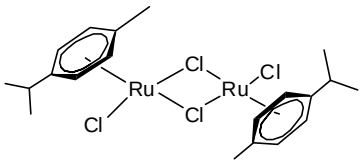


**93: Anal**. Calcd. for $C_{20}H_{28}Cl_4Ru_2$ (612.39 $gmol^{-1}$). Found (calcd): C 39.69 (39.23); H 4.70 (4.61).

*Synthesis of [Ru (η⁶-p-cymene)Cl₂(PZA)]* (**88**)

$[Ru(\eta^6\text{-}p\text{-cymene})Cl_2]_2$ (0.22 g, 0.36 mmol) was dissolved under nitrogen in dry degassed $CH_2Cl_2$ (13 mL). A solution of PZA (0.19 g, 0.72 mmol, two diastereomers ratio 1:1) in $CH_2Cl_2$ (7 mL) was added dropwise and the reaction was left under stirring at room temperature for 1 h. The volume was then reduced to approximately 10 mL and dry degassed diethyl ether (15 mL) was added to precipitate the product. The solid was isolated and washed with cold diethyl ether to afford the product as a red-orange powder (0.26 g, 63% yield), containing the two diastereoisomers in ratio 1:2.

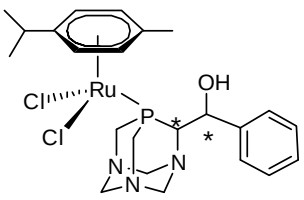


**88: S($H_2O$)$_{20°C}$**= 2.7 mg·$mL^{-1}$. **$^1$H NMR** (400.13 MHz, $CDCl_3$): $\delta$ (ppm) 7.41-7.30 (m, 5H, Ar); 5.65-5.51 (m, 3H, *p*-cym); 5.47-5.40 (m, 1H, C*H*OH); 5.22-5.19 (m, 1H, *p*-cym); 4.87-4.14 (m, 11 H,3 x NC$H_2$N, 2 x PC$H_2$N, PC*H*N ); 2.82-2.77 (m, 1H, C*H*$(CH_3)_2$); 2.20 (2.11) (s, 3H, *p*-cym C$H_3$); 1.30 (1.25) (d, $^1J_{HH}$ = 4.9 (2.3) Hz, 3H, CH-*Me*$_2$); 1.28 (1.23) (d, $^1J_{HH}$ = 4.9 (2.3) Hz, 3H, CH-*Me*$_2$) . **$^{31}$P {$^1$H} NMR** (161.97 MHz, $CDCl_3$): $\delta$ -40.32 (-28.71) (s). **$^{13}$C {$^1$H} NMR** (100.61 MHz, $CDCl_3$): $\delta$ 141.09 (141.52) (d, $^3J_{CP}$ = 9.1 Hz, Ar); 128.53 (127.99) (s, Ar); 128.16 (127.12) (s, Ar); 126.69 (126.28) (s, Ar); 108.53 (106.83) (s, *C*-CH$(CH_3)_2$); 99.86 (96.48) (s, *C*-$CH_3$); 89.69 (88.66) (s, *C*H *p*-cym); 87.52 (88.42) (s, *C*H *p*-cym); 83.64 (85.70) (s, *C*H *p*-cym); 83.49 (85.07) (s, *C*H *p*-cym); 75.88 (75.47) (s,NC$H_2$N); 73.54 (73.97)(s, NC$H_2$N); 72.12 (s, *C*HOH); 69.72 (68.71)(d, $^1J_{CP}$ = 9.4 Hz, P*C*HN); 67.51 (65.70) (d, $^3J_{CP}$ = 4.6 Hz, NC$H_2$N); 54.72 (51.25) (d, $^2J_{CP}$ = 12.8 Hz, P*C*$H_2$N); 45.50 (d, $^1J_{CP}$ = 18.8 Hz, P*C*$H_2$N); 31.10

(30.80) (s, C*C*H-$Me_2$); 22.54 (22.36) (s, CCH-*Me*$_2$); 22.49 (22.03) (s, CCH-*Me*$_2$); 19.03 (18.50) (s, C-*C*$H_3$). **IR** (KBr, $cm^{-1}$): $\nu_{(OH)}$ 3372 (br, s); $\nu_{(arom)}$ 1446; $\nu_{(CH3)}$ 1241 (s). **Anal**. Calcd. for $C_{23}H_{32}Cl_2N_3OPRu$ (569.47 $gmol^{-1}$). Found (calcd): C 45.16 (48.51); H 5.29 (5.66); N 6.41 (7.38).

*Synthesis of [Ru(η⁶-p-cymene)Cl₂{(S,R R,S)-(PZA-NMe₂)}]* (**89**)

Dry degassed $CH_2Cl_2$ (25 mL) was added under nitrogen to a Schlenk tube charged with ligand (*S*,*R R*,*S*)(PZA-N-$Me_2$ (0.20 g, 0.65 mmol) and [Ru($\eta^6$-*p*-cymene)$Cl_2$]$_2$ (0.20 g, 0.33 mmol). The resulting clear red solution was stirred for 2h at room temperature. The solvent was reduced to about half of the initial volume and upon addition of 15 mL of cold pentane, a red-pink precipitate was formed. This was filtered under nitrogen and washed with 5 mL of cold pentane, yielding 0.22 g of a red-pink powder (56% yield).

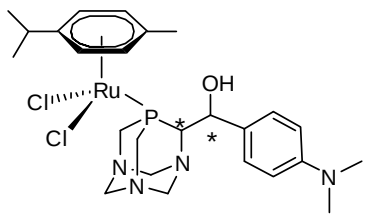


**89: S($H_2O$)$_{20°C}$**= 1.4 mg·$mL^{-1}$.**$^1$H NMR** (300.13 MHz, $CD_2Cl_2$): $\delta$ (ppm) 7.26 (d, $^3J_{HH}$ = 8.7 Hz, 2H, Ar); 6.75 (d, $^3J_{HH}$ = 8.7 Hz, 2H, Ar); 5.65-5.54 (m, 3H, *p*-cym);5.38-5.30 (m, 1H, C*H*OH); 5.23 (d, $^1J_{HH}$ = 5.9 Hz, 1H, *p*-cym); 4.65-4.35 (m, 9H, 3x NC$H_2$N + 1 x PC$H_2$N + PC*H*N); 4.25-4.15(m, 2H, PC$H_2$N) 2.97 (s, 6H, N(C$H_3$)$_2$); 2.79 (sept, $^1J_{HH}$ = 6.9 Hz, 1H, C*H*-$Me_2$); 2.19 (s, 3H, *p*-cym C$H_3$); 1.32 (d, $^1J_{HH}$ = 6.9 Hz, 3H, CH-*Me*$_2$); 1.30 (d, $^1J_{HH}$ = 6.9 Hz, 3H, CH-*Me*$_2$). **$^{31}$P {$^1$H} NMR** (121.50 MHz, $CD_2Cl_2$): $\delta$ -40.35 (s). **$^{13}$C {$^1$H} NMR** (75.47 MHz, $CD_2Cl_2$): $\delta$ 150.38 (s, Ar); 128.90 (d, $^3J_{CP}$ = 8.2 Hz, Ar); 127.51 (s, Ar); 112.17 (s, Ar); 108.10 (d, $^3J_{CP}$= 2.7 Hz, *C*-CH-$Me_2$); 99.41 (s, *C*-$CH_3$); 89.66 (d, $^2J_{CP}$ = 4.5 Hz, *C*H *p*-cym); 87.55 (d, $^2J_{CP}$ = 5.6 Hz, *C*H *p*-cym); 83.76 (s, *C*H *p*-cym); 83.48 (d, $^2J_{CP}$ = 3.7 Hz, *C*H *p*-cym); 75.84 (br s, N*C*$H_2$N); 73.60 (d, $^3J_{CP}$ = 6.6 Hz, N*C*$H_2$N); 71.63 (d, $^3J_{CP}$ = 2.6 Hz, *C*HOH); 69.57 (d, $^1J_{CP}$ = 9.5 Hz, P*C*HN); 67.43 (d, $^3J_{CP}$ = 7.4 Hz, N*C*$H_2$N); 54.78 (d, $^1J_{CP}$ = 13.5 Hz, P*C*$H_2$N); 45.25 (d, $^1J_{CP}$ = 18.8 Hz, P*C*$H_2$N); 40.34 (s, N(*C*$H_3$)$_2$); 31.02 (s, C*C*H-$Me_2$); 22.23 (s, CH-*Me*$_2$); 22.15 (s, CH-*Me*$_2$); 18.66 (s, CH-*C*$H_3$). **IR** (KBr, $cm^{-1}$): $\nu_{(OH)}$ 3383 (br, s); $\nu_{(arom)}$ 1611 (m), 1521 (m); $\nu_{(CH3)}$ 1241 (s). **Anal**. Calcd. for $C_{25}H_{37}Cl_2N_4OPRu$ (612.54 $gmol^{-1}$). Found (calcd): C 48.76 (49.02); H 5.01 (6.09); N 8.60 (9.15).

*Synthesis of [Ru(η⁶-p-cymene)I₂{(S,R R,S)-(PZA-NMe₂)}]* (**90**)

Following the synthetic procedure described above, the corresponding iodide analogue was obtained in 65% yield.

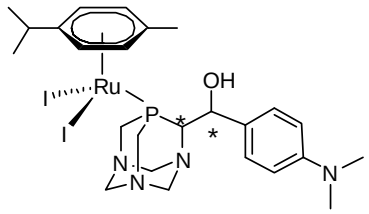


**90: . $^{1}$H NMR** (300.13 MHz, $CDCl_3$): $\delta$ 7.25 (d, $^{3}J_{HH}$ = 8.7 Hz, 2H, Ar); 6.73 (d, $^{3}J_{HH}$ = 8.7 Hz, 2H, Ar); 5.67 (d, $^{1}J_{HH}$= 5.8, 1H, *p*-cym); 5.63-5.55 (m, 2H, *p*-cym); 5.45 (dd, $^{1}J_{HH}$ = 7.3 Hz, $^{3}J_{HP}$ = 9.6 Hz, 1H, C*H*OH); 5.36 (d, $^{1}J_{HH}$= 5.8 Hz, 1H, *p*-cym); 4.82-4.42 (m, 9H, 3x NC$H_2$N + 1x PC$H_2$N + PC*H*N); 4.16-4.04 (m, 2H, PC$H_2$N); 3.64 (d, $^{1}J_{HH}$= 5.6 Hz, 1H, O*H*); 3.19 (sept, $^{1}J_{HH}$ = 5.0 Hz, 1H, C*H*-$Me_2$); 2.96 (s, 6H, N(C$H_3$)$_2$); 2.45 (s, 3H, *p*-cym C$H_3$); 1.31 (d, $^{1}J_{HH}$ = 6.9 Hz, 3H, CH-*Me*$_2$); 1.30 (d, $^{1}J_{HH}$ = 6.9 Hz, 3H, CH-*Me*$_2$). **$^{31}$P {$^{1}$H} NMR** (121.50 MHz, $CDCl_3$): $\delta$ -51.91 (s). **$^{13}$C {$^{1}$H} NMR** (75.47 MHz, $CDCl_3$): $\delta$ 150.35 (s, Ar); 128.11 (d, $^{3}J_{CP}$ = 6.1 Hz, Ar); 127.68 (s, Ar); 112.32 (s, Ar); 112.01 (d, $^{3}J_{CP}$= 3.1 Hz, *C*-CH(CH$_3$)$_2$); 101.28 (s, *C*-CH$_3$); 89.27 (d, $^{2}J_{CP}$ = 3.1 Hz, *C*H *p*-cym); 87.60 (d,2$^{3}J_{CP}$ = 3.3 Hz, *C*H *p*-cym); 83.93 (s, *C*H *p*-cym); 84.80 (d, $^{2}J_{CP}$ = 2.8 Hz, *C*H *p*-cym); 76.20 (d, $^{3}J_{CP}$ = 2.5 Hz, NCH$_2$N); 73.32 (d, $^{3}J_{CP}$ = 5.0 Hz, NCH$_2$N); 71.50 (d, $^{3}J_{CP}$ = 2.2 Hz, *C*HOH); 70.22 (d, $^{1}J_{CP}$ = 7.5 Hz, P*C*HN); 67.72 (d, $^{3}J_{CP}$ = 5.6 Hz, NCH$_2$N); 59.62 (d, $^{1}J_{CP}$ = 11.7 Hz, PCH$_2$N); 54.20 (d, $^{1}J_{CP}$ = 17.0 Hz, PCH$_2$N); 40.53 (s, N(CH$_3$)$_2$); 31.95 (s, C*C*H-Me$_2$); 23.71 (s, CH-*Me*$_2$); 22.15 (s, CH-*Me*$_2$); 20.71 (s, CH-*C*H$_3$). **IR** (KBr, cm$^{-1}$): $\nu_{(OH)}$ (br, s); 1241 (s). **Anal**. Calcd. for $C_{25}H_{37}I_2N_4OPRu$ (795.44 gmol$^{-1}$). Found (calcd): C 37.86 (37.75); H 4.86 (4.69); N 7.32 (7.04).

*Synthesis of (κ²-P,N)-[RuCl(η⁶-p-cymene){PTA-CH(1-MeIm)OH}]Cl* (**91**)

A 100 mL Schlenk flask was charged under a nitrogen atmosphere, with $[Ru(\eta^6\text{-}p\text{-cymene})Cl_2]_2$ (0.076 g, 0.124 mmol), PTA-CH(1-MeIm)OH (0.078 g, 0.290 mmol) and 25 mL $CHCl_3$. The clear red solution was heated to 60 $^{o}$C and stirred for 5 h under $N_2$. The resulting dark brown solution was filtered through Celite and the volume reduced to approximately 10 mL under vacuum. $Et_2O$ (10 mL) was added dropwise to produce a tan powder that was collected under $N_2$, washed with $Et_2O$ (2 x 5 mL) and dried *in vacuo*, yielding 0.12 g of the product (85.9 % yield).

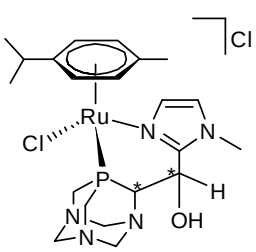

**91**: **S(H$_2$O)$_{20°C}$**= 320 mg·mL$^{-1}$. **$^1$H NMR** (400.13 MHz, $CDCl_3$): $\delta$ 7.76 (br s, 1H, NCHC*H*NCMe-Im); 6.93 (br s, 1H, NC*H*CHNMe-Im); 6.05 (br d, *J* = 5.5 Hz, 1H, C*H*-cym); 5.98 (br d, $^3J_{HP}$ = 5.4 Hz, 1H, C*H*-cym); 5.80 (br s, 1H, C*H*-cym); 5.55 (br s, 1H, C*H*-cym); 5.49 (br d, *J* = 10.1 Hz 2H, NC$H_2$N); 5.22 (br d, $^3J_{HP}$= 8.7 Hz 1H, PCHC*H*ImOH); 4.78 (br d, *J* = 9.2 Hz, 1H, PC*H*CHImOH); 4.60 (m, 3H, NC$H_2$N); 4.51 (br d, *J* = 14.9 Hz, 1H, PC$H_2$N); 4.40 (br d, *J* = 13.0 Hz, 1H, PC$H_2$N); 4.28 (br d, *J* = 13.0 Hz, 1H, PC$H_2$N); 4.10 (br d, *J* = 12.6 Hz, 1H, PC$H_2$N); 4.02 (s, 3H, N*Me*-Im); 3.47 (br s, 1H, PC$H_2$N); 2.68 (sept, *J* = 6.5 Hz, 1H, C*H*Me$_2$-cym); 1.81 (s, 3H, *Me*-cym); 1.29 (d, *J* = 6.8 Hz, 3H, CH*Me*$_2$-cym); 1.19 (d, *J* = 6.6 Hz, 3H, CH*Me*$_2$-cym). **$^{31}$P{$^1$H} NMR** (161.98 MHz, $CDCl_3$): $\delta$ 22.88 (s); -26.37 (s). **$^{13}$C{$^1$H} NMR** (100.03 MHz, $CDCl_3$): $\delta$ 149.53 (s, N*C*NMe-Im); 134.64 (s, N*C*=CNMe-Im); 122.22 (s, NC=*C*NCMe-Im); 105.47 (s, *C*Me-cym); 100.17 (s, *C*CHMe$_2$-cym); 98.05 (d, $^3J_{CP}$ = 6.7 Hz, *C*H-cym); 95.60 (d, $^3J_{CP}$ = 7.0 Hz, *C*H-cym); 82.79 (s, *C*H-cym); 81.75 (s, *C*H-cym); 76.51 (d, $^3J_{CP}$ = 2.6 Hz, N*C*N); 74.17 (d, $^3J_{CP}$ = 6.3 Hz, N*C*N); 68.18 (d, $^2J_{CP}$ = 9.2 Hz, **C*HOH); 66.72 (s, N*C*N); 59.22 (d, $^1J_{CP}$ = 13 Hz, P**C*N); 54.50 (d, $^1J_{CP}$ = 14 Hz, P*C*N); 52.56 (d, $^1J_{CP}$ = 19 Hz, P*C*N); 35.23 (s, N*Me*-Im); 30.63 (s, C*C*HMe$_2$-cym); 23.81 (s, CCH*Me*$_2$-cym); 20.89 (s, CCH*Me*$_2$-cym); 18.50 (s, C*Me*-cym); **IR** ($CH_2Cl_2$, cm$^{-1}$): $\nu_{(O-H)}$ 3370 (sh) ; $\nu_{(C=N)}$ 1604 cm$^{-1}$. **Anal**. Calcd. for $C_{21}H_{32}Cl_2N_5OPRu$ (573.4 gmol$^{-1}$). Found (calcd): C 44.10 (43.98); H 5.54 (5.62); N 12.44 (12.21).

*Synthesis of (κ²-P,N)-[RuCl(η⁶-p-cymene){PTA-C(1-MeIm)₂OH}]Cl* (**92**)

Following the same procedure, using 0.075 g (0.123 mmol) of $[Ru(\eta^6$-*p*-cymene$)Cl_2]_2$, and 0.10 g (0.293 mmol) of PTA-C(1-MeIm)$_2$OH, the product was obtained as a brown powder in 71.4% yield.

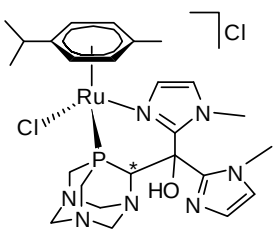

**92**: **S(H$_2$O)$_{20°C}$**= 170 mg·mL$^{-1}$. **$^1$H NMR** (400.13 MHz, $CD_2Cl_2$): $\delta$ 7.41 (s, 1H, NCHC*H*NCMe-Im); 6.97 (s, 1H, NC*H*CHNMe-Im); 6.86 (s, 1H, NCHC*H*NMe-Im); 6.81 (s, 1H, NC*H*CHNMe-Im); 6.08 (d, *J* = 6.3 Hz, 1H, C*H*-cym); 6.02 (d, *J* = 6.4 Hz, 1H,

C*H*-cym); 5.59 (br s, 1H, C*H*-cym); 5.56 (br s, 1H, C*H*-cym); 5.29 (br d, *J* = 13.5 Hz, 2H, NC*H*$_2$N); 4.60 (m, 4H, NC*H*$_2$N); 4.48 (br d, *J* = 13.3 Hz, 1H, PC*H*ClIm$_2$OH); 4.30 (br d, *J* = 13.3 Hz, 1H, PC*H*$_2$N); 4.23 (s, 3H, *NMe*-Im); 4.18 (br d, *J* = 13.7 Hz, 2H, PC*H*$_2$N); 4.02 (br d, *J* = 14.8 Hz, 1H, PC*H*$_2$N); 3.01 (s, 3H, N*Me*-Im); 2.80 (sept, *J* = 6.9 Hz, 1H, C*H*Me$_2$-cym); 2.05 (s, 3H, *Me*-cym); 1.36 (d, *J* = 6.9 Hz, 3H, CH*Me$_2$*-cym); 1.27 (d, *J* = 6.8 Hz, 3H, CH*Me$_2$*-cym). **$^{31}$P{$^1$H} NMR** (161.98 MHz, $CD_2Cl_2$): $\delta$ -19.77 (s). **$^{13}$C{$^1$H} NMR** (100.03 MHz, $CD_2Cl_2$): $\delta$ 150.39 (s, NCNMe-Im); 144.64 (d, $^3J_{CP}$ = 7.0 Hz, NCNMe-Im); 134.73 (s, NC=CNMe-Im); 127.31 (s, NC=CNMe-Im); 123.96 (s, NC=CNCMe-Im); 122.82 (s, NC=CNCMe-Im); 107.63 (s, CMe-cym); 105.67 (s, CCHMe$_2$-cym); 96.86 (d, $J_{CP}$ = 5.9 Hz, CH-cym); 95.69 (d, $J_{CP}$ = 7.4 Hz, CH-cym); 82.14 (s, CH-cym); 81.53 (s, CH-cym); 78.48 (s, NCN); 76.85 (d, $^3J_{CP}$ = 3.3 Hz, NCN); 74.07 (d, $^3J_{CP}$ = 6.7 Hz, NCN); 68.23 (d, $^2J_{CP}$ = 9.3 Hz, C*COHIm$_2$); 64.47 (d, $^1J_{CP}$ = 14.1 Hz, P*CN); 54.14 (d, $^1J_{CP}$ = 22.9 Hz, PCN); 52.85 (d, $^1J_{CP}$ = 19.3 Hz, PCN); 36.78 (s, N*Me*-Im); 36.65 (s, N*Me*-Im); 31.20 (s, CCHMe$_2$-cym); 22.48 (s, CCH*Me$_2$*-cym); 22.08 (s, CCH*Me$_2$*-cym); 19.28 (s, C*Me*-cym); **IR** ($CH_2Cl_2$, cm$^{-1}$): $\nu_{(O-H)}$ 3284 (sh) ; $\nu_{(C=N)}$ 1606 cm$^{-1}$. **Anal**. Calcd. for $C_{25}H_{36}Cl_2N_7OPRu$ (653.6 gmol$^{-1}$). Found (calcd): C 45.10 (45.94); H 5.58 (5.55); N 14.98 (15.01).

### 4.6.2. X-ray diffraction data collection

Single crystal X-ray diffraction data collection for compound **90** were carried out by using the same procedures reported in the experimental section of Chapter 2.

*X-ray crystal structure of [Ru($\eta^6$-p-cymene)I$_2${(S,R R,S)-(PZA-NMe$_2$)}]* (**90**)

The X-ray crystal structure of complex **90** shows that the complex crystallizes in a centro-symmetric space group and both the *S*,*R* and *R*,*S* are present in the crystal. The geometry around the ruthenium atom in **90** is an octahedron, where *p*-cymene occupies three coordination positions while two iodine atoms and one PZA-NMe$_2$ ligand occupy the other three. The Ru metal-carbon distances are between 2.187(10) and 2.276(10) that are slightly longer respect the corresponding distances

in the cation $[\{Ru(\eta^6\text{-}C_{10}H_{14})\}_2(Cl)_3]^+$.[33] The Phosphorus–Ruthenium distance is 2.340(3) and is comparable with the Ru-P distances in other PTA complexes. As in the previously reported Ir-PZA complex $[Cp^*IrCl_2(PZA)]$,[34] there is an intramolecular hydrogen bond between the hydroxyl hydrogen and one iodine atom (O1…I1 = 3.474(9). Figure 4.6 shows an ORTEP diagram of the structure and selected bond lengths and angles are reported in the caption.

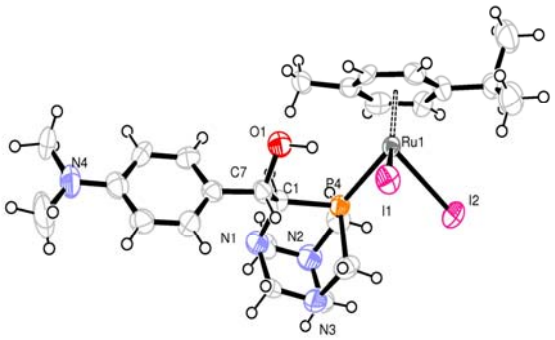


**Figure 4.6 .** ORTEP view of **90**. Ellipsoids drawn at 50% probability level. Selected bond lengths (Å) and angles (°): Ru1-P4=2.340(3); Ru1-I1=2.7366(12); Ru1-I2=2.7413(1); Ru-C17=2.239(11); Ru1-C18=2.201(12); Ru1-C19=2.193(12); Ru1-C20=2.276(11); Ru1-C21=2.247(10); Ru1-C22=2.187(10); P4-C3=1.854(12); P4-C2=1.849(12); P4-C1=1.877(11); P4-Ru1-I1=86.21(8); P4-Ru1-I2=86.46(8); I1-Ru1-I2=89.59(4); C3-P4-C2=98.7(6); C3-P4-C1=97.5(6); C2-P4-C1=97.7(5).

## 4.7 References


[1] Kovács, J.; Joó. F.; Bényei, A. C.; Laurenczy, G. *Dalton Trans*. **2004**, 2336-2340.
[2] Smoleński, P.; Pruchnik, F. P.; Ciunik, Z.; Lis, T. *Inorg*. *Chem*. **2003**, *42*, 3318-3322.
[3] Darensbourg, D. J.; Joó. F.; Kannisto, M.; Kathó, A.; Reibenspies, J. H. *Organometallics* **1992**, *11*, 1990-1993.
[4] Darensbourg, D. J.; Joó. F.; Kannisto, M.; Kathó, A.; Reibenspies, J. H.; Daigle, D. J. *Inorg*. *Chem*. **1994**, *33*, 200-208.
[5] Laurenczy, G.; Joó. F.; Nádasdi, L. *Inorg*. *Chem*. **2000**, *39*, 5083-5088.
[6] Mebi, C. A.; Frost, B. J. *Inorg*. *Chem*. **2007**, *46*, 7115-7120.
[7] Girotti, R.; Romerosa, A.; Mañas, S.; Serrano-Ruiz, M.; Perutz, R. N. *Inorg*. *Chem*. **2009**, *48*, 3692-3698.
[8] Akbayeva, D. N. ; Moneti, S.; Peruzzini, M.; Gonsalvi, L.; Ienco, L.; Vizza, F. *C. R. Chimie*, **2005**, *8*, 1491-1496.
[9] Akbaeva, D. N.; Gonsalvi, L.; Oberhauser, W.; Peruzzini, M.; Vizza, F.; Brügeller, P.; Romerosa, A.; Sava, G.; Bergamo, A. *Chem*. *Comm*. **2003**, 264-265.
[10] Bolaño, S.; Gonsalvi, L.; Zanobini, F.; Vizza, F.; Bertolasi, V.; Romerosa, A.; Peruzzini, M. *J. Mol. Cat. A*: *Chem*. **2004**, *224*, 61-70.
[11] Frost, B. J.; Mebi, C. A. *Organometallics* **2004**, *23*, 5317-5323.
[12] Mebi, C. A.; Frost, B. J. *Organometallics* **2005**, *24*, 2339-2346.
[13] Mebi, C. A.; Radhika, P. N.; Frost, B. J. *Organometallics* **2007**, *26*, 429-438.
[14] Mena-Cruz, A.; Lorenzo-Luis, P.; Romerosa, A.; Saoud, M.; Serrano-Ruiz, M. *Inorg. Chem*. **2007**, *46*, 6120-6128.
[15] Smith, C. A.; Sutherland-Smith, A. J.; Keppler, B. K.; Kratz, F.; Baker, E. N. *J. Biol. Inorg. Chem* **1996**, *1*, 424-431.
[16] Alessio, E.; Mestroni, G.; Bergamo, A.; Sava, G. *Curr. Top. Med. Chem*. **2004**, *4*, 1525-1535.
[17] Kratz, F.; Hartmann, M.; Keppler, B. K.; Messori, L. *J. Biol. Chem*. **1994**, *269*, 2581-2588.
[18] Allardyce, C. S.; Dyson, P. J.; Ellis, D. J. Heath, S. L. *Chem. Comm*. **2001**, 1396-1397.
[19] Ang, W. H.; Daldini, E.; Juillerat-Jeanneret, L.; Dyson, P. *Inorg. Chem*. **2007**, *46*, 9048-9050.
[20] Dyson, P. J.; Ellis, D. J.; Laurenczy, G. *Adv. Synth. Catal*. **2003**, *345*, 211-215.
[21] (a) Scolaro, C.; Bergamo, A.; Brescacin, L.; Delfino, R.; Cocchietto, M.; Laurenczy, G.; Geldbach, T.J.; Sava, G.; Dyson, P.J. *J. Med. Chem*. **2005**, *48*, 4161-4171. (b) Scolaro, C.; Geldbach, T. J.; Rochat, S.; Dorcier, A.; Gossen, C.; Bergamo, A.; Cocchietto, M.; Tavernelli, I.; Savva, G.; Rothlisberger, U.; Dyson, P. J. *Organometallics* **2006**, *25*, 756-765. (c) Renfrew, A. K.; Phillips, A. D.; Tapavicza, E.; Scopelliti, R.; Rothlisberger, U.; Dyson, P. J. *Organometallics*, **2009**, *28*, 5061-5071.
[22] (a) Romerosa, A.; Campos-Malpartida, T.; Lidrissi, C.; Saoud, M.; Serrano-Ruiz, M.; Peruzzini, M.; Garrido-Cárdenas, J. A.; Garciá-Maroto, F. *Inorg. Chem*. **2006**, *45*, 1289-1298. (b) Romerosa, A.; Saoud, M.; Campos-Malpartida, T.; Lidrissi, C.; Serrano-Ruiz, M.; Peruzzini, M.; Garrido, J. A.; Garciá-Maroto, F. Eur. *J. Inorg. Chem*. **2007**, 2803-2812.
[23] Wong, G. W.; Lee, W-C.; Frost, B. *J. Inorg. Chem*. **2008**, *47*, 612-620.
[24] Krogstad, D. A.; Guerriero A.; Ienco, A.; Peruzzini, M.; Bosquain, S. S.; Reginato, G.; Gonsalvi, L. manuscript in preparation.
[25] (a) Phillips, A. D.; Gonsalvi, L.; Romerosa, A.; Vizza, F.; Peruzzini, M. *Coord. Chem. Rev*. **2004**, *248*, 955-993. (b) Bravo, J.; Bolaño, S.; Gonsalvi, L.; Peruzzini, M. *Coord. Chem. Rev*. **2010**, *254*, 555-607.
[26] Renfrew, A. K.; Phillips, A. D.; Egger, A.; Hartinger, C. G.; Bosquain, S. S.; Nazarov, A. A.; Keppler, B. K.; Gonsalvi, L.; Peruzzini, M.; Dyson, P. J. *Organometallics* **2009**, *28*, 1165–1172.
[27] Caballero, A.; Jalon, F. A.; Manzano, B. R.; Espino, G.; Perez-Manrique, M.; Mucientes, A.; Poblete, F. J.; Maestro, M. *Organometallics*, **2004**, *23*, 5694-5706.
[28] (a) De la Encarnacion, E.; Pons, J.; Yanez, R.; Ros, J. *Inorg. Chim. Acta* **2005**, *358*, 3272-3276. (b) Moldes, I.; de la Encarnacion, E.; Ros, J.; Alvarez-Larena, A.; Piniella, J. F. *J. Organomet. Chem.* **1998**, *566*, 165-174.
[29] Hounjet, L. J.; Bierenstiel, M.; Ferguson, M. J.; McDonald, R.; Cowie, M. *Inorg. Chem*. **2010**, *49*, 4288-4300.

[30] Madrigal, C. A.; Garcia-Fernandez, A.; Gimeno, J.; Lastra, E. J. *Organomet*. *Chem*. **2008**, *693*, 2535-2540.
[31] (a) Baratta, W.; Rigo, P. *Eur. J*. *Inorg*. *Chem*. **2008**, *26*, 4041-4053. (b)De Vries, J. G.; Elsevier, C. J. *Handbook of Homogeneous Hydrogenation*, *vol.2*, Eds; HandWiley-VCH Verlag GmbH & Co KGaA: Weinheim, **2007**.
[32] Bennett, M. A.; Huang, T-N.; Matheson, T. W.; Smith, K. *Inorg*. *Synth*. **1982**, *21*, 74-75.
[33] Liu, L.; Zhanga, Q.-F,; Leung, W-H. *Acta Cryst*. **2004**, E60, m506-m508.
[34] Erlandsson, M.; Gonsalvi, L.; Ienco, A.; Peruzzini, M. *Inorg*. *Chem*. **2008**, *47*, 8-10.

# *Chapter 5*

# Rhodium PTA complexes and their catalytic hydroformylation studies with cyclodextrins

## 5.1 Overview

This Chapter describes the activity of PTA and some of its *lower rim* derivatives in rhodium-catalyzed hydroformylation reactions using cyclodextrins (CDs) as mass transfer promoters. Firstly, the description of known Rh-PTA complexes and a brief introduction on the most important features of cyclodextrins and their use in catalysis are reported. In the second part of this Chapter, the studies on the interaction of ligands PTA and its derivatives, [*N*-BzPTA]Cl (**73**) and [*tert*-butyl-*N*-BzPTA]Br (**72**), are described and their performances in catalytic hydroformylation reactions of terminal alkenes are discussed. This work has been carried out for its synthetic part in the laboratories in Florence and for the catalytic test at UCCS-CNRS Lens (France) as part of a bilateral CNR-CNRS collaboration. In the last part, the Chapter reports the experimental section describing all the details about association constants, NMR and surface-tension studies and all details about catalytic experiments carried out in the present study.

## 5.2 Introduction

As for ruthenium, rhodium-PTA based systems have received much attention due to their potential catalytic activity both in hydrogenation and hydroformylation reactions.[1] The water-soluble transition metal complex bearing PTA and Tpms (Tpms= tris(1-pyrazolyl)methansulfonate), [Rh(Tpms)(CO)(PTA)] was obtained in high yield in a single pot reaction by using $[Rh(CO)_2(\mu\text{-}Cl)]_2$, Li(Tpms) and PTA, without adding CO (Scheme 5.1). The X-ray crystal structure of the complex showed that the anionic tris(1-pyrazolyl)methansulfonate group acted as a bidentate $\kappa^2$-*N*,*N*-ligand, binding the Rh atom through the two pyrazolyl nitrogen atoms. PTA and CO completed the coordination sphere.[2]

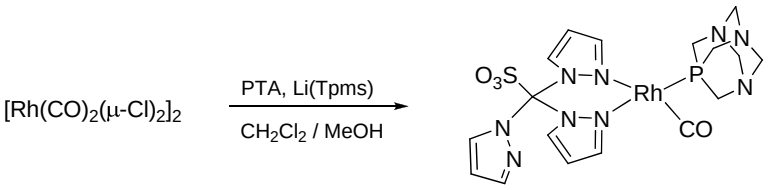


**Scheme 5.1.** Synthesis of [Rh(Tpms)(CO)(PTA)] complex.

The Rh(I) complex [Rh(acac)(CO)(PTA)] (acac= acteylacetonate) was synthesized by reacting $[Rh(acac)(CO)_2]$ with one equivalent of PTA in ethanol under refluxing conditions and was tested for catalytic hydrogenation of alkenes and allyl alcohol.[3] The catalytic tests, performed under biphasic water/substrate and $H_2$ pressure conditions, showed a selectivity of 90% in the hydrogenation of allyl alcohol to *n*-propanol and a TOF value of 143 $h^{-1}$ for the hydrogenation of 1-hexene. Complex $[RhCl(PTAH)(PTA)_2]Cl$ was found to be active in the C=C double bond hydrogenation (93% selectivity) of *trans*-cinnamaldehyde under biphasic conditions using $NaCO_2H$ as the hydrogen source.[4] In the *transfer hydrogenation* of allylbenzene, this complex resulted to be poorly selective, as it gave extensive isomerisation to *cis* and *trans*-propenylbenzene, and its recycling was limited to the fourth cycle.

By reacting $[RhCl(cod)]_2$ with the open-cage PTA derivatives PTN(R), the products $\kappa^1$-*P*-[RhCl(cod){PTN(R)}] (R= Me or Ph) were obtained in high yields as air- and moisture-stable yellow solids (Scheme 5.2).[5] Chloride abstraction forcing chelation

of the aminophosphine to yield $\kappa^2$-*P*,*N*-[RhCl(cod){PTN(R)}]($BAr^F_4$) (R=Me or Ph) was easily obtained by reacting the Rh(I) chloride parent species with $NaBAr^F_4$ in dichloromethane at room temperature. ($BAr^F_4$ = $[B\{C_6H_3(CF_3)_2\}_4]^-$).

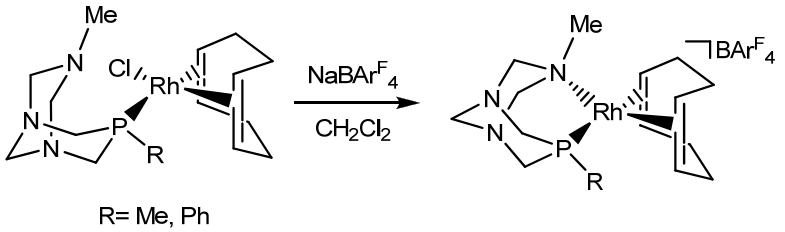


**Scheme 5.2.** Rh(I) complexes bearing the water soluble derivatives PTN(R).

The DFT studies on these complexes revealed significant changes to the PTN ligands on passing from the $\kappa^1$-P to the $\kappa^2$-P,N chelating mode and overall, PTN ligands had a preference for maintaining *P*-coordination to Rh. In contrast, a higher energy cost in terms of bond strain was associated to the *P*,*N* chelation, and, as consequence, the ligands could show in principle hemilabile behaviour in the presence of polar solvents or other types of nucleophiles. These complexes were all tested as catalysts for 1-hexene and styrene hydroformylation and *transfer hydrogenations* of benzylidene acetone (BZA) and acetophenone. High chemoselectivity to C=C bond hydrogenation was obtained with all complexes in the *transfer hydrogenation* in water of BZA using sodium formate. The hydrogenation of acetophenone was performed using the KOH/$^i$PrOH protocol and the $\kappa^1$-P species showed higher conversions (56-69%) than the $\kappa^2$-P,N chelate compounds. When tested as catalysts for 1-hexene hydroformylation in homogeneous phase, the Rh complexes showed to favour the formation of the linear aldehyde, while high conversions and high chemoselectivity to the branched aldehydes were obtained as expected in the hydroformylation of styrene.

Direct reaction of the rhodium dimer $[Cp^*RhCl(\mu\text{-}Cl)]_2$ with two or four equivalents of PTA or [mPTA]Cl afforded the series of water-soluble complexes reported in Scheme 5.3.[6] These compounds were evaluated for anticancer activity *in vitro*, using HT29 colon carcinoma, A549 lung carcinoma and T47D breast carcinoma cells, and their activity was compared to that of $[RuCl_2(\eta^6\text{-}p\text{-cymene})(PTA)]$, (RAPTA-C.)[7] In the

HT29 cell line, the nearest congener to RAPTA-C, $[Cp^*RhCl_2(PTA)]$ demonstrated a very similar cytotoxicity profile. Furthermore, $[Cp^*RhCl_2(PTA)]$ proved significantly more cytotoxic in A549 cells and $[Cp^*RhCl(PTA)_2]Cl$ more cytotoxic in T47D cell line, both relative to RAPTA-C.

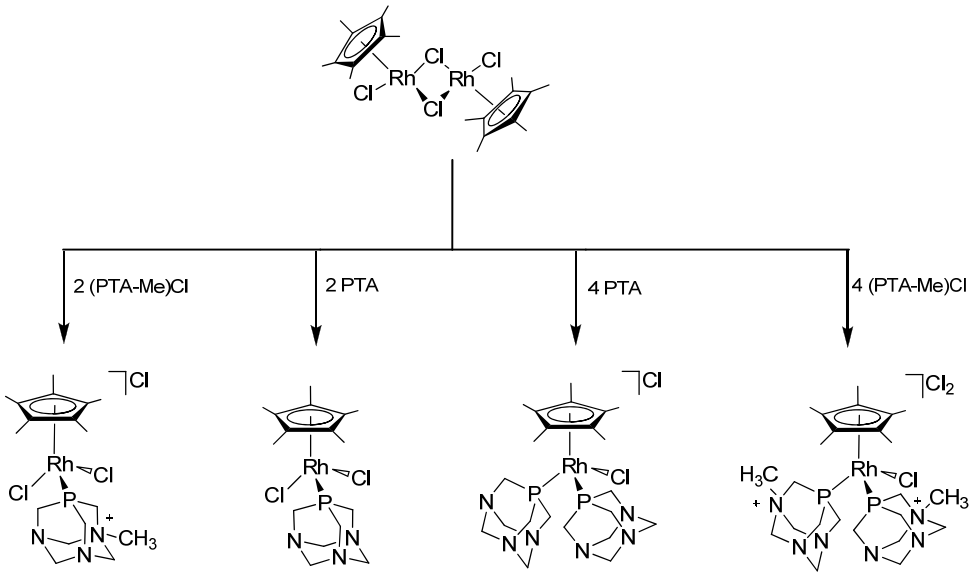


**Scheme 5.3.** Synthesis of some Rh-PTA complexes as potential anticancer drugs.

The two rhodium hydride compounds featuring alkylated PTA derivatives, $[RhH(mPTA)_4]I_4$ and $[RhH(mPTA)_4]I_4$ were prepared by addition of one equivalent of phosphine to $[Rh(CO)(PTA_R)_3]I_3$ (R= Me or Et) and subsequent treatment with $NaBH_4$.[8] These two hydrides were very stable to air and moisture as solids and could be stored for several months in deoxygenated water. Finally, other examples of transition-metal complexes bearing the *lower rim* modified PTA ligands, $PTA_{R3}$, are given by the Rh compounds $[RhCl(CO)(PTA_{R3})_2]$ (R= Ph, or $C_6H_4OCH_3$, or $C_6H_4CN$), which were obtained by reacting $[RhCl(CO)(PPh_3)_2]$ with the appropriate amount of ligand in benzene.[9] Since modifications of the triazacyclohexane ring alter the steric properties of the phosphine with minimal change to electronics, comparison of $\nu_{CO}$ IR stretching bands for a series of *trans*-$[RhCl(CO)(PTA_{R3})_2]$ complexes, indicated that these ligands were electronically similar and less electron-donating than PTA.

## 5.3 Cyclodextrins: supramolecular hosts for organometallic compounds

As already discussed, the use of biphasic aqueous catalysis is not widely applied because of the low solubility of most organic substrates in water and also by the need to synthesize water-soluble ligands or stabilizing agents in order to constrain the catalyst in water. Indeed, poorly water-soluble ligands react far too slowly under aqueous biphasic conditions for economically viable industrial applications and the synthesis of water-soluble ligands or stabilizing agents is often difficult and expensive.[10] Among the possible approaches to circumvent these problems, the use of cyclodextrins (CDs) proved to be one of the more promising.[11] The most current cyclodextrins contain six (α-CD), seven (β-CD) or eight (γ-CD) D-glucopyranose units (Figure 5.1).[12]

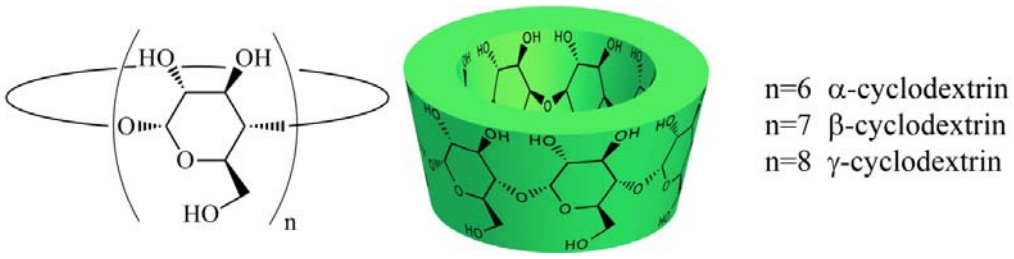


**Figure 5.1.** Chemical structure of native cyclodextrins.

The specific coupling of the glucose monomer determines a rigid conical molecular structure whose inner surface is hydrophobic and outer surface hydrophilic. The internal cavity can accommodate a wide range of guest molecules, which are bound at least partially within the cavity of the CD. The driving forces for the inclusion complexation of CD with substrates are attributed in most cases to several factors, such as van der Waals forces, hydrophobic interactions, electronic effects and steric factors.[13] The inclusion generally modifies the chemical, electrochemical and photochemical properties of organometallic compounds. The interaction between the organometallic complex and the CD can generate different types of adducts (Figure 5.2). In fact, the CD can behave as a second-sphere ligand, binding noncovalently the first-sphere ligands of the metal centre (a, Figure 5.2); the CD can

act simultaneously as a first- and second-sphere ligand, attaching covalently one ligand of the organometallic compound and including another ligand of the complex into its cavity (b, Figure 5.2); the CD can still bind a ligand of the complex and temporarily include in its cavity a substrate which reacts with the organometallic complex (c, Figure 5.2); and finally, the cyclodextrin can include in its cavity an hydrophobic substrate which binds a water-soluble organometallic catalyst (d, Figure 5.2).[14] Formation of such inclusion complexes can induce in some cases a decrease in the activity and selectivity[15] or a modification of the catalyst structure.[16]

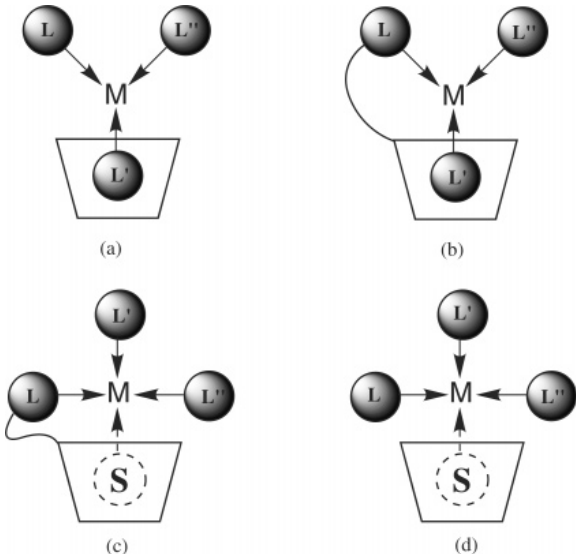


**Figure 5.2.** Different adducts generated by the interaction organometallic complex/CD. Adapted from ref. 14.

Many synthetic protocols have been developed for selective modifications of CDs, which provide the opportunity to fine-tune their physicochemical properties, such as solubility and surface activity.[17] A wide range of catalytic reactions, including hydrogenation, hydroformylation, oxidation, reduction and C–C coupling reactions have been successfully achieved in aqueous media by using chemically modified CDs.[18] In many reactions, chemically modified CDs exhibited a better catalytic activity than native CDs, such as in the hydrogenation of aldehydes[19] or in hydroformylation reactions.[20] For example, the randomly methylated β-cyclodextrin, RAME-β-CD (Figure 5.3), in the catalytic system together with the

metal and the water-soluble ligand, could be quantitatively recovered and the phase separation between the organic and aqueous phase resulted to be fast with this modified CD.

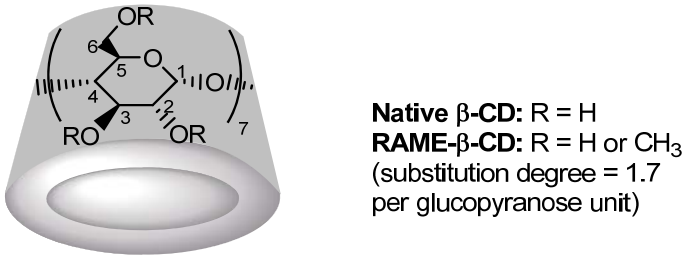


**Figure 5.3.** Structure of the native and the chemical modified β-cyclodextrins.

In addition, with RAME-β-CD no increase in catalyst leaching into the organic phase was observed. Interestingly, chemically modified CDs can also been used to perform substrate-selective reactions which are difficult to achieve with conventional transition metal catalysts.[21] In fact, when the organic phase contains a mixture of isomers, the water-soluble catalyst reacts with the isomer which preferentially interacts with the CD cavity, inducing substrate selectivity. This type of catalytic system exhibits enzyme-like properties. In several studies, it was demonstrated that, by using different structural isomers, the substrate selectivity strongly depended on the water solubility and the structures of isomers. Thus, high substrate selectivity could only be observed with highly water-insoluble isomers which showed pronounced structural differences.[22] Experimental data about surface tension and association constant measurements[23] and molecular dynamic simulations,[24] showed that chemically modified CDs favour the contact between the organometallic catalyst and the substrate at the interface or into the bulk aqueous phase according to the nature of the substrate. Indeed, when a mechanism of inverse phase catalysis is proposed for partially water-soluble substrates, the reaction of highly water-insoluble substrates is believed to occur by an interfacial catalysis mechanism. A cartoon-like description is shown in Figure 5.4.

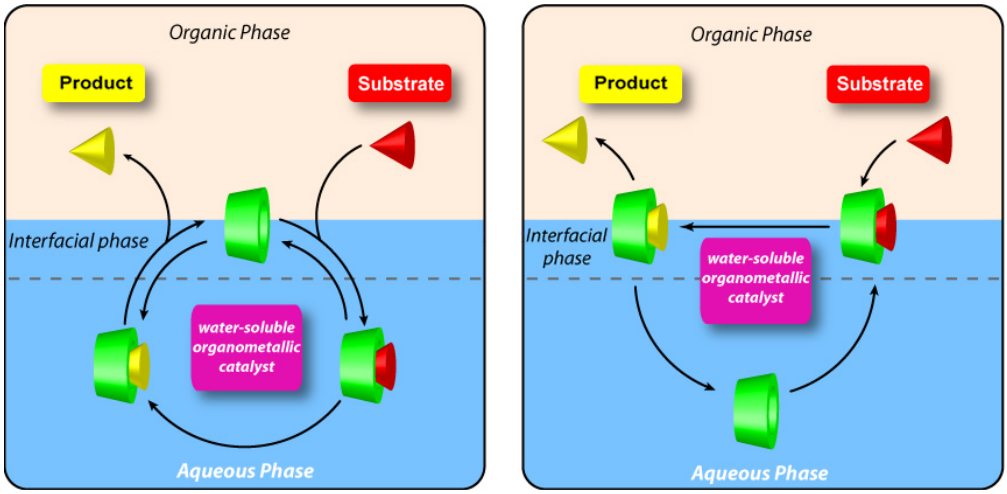


**Figure 5.4.** (a) Inverse phase transfer catalysis (b) Interfacial catalysis. Taken from ref. 18.

## 5.4 Hydroformylations of higher olefins with PTA and derivatives in the presence of CDs

Hydroformylation reactions are of great interest for industrial applications and the Rhurchemie/Rhône-Poulenc process is one of the main important examples. This hydroformylation process is performed in water on lower olefins such as propene and butene by using water-soluble Rh-organometallic catalysts.[25] However, although this system can be applied to lower olefins, it does not work on higher olefins. To circumvent this problem and to perform hydroformylation reactions of long chain olefins in water, the use of cycoldextrins can be one of the possible solution. As previously discussed, the performances of the CD-based biphasic system may be affected by detrimental interactions between the CD and the water-soluble ligand which has the function to stabilize the catalyst in water. TPPTS (tris-*m*-sulfonated triphenylphosphine), which is the water-soluble phosphine used in the Rhône-Poulenc process, forms a 1:1 inclusion complex with RAME-β-CD, inducing the formation of phosphine low-coordinated rhodium species and causing a subsequent decrease in the regioselectivity of hydroformylation reaction.[26]

In consideration of the behaviour of TPPTS ligand with RAME-β-CD, we decided to test PTA and its *lower rim* derivative [*N*-BzPTA]Cl (**73**) (1-benzyl-1,3,5-triaza-7-

phosphaadamantane chloride, Figure 5.5), in Rh-catalyzed hydroformylation of 1-decene in presence of RAME-β-CD as mass transfer promoter.[27]

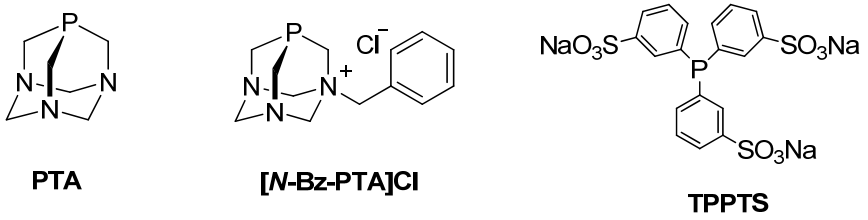


**Figure 5.5.** PTA, [*N*-BzPTA]Cl and TPPTS.

Interactions between RAME-β-CD and the two phosphines in water have first been studied to evaluate the ability of the ligands to include into the CD cavity. By using the spectral displacement method (UV-vis spectroscopy) with methyl orange as competitor of the ligand, no spectral variation was detected, indicating the absence of interaction between PTA and [*N*-BzPTA]Cl and RAME-β-CD. The inclusion constants calculated also with the less hindered native β-CD, both for PTA ($K_{inc}$= 63 $M^{-1}$) and for [*N*-BzPTA]Cl ($K_{inc}$= 11 $M^{-1}$), resulted to be lower in comparison with that of TPPTS ($K_{inc}$= *ca* $10^5$ $M^{-1}$). These low values are in contrast with the large association constants reported in the literature with CDs and PTA structurally close derivatives, such as adamantyl compounds. NMR experiments also corroborated the abovementioned results as no contact was detected in the 2D T-ROESY spectrum of a 1:1 mixture of RAME-β-CD and PTA. Probably, the low inclusion level was due to the ability of nitrogen and phosphorus atoms to form hydrogen bonding with water, preventing the inclusion of PTA and its *lower rim* derivative in the hydrophobic cavity of RAME-β-CD. Additionally, the absence of interaction could also be rationalized by the presence of hindered methyl groups on the CD which prevent a recognition process between both compounds. As a conclusion of these data, it appeared that both PTA and [*N*-BzPTA]Cl could be considered as non-interacting phosphines with respect to RAME-β-CD and so, the CD cavity would be not poisoned by the two ligands.

In consideration of these results, we decided to evaluate the performances of PTA and [*N*-BzPTA]Cl as rhodium water-soluble stabilizing ligands in catalytic

hydroformylation of 1-decene in the presence of RAME-β-CD (Scheme 5.4). 1-decene has been chosen as model substrate for its hydrophobic character, while RAME-β-CD was preferred to the native-β-CD for its better adsorption ability at the organic/aqueous interface.[23]

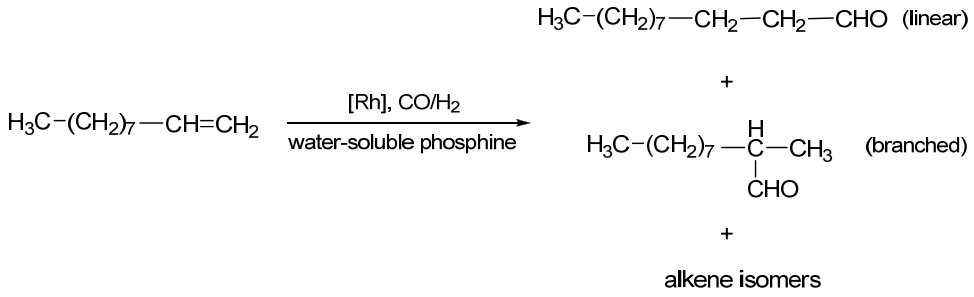


**Scheme 5.4.** Hydroformylation of 1-decene.

**Table 5.1.** Biphasic Rh-catalyzed hydroformylation of 1-decene with PTA, [*N*-BzPTA]Cl and TPPTS in the presence of RAME-β-CD. Adapted from ref. 27.

| ENTRY | PHOSPHINE | CD | T (°C) | CONV. (%)[b] | SELECT. (%)[c] | l/b RATIO[d] |
|---|---|---|---|---|---|---|
| **1** | TPPTS | – | 80 | 3 | 59 | 2.8 |
| **2** | TPPTS | – | 100 | 28 | 42 | 2.9 |
| **3** | TPPTS | – | 120 | 50 | 30 | 3.0 |
| **4** | TPPTS | RAME-β-CD | 80 | 95 (65[e]) | 96 | 1.8 |
| **5** | TPPTS | RAME-β-CD | 100 | 100 (74[e]) | 88 | 1.9 |
| **6** | TPPTS | RAME-β-CD | 120 | 100 (85[e]) | 73 | 2.2 |
| **7** | PTA | – | 80 | <1 | n.d. | n.d. |
| **8** | PTA | – | 100 | 2 | 90 | 1.9 |
| **9** | PTA | – | 120 | 81 | 96 | 1.9 |
| **10** | PTA | RAME-β-CD | 80 | <1 | n.d. | n.d. |
| **11** | PTA | RAME-β-CD | 100 | 11 | 98 | 1.9 |
| **12** | PTA | RAME-β-CD | 120 | 94 | 99 | 1.7 |
| **13** | [*N*-BzPTA]Cl | – | 80 | 19 | 98 | 1.9 |
| **14** | [*N*-BzPTA]Cl | – | 100 | 77 | 99 | 1.8 |
| **15** | [*N*-BzPTA]Cl | RAME-β-CD | 80 | 24 | 98 | 1.9 |
| **16** | [*N*-BzPTA]Cl | RAME-β-CD | 100 | 86 | 96 | 1.8 |

[a] $Rh(acac)(CO)_2$, 4.07 x $10^{-2}$ mmol; phosphine, 0.21 mmol; CD, 0.48 mmol; $H_2O$, 11.5 mL; 1-decene, 20.35 mmol; 1500 rpm; $CO/H_2$ (1:1), 50 bar; time, 6h. [b] calculated with respect to the starting olefin.
[c] (mol of aldehydes/mol of converted olefins) x 100. The side products were mainly isomeric olefins.
[e] After 3h reaction time.

All the catalytic experiments were carried out in water at various temperatures under $CO/H_2$ pressure (50 bar) for 6h. Catalytic tests in the presence of TPPTS instead of PTA or [*N*-BzPTA]Cl under the same conditions were run for comparison. The results of the catalytic experiments are reported in Table 5.1.

The first catalytic tests carried out with TPPTS in absence of RAME-β-CD, showed very low conversions, while in the presence of CD the conversions were higher, but alkene isomerization by-products were formed along with aldehydes as an effect of temperature increase (entries 4-6). Moreover, due to the formation of a RAME-β-CD/TPPTS supramolecular complex and the resulting displacement of the equilibrium in favor of phosphine low-coordinated rhodium species, the linear to branched aldehyde ratio (l/b) dropped from 2.8 to 1.8 at 80 °C (entries 1 and 4). The increase of temperature, causing the decrease in the RAME-β-CD/TPPTS association constant, logically determined an increase in l/b ratio but still poorly significant (1.8 at 80 °C *vs*. 2.2 at 120 °C). As PTA has a more basic character than TPPTS,[1a] a higher reaction temperature was required to generate the catalytically active Rh-species. In fact, in absence of RAME-β-CD, a conversion of 81% was achieved at 120 °C after 6h (entry 9). The addition of RAME-β-CD to the PTA-containing catalytic solution, at the same temperature (120 °C) resulted in an increase of the conversion to 94% (entry 12). Interestingly, contrary to the reduction in chemoselectivity previously observed with TPPTS at 120 °C, increasing the temperature with PTA as ligand did not alter the chemoselectivity of the hydroformylation reaction. Indeed, 98% and 99% aldehydes were produced during the course of the reaction at 100 and 120 °C respectively, along with small amounts of isomerized alkenes (entries 11 and 12). Additionally, in contrast to TPPTS where the formation of an inclusion complex with RAME-β-CD determined a loss in the l/b ratio, the linear to branched aldehydes ratio remained unchanged with PTA as water-soluble phosphine regardless of the presence of the cyclodextrin. This could be interpreted as no interaction occurring between RAME-β-CD and PTA and so high-coordinated catalytic species were favored. As a consequence, the choice in the formation of linear or branched aldehydes for the catalyst was not perturbed and the l/b ratio remained constant.

When the catalytic runs were carried out by using [*N*-BzPTA]Cl as water soluble ligand, a better conversion was obtained also respect to that obtained with PTA (19% for [*N*-BzPTA]Cl and <1% for PTA at 80 °C; 77% for [*N*-BzPTA]Cl and 2% for PTA at 100 °C in absence of RAME-β-CD). This behaviour is indicative of the more acidic and surface-active character of this phosphine. In fact, the phosphine basicity calculated in $D_2O$ from the first order phosphorus-selenium coupling constants ($^1J_{P\text{-}Se}$), gave values of 755Hz for Se=PTA and of 817Hz for [*N*-Bz(Se=PTA)]Cl. This higher $^1J_{P\text{-}Se}$ value indicated that [*N*-BzPTA]Cl is less electron rich than PTA[28] and thus at 80 °C the catalyst was already active. Moreover, the surface activity of [*N*-BzPTA]Cl seemed also to be responsible for this increase in activity due to its amphiphilic structure and the surface tension $\gamma$ dropped at lower concentration both for [*N*-BzPTA]Cl and the phosphine TPPTS. This was also corroborated by the low impact of the addition of RAME-β-CD on the activity of the catalytic system and so the role of the CD as mass transfer promoter became less significant. As observed above with PTA, the chemo- and regioselectivity were not strongly affected by the presence of RAME-β-CD, the selectivity in obtaining aldehydes resulted to be very high (>98%) and the l/b ratio was the same in comparison to the tests performed without the CD. These results confirm the absence of interaction between [*N*-BzPTA]Cl and the cyclodextrin as already explained for PTA. Although the use of [*N*-BzPTA]Cl determined many advantages in terms of catalytic activity performance, its surface activity hampered the decantation process of the biphasic system at the end of the reaction due to the formation of an emulsion.

For this reason we decided to test the new *lower rim* PTA derivative [*tert*-butyl-*N*-BzPTA]Br (**72**) (4'-tert-butyl-1-benzyl-1,3,5-triaza-7-phosphaadamantane bromide, Figure 5.6) in catalytic hydroformylation reactions in the presence of native-β-CD and RAME-β-CD, and to study how the introduction of the *tert*-butyl group could affect the catalytic performances.[29]

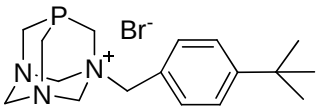


**Figure 5.6.** The new *lower rim* derivative [*tert*-butyl-*N*-BzPTA]Br.

Indeed, it is well known that *tert*-butylphenyl subunits are easily recognized by the internal cavity of β-cyclodextrins and numerous van der Waals interactions between the guest and the inner walls can be established. The determination of ligand basicity through first order phosphorus-selenium coupling constants resulted in a $^{1}J_{P\text{-}Se}$ value of 815 Hz and so [*tert*-butyl-*N*-Bz-PTA]Br is slightly more basic than [*N*-BzPTA]Cl ($^{1}J_{P\text{-}Se}$= 817 Hz).[27] This result was coherent with the electron-donating effect of the 4-*tert*-butyl substituent. Surface tension measurements revealed the hydrophobic feature of this ligand and as for [*N*-BzPTA]Cl, a regular decrease in the interfacial tension $\gamma$ with the concentration was observed (Figure 5.7). No critical micellar concentration (cmc) could be detected in the studied concentration range.

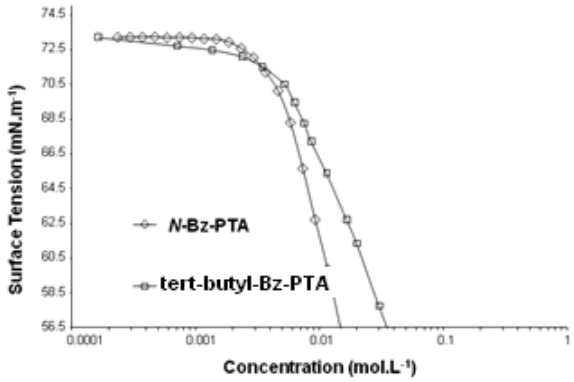


**Figure 5.7.** Comparison of surface tension curves of [*N*-Bz-PTA]Cl and [*tert*-butyl-*N*-Bz-PTA]Br. Adapted from ref. 29.

Due to the insolubility of [*tert*-butyl-*N*-Bz-PTA]Br beyond 25 $mM^{-1}$ at room temperature, the impact of the ligand on $\gamma$ was measured at low concentrations, clearly showing its ability to adsorb at the aqueous/air interface. Interestingly, the addition of one equivalent of RAME-β-CD on an aqueous solution of it caused an increase of the surface tension $\gamma$ to 57.2 $mN \cdot m^{-1}$, which is an intermediate value between that of the pure ligand (54.6 $mN \cdot m^{-1}$) and that of pure CD (58.0 $mN \cdot m^{-1}$).

This observation suggested that RAME-β-CD concealed the amphiphilic character of [*tert*-butyl-*N*-Bz-PTA]Br because of the inclusion of *tert*-butylphenyl group into the CD cavity. Furthermore, in contrast with [*N*-Bz-PTA]Cl, at 80 °C the association constants between [*tert*-butyl-*N*-Bz-PTA]Br and both RAME-β-CD and native-β-CD, calculated with Isothermal Titration Calorimetry (ITC) method, showed strong interactions. In addition, at room temperature and at 80 °C, correlations were also detected in 2D T-ROESY spectra containing an equimolar amount of CDs and ligand.
Thus, knowing that [*tert*-butyl-*N*-Bz-PTA]Br had a strong affinity for both RAME-β-CD and native-β-CD, we decided to test its catalytic activity in hydroformylation reactions. The catalytic runs were first performed on 1-decene, the same substrate used with PTA and [*N*-Bz-PTA]Cl, and then on higher olefins, such as 1-dodecene and 1-tetradecene. The catalytic reactions were carried out with $Rh(acac)(CO)_2$ precursor at different temperatures by using in all cases a $CO/H_2$ pressure (1:1, 50 bar) at 6 h. The results are reported in Table 5.2, which includes also the previous results obtained with [*N*-Bz-PTA]Cl (entries 1-4) for an easier comparison. At 80 °C, [*tert*-butyl-*N*-Bz-PTA]Br appeared to be an effective ligand as the conversion was close to that obtained with [*N*-Bz-PTA]Cl in hydroformylation of 1-decene (26% *vs*. 19%) and much more effective than TPPTS for which a very low conversion (3%) was measured in the same catalytic conditions (Table 5.1).[27] When the temperature was increased to 100 and 120 °C, logically an increase in the conversion was observed as the formation of the active species was favoured. Astonishingly, at 80 °C, the addition of an excess RAME-β-CD led to a drop in the catalytic activity (from 26% to 10% conversion, entries 5,6). Similar results were obtained also with 1-dodecene (from 39% to 11% conv., entries 13, 14) and 1-tetradecene (from 53% to 14% conv., entries 19, 20). Conversely, at 100 and 120 °C the addition of excess RAME-β-CD resulted in a marked increase in catalytic activity. In fact, at 100 °C the conversion increased from 56% to 72% for 1-decene, from 49% to 75% for 1-dodecene and from 53% to 88% for 1-tetradecene.

**Table 5.2.** Biphasic rhodium-catalyzed hydroformylation reactions.[29]

| Entry | Olefin | Phosphine | CD | T (°C) | Conv.(%)[b] | Select.(%)[c] | l/b ratio[d] |
|---|---|---|---|---|---|---|---|
| **1** | 1-decene | *N*-Bz-PTA | - | 80 | 19 | 98 | 1.9 |
| **2** | 1-decene | *N*-Bz-PTA | RAME-β-CD | 80 | 24 | 98 | 1.9 |
| **3** | 1-decene | *N*-Bz-PTA | - | 100 | 77 | 99 | 1.8 |
| **4** | 1-decene | *N*-Bz-PTA | RAME-β-CD | 100 | 86 | 96 | 1.8 |
| **5** | 1-decene | **72** | - | 80 | 26 | 99 | 2.1 |
| **6** | 1-decene | **72** | RAME-β-CD | 80 | 10 | 97 | 1.8 |
| **7** | 1-decene | **72** | Native-β-CD | 80 | 9 | 97 | 1.9 |
| **8** | 1-decene | **72** | - | 100 | 56 | 99 | 1.7 |
| **9** | 1-decene | **72** | RAME-β-CD | 100 | 72 | 99 | 2.0 |
| **10** | 1-decene | **72** | Native-β-CD | 100 | 78 | 95 | 1.8 |
| **11** | 1-decene | **72** | - | 120 | 94 | 99 | 1.9 |
| **12** | 1-decene | **72** | RAME-β-CD | 120 | 98 | 99 | 1.8 |
| **13** | 1-dodecene | **72** | - | 80 | 39 | 96 | 1.5 |
| **14** | 1-dodecene | **72** | RAME-β-CD | 80 | 11 | 99 | 1.7 |
| **15** | 1-dodecene | **72** | Native-β-CD | 80 | 8 | 98 | 1.7 |
| **16** | 1-dodecene | **72** | - | 100 | 49 | 98 | 1.5 |
| **17** | 1-dodecene | **72** | RAME-β-CD | 100 | 75 | 99 | 1.7 |
| **18** | 1-dodecene | **72** | Native-β-CD | 100 | 71 | 98 | 1.6 |
| **19** | 1-tetradecene | **72** | - | 80 | 53 | 93 | 1.7 |
| **20** | 1-tetradecene | **72** | RAME-β-CD | 80 | 14 | 95 | 1.6 |
| **21** | 1-tetradecene | **72** | Native-β-CD | 80 | 11 | 98 | 2.1 |
| **22** | 1-tetradecene | **72** | - | 100 | 57 | 97 | 1.5 |
| **23** | 1-tetradecene | **72** | RAME-β-CD | 100 | 88 | 97 | 1.9 |
| **24** | 1-tetradecene | **72** | Native-β-CD | 100 | 66 | 98 | 1.7 |

[a] $Rh(acac)(CO)_2$,$4.07 \times 10^{-2}$ mmol; water-soluble ligand, 0.21 mmol; cyclodextrin,0.48 mmol; $H_2O$, 11.5 mL; 1-alkene, 20.35 mmol; 1500 rpm, $CO/H_2$ (1/1), 50 bar,time, 6 h. [b] Calculated with respect to the starting olefin. [c] (mol. of aldehydes)/(mol of converted olefins) × 100. The side products were mainly isomeric olefins. [d] Ratio of linear to branched aldehyde product.

Thus, RAME-β-CD affected the conversion either positively or negatively depending on the reaction temperature. This could be explained in the strength of the interaction of RAME-β-CD/**72** depending on the temperature. At 80 °C, the surface active character of **72** and its adsorption ability at the aqueous/organic interface were masked due to inclusion of the hydrophobic part of **72** in the RAME-β-CD cavity ($K_{ass}$ = 5447 $M^{-1}$). Hence, most of the catalytically active species were confined in the aqueous phase and only a few of them were present at the aqueous/organic interface resulting in a decrease in catalytic activity. On the

contrary, at 100 or 120 °C the markedly higher activities were indicative of a change in the behavior of the catalytic system components. Although the RAME-β-CD/**72** association constant determination at 100 °C could not be performed for experimental reasons (ITC measurements requires an aqueous phase under atmospheric pressure), it is well known that the association constant values decrease with the temperature. Hence, at 100 °C we postulate that the concentrations of "free" ligand and RAME-β-CD increase in solution (Figure 5.8). The surface activity of **1** being revealed, an increase in the catalytic activity at the aqueous/organic interface was then observed. More RAME-β-CDs were then available to promote the mass transfer by inclusion of higher olefins in their cavity, thus participating to the catalytic activity enhancement.

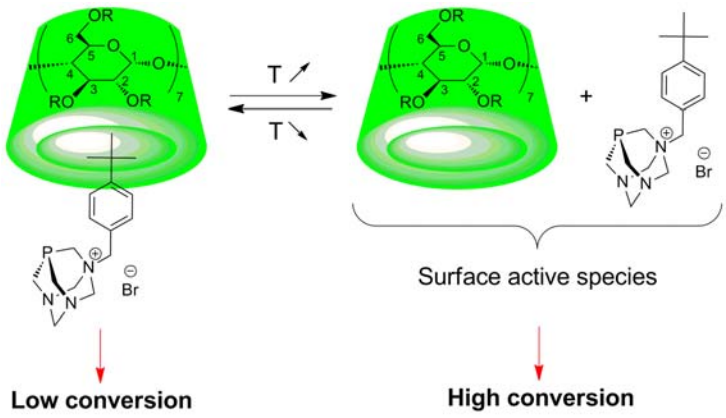


**Figure 5.8.** Change of the RAME-β-CD/[*tert*-butyl-*N*-Bz-PTA]Br inclusion complex depending on the temperature.

The implication of both the ligand surface activity and RAME-β-CD properties has been indirectly confirmed by replacing RAME-β-CD with native β-CD. At 80 °C, the native β-CD/**72** association constant ($K_{ass}$ = 4934 $M^{-1}$) was similar to that measured for RAME-β-CD. Although only a slight difference in conversion was evidenced between the native β-CD and RAME-β-CD at 80 °C (11% *vs*. 14% conv. for 1-tetradecene), a significant variation was measured at 100 °C (66% *vs*. 88% conv.). Furthermore, the chemoselectivity of the reaction resulted to be independent on the length of the terminal alkene. In fact, increasing the length of the hydrocarbon chain from 10 to 14 carbons did not significantly modify the chemoselectivity of the

reaction. A similar trend was observed for the regioselectivity as no significant variation in the l/b ratio was observed whatever the olefin. Interestingly, both the chemo- and regio-selectivity was independent on the presence or absence of RAME-β-CD suggesting that the catalytically active species proved to be stable under these conditions. This observation was opposite to what was previously observed with TPPTS.[16]

Finally, at the end of the catalytic experiments performed with ligand [*tert*-butyl-*N*-BzPTA]Br, no formation of emulsion was observed. Contrary to what observed for [*N*-BzPTA]Cl, a clear separation and an easily recovery of both aqueous and organic phases were obtained with **72**.

## 5.5 Conclusions

The water soluble phosphines PTA, [*N*-BzPTA]Cl and [*tert*-butyl-*N*-BzPTA]Br have been used as ligands in hydroformylation reactions catalyzed by rhodium complexes. All the phosphines showed to increase the stability of the catalytic species without affecting the chemo- and regioselectivity of the hydroformylation reaction of terminal alkenes. The catalytic experiments using 1-decene as substrate, by using PTA and its mono-benzylated derivative [*N*-BzPTA]Cl showed an increase in the reaction conversions in comparison with the results obtained with the sulfonated ligand TPPTS. The association constants on PTA and [*N*-BzPTA]Cl with RAME-β-CD which were close to zero, confirmed that the two phosphines can be considered as non-interacting ligands. The absence of interaction between the CD mass transfer promoter and the PTA-based ligands, had beneficial effects on the chemo- and regioselectivity and did not cause an alteration of the catalytic performances. The results obtained with RAME-β-CD and [*tert*-butyl-*N*-BzPTA]Br indicated that this water soluble phosphine acts as an interacting ligand depending on the temperature. The binding affinity of its *tert*-butylphenyl group for the RAME-β-CD cavity was influenced by the temperature, decreasing at T higher than 80 °C. Stabilizing the rhodium catalyst in the aqueous phase already at 80 °C, RAME-β-CD revealed the surface activity of [*tert*-butyl-*N*-BzPTA]Br over 100 °C, increasing the

catalytic activity without affecting either the chemo- and regio-selectivity. Additionally, by using the system RAME-β-CD/**72** a rapid decantation was observed at the end of the reaction, giving an added value to this thermoregulated process.

## 5.6 Experimental Section

### 5.6.1 General procedures

RAME-β-CD was purchased from Wacker Chemie GmbH and was used as received. RAMEB was of pharmaceutical grade (Cavasol® W7M Pharma) and its degree of substitution was equal to 1.7.[30] TPPTS was synthesized as reported in the literature.[31] Other chemicals were purchased from Acros and Aldrich Chemicals in their highest purity. All solvents were used as supplied without further purification. Distilled water was used in all experiments.

#### *5.6.1.1 NMR measurements*

NMR spectra were recorded at 25 °C on Bruker DRX300 spectrometers operating at 300 MHz for $^{1}H$ nuclei, 75.5 MHz for $^{13}C$ nuclei and 121.5 MHz for $^{31}P$ nuclei. $^{31}P\{^{1}H\}$ NMR spectra were recorded with an external reference (85% $H_3PO_4$). $D_2O$ (99.92% isotopic purity) was purchased from Euriso-Top. The 2D T-ROESY experiments were run using the software supplied by Bruker. T-ROESY experiments were preferred to classical ROESY experiments as this sequence provides reliable dipolar cross-peaks with a minimal contribution of scalar transfer. Mixing times for T-ROESY experiments were set at 300 ms. Data matrix for the T-ROESY was made of 512 free induction decays, 1 K points each, resulting from the co-addition of 32 scans. The real resolution was 1.5–6.0 Hz/point in F2 and F1 dimensions, respectively. They were transformed in the nonphase-sensitive mode after QSINE window processing.

### *5.6.1.2 Determination of the phosphine basicity*

Phosphine selenides were synthesized by stirring overnight at room temperature excess selenium (10 equiv.) with the phosphine (250 mg) in absolute ethanol (15 mL) under nitrogen for 15 h. The resulting mixture was directly analyzed by $^{31}P\{^{1}H\}$ NMR without any purification. In all cases, NMR spectra exhibit the presence of phosphine selenides characterized by a singlet with two satellites due to only 7.6% of active selenium isotope ($^{77}Se$) in NMR spectroscopy.[32]

### *5.6.1.3 Determination of association constants*

For PTA and [*N*-BzPTA]Cl, the determination of the association constants was based on a spectral displacement method by using methyl orange (MO) in its basic form.[33] The addition of the phosphine ligands to a solution containing RAME-β-CD and MO led to the formation of the RAME-β-CD/PTA complex which decreased the concentration of the RAME-β-CD/MO complex initially present. The resulting absorbance variation and therefore the association constants, were directly linked to the added concentration of PTA or [*N*-BzPTA]Cl and to the formation of RAME-β-CD/phosphine inclusion complex. The UV-vis spectra were recorded between 520 and 530 nm using a PerkinElmer Lambda 2S double beam spectrometer and a quartz cell with optical path length of 1.00 cm at 298 K. The control of the temperature was operated by using a thermostated bath linked to the cell holder (accuracy: ± 1.1 K). PTA and [*N*-BzPTA]Cl were dissolved in phosphate buffer at pH 5.8 and the concentrations for MO, RAME-β-CD and phosphine were fixed at 0.1, 0.2 and 1mM, respectively. The first derivatives of these spectra were used for quantitative analysis by an algorithmic treatment.

In the case of [*tert*-butyl-*N*-BzPTA]Br the association constant were measured by the method of Isothermal Titration Calorimetry (ITC). An isothermal calorimeter ($ITC_{200}$, MicroCal Inc., USA) was used to determine simultaneously the formation constant and the inclusion enthalpy and entropy of the studied complexes. The titration protocol used was that of 204.5 µL of degassed aqueous solution of and [*tert*-butyl-*N*-BzPTA]Br (phosphate buffer, pH 6.2) was titrated with the RAME-β-CD

solution (same buffer) in a 40 µL syringe. Concentrations of RAME-β-CD and [*tert*-butyl-*N*-BzPTA]Br in stock solutions were respectively equal to 2.5 mM and 0.125 mM. Each titration was realised at 343 K in order to be as close as possible to the catalytic conditions. Such a temperature also implies a perfect homogeneous solution of [*tert*-butyl-*N*-BzPTA]Br. After a prior injection of 0.4 µL, 10 aliquots of 3.7 µL of CD solution were delivered over 7.4 s and the corresponding heat flow was recorded as a function of time. The time interval between two consecutive injections was 100 s and agitation speed was 1000 rpm for all experiments. In addition, the heat consecutive to RAME-β-CD dilution was eliminated by performing blank titrations. The areas under the peak following each injection (obtained by integration of the raw signal) were then expressed as the heat effect per mole of added RAME-β-CD. Stoichiometries, binding constants and inclusion enthalpies were finally determined by nonlinear regression analysis of the binding isotherms, using built-in binding models within MicroCal Origin 7.0 software package (MicroCal, Northampton, MA). Each titration experiment was performed three times to ensure reproducibility of the results. Formation constants were then evaluated at different temperatures by means of the Van't Hoff equation, with the assumption that inclusion enthalpy and entropy are constant over the temperature scale.

#### *5.6.1.4 Surface tension measurements*

The interfacial tension measurements were performed using a KSV Instruments digital tensiometer (Sigma 70) with a platinum plate. The precision of the force transducer of the surface tension apparatus was 0.1 mN/m. The experiments were performed at 25 °C ± 0.5 °C controlled by a thermostated bath Lauda (RC6 CS). The samples were freshly prepared by dissolving the desired amount of the phosphine ligand in ultra pure water.

### 5.6.2 Catalytic experiments procedures

All catalytic reactions were performed under nitrogen using standard Schlenk techniques. In a typical experiment, $Rh(acac)(CO)_2$ (0.04 mmol), the water-soluble phosphine ligand (0.21 mmol), and RAME-β-CD (0.48 mmol) were dissolved in 11.5 mL of degassed and distilled water. The resulting aqueous phase and an organic phase composed of the olefin (20.35 mmol) were charged under an atmosphere of $N_2$ into the 50 mL reactor, which was heated at the desired temperature. Mechanical stirring equipped with a multipaddle unit was then started (1500 rpm), and the autoclave was pressurized with 50 atm of $CO/H_2$ (1:1) from a gas reservoir connected to the reactor through a high-pressure regulator valve allowing to keep constant the pressure in the reactor throughout the whole reaction. At the end of the reaction after decantation, the organic phase was analysed on a Shimadzu GC-17 A gas chromatograph equipped with a methylsilicone capillary column (30 m x 0.32 mm) and a flame ionization detector (GC:FID). For kinetic measurements, the time of the addition of $CO/H_2$ was considered as the beginning of the reaction.

## 5.7 References


[1] (a) Phillips, A. D.; Gonsalvi, L.; Romerosa, A.; Vizza, F.; Peruzzini, M. *Coord*. *Chem*. *Rev*. **2004**, *248*, 955-993. (b) Bravo, J.; Bolaño, S.; Gonsalvi, L.; Peruzzini, M. *Coord*. *Chem*. *Rev*. **2010**, *254*, 555-607.

[2] Smolénski, P.; Dinoi, C.; Guedes da Silva, M. F. C.; Pombeiro, A. J. L. *J*. *Organomet*. *Chem*. **2008**, *693*, 2338-2344.

[3] Pruchnik, F. P.; Smolénski, P.; Wajida-Hermanowicz, K. *J*. *Organomet*. *Chem*. **1998**, *570*, 63-69.

[4] Darensbourg, D. J.; Stafford, N. W.; Joó, F.; Reinbenspies, J. H. *J*. *Organomet*. *Chem*. **1995**, *488*, 99-108.

[5] Phillips, A. D.; Bolaño, S.; Bosquain, S. S.; Daran, J.-C.; Malacea, R.; Peruzzini, M.; Poli, R.; Gonsalvi, L. *Organometallics*, **2006**, *25*, 2189-2200.

[6] Dorcier, A.; Hartinger, C. G.; Scopelliti, R.; Fish, R. H.; Keppler, B. K.; Dyson, P. J. *J*. *Inorg*. *Biochem*. **2008**, *102*, 1066-1076.

[7] Dorcier, A.; Ang, W-H.; Bolaño, S.; Gonsalvi, L.; Juillerat-Jeannerat, L.; Laurenczy, G.; Peruzzini, M.; Phillips, A. D.; Zanobini, F.; Dyson, P. J. *Organometallics*, **2006**, *25*, 4090-4096.

[8] Pruchnik, F. P.; Smolénski, P.; Galdecka, E.; Galdecki, Z. S. *Inorg*. *Chim*. *Acta* **1999**, *293*, 110-114.

[9] Huang, R.; Frost, B. J. *Inorg*. *Chem*. **2007**, *46*, 10962-10964.

[10] Cole-Hamilton, D. J.; Tooze, R. P. *Catalyst Separation, Recovery and Recycling: Chemistry and Process Design*. Series: Catalysis by Metal Complexes, Eds Springler: Dodrecht, The Netherlands, **2006**.

[11] Monflier, E.; Komiyama, M. *Cyclodextrins and Catalysis. Cyclodextrins and Their Complexes: Chemistry, Analytical Methods, Applications*. Dodziuk, H. Eds. Wiley-VCH: Weinheim, Germany, **2006**.

[12] Wenz, G. *Angew*. *Chem*. *Int*. *Ed*. *Engl*. **1994**, *33*, 803

[13] Rekharsky, M. V., Inoue, Y. *Chem*. *Rev*. **1998**, *98*, 1875-1918.

[14] Hapiot, F.; Tilloy, S.; Monflier, E. *Chem*. *Rev*. **2006**, *106*, 767-781.

[15] Binkowski, C.; Cabou, J.; Bricout, H.; Hapiot, F.; Monflier, E. *J. Mol. Cat. A: Chem*. **2004**, *215*, 23-32.

[16] Monflier, E.; Bricout, H.; Hapiot, F.; Tilloy, S.; Aghmiz, A.; Masdeu-Bulto, A. M. *Adv. Synth. Catal*. **2005**, *347*, 1301-1307.

[17] Khan, A. r.; Forgo, P.; Stine, K. J.; D'Souza, V. T. *Chem*. *Rev*. **1998**, *98*, 1977-1996.

[18] Bricout, H.; Hapiot, F.; Ponchel, A.; Tilloy, S.; Monflier, E. *Sustainability* **2009**, *1*, 924-945.

[19] (a) Tilloy, S.; Brocout, H.; Monflier, E. *Green Chem*. **2002**, *4*, 188-193. (b) Monflier, E. ; Tilloy, S.; Castanet, Y.; Mortreux, A. *Tetrahedron Lett*. **1998**, *39*, 2959-2960.

[20] (a) Monflier, E.; Tilloy, S.; Fremy, G.; Castanet Y.; Mortreaux, A. Tetrahedron Lett. 1995, 36, 9481-9484. (b) Dessoudeix, M.; Urrutigoïty, M.; Kalck, P. Eur. *J*. *Inorg*. *Chem*. **2001**, *7*, 1797-1800.

[21] Bricout, H.; Caron, L.; Bormann, D.; Monflier, E. *Catal*. *Today* **2001**, *66*, 355-361.

[22] (a) Torque, C.; Bricout, H.; Hapiot, F.; Monflier, E. *Tetrahedron* **2004**, *60*, 6487-6493. (b) Cabou, J.; Bricout, H.; Hapiot, F.; Monflier, E. *Catal Commun*. **2004**, *5*, 265-270.

[23] Leclerq, L.; Bricout, H.; Tilloy, S.; Monflier, E. *J*. *Colloid Interf*. *Sci*. **2007**, *307*, 481-487.

[24] Sieffert, N.; Wipff, G. *Chem*. *Eur*. *J*. **2007**, *13*, 1978-1990.

[25] (a) Kuntz, E. G. *CHEMTECH* **1987**, *17*, 570-575. (b) Cornlis, B.; Kuntz, E. G. *J*. *Organomet*. *Chem*. **1995**, *502*, 177-186.

[26] Monflier, E.; Bricout, H.; Hapiot, F.; Tilloy, S.; Aghmiz, A.; Masdeu-Bulto, A. M. *Adv. Synth. Catal*. **2004**, *346*, 425-431.

[27] Legrand, F-X.; Hapiot, F.; Tilloy, S.; Guerriero, A.; Peruzzini, M.; Gonsalvi, L. *Appl*. *Cat*. *A*: *Gen*. **2009**, *362*, 62-66.

[28] Otto, S.; Ionescu, A.; Roodt, A. *J*. *Organomet*. *Chem*. **2005**, *690*, 4337-4342.

[29] Six, N.; Guerriero, A.; Landy, D.; Peruzzini, M.; Gonsalvi, L.; Hapiot, F.; Monflier, E. Manuscript in preparation.

[30] Legrand, F.-X.; Sauthier, M.; Flahaut, C.; Hachani, J.; Elfakir, C.; Fourmentin, S.; Tilloy, S.; Monflier, E. *J. Mol. Catal. A: Chem*. **2009**, *303*, 72-77.

[31] Gärtner, R.; Cornils, B.; Springer, H.; Lappe, P.**1982**, DE Pat. 3, 235, 030.

[32] Genine, E.; Amengual, R.; Michelet, V.; Savignac, M.; Jutand, A.; Neuville, L.; Genêt, J. P. *Adv*. *Synth*. *Catal*. **2004**, *346*, 1733-1741.

[33] Landy, D.; Fourmentin, S.; Salome, M. Surpateanu, G. *J*. *Incl*. *Phenom*. **2000**, *38*, 187-198.

# *Chapter 6*

## Appendix

# 6.1 Appendix to Chapter 2

## *6.1.1 Structure Determination for ligand (R,S S,R)PZA(O)* (78)

The crystal data for compound (*R*,*S S*,*R*)PZA(O) (**78**) are presented in Table 6.1.

**Table 6.1.** Crystal data and structure refinement for (*R*,*S S*,*R*)PZA(O) (78).

| | |
|---|---|
| Empirical formula | $C_{13}H_{18}N_3O_2P$ |
| Formula weight | 279.27 |
| Temperature | 293(2) K |
| Wavelength | 0.71073 Å |
| Crystal system | Monoclinic |
| Space group | P 1 21/c 1 |
| Unit cell dimensions | a = 10.485(3) Å $\alpha$= 90° |
| | b = 11.337(4) Å $\beta$= 97.97(3)° |
| | c = 11.004(5) Å $\gamma$= 90° |
| Volume | 1295.4(8) $Å^3$ |
| Z | 4 |
| Density (calculated) | 1.432 $Mg/m^3$ |
| Absorption coefficient | 0.214 $mm^{-1}$ |
| F(000) | 592 |
| Crystal size | 0.50 x 0.50 x 0.05 $mm^3$ |
| Theta range for data collection | 1.96 to 24.96°. |
| Index ranges | -12<=h<=12, 0<=k<=13, 0<=l<=13 |
| Reflections collected | 2408 |
| Independent reflections | 2277 [R(int) = 0.0587] |
| Completeness to theta = 24.96° | 99.6 % |
| Absorption correction | None |
| Max. and min. transmission | 0.9894 and 0.9003 |
| Refinement method | Full-matrix least-squares on $F^2$ |
| Data / restraints / parameters | 2277 / 0 / 176 |
| Goodness-of-fit on $F^2$ | 1.047 |
| Final R indices [I>2sigma(I)] | R1 = 0.0787, wR2 = 0.1391 |
| R indices (all data) | R1 = 0.1930, wR2 = 0.1708 |
| Largest diff. peak and hole | 0.292 and -0.324 $e.Å^{-3}$ |

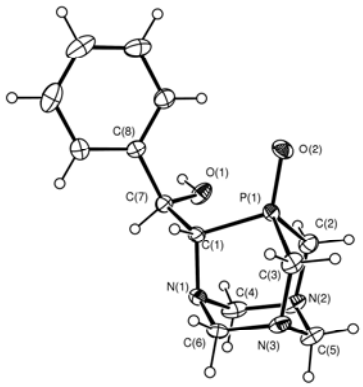


**Figure 6.1.** Asymmetric units of *(R,S S,R)*PZA(O). Ellipsoids are shown at 30% of probability**.**

**Table 6.2.** Bond lenghts [Å] and angles [°]for PZA(O).

| | | | |
|---|---|---|---|
| P(1)-O(2) | 1.490(4) | C(3)-H(3B) | 0.9700 |
| P(1)-C(2) | 1.808(6) | C(4)-H(4A) | 0.9700 |
| P(1)-C(3) | 1.818(5) | C(4)-H(4B) | 0.9700 |
| P(1)-C(1) | 1.833(6) | C(5)-H(5A) | 0.9700 |
| O(1)-C(7) | 1.432(7) | C(5)-H(5B) | 0.9700 |
| O(1)-H(1A) | 0.85(6) | C(6)-H(6A) | 0.9700 |
| N(1)-C(6) | 1.468(7) | C(6)-H(6B) | 0.9700 |
| N(1)-C(4) | 1.469(8) | C(7)-C(8) | 1.527(7) |
| N(1)-C(1) | 1.502(6) | C(7)-H(7) | 0.9800 |
| N(2)-C(4) | 1.457(8) | C(8)-C(13) | 1.367(8) |
| N(2)-C(5) | 1.461(8) | C(8)-C(9) | 1.381(8) |
| N(2)-C(2) | 1.493(7) | C(9)-C(10) | 1.392(9) |
| N(3)-C(6) | 1.455(7) | C(9)-H(9) | 0.9300 |
| N(3)-C(5) | 1.461(8) | C(10)-C(11) | 1.371(10) |
| N(3)-C(3) | 1.485(7) | C(10)-H(10) | 0.9300 |
| C(1)-C(7) | 1.527(7) | C(11)-C(12) | 1.369(10) |
| C(1)-H(1) | 0.9800 | C(11)-H(11) | 0.9300 |
| C(2)-H(2A) | 0.9700 | C(12)-C(13) | 1.381(8) |
| C(2)-H(2B) | 0.9700 | C(12)-H(12) | 0.9300 |
| C(3)-H(3A) | 0.9700 | O(2)-P(1)-C(2) | 117.7(3) |
| O(2)-P(1)-C(3) | 115.0(2) | O(2)-P(1)-C(1) | 117.7(2) |

| | | | |
|---|---|---|---|
| C(7)-O(1)-H(1A) | 106(4) | N(2)-C(5)-H(5A) | 108.4 |
| C(6)-N(1)-C(4) | 108.4(5) | N(3)-C(5)-H(5A) | 108.4 |
| C(6)-N(1)-C(1) | 111.4(4) | N(2)-C(5)-H(5B) | 108.4 |
| C(4)-N(1)-C(1) | 112.3(4) | N(3)-C(5)-H(5B) | 108.4 |
| C(4)-N(2)-C(5) | 109.3(5) | H(5A)-C(5)-H(5B) | 107.5 |
| C(4)-N(2)-C(2) | 110.0(4) | N(3)-C(6)-N(1) | 115.4(5) |
| C(5)-N(2)-C(2) | 110.7(5) | N(3)-C(6)-H(6A) | 108.4 |
| C(6)-N(3)-C(5) | 108.3(5) | N(1)-C(6)-H(6A) | 108.4 |
| C(6)-N(3)-C(3) | 109.8(4) | N(3)-C(6)-H(6B) | 108.4 |
| C(5)-N(3)-C(3) | 110.0(5) | N(1)-C(6)-H(6B) | 108.4 |
| N(1)-C(1)-C(7) | 111.4(4) | H(6A)-C(6)-H(6B) | 107.5 |
| N(1)-C(1)-P(1) | 106.7(3) | O(1)-C(7)-C(8) | 110.7(4) |
| C(7)-C(1)-P(1) | 118.6(4) | O(1)-C(7)-C(1) | 108.7(5) |
| N(1)-C(1)-H(1) | 106.5 | C(8)-C(7)-C(1) | 113.1(4) |
| C(7)-C(1)-H(1) | 106.5 | O(1)-C(7)-H(7) | 108.1 |
| P(1)-C(1)-H(1) | 106.5 | C(8)-C(7)-H(7) | 108.1 |
| N(2)-C(2)-P(1) | 109.5(4) | C(1)-C(7)-H(7) | 108.1 |
| N(2)-C(2)-H(2A) | 109.8 | C(13)-C(8)-C(9) | 119.1(5) |
| P(1)-C(2)-H(2A) | 109.8 | C(13)-C(8)-C(7) | 121.6(5) |
| N(2)-C(2)-H(2B) | 109.8 | C(9)-C(8)-C(7) | 119.2(5) |
| P(1)-C(2)-H(2B) | 109.8 | C(8)-C(9)-C(10) | 120.1(6) |
| H(2A)-C(2)-H(2B) | 108.2 | C(8)-C(9)-H(9) | 119.9 |
| N(3)-C(3)-P(1) | 111.3(4) | C(10)-C(9)-H(9) | 119.9 |
| N(3)-C(3)-H(3A) | 109.4 | C(11)-C(10)-C(9) | 120.4(7) |
| P(1)-C(3)-H(3A) | 109.4 | C(11)-C(10)-H(10) | 119.8 |
| N(3)-C(3)-H(3B) | 109.4 | C(9)-C(10)-H(10) | 119.8 |
| P(1)-C(3)-H(3B) | 109.4 | C(10)-C(11)-C(12) | 119.0(6) |
| H(3A)-C(3)-H(3B) | 108.0 | C(10)-C(11)-H(11) | 120.5 |
| N(2)-C(4)-N(1) | 115.0(5) | C(12)-C(11)-H(11) | 120.5 |
| N(2)-C(4)-H(4A) | 108.5 | C(11)-C(12)-C(13) | 121.0(7) |
| N(1)-C(4)-H(4A) | 108.5 | C(11)-C(12)-H(12) | 119.5 |
| C(13)-H(13) | 0.9300 | C(13)-C(12)-H(12) | 119.5 |
| H(4A)-C(4)-H(4B) | 107.5 | C(8)-C(13)-C(12) | 120.4(6) |

### *6.1.2 Structure Determination for ligand (S,R R,S)PZA-NMe$_2$* (75a)

The crystal data for compound (*S*,*R R*,*S*)PZA-NMe$_2$ (**75a**) are presented in Table 6.3.

**Table 6.3.** Crystal data and structure refinement for (*S*,*R R*,*S*)PZA-NMe$_2$ (**75a**)

| | |
|---|---|
| Empirical formula | $C_{15}H_2N_4OP$ |
| Formula weight | 306.34 |
| Temperature | 298(2) K |
| Wavelength | 0.71069 Å |
| Crystal system | Monoclinic |
| Space group | P 1 21/c 1 |
| Unit cell dimensions | a= 16.5675(19) Å $\alpha$= 90° |
| | b= 7.7963(8) Å $\beta$=108.984(13)° |
| | c= 12.4241(16) Å $\gamma$= 90° |
| Volume | 1517.5(3) Å$^3$ |
| Z | 4 |
| Density (calculated) | 1.341 Mg/m$^3$ |
| Absorption coefficient | 0.187 mm$^{-1}$ |
| F(000) | 656 |
| Crystal size | 0.4 x 0.2 x 0.15 mm$^3$ |
| Theta range for data collection | 3.90 to 32.36°. |
| Index ranges | -24<=h<=24, -8<=k<=11, -17<=l<=18 |
| Reflections collected | 11990 |
| Independent reflections | 4915 [R(int) = 0.0400] |
| Completeness to theta = 25.00° | 99.4 % |
| Absorption correction | Semi-empirical from equivalents |
| Max. and min. transmission | 0.9696 and 0.873 |
| Refinement method | Full-matrix least-squares on F$^2$ |
| Data / restraints / parameters | 4915 / 0 / 195 |
| Goodness-of-fit on F$^2$ | 0.946 |
| Final R indices [I>2sigma(I)] | R1 = 0.0566, wR2 = 0.1332 |
| R indices (all data) | R1 = 0.1047, wR2 = 0.1479 |
| Largest diff. peak and hole | 0.378 and -0.268 e.Å$^{-3}$ |

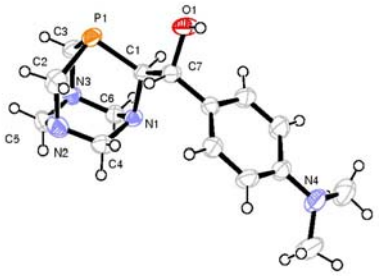


**Figure 6.2.** Asymmetric units of (*S*,*R R*,*S*)PZA-$NMe_2$. Ellipsoids are shown at 50% of probability**.**

**Table 6.4.** Bond lenghts [Å] and angles [°] for (*S*,*R R*,*S*)PZA-$NMe_2$.

| | |
|---|---|
| P(1)-C(3) 1.8503(19) | C(7)-H(7) 0.9800 |
| P(1)-C(2) 1.859(2) | C(8)-C(13) 1.373(2) |
| P(1)-C(1) 1.8695(16) | C(8)-C(9) 1.382(3) |
| C(1)-N(1) 1.476(2) | C(9)-C(10) 1.375(3) |
| C(1)-C(7) 1.531(2) | C(9)-H(9) 0.9300 |
| C(1)-H(1) 0.9800 | C(10)-C(11) 1.394(3) |
| C(2)-N(2) 1.476(3) | C(10)-H(10) 0.9300 |
| C(2)-H(2A) 0.9700 | C(11)-N(4) 1.384(2) |
| C(2)-H(2B) 0.9700 | C(11)-C(12) 1.389(3) |
| C(3)-N(3) 1.470(2) | C(12)-C(13) 1.379(3) |
| C(3)-H(3A) 0.9700 | C(12)-H(12) 0.9300 |
| C(3)-H(3B) 0.9700 | C(13)-H(13) 0.9300 |
| C(4)-N(1) 1.455(2) | C(14)-N(4) 1.434(3) |
| C(4)-N(2) 1.469(2) | C(14)-H(14A) 0.9600 |
| C(4)-H(4A) 0.9700 | C(14)-H(14B) 0.9600 |
| C(4)-H(4B) 0.9700 | C(14)-H(14C) 0.9600 |
| C(5)-N(2) 1.460(3) | C(15)-N(4) 1.448(3) |
| C(5)-N(3) 1.467(3) | C(15)-H(15A) 0.9600 |
| C(5)-H(5A) 0.9700 | C(15)-H(15B) 0.9600 |
| C(5)-H(5B) 0.9700 | C(15)-H(15C) 0.9600 |
| C(6)-N(1) 1.456(2) | O(1)-H(1W) 0.91(2) |
| C(6)-N(3) 1.469(2) | C(3)-P(1)-C(2) 95.69(9) |
| C(6)-H(6A) 0.9700 | C(3)-P(1)-C(1) 94.68(8) |
| C(6)-H(6B) 0.9700 | C(2)-P(1)-C(1) 97.08(9) |
| C(7)-O(1) 1.420(2) | N(1)-C(1)-C(7) 112.86(13) |
| C(7)-C(8) 1.504(2) | N(1)-C(1)-P(1) 112.67(11) |

| | |
|---|---|
| C(7)-C(1)-P(1) 111.62(11) | C(8)-C(7)-H(7) 108.9 |
| N(1)-C(1)-H(1) 106.4 | C(1)-C(7)-H(7) 108.9 |
| P(1)-C(1)-H(1) 106.4 | C(13)-C(8)-C(9) 116.69(16) |
| N(2)-C(2)-P(1) 115.02(13) | C(13)-C(8)-C(7) 121.30(17) |
| N(2)-C(2)-H(2A) 108.5 | C(9)-C(8)-C(7) 122.01(17) |
| P(1)-C(2)-H(2A) 108.5 | C(10)-C(9)-C(8) 122.11(19) |
| N(2)-C(2)-H(2B) 108.5 | C(10)-C(9)-H(9) 118.9 |
| P(1)-C(2)-H(2B) 108.5 | C(8)-C(9)-H(9) 118.9 |
| H(2A)-C(2)-H(2B) 107.5 | C(9)-C(10)-C(11) 121.14(19) |
| N(3)-C(3)-P(1) 115.12(12) | C(9)-C(10)-H(10) 119.4 |
| N(3)-C(3)-H(3A) 108.5 | C(11)-C(10)-H(10) 119.4 |
| P(1)-C(3)-H(3A) 108.5 | N(4)-C(11)-C(12) 121.87(18) |
| N(3)-C(3)-H(3B) 108.5 | N(4)-C(11)-C(10) 121.59(18) |
| P(1)-C(3)-H(3B) 108.5 | C(12)-C(11)-C(10) 116.50(17) |
| H(3A)-C(3)-H(3B) 107.5 | C(13)-C(12)-C(11) 121.38(18) |
| N(1)-C(4)-N(2) 115.13(15) | C(13)-C(12)-H(12) 119.3 |
| N(1)-C(4)-H(4A) 108.5 | C(11)-C(12)-H(12) 119.3 |
| N(2)-C(4)-H(4A) 108.5 | C(8)-C(13)-C(12) 122.06(18) |
| N(1)-C(4)-H(4B) 108.5 | C(8)-C(13)-H(13) 119.0 |
| N(2)-C(4)-H(4B) 108.5 | C(12)-C(13)-H(13) 119.0 |
| H(4A)-C(4)-H(4B) 107.5 | N(4)-C(14)-H(14A) 109.5 |
| N(2)-C(5)-N(3) 114.28(14) | N(4)-C(14)-H(14B) 109.5 |
| N(2)-C(5)-H(5A) 108.7 | H(14A)-C(14)-H(14B) 109.5 |
| N(3)-C(5)-H(5A) 108.7 | N(4)-C(14)-H(14C) 109.5 |
| N(2)-C(5)-H(5B) 108.7 | H(14A)-C(14)-H(14C) 109.5 |
| N(3)-C(5)-H(5B) 108.7 | H(14B)-C(14)-H(14C) 109.5 |
| H(5A)-C(5)-H(5B) 107.6 | N(4)-C(15)-H(15A) 109.5 |
| N(1)-C(6)-N(3) 114.04(13) | N(4)-C(15)-H(15B) 109.5 |
| N(1)-C(6)-H(6A) 108.7 | H(15A)-C(15)-H(15B) 109.5 |
| N(3)-C(6)-H(6A) 108.7 | N(4)-C(15)-H(15C) 109.5 |
| N(1)-C(6)-H(6B) 108.7 | H(15A)-C(15)-H(15C) 109.5 |
| N(3)-C(6)-H(6B) 108.7 | H(15B)-C(15)-H(15C) 109.5 |
| O(1)-C(7)-C(8) 111.87(15) | C(4)-N(1)-C(6) 108.00(13) |
| O(1)-C(7)-C(1) 104.64(14) | C(4)-N(1)-C(1) 113.09(13) |
| C(8)-C(7)-C(1) 113.59(13) | C(6)-N(1)-C(1) 110.72(13) |
| O(1)-C(7)-H(7) 108.9 | C(5)-N(2)-C(4) 108.33(15) |

## 6.2 Appendix to Chapter 4

### *6.2.1 Structure determination for complex [RuI$_2$(p-cymene){(S,R R,S)PZA-NMe$_2$}]* **(90)**

The crystal data for compound [RuI$_2$(p-cymene){(*S*,*R R*,*S*)PZA-NMe$_2$}] (**90**) are presented in Table 6.5.

**Table 6.5.** Crystal data and structure refinement for [RuI$_2$(p-cymene){(*S*,*R R*,*S*)PZA-NMe$_2$}] (**90**)

| | |
|---|---|
| Empirical formula | $C_{25}H_{37}I_2N_4OPRu$ |
| Formula weight | 795.43 |
| Temperature | 293(2) K |
| Wavelength | 0.71069 Å |
| Crystal system | Monoclinic |
| Space group | P 1 21/c 1 |
| Unit cell dimensions | a = 13.0146(8) Å $\alpha$= 90° |
| | b = 8.2283(4) Å $\beta$= 101.651(8)° |
| | c = 27.105(3) Å $\gamma$= 90° |
| Volume | 2842.8(4) Å$^3$ |
| Z | 4 |
| Density (calculated) | 1.858 Mg/m$^3$ |
| Absorption coefficient | 2.804 mm$^{-1}$ |
| F(000) | 1552 |
| Crystal size | 0.4 x 0.35 x 0.2 mm$^3$ |
| Theta range for data collection | 3.74 to 28.88°. |
| Index ranges | -17<=h<=16, -9<=k<=10, -28<=l<=33 |
| Reflections collected | 11981 |
| Independent reflections | 5769 [R(int) = 0.0455] |
| Completeness to theta = 25° | 92.9 % |
| Absorption correction | Semi-empirical from equivalents |
| Max. and min. transmission | 0.57 and 0.299358 |
| Refinement method | Full-matrix least-squares on F$^2$ |
| Data / restraints / parameters | 5769 / 0 / 315 |
| Goodness-of-fit on F$^2$ | 1.202 |
| Final R indices [I>2sigma(I)] | R1 = 0.0948, wR2 = 0.1393 |
| R indices (all data) | R1 = 0.1292, wR2 = 0.1509 |
| Largest diff. peak and hole | 1.124 and -1.141 e.Å$^{-3}$ |

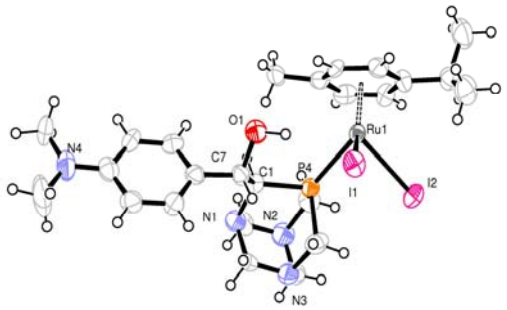


**Figure 6.3.** Asymmetric units of [$RuI_2$(p-cymene){(S,R R,S)PZA-$NMe_2$}] (n). Ellipsoids are shown at 50% of probability.

**Table 6.6.** Bond lenghts [Å] and angles [°] for [$RuI_2$(p-cymene){(S,R R,S)PZA-$NMe_2$}] (**90**).

| | |
|---|---|
| Ru(1)-C(22) 2.187(10) | O(1)-H(1W) 0.77(13) |
| Ru(1)-C(19) 2.193(12) | C(1)-C(7) 1.535(15) |
| Ru(1)-C(18) 2.201(12) | C(7)-C(8) 1.502(16) |
| Ru(1)-C(17) 2.239(11) | C(8)-C(9) 1.376(15) |
| Ru(1)-C(21) 2.247(10) | C(8)-C(13) 1.374(16) |
| Ru(1)-C(20) 2.276(11) | C(9)-C(10) 1.378(16) |
| Ru(1)-P(4) 2.340(3) | C(10)-C(11) 1.395(17) |
| Ru(1)-I(1) 2.7366(12) | C(11)-C(12) 1.406(18) |
| Ru(1)-I(2) 2.7413(12) | C(12)-C(13) 1.362(17) |
| P(4)-C(3) 1.854(12) | C(16)-C(17) 1.510(16) |
| P(4)-C(2) 1.849(12) | C(17)-C(18) 1.401(17) |
| P(4)-C(1) 1.877(11) | C(17)-C(22) 1.407(16) |
| N(1)-C(4) 1.469(16) | C(18)-C(19) 1.394(17) |
| N(1)-C(6) 1.470(15) | C(19)-C(20) 1.427(15) |
| N(1)-C(1) 1.487(13) | C(20)-C(21) 1.394(16) |
| N(2)-C(4) 1.448(17) | C(20)-C(23) 1.511(16) |
| N(2)-C(5) 1.476(17) | C(21)-C(22) 1.426(16) |
| N(2)-C(2) 1.472(15) | C(23)-C(25) 1.521(18) |
| N(3)-C(6) 1.439(16) | C(23)-C(24) 1.528(18) |
| N(3)-C(5) 1.461(18) | C(22)-Ru(1)-C(19) 78.2(5) |
| N(3)-C(3) 1.482(15) | C(22)-Ru(1)-C(18) 66.5(5) |
| N(4)-C(11) 1.373(16) | C(19)-Ru(1)-C(18) 37.0(4) |
| N(4)-C(14) 1.425(18) | C(22)-Ru(1)-C(17) 37.0(4) |
| N(4)-C(15) 1.431(19) | C(19)-Ru(1)-C(17) 66.2(5) |

| | | | |
|---|---|---|---|
| O(1)-C(7) | 1.430(13) | C(18)-Ru(1)-C(17) | 36.8(5) |
| C(22)-Ru(1)-C(21) | 37.5(4) | C(3)-P(4)-Ru(1) | 119.5(4) |
| C(19)-Ru(1)-C(21) | 65.8(5) | C(2)-P(4)-Ru(1) | 113.1(4) |
| C(18)-Ru(1)-C(21) | 78.7(4) | C(1)-P(4)-Ru(1) | 125.4(3) |
| C(17)-Ru(1)-C(21) | 67.0(4) | C(4)-N(1)-C(6) | 107.5(10) |
| C(22)-Ru(1)-C(20) | 66.2(4) | C(4)-N(1)-C(1) | 112.1(9) |
| C(19)-Ru(1)-C(20) | 37.2(4) | C(6)-N(1)-C(1) | 112.2(9) |
| C(18)-Ru(1)-C(20) | 67.0(4) | C(4)-N(2)-C(5) | 108.2(12) |
| C(17)-Ru(1)-C(20) | 78.6(4) | C(4)-N(2)-C(2) | 110.4(10) |
| C(21)-Ru(1)-C(20) | 35.9(4) | C(5)-N(2)-C(2) | 111.3(11) |
| C(22)-Ru(1)-P(4) | 117.9(3) | C(6)-N(3)-C(5) | 108.7(11) |
| C(19)-Ru(1)-P(4) | 123.9(3) | C(6)-N(3)-C(3) | 111.7(10) |
| C(18)-Ru(1)-P(4) | 97.0(3) | C(5)-N(3)-C(3) | 110.5(11) |
| C(17)-Ru(1)-P(4) | 94.6(3) | C(11)-N(4)-C(14) | 121.4(12) |
| C(21)-Ru(1)-P(4) | 154.8(3) | C(11)-N(4)-C(15) | 120.2(13) |
| C(20)-Ru(1)-P(4) | 161.1(3) | C(14)-N(4)-C(15) | 118.3(13) |
| C(22)-Ru(1)-I(1) | 93.3(3) | C(7)-O(1)-H(1W) | 107(10) |
| C(19)-Ru(1)-I(1) | 149.3(3) | N(1)-C(1)-C(7) | 111.2(9) |
| C(18)-Ru(1)-I(1) | 158.7(4) | N(1)-C(1)-P(4) | 110.1(7) |
| C(17)-Ru(1)-I(1) | 122.1(3) | C(7)-C(1)-P(4) | 115.3(7) |
| C(21)-Ru(1)-I(1) | 89.4(3) | N(1)-C(1)-H(1) | 106.5 |
| C(20)-Ru(1)-I(1) | 112.4(3) | C(7)-C(1)-H(1) | 106.5 |
| P(4)-Ru(1)-I(1) | 86.21(8) | P(4)-C(1)-H(1) | 106.5 |
| C(22)-Ru(1)-I(2) | 155.6(3) | N(2)-C(2)-P(4) | 112.6(9) |
| C(19)-Ru(1)-I(2) | 87.0(3) | N(2)-C(2)-H(2A) | 109.1 |
| C(18)-Ru(1)-I(2) | 111.6(4) | P(4)-C(2)-H(2A) | 109.1 |
| C(17)-Ru(1)-I(2) | 148.3(3) | N(2)-C(2)-H(2B) | 109.1 |
| C(21)-Ru(1)-I(2) | 118.4(3) | P(4)-C(2)-H(2B) | 109.1 |
| C(20)-Ru(1)-I(2) | 90.3(3) | H(2A)-C(2)-H(2B) | 107.8 |
| P(4)-Ru(1)-I(2) | 86.46(8) | N(3)-C(3)-P(4) | 112.2(9) |
| I(1)-Ru(1)-I(2) | 89.59(4) | P(4)-C(3)-H(3A) | 109.2 |
| C(3)-P(4)-C(2) | 98.7(6) | N(3)-C(3)-H(3B) | 109.2 |
| C(3)-P(4)-C(1) | 97.5(6) | P(4)-C(3)-H(3B) | 109.2 |
| C(2)-P(4)-C(1) | 97.7(5) | N(2)-C(4)-N(1) | 114.8(10) |

# *Curriculum Vitae*

# PERSONAL DETAILS

**ANTONELLA GUERRIERO**

*Date and Place of Birth*: 13.01.1981, Sant'Arcangelo (PZ), Italy

*Home Address*: via R. Giuliani n° 3, Firenze, Italy

*Telephone and Mobile*: 0550515202, +39.3391089185

*Electronic Mail*: antoguerri@yahoo.com

antonella.guerriero@iccom.cnr.it

## EDUCATION

- Doctoral Candidate (Dottorato in Scienze Chimiche, Ciclo XXIII, a.a. 2010, University of Florence). Supervisors: Dr. Gianna Reginato, Dr. Luca Gonsalvi.
- Master in "Drug Design and Synthesis", at University of Siena, on December 2006. Final evaluation: excellent. Master thesis on "Fragment-Based approach for the design of new matrix metalloproteinase (MMP) inhibitors". Supervisor: Dr. Alessandro Mordini.
- Degree in Pharmacy, at University of Florence in July 2005. Final mark: 110/110 cum Laude. Degree thesis on "Design and synthesis of heterocondensated piridazinone derivatives as potential antiplatelet drugs" Supervisors: Prof. Vittorio Dal Piaz, Dr. Maria Paola Giovannoni.
- High school diploma, Maturità Scientifica at liceo Scientifico Galileo Galilei of Sant'Arcangelo (PZ). Final mark: 90/100.

## EXPERIENCES

- 2010: CNR Research Grant on "Hydrgen Production from renewable sources and release on demand via chemical storage (PIRODE) and "Program of Advanced Research for Production, Storage and Utilization of Hydrogen as Energy Vector " (FIRENZE HYDROLAB), at Istituto di Chimica dei Composti OrganoMetallici (ICCOM-CNR) Supervisor: Dr. Luca Gonsalvi.
- 2008/2010: CNR Research Grant on "Synthesis of new water-soluble phosphines and their transition metal complexes for pharmacological activity and use in catalysis for valorisation of renewable energies" at Istituto di

Chimica dei Composti OrganoMetallici (ICCOM-CNR). Supervisor: Dr. Luca Gonsalvi.

- 2006: Master stage of about six months in organic synthesis and molecular modelling at Organic Department of University of Florence and ProtEra s.r.l. Polo Scientifico - Sesto Fiorentino (FI). Supervisor: Dr. Alessandro Mordini.

## TECHNICAL SKILLS

- Good knowledge of organic and organometallic synthetic procedures; manipulation and purification of air-sensitive compounds.
- Purification of solvents and purification of compounds through distillation, sublimation, crystallization and column chromatography.
- Use of NMR (multinuclear, variable temperature), GC, GC-MS and IR instruments.
- Use of Parr autoclaves for hydrogenation reactions under pressure of gas.

## FOREIGN LANGUAGES

- Good knowledge of oral and written English.
- Good knowledge of oral and written French.
- Elementary knowledge of oral and written German.

## COMPUTER SKILLS

- Good knowledge of Windows 95/98/2000/XP (Excel, Word, Power Point, Outlook), ChemDraw (software of graphic chemistry), Beilstein Commander and SciFinder (bibliographical search), Internet.

## PUBBLICATIONS

1. “Aqueous rhodium-catalyzed hydroformylation of 1-decene in the presence of randomly methylated β-cyclodextrin and 1,3,5-triaza-7-phosphaadamantane derivatives”. F-X. Legrand, F. Hapiot, S. Tilloy, A. Guerriero, M. Peruzzini, L. Gonsalvi, E. Monflier *Applied Catalysis A: General* **2009**, *362*, 62-66.

2. "Rhenium Allenylidenes and Their Reactivity toward Phosphines: A Theoretical Study" Coletti, C.; Gonsalvi, L.; Guerriero, A.; Marvelli, L.; Peruzzini, M.; Reginato, G., Re, N. *Organometallics* **2010**, *29,* 5982-5993.

**In preparation:**

1. "Iridium(I) Complexes of Upper Rim Functionalized PTA Derivatives a Catalysts for C=O vs C=C bond Hydrogenations (PTA =7phospha-1,3,5-triazaadamantane)" Guerriero, A.; Erlandsonn, M.; Ienco, A.; Krogstad, D. A.; Peruzzini, M.; Reginato, G.; Gonsalvi, L. *Organometallics*, submitted for pubblication
2. "Imidazolyl-PTA Derivatives as Water Soluble (P,N) Ligand for Ru-catalyzed Hydrogenations (PTA=7phospha-1,3,5-triazaadamantane)" Krogstad, D. A.; Guerriero, A.; Ienco, A.; Peruzzini, M.; Bosquain, S.; Reginato, G.; Gonsalvi, L., in preparation
3. "Rhenium Allenylidenes bearing an electron-withdrawing (p-nitrophenyl)group and Their Reactivity toward Phosphines: a combined experimental and Theoretical Study" Coletti, C.; Gonsalvi, L.; Guerriero, A.; Marvelli, L.; Peruzzini, M.; Reginato, G., Re, N., in preparation
4. "Supramolecular Controlled Surface Activty of an Amphiphilic Ligand. Application to Biphasic-Hydroformylation of Higher Olefins" Six, N.; Guerriero, A.; Landy, D.; Peruzzini, M.; Gonsalvi, L.; Hapiot, F.; Monflier, E., in preparation

## ORAL COMUNICATIONS – Personally presented

1. *Cost Action D40 "Innovative Catalysis: New Processes and Selectivities"*, Bratislava (SK), 27-28 April 2009. "Derivatisation of 1,3,5-triaza-7-phosphadamantane (PTA): towards enantioselective catalytic processes in water phase". **A. Guerriero**, L. Gonsalvi , A. Mordini, M. Peruzzini, G. Reginato, A. Rossin.
2. *International School of Organometallic Chemistry 7$^{th}$ Edition*, Camerino, 5-9 Sptember 2009. Flash presentation "Upper rim functionalisation of the water

soluble phosphine PTA and use of the related Ru and Ir complexes in catalytic hydrogenations". **A. Guerriero**, G. Reginato, M. Peruzzini, L. Gonsalvi.

3. *Meeting PRIN 2007*, Bologna, 18 December 2009. "New functionalizations of the water soluble phosphine PTA, coordination chemistry and applications in catalityc reactions in aqueous media". **A. Guerriero**, L. Gonsalvi, M. Peruzzini, G. Reginato, D.A. Krogstad.
4. *XV Edizione della Scuola Nazionale di Chimica Organometallica per dottorandi*, Bertinoro (F-C), 23-27 May 2010. "New upper rim derivatives of PTA, coordination chemistry and applications in catalytic hydrogenations and hydroformilations in water". **A. Guerriero**, L. Gonsalvi, G. Reginato, M. Peruzzini, D. A. Krogstad.

## ORAL COMUNICATIONS

1. *Cost Action D40 "Innovative Catalysis: New Processes and Selectivities"*, Tarragona (Spain), 20-22 May 2008. "Synthesis of new polyfunctionalised phosphines by synthetic elaboration of naturally occurring amino acids and selective transformation of PTA". **G. Reginato**, A. Mordini, M. Peruzzini, L. Gonsalvi, A. Guerriero, M. Erlandsson.
2. *Cost Action D40 "Innovative Catalysis: New Processes and Selectivities"*, Turku (N), 26- 28 May 2009. "Derivatization of 1,3,5-triaza-7-phosphaadamantane (PTA) for application to enantioselective catalytic processes in water phase". **G. Reginato**, A. Mordini, M. Peruzzini, L. Gonsalvi, A. Guerriero, F. Faigl.
3. *Nesmeyanov International Conference "Chemistry of Organoelement Compounds: Results and Prospects"*, Mosca, 28 September-2 October 2009. "The quest for advanced tailoring of water soluble phosphines. Upper rim functionalisation of PTA and applications of catalytic hydrogenation reactions". **A. Rossin**, M. Erlandsson, L. Gonsalvi, A. Guerriero, M. Peruzzini, G. Reginato, C. Tiozzo.
4. *Cost Action D40 "Innovative Catalysis: New Processes and Selectivities"*, Ankara (Turkey), 25-27 May 2010. "New upper rim derivatives of PTA: coordination

chemistry and applications in catalytic hydrogenations in water". **G. Reginato**, A. Guerriero, L. Gonsalvi, M. Peruzzini, D.A. Krogstad, A. Mordini.

## POSTER PRESENTATIONS

1. *VIII Congresso del Gruppo Interdivisionale di Chimica Organometallica (Co.G.I.C.O.)*, Perugia, 25-28 June 2008. "NMR and DFT Studies on the nucleophilic Addition of Phosphines to Cγ-Activated Rhenium Allenylidenes". **A. Guerriero**, C. Coletti, L. Gonsalvi, L. Marvelli, N. Re, G. Reginato, M. Peruzzini.
2. *16$^{th}$ International Symposium on Homogeneous Catalysis (ISHC XVI)*, Florence, 6-11 July 2008. "Synthesis of diastereomerically enriched analogues of the water soluble phosphine PTA and use in catalytic hydrogenations". **A. Guerriero**, M. Erlandsson, A. Ienco, G. Reginato, M. Peruzzini, L. Gonsalvi.
3. *Scuola di catalisi GIC "Dal Catalizzatore al Processo: Principi, Strategie e Mode"*, Certosa di Pontignano (Siena), 3-6 November 2008. "Synthesis of diastereomerically enriched analogues of the water soluble phosphine PTA and use in catalytic hydrogenations". **A. Guerriero**, M. Erlandsson, A. Ienco, G. Reginato, M. Peruzzini, L. Gonsalvi.
4. *9° Congresso del Gruppo Interdivisionale di Chimica Organometallica della Società Chimica Italiana (Co.G.I.C.O.)*, Florence, 8-11 June 2010. "Iridium (I) and Ruthenium (II) complexes of *upper rim* functionalised PTA ligands as catalysts for hydrogenations in water and biphasic media". **A. Guerriero**, L. Gonsalvi, D.A. Krogstad, M. Peruzzini, G. Reginato. Member of the organizing committee.
5. *9$^{th}$ International Symposium on Carbanion Chemistry*, Florence, 20- 24 July 2010. "Upper rim derivatives of the water-soluble phosphine PTA via selective lithiation reactions". **A. Guerriero**, L. Gonsalvi, M. Peruzzini, G. Reginato, D.A. Krogstad. Member of the organizing committee.

## SCHOOLS AND MEETINGS

1. Course *"Avance Base" NMR* of Bruker Italy, Milan, 27-30 October 2008.
2. *Scuola di catalisi GIC "Dal Catalizzatore al Processo: Principi, Strategie e Mode"*, Certosa di Pontignano (Siena), 3-6 November 2008.

3. *International School of Organometallic Chemistry 7th Edition*, Camerino, 5-9 Sptember 2009.
4. *XV Edizione della Scuola Nazionale di Chimica Organometallica per dottorandi*, Bertinoro (F-C), 23-27 May 2010.
5. *6th European Workshop on Phosphorus Chemistry (EWPC-6),* Florence, 26-27 March 2009.
6. *2nd Nano-Host Workshop* "Selective processes by homogeneous supported catalysts", Florence, 17 February 2010.

**Member of the local organizing committee at the following meetings**

1. *6th European Workshop on Phosphorus Chemistry (EWPC-6),* Florence, 26-27 March 2009
2. *9° Congresso del Gruppo Interdivisionale di Chimica Organometallica della Società Chimica Italiana (Co.G.I.C.O.)*, Florence, 8-11 June 2010.
3. *9th International Symposium on Carbanion Chemistry*, Florence, 20- 24 July 2010.

# *Ringraziamenti*

Non ci posso credere siamo finalmente arrivati ai ringraziamenti (!!!).

Innanzitutto vorrei ringraziare la Dott.ssa Gianna Reginato, la quale per prima mi ha proposto di fare questo dottorato e mi ha seguita per tutto l'arco dei tre anni, con pazienza e costanza, sostenendomi in alcuni momenti di scoraggiamento. Il rapporto che si è creato durante questi anni trascorsi insieme, penso vada oltre quello esclusivamente lavorativo e questo è per me un valore aggiunto. I miei ringraziamenti vanno poi al Dr. Luca Gonsalvi, il quale mi ha affidato il progetto di cui si occupa da tanti anni, seguendomi sempre nel lavoro, compreso quello finale della tesi, e coinvolgendomi in diversi progetti. Naturalmente non posso non ringraziare il dr. Maurizio Peruzzini, che mi ha accolta nel suo gruppo di ricerca e quando necessario è sempre stato disponibile per consigli e spiegazioni.

A questo punto finiti i capi… Ringrazio il Prof. Frédéric Hapiot del CNRS di Lens (Francia) con il quale ho lavorato due mesi nei nostri laboratori e un mese nel suo laboratorio in Francia, dove mi ha ospitata per uno stage. Con Frédéric mi sono trovata sempre molto bene e soprattutto durante il mio periodo a Lens, si è mostrato sempre gentile e disponibile. Ringrazio poi il Prof. Donald Krogstad del Concordia College (Università del Minnesota USA), con il quale ho condiviso l'ultimo anno di lavoro. Oltre ad essere sempre presente e disponibile in laboratorio, è sempre stato affabile e con lui come con Frédéric, il tempo passato insieme mi ha arricchito non solo da un punto di vista lavorativo, ma soprattutto umano. Tra le persone da ringraziare anche tutti quelli che fanno parte del mio stesso gruppo di ricerca e tutte le persone che lavorano nel nostro istituto. In modo particolare Barbara, Valentina, Vincenzo e Carlo che fanno parte della mia vita anche al di fuori del laboratorio.

Ringrazio infine tutte le persone che in questi anni mi sono state senza dubbio più vicine. Per primi i miei genitori e poi mia sorella, Claudio, Lorenzo e tutte le altre persone della mia famiglia a cui tengo tantissimo.

# *Acknowledgements*

I can't believe it, finally I' m to the last page for the acknowledgments (!!!).

First of all, I want to thank Dr. Gianna Reginato, who suggested to me to attend this PhD and supported me along the three years, with patience and constancy, and helped me in overcoming some periods of pessimism. I think that our relationship is not only of working nature and this is very important for me. I want to thank also Dr. Luca Gonsalvi, who disclosed me his research project, following always my work also in the last part of writing this thesis and involved me in several projects. Certainly, I thank Dr. Maurizio Peruzzini, who accepted me in his research group and, when necessary, was always ready for suggestions and enlightenments.

So I finished with my bosses… I want to thank Prof. Frédéric Hapiot of CNRS of Lens (France), with whom I worked for two months at ICCOM and one month in his laboratories in Lens. With Frédéric, I had a very nice time and especially when I was in Lens, he has been very kind and helpful. I want also thank Prof. Donald Krogstad of Concordia College (University of Minnesota, USA). We worked together during the last year. He has been friendly and always available. The time I spent with both of them has been important not only from the point of view of the working skillness but also for my experience of life. I want also to thank all the people of my research team and the people who work in our institute. Particularly, Barbara, Valentina, Vincenzo and Carlo who are not only colleagues but also friends.

Finally, I thank the most important persons of my life. For first, my parents and my sister and then Claudio, Lorenzo and all the others of my family that I love a lot.